Alternative approaches to the prevention of coronary In-stent restenosis

Dr. Keith E. Robertson

BSc (Med.Sci.) MB ChB MRCPSG

Submitted in fulfilment of the requirements of the degree of Doctor of Philosophy

Institute of Cardiovascular and Medical Sciences
Faculty of Medicine
University of Glasgow

February 2014

Abstract

Cardiovascular disease (CVD) has become the most common cause of mortality worldwide, accounting for approximately 30% of all deaths. The primary pathological process that underlies it is atherosclerosis. Atherosclerosis leads to the development of flow-limiting lesions that accumulate over years to decades under the stimulus of genetic and environmental factors. These contribute to both impaired tissue oxygen delivery with resultant clinical symptoms and acute coronary syndromes carrying a significant burden of morbidity and mortality. Within the UK population, 28% of premature deaths in men and 20% in women are attributable to CVD carrying an estimated £30bn annual economic cost.

Myocardial revascularisation in the form of coronary artery bypass grafting (CABG) and percutaneous coronary intervention (PCI) are established therapies for both acute coronary syndromes and symptomatic chronic disease refractory to pharmacological therapy. CABG remains the standard for patients with complex multi-vessel disease however in patients with less complex disease PCI is a reasonable alternative, and remains the gold-standard for patients with simple, focal CAD. The long-term results of CABG are limited by the failure of conduit grafts leading to recurrent symptoms, MI and/or repeat revascularization that carries with it a significant excess risk. Despite advancements in surgical technique and adjunctive medical therapy, the commonly used saphenous vein grafts are constrained by a cumulative graft failure rate of 50% at 10 years. Intracoronary stents, used for PCI are limited by the restenosis or thrombosis of stented vessel segments, phenomena that also confer significant morbidity and mortality. Vein graft disease (VGD) and in-stent restenosis (ISR)/thrombosis share similar pathological features related to the response to vessel injury, principally thrombosis, the development of neointimal hyperplasia, impaired endothelialisation and accelerated atherosclerosis.

Gene-therapy remains a potential alternative to the use of pharmacotherapy for the prevention and treatment of these important clinical entities. Preclinical studies have provided a greater understanding of the underlying mechanistic pathways in both VGD and ISR and have provided insight into potential pathophysiological targets for manipulation with gene therapy. However, as yet, translation to the clinical setting has been less successful.

Although stent technology and associated clinical outcomes continue to improve, preclinical studies suggest that gene therapy with a safe and stable vector expressing

endogenous proteins that restore normal vessel physiology can be an intuitive alternative to cytotoxic drugs for the prevention of stent complications.

The principal aim of this PhD was to investigate alternative approaches to the prevention of coronary in-stent restenosis. It was initially planned to do this using a gene therapy approach with development and delivery of therapeutic viral vectors to a large animal model of ISR. Subsequently an interest was taken in the role of microRNAs in the development of neointimal hyperplasia and the potential for their therapeutic modulation in the prevention of ISR and use as cardiovascular biomarkers.

Initial experiments focused on the assessment of adenoviral and lentiviral vectors for the transduction of human coronary artery smooth muscle cells (HCASMC). The dedifferentiation of vascular smooth muscle cells (VSMC) to a proliferative and migratory phenotype from their differentiated contractile state is a key process in the development of neointimal hyperplasia. Unmodified adenoviral (Ad5) and second-generation lentiviral vectors were used to transduce HCASMC *in vitro*. Successful gene expression was achieved with both vectors, however, in keeping with previous studies significant transduction with Ad5 could only be obtained at higher viral concentrations. Lentivirus was much more efficient, showing significant cell transduction at low viral doses. It was initially planned to take this vector forward to an *in vivo* model but it unfortunately proved time consuming and prohibitively expensive to produce in large enough titres. Adenoviral vectors were therefore used for *in vivo* delivery. A local delivery catheter approach, for the delivery of an adenoviral vector was tested *ex vivo* and successful viral transduction of explanted porcine coronary arteries was obtained.

The Clearway RX^{TM} (Atrium Medical) perfusion balloon catheter was designed to deliver a therapeutic agent directly to intra-coronary lesions. It was therefore hypothesized that it may be able to effectively deliver a gene-delivery vector. A porcine model of coronary stent delivery and overexpansion has been shown to develop consistent vessel injury and the development of neointima. This was therefore used to assess the ability of the Clearway RX to deliver an adenovirus expressing β-galactosidase. Measurable viral transduction of the arterial wall was not obtained most likely due to the Clearway being unable to maintain viral contact with the vessel for long enough to achieve significant transduction. Similar issues affected the only other commercially available local delivery catheter, the GENIE^{TM} which forms a therapeutic drug reservoir between two occlusive

balloons. Again, long enough incubation times to mediate unmodified Ad5 arterial transduction could not be obtained and the pigs tolerated the procedures poorly.

To overcome these issues a virus-coated stent was developed using the spray-coatable Yukon^{TM} stent system and a Poloxamer 407 gel with thermoreversible properties. Poloxamer 407 has previously been used to successfully augment adenoviral transduction in small animal models. This system was therefore tested in the porcine model. No viral transduction of the vessel wall was obtained and analysis of distal organ sites confirmed off-target viral sequestration.

Interest turned to the investigation of the role of microRNAs (miRs) in the development of in-stent restenosis. miRs are short, non-coding ribonucleic acids that act to control gene expression at a posttranscriptional level. Several miRs have been shown to play key roles in establishing smooth muscle and endothelial cell fate, tissue homeostasis and are now implicated in the complex regulation of the phenotype of cell types involved in vascular remodelling and the development of ISR. Using *in vitro* models of VSMC proliferation and migration, the dynamic expression of regulatory miRs implicated in the control of VSMC phenotype was assessed. These experiments suggested that miR-21, miR-146a, miR-221 and miR-365 overexpression may contribute to the promotion of a dedifferentiated VSMC phenotype in the development of human neointimal lesions. The results for miR-143 and miR-145 were less clear however.

It was hypothesised that expression patterns of these regulatory miRs in the vasculature would alter in response to stent-induced injury. All previously reported studies in this area have used *in-vitro* or *in-vivo* rodent models of vascular injury. A more clinically relevant large animal (porcine) model of in-stent restenosis was therefore utilised to assess the expression levels of miRs previously reported to play a role in VSMC regulation as well as novel targets. RNA was extracted from vessels snap frozen at the time of sacrifice and changes in miR expression within the vessel wall were determined using quantitative real time PCR (qRT-PCR). Using an electrolysis method to achieve stent dissolution it was possible to use *in-situ* hybridization to co-localise dysregulated miRs within neointimal lesions. Both miR-21 and the miR-143/miR-145 cluster appear to play a key role in the regulation of VSMC phenotypic switch and are shown to be both dynamic and significantly upregulated in developing neointima following stent implantation. This localised upregulation in the miR-143/miR-145 cluster, despite a consistent overall

"whole-vessel" downregulation, is particularly novel and differs from previously published findings. This has important implications towards future therapeutic manipulation.

Additionally, and consistent with suggestions that microRNAs operate in regulatory networks, a panel of novel miRs, including miR-142, have been identified that may play an important role in the development of ISR and merit future investigation.

Finally, experiments were performed to investigate the potential role of circulating miRs as biomarkers in patients undergoing CABG surgery. RNA was extracted from serum pre- and post-surgery and the dynamic and temporal expression of a panel of miRs associated with both acute and stable chronic coronary artery disease determined using qRT-PCR. Correlation analysis was performed with classical biomarkers and peri-operative factors. Dynamic changes were seen in circulating levels of miR-133a (which was seen to correlate with the biomarker troponin T), miR-122, miR-92a and miR-126. Although patient numbers were small, and this data is therefore observational, it is the first to investigate a temporal serum profile of dynamic miRs in the setting of uncomplicated CABG and show early potential for their use as biomarkers. It also adds to the growing evidence for the presence of a circulating microRNA network for cardiovascular disease that may hold significant future potential for therapeutic manipulation in specific pathological settings.

Although the initial aims of developing a therapeutic gene therapy vector for the prevention of in-stent restenosis and its delivery to and testing in a large animal *in vivo* model were not achieved, this thesis adds to the understanding of the developing and increasingly complex role played by microRNAs in the setting of vascular remodelling following coronary stent implantation. It is hoped that the therapeutic modulation of miR levels could become an effective approach for the prevention of ISR and optimisation of patient outcomes in the clinical setting.

Table of Contents

Abstract ..... **ii**
List of Tables ..... **xi**
List of Figures ..... **xii**
Acknowledgement ..... **xiv**
Author's declaration ..... **xvi**
List of Publications ..... **xvii**
Definitions & Abbreviations ..... **xix**

1 Introduction **1**

1.1 Cardiovascular Disease 2
1.2 Revascularization for Coronary Artery Disease 3
1.3 Mechanisms of Vein Graft Disease and In-stent restenosis 9
1.3.1 Vein Graft Disease 9
1.3.2 In-stent Restenosis 10
1.4 Cardiovascular Gene Therapy 14
1.4.1 Identification of Therapeutic Targets 14
1.4.1.1 Vein Graft Disease 14
1.4.1.2 In-stent Restenosis 16
1.4.1.3 Neointimal Hyperplasia 16
1.4.1.4 Extracellular Matrix Formation 19
1.4.1.5 Endothelialisation 20
1.4.2 Development of Gene Therapy Vectors 23
1.4.2.1 Non-viral Vectors 23
1.4.2.2 Retroviruses 23
1.4.2.3 Adenoviruses 24
1.4.2.4 Adeno-associated Viruses 30
1.4.2.5 Lentiviruses 31
1.4.3 Delivery of a Therapeutic Vector to the Target Tissue 33
1.4.3.1 Stent Models 33
1.4.3.2 Thrombosis 35
1.5 Human Perspectives and Clinical Trials 36
1.5.1 In-stent Restenosis 36
1.6 MicroRNA 39
1.6.1 MicroRNA Processing and Function 39
1.6.1.1 MicroRNA Biogenesis 39
1.6.2 MicroRNAs in the vasculature 42
1.6.2.1 Complex role of miR-21 in restenosis 44
1.6.2.2 MiR-143/145 45
1.6.2.3 MiR-221 48

1.6.2.4 miR-92a and miR-126 48
1.6.2.5 miR-146a 49
1.6.2.6 miR-155 50
1.6.2.7 miR-133a 50
1.7 HYPOTHESIS 51

2 Materials & Methods 52

2.1 CHEMICALS 53
2.2 CELL LINES 53
2.3 TISSUE AND CELL CULTURE 53
2.3.1 Preparation of smooth muscle cells from saphenous vein explants 54
2.3.2 Maintenance of established cell lines 54
2.3.3 Cryopreservation and recovery of cultured cell lines 55
2.4 PRODUCTION OF VIRAL VECTORS 56
2.4.1 Recombinant Ad5 production 56
2.4.2 AdGFP purification through caesium chloride gradient 56
2.4.3 Virus titration by end-point dilution assay 57
2.4.4 Quantification of virus particles 57
2.4.5 Recombinant Ad5 expressing LacZ 58
2.4.6 Production of Lentivirus expressing eGFP 58
2.4.7 Concentration of Lentivirus 59
2.4.8 Calculation of virus titre in 293T cells 59
2.5 VIRUS TRANSDUCTIONS 63
2.5.1 Virus cell binding 63
2.5.2 Determination of Protein Concentration in Cell and Tissue Lysates 63
2.5.3 GFP transgene quantification 64
2.5.4 B-galactosidase transgene quantification 64
2.5.5 LacZ staining 65
2.6 HAEMAGGLUTINATION ASSAY 66
2.6.1 Preparation of erythrocytes 66
2.6.2 Haemagglutation Analysis 66
2.7 GENERAL MOLECULAR BIOLOGY TECHNIQUES 67
2.7.1 Vascular Smooth Muscle Cell Stimulation 67
2.7.2 Cell migration 68
2.7.3 RNA extraction 68
2.7.3.1 Total RNA extraction from cells 68
2.7.3.2 Total RNA extraction from tissue 69
2.7.4 cDNA synthesis 70
2.7.5 Quantitative Real Time Polymerase Chain Reaction 70
2.8 HISTOLOGY 71
2.8.1 Stent Electrolysis 71
2.8.2 En-face β-galactosidase staining 73

2.8.3 Paraffin processing....73
2.8.4 Tissue Sectioning....74
2.8.5 Haematoxylin and Eosin Staining....74
2.8.6 Immunohistochemistry (IHC)....75
2.8.6.1 Antigen retrival....75
2.8.6.2 Quenching....75
2.8.6.3 Antibody binding....75
2.8.7 In-situ hybridisation....76
2.8.7.1 Preparation....76
2.8.7.2 Unmasking and Deproteinating Sections....77
2.8.7.3 Hybridisation....77
2.8.7.4 Stringency washing....78
2.8.7.5 Immunological detection....78
2.8.7.6 Colour solution....78
2.9 MICROSCOPE IMAGING....79
2.9.1 Morphometric analysis....79
2.10 EX-VIVO METHODS....80
2.10.1 Delivery of adenovirus to ex-vivo porcine coronary arteries using the Clearway™ RX Therapeutic Perfusion Catheter....80
2.11 *IN*-VIVO METHODS....82
2.11.1 Ethics and Legislation....82
2.11.2 Animals and Environment....82
2.11.3 Coronary Angiography Procedural Technique....82
2.11.3.1 General Considerations....82
2.11.3.2 Periprocedural pharmacotherapy....84
2.11.3.3 Anaesthesia....84
2.11.3.4 Arterial access....85
2.11.3.5 Coronary catheterization....85
2.11.3.6 Closure....87
2.11.3.7 Recovery....87
2.11.3.8 Animal sacrifice....87
2.11.4 Coronary Stent Model....87
2.11.5 Development of in-stent restenosis....88
2.11.6 Local delivery of viral vectors....88
2.11.6.1 Development of Model and Initial Problems....88
2.11.6.2 Viral Gene Delivery using Clearway™ RX and GENIE™....89
2.11.7 Stent-based delivery of viral vectors....92
2.11.7.1 Poloxamer 407....92
2.11.7.2 Yukon stent system....93
2.11.7.3 Stent preparation and delivery....93
2.11.8 MicroRNA expression in neointima....96
2.11.8.1 Optical coherence tomography....96
2.12 MICRORNA LEVELS IN CABG PATIENTS....97

2.12.1 Study Population 97
2.12.2 RNA isolation 97
2.12.3 Quantitative real time polymerase chain reaction (qRT-PCR) 98
2.12.4 Data Analysis and Normalisation 98
2.13 STATISTICAL ANALYSIS 99
2.13.1 Software 99
2.13.2 In Vitro 99
2.13.3 In-vivo 99
2.13.4 MicroRNAs in CABG patients 99

3 Local Delivery of Viral Vectors in a Porcine Coronary Stent Model 100

3.1 INTRODUCTION 101
3.2 RESULTS 102
3.2.1 Manufacture and testing of Viral Vectors 102
3.2.1.1 Transduction of Human Saphenous Vein Smooth Muscle Cells Using an Adenovirus expressing Green Fluorescent Protein 102
3.2.1.2 Transduction of Human Saphenous Vein Smooth Muscle Cells Using a Lentiviral Vector expressing Green Fluorescent Protein 102
3.2.2 Haemagglutination 106
3.2.3 Delivery of adenoviral vector to ex-vivo porcine coronary arteries using the Clearway™ RX Therapeutic Perfusion Catheter 108
3.2.3.1 Adenovirus expressing Green Fluorescent Protein 108
3.2.3.2 Adenovirus expressing LacZ 108
3.2.4 Local Delivery of Viral Vectors in a Porcine model of Intracoronary Stenting 111
3.2.4.1 Viral Gene Delivery using Clearway™ RX 111
3.2.4.2 Viral Gene Delivery using GENIE™ 113
3.2.5 Stent-based delivery of viral vectors 116
3.2.5.1 Poloxamer 407 116
3.2.5.2 Effect of Poloxamer 407 on transduction of HCASMC *in-vitro* 117
3.2.5.3 Delivery of RAd 35 stents 122
3.3 DISCUSSION 126

4 Role of MicroRNAs in a Porcine model of In-stent Restenosis 134

4.1 Introduction 135
4.2 Results 136
4.2.1 Changes in microRNA expression levels as HCASMCs proliferate 136
4.2.2 MicroRNA expression alters as HCASMC switch to a migratory phenotype 144
4.2.3 In-vivo Porcine model of In-stent Restenosis 149
4.2.3.1 Histology 149
4.2.3.2 Choice of endogenous control 153
4.2.3.3 Expression of MiR-21/221 155

4.2.3.4 Expression of MiR-143/145 155
4.2.3.5 Other Vascular MicroRNAs 155
4.2.3.6 Localisation of miR-21 159
4.2.3.7 Localisation of miR-143/145 expression in neointima 159
4.2.3.8 Novel MicroRNAs Dysregulated in Restenosis 163
4.3 Discussion 167

5 Dynamic changes in circulating microRNA levels in patients undergoing Coronary Artery Bypass Surgery 178

5.1 INTRODUCTION 179
5.2 RESULTS 182
5.2.1 Demographics 182
5.2.2 Panel of MicroRNAs Studied 182
5.2.3 Temporal Changes in Circulating MicroRNA Levels 186
5.2.4 Correlation with Existing Biomarkers 193
5.2.5 Relationship to Intra-operative Factors 196
5.2.6 Relationship to Renal and Liver Function 196
5.3 DISCUSSION 203

6 Final Discussion 207

List of References ..... Error! Bookmark not defined.

List of Tables

Table 1-1 Indications for revascularization in stable angina or silent ischaemia....4
Table 1-2 Clinical trials of gene therapy for the prevention of in-stent restenosis 38
Table 1-3 MicroRNAs implicated in the vessel response to injury and development of neointimal hyperplasia 42
Table 3-1 Viral vector delivery to the porcine model with GENIE catheter 116
Table 3-2 Delivery of RAd35 using Poloxamer 407-coated stents....123
Table 4-1 Mean cycle thresholds (Ct) of potential endogenous control microRNAs 153
Table 5-1 Patient's Baseline Characteristics....183
Table 5-2 Intra-Operative Characteristics....184
Table 5-3 Post-Operative Course....185
Table 5-4 Serum levels of C-reactive protein and cardiac isoform of Troponin T 193

List of Figures

Figure 1-1 Development of neointimal hyperplasia....13
Figure 1-2 Vascular gene therapy for the prevention of ISR and VGD....15
Figure 1-3 Cellular uptake mechanisms of Adenovirus serotype 5 viral vectors....29
Figure 1-4 The microRNA biogenesis pathway....41
Figure 1-5 MicroRNAs implicated in the vessel injury response, vascular remodelling, and angiogenesis 43
Figure 1-6 Summary of signalling pathways mediating effects of miR-143/miR-145 cluster on VSMC phenotype 46
Figure 2-1 Stent dissolution using electrolysis method....72
Figure 2-2 *In-situ* hybridization for microRNA....76
Figure 2-3 Clearway™ RX Therapeutic Perfusion Catheter (Atrium Medical) 80
Figure 2-4 Theatre set-up for coronary angiography 83
Figure 2-5 Arterial Access 86
Figure 2-6 Stent delivery to porcine Left Anterior Descending (LAD) artery....88
Figure 2-7 GENIE™ local drug delivery system....89
Figure 2-8 GENIE™ local drug delivery system....90
Figure 2-9 Schematic for delivery of viral vector using a pressure syringe....91
Figure 2-10 Chemical structure of Poloxamer 407 (BASF)....92
Figure 2-11 Poloxamer 407 as a thermo-reversible gel....93
Figure 2-12 Yukon® stent system (Translumina)....95
Figure 3-1 Transduction of VSMC with Ad5 expressing eGFP 103
Figure 3-2 Transduction of VSMC with SFFV lentivirus expressing eGFP....104
Figure 3-3 Viral transduction of human smooth muscle cells....105
Figure 3-4 Haemagglutination Assay....107
Figure 3-5 AdGFP delivery via Clearway RX to *ex-vivo* porcine arteries....109
Figure 3-6 AdLacZ delivery via Clearway RX to ex-vivo porcine arteries 110
Figure 3-7 Delivery of AdLacZ to stented porcine coronary arteries using Clearway RX 112
Figure 3-8 Time taken to deliver viral vector and total inflation times for GENIE™ 114
Figure 3-9 Delivery of AdLacZ to stented porcine coronary arteries using GENIE™ 115
Figure 3-10 Effect of Poloxamer 407 on transduction of HCASMC by AdLacZ....118
Figure 4-1 Change in expression level of miR-21 with HCASMC phenotypic switch....137
Figure 4-2 Change in expression level of miR-146a with HCASMC phenotypic switch....138
Figure 4-3 Expression level of miR-146b with HCASMC phenotypic switch 139
Figure 4-4 Change in expression level of miR-365 with HCASMC phenotypic switch....140
Figure 4-5 Expression level of miR-221 with HCASMC phenotypic switch 141
Figure 4-6 Expression level of miR-143 and miR-145 with HCASMC phenotypic switch 142
Figure 4-7 Expression level of miR-133a with HCASMC phenotypic switch 143
Figure 4-8 *In vitro* scratch migration assay....145
Figure 4-9 Change in expression level of miR-21 and miR-221 with HCASMC switch to a migratory phenotype 146

Figure 4-10 Change in expression level of miR-143 and miR-145 with HCASMC switch to a migratory phenotype 147
Figure 4-11 Expression level of miR-146a and miR-146b with HCASMC switch to a migratory phenotype 148
Figure 4-12 Morphometric analysis of porcine arteries treated with bare-metal stents 150
Figure 4-13 "Virtual" histology of BMS vs. DES at 28 days obtained using OCT 151
Figure 4-14 Comparison of neointimal area as measured by OCT and H&E morphometry 152
Figure 4-15 Scatter plots of raw Ct values for potential porcine endogenous controls 154
Figure 4-16 Expression levels of microRNAs upregulated in a porcine model of coronary in-stent restenosis 156
Figure 4-17 Expression levels of microRNAs downregulated in a porcine model of coronary in-stent restenosis 157
Figure 4-18 Expression profiles of vascular microRNAs not significantly altered in response to vessel injury and stent implantation in porcine model 158
Figure 4-19 miR-21 localisation in stented porcine vessels 160
Figure 4-20 miR-143/miR-145 localisation in stented porcine vessels 161
Figure 4-21 Immunolocalization of cells expressing miR-143 and miR-145 in stented porcine coronary arteries 162
Figure 4-22 Change in expression of miR-142-3p and miR-142-5p in response to coronary stent insertion 164
Figure 4-23 Other novel microRNAs dysregulated in porcine ISR model 165
Figure 4-24 Investigated microRNAs with no change in expression in porcine ISR model 166
Figure 5-1 Circulating microRNA levels in serum from patients undergoing CABG – miRs showing increase or no change 187
Figure 5-2 Circulating levels of microRNAs showing a post-op reduction 188
Figure 5-3 Comparison of normalisation methods for miR-133a 189
Figure 5-4 Comparison of normalisation methods for miR-122 190
Figure 5-5 Comparison of normalisation methods for miR-92a 191
Figure 5-6 Comparison of normalisation methods for miR-126 192
Figure 5-7 Correlation between change in circulating miR-133a levels and rise in serum Troponin T at day 1 post-op 194
Figure 5-8 Absence of correlation between circulating microRNAs and rise in serum Troponin T 195
Figure 5-9 Absence of correlation between circulating miR-133a or miR-122 and intra-operative factors 197
Figure 5-10 Absence of correlation between circulating miR-92a or miR-126 and intra-operative factors (POD1) 198
Figure 5-11 Absence of correlation between circulating miR-92a or miR-126 and intra-operative factors (POD5) 199
Figure 5-12 Renal function in the peri-operative period 200
Figure 5-13 Hepatic function in the peri-operative period 201
Figure 5-14 Absence of correlation between circulating microRNAs and change in serum creatinine 202

Acknowledgement

Firstly I would like to greatly acknowledge and thank my supervisors Dr. Simon Kennedy, Professor Keith Oldroyd and Professor Andrew Baker. Their wisdom, advice, encouragement, patience and guidance were gratefully received and I hugely appreciate all the time and effort they have dedicated to me. A little “gentle” encouragement also helped at times!

Thank you to the British Heart Foundation who funded my PhD and were also very understanding and helpful when clinical pressures threatened my plans to complete this degree. To this end, thank you also to the Faculty of Medicine at the University of Glasgow, particularly Professor Mary Ann Lumsden, who displayed welcome support and understanding.

Many thanks also to the staff of the GCRC, particularly the Baker group, who displayed remarkable patience, despite my naivety in the lab, and taught me the skills and techniques I needed to complete my project. Special mention must go out to Nicola Hamilton and Gregor Aitchison for looking after me in the lab and particularly Dr. Robert McDonald whose advice and experience I relied on frequently. Also a huge thanks to my room 423 office buddies over the years: Dave Carty, Stacy Wood, Margaret Duffy, Crawford “tea-boy” Halliday and Emily Ord. Their banter, cups of tea and endless enthusiasm definitely helped keep me going.

Thank you to the staff of the BPU at the University of Strathclyde, particularly Linda Horan, Kevin O'Halloran and Steven McDonald, for their invaluable assistance in performing the *in vivo* experiments.

Both heartfelt thanks and also an apology goes out to all my many friends out-with science and medicine, who have been not only supportive and encouraging but also understanding with regards to all the missed social gatherings and periods of non-communication. You know who you are.

To my wonderful family; Mum, Dad and brother Niall and in-laws Maggie and Les who could not have been more supportive or encouraging, both in this and everything else I do.

Lastly my amazing wife Nina, who I absolutely could not have done this without. Your support and love have been unwavering and I will always be in you debt. Thank you so much. I dedicate this to you, and our wee boy Ruaridh, whose arrival almost a year ago gave me a new and welcome drive and focus.

Author's declaration

I declare that this thesis has been written entirely by myself and is a record of work that I have performed, excluding the PCNA staining in Figure 4-24, which was performed by Dr. Robert McDonald and the TaqMan Low-Density microRNA microarray analysis of porcine vascular tissue (Page 160-161, Table 4-2, Figure 4-18) which was performed by Dr. Robert McDonald and Dr. Katie White. This thesis has not been previously submitted for a higher degree. The research was carried out in the Institute of Cardiovascular and Medical Sciences, University of Glasgow under the supervision of Professor A.H. Baker and the Biological Procedures Unit, University of Strathclyde under the supervision of Dr. Simon Kennedy.

Keith Robertson

February 2014

List of Publications

Papers

McDonald RA, White KM, Wu J, Cooley BC, **Robertson KE**, Halliday CA, McClure JD, Francis S, Lu R, Kennedy S, George SJ, Wan S, van Rooij E, Baker AH (2013). miRNA-21 is dysregulated in response to vein grafting in multiple models and genetic ablation in mice attenuates neointima formation. *Eur Heart J*; 34(22):1636-43

Robertson KE, McDonald RA, Oldroyd KG, Nicklin SA, Baker AH (2012). Prevention of coronary in-stent restenosis and vein graft failure: does vascular gene therapy have a role? *Pharmacol Ther*;136(1):23-34

Caruso P, MacLean MR, Khanin R, McClure J, Soon E, Southgate M, MacDonald RA, Greig JA, **Robertson KE**, Masson R, Denby L, Dempsie Y, Long L, Morrell NW, Baker AH (2010). Dynamic changes in lung microRNA profiles during the development of pulmonary hypertension due to chronic hypoxia and monocrotaline. *Arterioscler Thromb Vasc Biol*; 30(4):716-23

Abstracts

Halliday CA[1], **Robertson KE**[1], McDonald RA, Kennedy S, Oldroyd KG, Douglas G, Channon KM, Baker AH (2013). MicroRNA 21 is Upregulated Following Coronary Artery Stenting and Genetic Deletion Limits Neointima Formation. *Eur Heart J* 34 (suppl 1):806. Oral presentation at European Society of Cardiology 2013 Annual Conference – Amsterdam.

Halliday CA[1], **Robertson KE**[1], McDonald RA, Kennedy S, Oldroyd KG, Douglas G, Channon KM, Baker AH (2013). The Role of MicroRNA 21 in Porcine and Murine Models of In-Stent Restenosis. Oral presentation at Scottish Cardiovascular Forum 2013

Robertson KE, Kennedy S, McDonald RA, Oldroyd KG, Baker AH (2012). Identification of MicroRNAs Dysregulated in a Porcine Model of Coronary In-stent Restenosis.

[1] Joint first authors

Circulation 126:A18304. Poster presentation at American Heart Association Scientific Sessions 2012 – Los Angeles.

McDonald RA, White KM, **Robertson KE**, Hu J, Lu R, George SJ, Wan S, Baker AH (2012). Dysregulation of the miR143/145 Cluster and miR133a During Progression of Vein Graft Neointima Formation. *Circulation* 126:A18427. Presentation at American Heart Association Scientific Sessions 2012 – Los Angeles.

McDonald RA, Wu J, White KM, **Robertson KE**, Cooley BC, Lu R, Hu J, Kennedy S, Wadsworth RM, George SJ, Wan S, Baker AH (2012). MicroRNA Analysis in Experimental Models of Vein Graft Neointima Formation Indentifies a Critical Role For Mir-21 in Neointima Formation. *Circulation* 126:A18255. Presentation at American Heart Association Scientific Sessions 2012 – Los Angeles.

Robertson KE, Hu J, McDonald RA, Oldroyd KG, Wan S, Baker AH (2012). Circulating microRNAs as potential biomarkers in patients undergoing coronary artery bypass graft surgery. *Eur Heart J* 33 (Abstract Supplement):345. Oral presentation at European Society of Cardiology 2012 Annual Conference – Munich.

Definitions & Abbreviations

AA	Abdominal Aorta
AAV	Adeno-associated virus
ACE	Angiotensin converting enzyme
ACS	Acute coronary syndromes
Ad	Adenovirus
AdV	Adenovirus serotype 5 vector
ALP	Alkaline phosphatase
α-SMA	Smooth Muscle alpha-actin
ALT/GPT	Alanine transaminase/Glutamic Pyruvic Transaminase
AP	Alkaline Phosphatase
Bcl-2	B-cell lymphoma 2
bFGF	Basic fibroblast growth factor
BMP	Bone morphogenic proteins
BMS	Bare metal stent
BSA	Bovine Serum Albumin
CA	Carotid Artery
CABG	Coronary Artery Bypass Graft surgery
CAD	Coronary Artery Disease
CAR	Coxsackie and Adenovirus Receptor
cDNA	Complementary Deoxyribonucleic Acid
CMV	Cytomegalovirus

CO_2	Carbon dioxide
CPB	Cardiopulmonary bypass
CPD	Citrate Phosphate Dextrose
CRP	C-reactive protein
CsCl	Caesium Chloride
CSE	Cystathionine gamma-lysase
Ct	Cycle Threshold
cTnT	Cardiac isoform of Troponin T
CVD	Cardiovascular Disease
Cx	Circumflex coronary artery
DC	Direct current
DEPC	Diethyl Pyrocarbonate
DES	Drug-eluting stent
DIG	Digoxigenin
DMEM	Dulbecco’s Modified Eagle Medium
dNTP	Deoxyribonucleotide
dNTPs	deoxynucleotide triphosphates
DPBS	Dulbecco's Phosphate-Buffered Saline
dTTP	Deoxythymidine triphosphate
E2F	Elongation Factor
EC	Endogenous control
EC	Endothelial Cell
ECG	Electrocardiogram

ECM	Extra-Cellular Matrix
EDTA	Ethylene Diamine Tetraacetic Acid
ESC	European Society of Cardiology
FAM	6-carboxyfluorescein
FCS	Foetal Calf Serum
FX	Coagulation factor X
GFP	Green Fluorescent Protein
H&E	Haematoxylin and Eosin
H_2O_2	Hydrogen Peroxide
H_2S	Hydrogen sulphide
HBSS	Hank's Balanced Salt Solution
HCASMC	Human Coronary Artery Smooth Muscle Cells
HCL	Hydrogen chloride
HSPG	Heparan Sulphate Proteoglycans
HSVSMC	Human Saphenous Vein Smooth Muscle Cells
ICC	Immunocytochemistry
ICLV	Integrase-competent lentiviral vectors
IDLV	Integrase-deficient lentiviral vectors
IH	Intimal Hyperplasia
IHC	Immunohistochemistry
IL-1α	Interleukin-1alpha
IM	Intra-muscular
ISH	*In-situ* Hybridisation

ISR	In-stent Restenosis
IV	Intravenous
IV	Intra-venous
JV	Jugular Vein
KLF2	Krueppel-like factor 2
KLF4	Krueppel-like factor 4
KLF5	Krueppel-like factor 5
LAD	Left Anterior Descending coronary artery
LAO	Left anterior oblique
LMS	Left main stem
LNA	Locked nucleic acid
LV	Left ventricle
mAb	Monoclonal antibody
MHC	Myosin Heavy Chain
MI	Myocardial infarction
miR	Micro Ribonucleic Acid
MOI	Multiplicity of Infection
MOI	Multiplicity of Infection
mRNA	Messenger Ribonucleic Acid
MRTFs	Myocardin-related Transcription Factors
mTOR	Mechanistic target of rapamycin
NIH	Neointimal Hyperplasia
NO	Nitric Oxide

NOS	Nitric Oxide Synthase
NSTEMI	Non-ST-segment elevation myocardial infarction
OCT	Optical Coherence Tomography
ODN	Oligodeoxynucleotides
OMT	Optimal medical therapy
P/L	Plasmid/Liposome
PBS	Phosphate Buffered Saline
PCI	Percutaneous Coronary Intervention
PCNA	Proliferating Cell Nuclear Antigen
PDCD4	Programmed cell death 4
PDGF	Platelet Derived Growth Factor
PES	Paclitaxel-eluting stent
PFA	Paraformaldehyde
pfu	Plaque forming units
PO	Per os
POBA	Plain old balloon angioplasty
pre-miR	Precursor microRNA
pri-miR	Primary microRNA
PTEN	Phosphatase and tensin homology deleted on chromosome 10
qRT-PCR	Quantitative Real Time Polymerase Chain Reaction
RAO	Right anterior oblique
RBC	Red Blood Cells
RCA	Right Coronary Artery

RNA	Ribonucleic Acid (Davis et al., 2008)
RT	Reverse Transcription
SDS	Sodium Dodecyl Sulphate
SES	Sirolimus-eluting stent
SMC	Smooth Muscle Cell
SP-1	Specificity protein-1
SRF	Serum Response Factor
SSC	Saline-sodium Citrate
ST	Stent thrombosis
STEMI	ST-segment elevation myocardial infarction
SV	Saphenous Vein
SVG	Saphenous Vein Graft
TAMRA	Tetramethylrhodamine
TGF	Transforming Growth Factor
TGF-β	Transforming growth factor β
TIMP	Tissue Inhibitor of Metalloproteinases
TMEM49	Transmembrane protein 49
UA	Unstable angina
v/v	%volume/volume
VC	Vena Cava
VEGF	Vascular Endothelial Growth Factor
VF	Ventricular fibrillation
VGD	Vein Graft Disease

VSMC	Vascular Smooth Muscle Cell
VT	Ventricular tachycardia
w/v	%weight/volume

1 Introduction

1.1 Cardiovascular Disease

Cardiovascular disease (CVD) has become the most common cause of mortality worldwide, accounting for approximately 30% of all deaths (Libby and Braunwald, 2008). This all-encompassing label refers to a spectrum of pathologies affecting the heart and circulatory system, including, coronary artery disease, congestive cardiac failure, disorders of cardiac rhythm, structural disorders of the cardiac muscle or valves, pericardial disease, congenital disease, peripheral arterial disease and stroke. The primary pathology that underlies a significant majority of these distinct disorders is atherosclerosis.

Atherosclerosis leads to the development of flow-limiting lesions that develop from early adolescence and accumulate over years to decades under the stimulus of a variety of genetic and environmental factors (Libby, 2013). These atherosclerotic lesions ultimately can lead to impaired tissue oxygen delivery and resultant clinical symptoms such as angina pectoris or intermittent claudication. Acutely, additional factors such as plaque rupture, inflammation and thrombosis result in unstable lesions leading to occlusive myocardial infarction (MI) or acute coronary syndromes (ACS) that carry a significant burden of morbidity and mortality. Within the UK population, 28% of premature deaths in men and 20% in women are attributable to CVD carrying an estimated £30bn annual economic cost (BHF, 2012). Almost half of these deaths are directly attributable to atherosclerotic coronary artery disease.

The rise in evident atherosclerosis among populations is driven by industrialization, urbanization and the associated changes in lifestyle they bring (Libby and Braunwald, 2008). Conventional risk factors for the development and progression of atherosclerosis include hypertension, hypercholesterolaemia, diabetes, sedentary lifestyle, obesity, smoking and family history (Bayturan et al., 2010, Frey et al., 2011, Kronmal et al., 2007, Nicholls et al., 2010, Otaki et al., 2013, Pekkanen et al., 1990, Perk et al., 2012). Although CVD mortality is changing, with declining age-standardized rates in Europe and the USA, they remain high and are even increasing in low- and middle-income countries due to this spread of risk factors and increased longevity through improved nutrition and public health measures. These reductions in mortality seen in high-income countries can be predominately explained by the combination of preventive methods leading to attenuation of the above risk factors (>50%) and advancing pharmacotherapeutics (~40%) (Perk et al., 2012).

1.2 Revascularization for Coronary Artery Disease

Advancements in medical therapy have proven to be effective in both controlling symptoms and reducing the morbidity and mortality associated with CVD. Optimal medical therapy (OMT), comprises the combination of intensive lifestyle and risk factor modification with pharmacological therapy including, primarily, anti-platelet agents, HMG-CoA reductase inhibitors (statins), β-blockers and angiotensin-converting enzyme (ACE) inhibitors (Boden et al., 2007, Wijns et al., 2010). Despite these improvements in non-invasive therapies there are key situations when an invasive revascularization strategy is required (Levine et al., 2011, Wijns et al., 2010).

Myocardial revascularisation in the form of PCI or CABG has undergone many technological advances and extensive study and validation. In patients presenting with acute coronary syndromes (ACS) restoration of coronary flow immediately (STEMI) or at an early time-point (NSTEMI) by revascularisation (principally PCI) has been shown to confer significant benefits in terms of symptom control and improved prognosis (Hamm et al., 2011, Steg et al., 2012). However, in patients with more stable CAD the presence of ischaemia, resulting in symptoms that cannot be adequately controlled by OMT or carrying an additional prognostic significance, is required for there to be any benefit in outcome following revascularisation (Wijns et al., 2010). The ESC recommendations for revascularisation in stable CAD are summarised in Table 1.1.

Arterial bypass surgery has been a mainstay in the treatment of occlusive coronary artery disease since its introduction in 1968 (Favaloro, 1968). When PCI was first introduced in 1977 (Gruntzig, 1978, Gruntzig et al., 1979), it was thought to only be appropriate for patients with focal single vessel disease however, with the expansion and advancement of operator ability and device technologies, the use of PCI has expanded to treat patients with increasingly complex disease involving multiple vessels and/or the left main (LMS) coronary artery (Mohr et al., 2013).

In the UK, numbers of CABG procedures performed have fallen to ~18,000 per annum while the growth in PCI has been exponential rising from less than 10,000 in 1991 to >85,000 in 2010 (BHF, 2012). PCI is therefore now one of the most frequently performed invasive medical procedures in current clinical practice (Garg and Serruys, 2010b).

Table 1-1 Indications for revascularization in stable angina or silent ischaemia

Adapted from European Society of Cardiology Guidelines on Myocardial Revascularization (Wijns *et al*, European Heart Journal (2010) 31, 2501–2555)

	Indications for revascularization
Prognosis	Left main stem>50% stenosis and documented ischaemia or measurable impaired coronary blood flow (if <90%)
	Proximal LAD stenosis >50% and documented ischaemia or measurable impaired coronary blood flow (if <90%)
	2-vessel or 3-vessel disease with impaired left ventricular function
	Proven large area of ischaemia (>10% LV)
	Single remaining patent vessel >50% stenosis and documented ischaemia or measurable impaired coronary blood flow (if <90%)
Symptoms	Any stenosis >50% with limiting angina or angina equivalent, unresponsive to OMT
	Dyspnoea/CHF and >10% LV ischaemia/viability supplied by >50% stenotic artery

Transluminal angioplasty; the widening of a vessel lumen to improve downstream blood flow using a percutaneously delivered catheter, was the first described method of "minimally-invasive" (i.e. non-surgical) revascularisation. It was first performed in peripheral arteries in 1964 (Dotter and Judkins, 1964) and in coronary arteries in 1977 (Gruntzig, 1978). Balloon dilatation of obstructive or occlusive coronary lesions, or "plain old balloon angioplasty" (POBA) as it became known became an important treatment for significant angina. It was however limited by significant complications, principally acute vessel closure due to coronary dissection or restenosis (luminal re-narrowing) caused by elastic recoil of the ballooned vessel segment and negative vessel re-modelling (de Feyter et al., 1994).

This led to the development of coronary stents, the first of which was implanted in 1986 (Sigwart et al., 1987). An in-situ stent provides a scaffold that prevents acute vessel closure and late constrictive recoil and their introduction reduced rates of emergency CABG (Roubin et al., 1992, Sigwart et al., 1988). These early stents carried a significant risk of occlusive stent thrombosis and subsequently increased bleeding secondary to the anticoagulants prescribed to prevent it. Advancements in stent technology (Fischman et al., 1994, Serruys et al., 1994), use of dual antiplatelet therapy (Barragan et al., 1994, Schomig

et al., 1996) and improved technique leading to adequate stent deployment (Colombo et al., 1995, Cutlip et al., 1999) led to stents becoming widely accepted and the default option when performing PCI (Serruys et al., 2006).

Bare metal stents (BMS) although hugely effective and now widely used, remained limited by a small risk of subacute stent thrombosis (~0.5%) and primarily by in-stent neointimal hyperplasia resulting in restenosis rates of between 15% to 30% (Moliterno, 2005). To combat this, many techniques were tried such as laser atherectomy, brachytherapy and systemic and local drug delivery however most were disappointing (Sharma et al., 2011). The next step in the evolution of PCI was the development of a stent that would not restenose to the same degree and therefore reduce the need for repeat revascularisation procedures. Drug-eluting stents (DES) were introduced in 2002 and promised a significant reduction in rates of restenosis compared to BMS (Morice et al., 2002). These impressive results led to huge uptake and by 2005 80-90% of all PCI cases in the USA involved a DES (Jeremias and Kirtane, 2008).

Safety concerns relating to these first-generation DES, eluting the antiproliferative agents sirolimus or paclitaxel, emerged in 2006. Published and presented results from meta-analyses of SES and PES compared to BMS (Camenzind et al., 2007, Nordmann et al., 2006), a clinical trial (Pfisterer et al., 2006) and a large Swedish registry (Lagerqvist et al., 2007) suggested higher rates of late clinical events (such as death and myocardial infarction) due to stent thrombosis (ST) in those receiving DES. This resulted in a rapid decline in DES use and provided a major stimulus for ongoing research into improving outcomes following PCI.

After careful thought and input from large regulatory bodies such as the FDA and ESC, concerns were raised about the methods used in these assessments of DES safety. Multiple independent patient-level meta-analyses of the initial DES trials were performed using standardised clinical outcomes and these concluded that overall rates of death and MI did not significantly differ between DES and BMS (Stettler et al., 2007, Kastrati et al., 2007, Spaulding et al., 2007, Mauri et al., 2007, Stone et al., 2007b). However, analysis of large patient registries revealed that the risk of very-late ST (>1 year post stent implantation) persisted and was estimated at between 0.4-0.6% per annum for at least 5-years post-implantation (James et al., 2009, Pinto Slottow et al., 2008, Wenaweser et al., 2008). Multiple causative factors for stent thrombosis have been identified with acute events being more likely due to procedural considerations such as stent underdeployment or

undersizing or insufficient platelet inhibition (Holmes et al., 2010, van Werkum et al., 2009). Very late events are more-likely due to pathological delayed vessel healing, impaired endothelialisation, hypersensitivity reactions, inflammation, neoatherosclerosis and vascular dysfunction within the stented segements and potentially all secondary to the eluted cytotoxic and cytostatic drugs and the stent polymer (Hara et al., 2010, Joner et al., 2006, Nakazawa et al., 2011). The clinical importance of ST should not be underestimated as 70-80% of patients with ST present with MI and of those with definite ST up to one-third will die (Mauri et al., 2007).

Although the introduction of DES has led to a significant reduction in rates of ISR it has not been eliminated. Late lumen loss has been shown to continue out to at least 5 years in some patients having received first-generation DES which is felt to indicate incomplete vascular healing, possibly driven by the stent polymer (Raber et al., 2011). It did not appear, however, that this late luminal loss contributed to adverse clinical outcomes.

The above ongoing safety concerns alongside the desire to improve vascular healing have led to the development of a multitude of newer generation DES incorporating new stent design and materials, more biocompatible polymers, improved drug kinetics and even biodegradable polymers and bioresorbable platforms (Garg and Serruys, 2010c).

The choice of antiproliferative drug has become an important consideration for improving outcomes post-PCI. Sirolimus (rapamycin) is a macrocyclic lactone that induces cell cycle arrest in VSMC through the inhibition of mTOR, thus reducing neointimal formation (Poon et al., 1996). Paclitaxel inhibits VSMC proliferation by inducing cytostasis through the stabilisation of microtubules which in turn impairs cell division (Axel et al., 1997). Overall, SES are superior to PES with regards to late lumen loss and repeat revascularisation when compared in clinical trials (Schomig et al., 2007). Newer-generation DES have therefore manly used macrolytic lactones, similar to sirolimus, but offering differences in degrees of immunosuppression and rate of drug absorption.

Other pharmacotherapeutic regimens to prevent NIH, delivered both systemically and locally have been investigated, however in general results have been disappointing and overshadowed by the use of DES. Antiplatelet and anticoagulant agents, although effective in reducing abrupt vessel closure due to acute ST do not prevent ISR (Kastrati et al., 1997). Many other agents including lipid-lowering drugs, ACE inhibitors, steroids, anti-inflammatory agents, calcium antagonists and growth factor antagonists have proven

disappointing in clinical trials despite some promise in pre-clinical studies (Faxon, 2002). This is likely in the main due to the difficulty in achieving adequate drug levels at the site of PCI without significant systemic toxicity (Sharma et al., 2011). Local drug delivery, intuitively, should allow a greater local drug concentration (and maximal tissue effect) for a lower overall dose (and minimised toxicity) than could be achieved if the agent was delivered systemically. Again, this approach has been shown to be effective in preclinical PCI studies using a variety of pharmacologic agents and delivery devices (Schwartz et al., 2004). There have been several obstacles to the development of safe and effective intracoronary drug delivery and one of the most important, particularly with regard to future use of gene-therapy, is the development of a suitable delivery device (Brieger and Topol, 1997). The optimal device will enable delivery of a therapeutic dose of drug with minimal disruption to the vessel wall and without limitation of distal blood flow.

The optimal method of revascularization for patients with complex disease has been fiercely debated with many clinical trials having been performed comparing outcomes of CABG with contemporary PCI (DES) in various groups, including those with LMS and/or multi-vessel disease, diabetes, the elderly and stable or unstable symptoms (Boudriot et al., 2011, Buszman et al., 2008, Chieffo et al., 2010, Kapur et al., 2010, Moshkovitz et al., 2012, Park et al., 2010, Park et al., 2011, Rodriguez et al., 2006, Serruys et al., 2010, Wu et al., 2010, Yan et al., 2011, Serruys et al., 2009). With such a complex and heterogeneous group of patients and also study limitations such as non-randomized patient selection, insufficient statistical power and the constant evolution of stent technology it is clear why the choice of revascularization strategy can be complex. PCI is a less invasive treatment than CABG, with associated shorter duration of required hospital stay and recuperation and lesser incurred short-term economic costs (Wijns et al., 2010). Many of the above studies, however, have suggested that CABG when compared to PCI results in a significantly reduced requirement for repeat revascularization and it has been reported that surgery may confer improved relief from angina and a better quality of life (Cohen et al., 2012). A large collaborative analysis of these previously described studies, covering 7812 patients with multi-vessel CAD, showed a similar all cause mortality with both procedures at a median follow-up time of 5.9 years (Hlatky et al., 2009). It also suggested that CABG may confer a mortality benefit in some subgroups, principally diabetics and the elderly (Hlatky et al., 2009).

The SYNergy between percutaneous coronary intervention with TAXus and cardiac surgery (SYNTAX) trial was the first randomized trial to compare CABG and PCI in

patients with very complex CAD (Serruys et al., 2009). It enrolled patients with de-novo LMS and/or three-vessel disease and randomized them to either PCI with a first-generation paclitaxel-eluting DES or CABG (Ong et al., 2006). At 1 year, patients undergoing CABG displayed significantly lower rates of the primary end-point (a composite of death, MI, re-revascularization and stroke) than those who had PCI (Serruys et al., 2009). This was completely driven, however, by significantly higher rates of repeat revascularization in the PCI group, and no significant differences were seen in the composite of death, stroke and MI. The SYNTAX study also allowed creation of a score estimating the baseline severity of a patient's coronary disease. This score split trial patients into three tertiles, low (0-22), intermediate (23-32) and high-risk ($\geq$33). In patients with a low score, there was no significant difference in any clinical outcomes between the two groups at 5 years follow-up (Mohr et al., 2013). In the intermediate severity group, CABG conferred a lower risk of MI and repeat revascularization but this did not translate to any difference in mortality (Mohr et al., 2013). In high risk patients, CABG conferred a lower mortality than PCI at 5 years follow-up (Mohr et al., 2013).

This study suggests a place for both CABG and PCI in the modern management of patients with CAD. CABG remains the standard for patients with complex multi-vessel disease however in patients with less complex disease PCI is a reasonable alternative, and remains the gold-standard for patients with simple, focal CAD or those unsuitable for CABG surgery. Ongoing clinical trials comparing CABG with modern stent technology and emerging techniques, such as the fractional flow reserve assessment of coronary blood flow, hope to refine our understanding of this complex area further.

1.3 Mechanisms of Vein Graft Disease and In-stent restenosis

1.3.1 Vein Graft Disease

When performing CABG surgery, surgeons can use the left or right internal mammary artery, radial artery segments or even synthetic grafts, however, autologous saphenous veins are the most widely used conduit, particularly for grafting to the circumflex or right coronary arteries and their branches. The long-term results of CABG are limited by failure of these conduits leading to recurrent symptoms, MI and/or repeat revascularization that carries with it a significant excess risk compared to native vessel PCI (Lopes et al., 2012, Mehilli et al., 2011, Motwani and Topol, 1998). When saphenous vein grafts (SVG) are used, 10% of all grafts will fail early (within 1 month) due to thrombotic occlusion, another 15% will fail within 1 year due to intimal thickening and a further 25% will fail following this due to accelerated atherosclerosis (Hata et al., 2007) leading to a cumulative graft failure rate of 50% at 10 years (Parang and Arora, 2009). Over 90% of all CABG procedures in the UK, and over 95% in the USA, comprise a combination of a single left internal mammary graft and SVG for all other conduits (Bridgewater et al., 2009, Tabata et al., 2009). This is despite an estimate that total arterial revascularization can be performed in approximately 80% of all cases and confers a 5-15% improvement in mortality at 10 years (Tatoulis, 2013).

The use of a SVG as a conduit results in exposing a thin-walled vein to the high-pressure arterial system, resulting in a complex series of biological changes. Within the first few days following SVG implantation, a proportion of vein grafts fail due to thrombosis as a result of endothelial injury which in turn develops due to a combination of mechanical injury during surgical preparation of the vein, arterial shear stress and ischaemia resulting from removal of the vaso vasorum (Bryan and Angelini, 1994). During the first 24 hours, SVG undergo a period of ischaemia followed by reperfusion which triggers VSMC and EC cytotoxicity through the generation of reactive oxygen species such as superoxide (West et al., 2001). Subsequently, the graft is then targeted by an acute inflammatory response involving the recruitment of inflammatory cells (neutrophils, monocytes) and ongoing oxidative stress (Shi et al., 2001). Vessel remodeling, through the migration and increased proliferation of medial VSMC into the intima and subsequent deposition of ECM occurs during the first week post-implantation. This cascade results in the development of intimal

hyperplasia (Newby, 1997). This resultant thickened intima is highly susceptible to the infiltration of monocytes, that differentiate into macrophages and subsequently foam cells through the uptake of lipids. These foam cells contribute to accelerated atherosclerosis which results in diffuse, concentric, friable plaques with poorly developed or absent fibrous caps, susceptible to plaque rupture, thrombosis and graft occlusion (Schwartz et al., 1995, Virmani et al., 1988). The molecular mechanisms underlying the development of VGD will be discussed in further detail in section 1.4, with respect to molecular targets for vascular gene therapy. The development of intimal hyperplasia is summarized in Figure 1.1.

A degree of protection against these pathological processes can be obtained through the use of pharmacological therapies. Aggressive lipid-lowering with statins affords a reduction in atheroma formation and an associated improvement in vein graft survival (Shah et al., 2008). Antiplatelet and anticoagulant agents provide a reduction in acute thrombosis, but systemic anticoagulation carries a significant risk of bleeding (Yusuf et al., 2001). Despite advancements in pharmacotherapy SVG failure rate has not significantly improved over the last 20 years.

Some improvement in graft survival has been afforded by advancement in surgical technique. Vascular injury, caused by surgical preparation of the vein graft, is the principal cause of the endothelial injury and dysfunction that promotes platelet aggregation and thrombosis and the development of intimal thickening. Standard practice when harvesting saphenous veins is to strip the adventitial layer and distend the segment with normal saline to avoid vasospasm. A “no-touch” technique, where the graft is harvested with surrounding tissue intact and distention is avoided has been shown to improve patency rates in both preclinical (Tsui et al., 2002a) and clinical studies (Souza et al., 2002). The use of “off-pump” surgery and endoscopic saphenous vein harvesting do not lead to an improvement in SVG patency, with the endoscopic technique actually proving to be inferior to open harvesting in a clinical trial (Zenati et al., 2011).

1.3.2 In-stent Restenosis

As previously discussed, the field of PCI has grown rapidly over the past 36 years. The observation that success in expanding a narrowed arterial lumen with a balloon was limited by acute vessel closure secondary to coronary dissection in the short term and restenosis due to elastic recoil, negative remodelling and neointimal hyperplasia (resulting in

recurrent symptoms and a requirement for repeat intervention) in the long term led to the development of adjunctive devices.

Bare metal coronary stents (BMS), first introduced in 1986, became widely used by the mid-1990s (Al Suwaidi et al., 2000). Stent insertion allowed treatment of the acute complications of PCI such as coronary dissection/occlusion and reduced the requirement for emergency CABG. Again limitations quickly became evident such as the requirement for dual antiplatelet therapy to prevent early thrombotic occlusion and a reduced, but still highly significant (15-30%) rate of ISR due to increased neointimal hyperplasia induced by stent injury (Hoffmann et al., 1996, Elezi et al., 1998).

This neointimal growth is a multifactorial response to mechanical vessel injury at the time of PCI. The radial force required to dilate the delivery balloon and deploy a stent results in fracturing or tearing of atherosclerotic plaque, endothelium and the intimal and medial layers of the artery wall. This stent-induced vascular injury results in endothelial dysfunction and local apoptosis of medial VSMC which in turn acts as a trigger for a regenerative repair response (Isner et al., 1995). Comprising this repair pathway are a number of processes including thrombus deposition and leukocyte trafficking to the stent site (Mitra and Agrawal, 2006), release of growth factors (Raines, 2004) and eicosanoids (e.g. thromboxane A_2) (Jones et al., 1995), local thrombin production (Gallo et al., 1998) and release of vasoactive agents (e.g. angiotensin II) (Tanski et al., 2004) all of which are known to be mitogenic stimuli for VSMC. It has been shown that dysregulation of this repair response is primarily responsible for the excessive VSMC proliferation and subsequent formation of a stenotic lesion that encroaches upon the vessel lumen (Komatsu et al., 1998). Platelet-derived growth factor beta (PDGF-β) is one of the most potent VSMC mitogens and induces proliferation via the activation of biphasic extracellular signal-regulated kinase, phosphoinositide-3 kinase and Akt which results in downstream progression of the cell cycle through G_1/S phase (Millette et al., 2005). For a period of 18 months following stent implantation, neointimal lesion VSMC content is in the region of 66% (Farb et al., 2004). This subsequently reduces to ~12% due to an increase in extracellular matrix (ECM) deposition within the lesion (Farb et al., 2004). Under the stimulation of transforming growth factor-beta (TGF-β), VSMC produce a proteoglycan-rich ECM that contributes to neointimal lesion thickness in the later stages (Schmidt et al., 2006). Additionally, an inflammatory component mediated by infiltration of macrophages and other mediators plays a key role in neointimal progression (Welt and Rogers, 2002). Neointimal development leads to luminal narrowing, reduction in coronary blood flow and

resultant recurrent symptoms and requirement for repeat revascularisation (with repeat exposure to its associated risks) and in some cases thrombotic occlusion leading to MI. These described mechanisms underpinning the development of neointimal hyperplasia and its role in ISR have been well characterised in animal models of vessel injury and atherosclerosis correlated with human autopsy findings (Schwartz et al., 2004, Geary et al., 1996). The above molecular pathways are summarised in Figure 1.1.

Many studies have been performed with the aim of reducing ISR using locally or systemically delivered pharmaceutical agents but with limited success (Wilensky et al., 2000, Holmes et al., 2002). Ultimately significant progress was achieved with the development of the first drug-eluting stent (DES) delivering sirolimus via a synthetic non-erodible polymer [polyethylene-co-vinyl acetate (PEVA) and poly n-butyl methacrylate (PBMA)] coating (Moses et al., 2003, Sousa et al., 2001). Although the use of DES has produced a marked reduction in rates of ISR they continue to exhibit a risk of stent thrombosis which occurs due to a combination of incomplete endothelialisation of stent struts, intolerance/resistance to or poor compliance with antiplatelet therapy or an inflammatory response to the polymer coating (Virmani et al., 2004). Although reduced, in certain situations ISR can still occur with DES (Dangas et al., 2010).

Figure 1-1 Development of neointimal hyperplasia

Vascular injury leads to activation of endothelial cells and thrombotic adhesion of platelets and circulating leukocytes. The subsequent development of a cytokine-rich pro-inflammatory microenvironment leads to proliferation and migration of medial smooth muscle cells (SMC) into the neointima after degradation of the basement membrane, accompanied by increased synthesis and deposition of collagen-rich extracellular matrix. Superimposed atherosclerosis further increases neointimal size, resulting in significant vascular occlusion and recurrence of clinical symptoms and syndromes. Taken from McDonald *et al*, Cardiovasc Res. 2012 Mar 15;93(4):594-604.

1.4 Cardiovascular Gene Therapy

There are three main factors to consider in the assessment of cardiovascular gene delivery. First is the identification of a suitable molecular target and therapeutic gene (or genes) to be expressed. Second, is to combine the gene of interest with an efficient and safe delivery vector. Third, is to develop a suitable process or device to effectively deliver the vector to the target cells/tissue/organ (Zuckerbraun and Tzeng, 2002, Rosenzweig, 2003, Gaffney et al., 2007). A summary schematic of a gene therapy approach to VGD and ISR is shown in Figure 1.2.

1.4.1 Identification of Therapeutic Targets

Preclinical studies have allowed a greater understanding of the underlying mechanistic pathways in both VGD and ISR and have provided insight into potential pathophysiological targets for manipulation with gene therapy. To achieve this, these studies have mainly relied on available *in vivo* animal models with additional *in vitro* proof of concept experiments.

1.4.1.1 Vein Graft Disease

Gene delivery can be achieved *ex vivo* with exposure of the harvested graft or by intra- or peri-vascular delivery devices. Major models in use include a porcine model of SV or internal jugular vein (JV) anastomosed to the carotid artery (CA) and also a rabbit model of JV to CA. Some groups have chosen to use a hypercholesterolaemic rabbit to look at effects on atherosclerosis and late VGD. Rodent models have also been extensively used including mouse JV or inferior vena cava to carotid artery and rat epigastric vein to common femoral artery. Less commonly, canine, ovine and non-human primate models have been employed (Schachner et al., 2006).

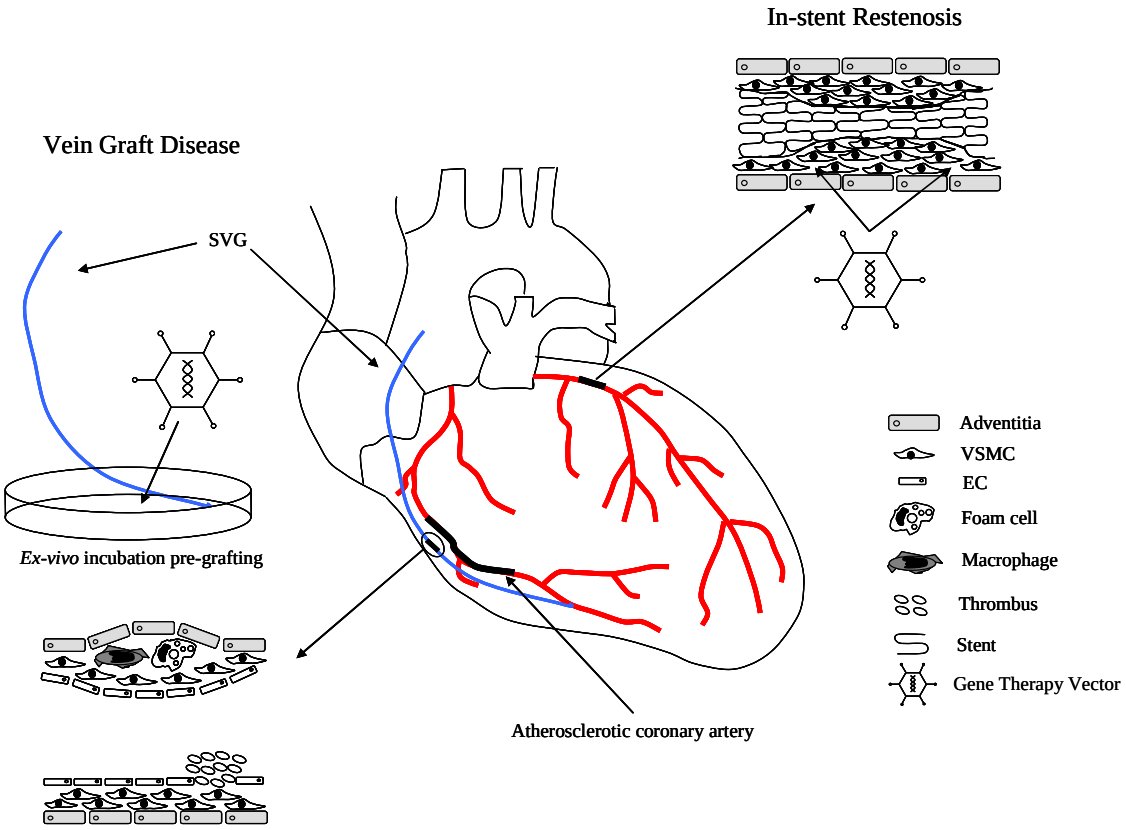

Figure 1-2 Vascular gene therapy for the prevention of ISR and VGD

During CABG surgery, saphenous veins are extracted from the patient's leg prior to being grafted proximally to the aorta and distally beyond the area of significant coronary disease producing a "bypass" for blood flow. This provides a useful window pre-grafting where the vein can be incubated ex vivo with a therapeutic vector targeting mechanisms underlying vein graft disease including thrombosis, intimal hyperplasia and accelerated atherosclerosis (left of diagram). Following percutaneous coronary intervention, (right of diagram) in-stent restenosis (ISR) can limit blood flow and result in clinically significant symptoms and acute coronary syndromes. Gene therapy vectors targeting the pathophysiological mechanisms underlying ISR could be utilised by local delivery devices post-stent placement or, more favourably, by "gene-eluting" stents which have the active agent deliverable from the stent surface. SVG – saphenous vein graft. VSMC – vascular smooth muscle cell. EC – endothelial cell.

1.4.1.2 In-stent Restenosis

Compared with VGD models, access to target tissue for *in viv*o ISR studies is more complex. Initial mechanistic studies relied on “balloon injury” models, typically rat carotid artery, rabbit iliac artery and aorta or porcine femoral or coronary arteries. Subsequently these models were adapted to allow delivery of gene therapy. Initially delivery experiments focused on a variety of different balloons and catheters to transfer genes of interest to the vessel wall following balloon injury or stent deployment. As clinical utility favors use of a stent model over balloon injury, interest has switched to “gene-eluting” platforms (Sharif et al., 2004). *In vivo* stent models tend to utilize larger animals such as rabbits, pigs and monkeys however a rat carotid stent (Gaffney et al., 2007) as well as complex mouse models (Chamberlain et al., 2010, Ali et al., 2007) are also in use.

1.4.1.3 Neointimal Hyperplasia

A large body of work exists targeting the cell cycle to prevent stent restenosis. The first studies focused on cytotoxic gene therapy, aiming for inhibition of DNA synthesis in the S phase to reduce VSMC proliferation. Adenoviral delivery of herpes simplex virus thymidine kinase (HSV-tk) which converts co-administered ganciclovir to a toxic metabolite resulted in a significant reduction of NIH in balloon injured porcine iliac (Ohno et al., 1994) and rat carotid arteries (Guzman et al., 1994, Chang et al., 1995c). This suppression of NIH was also seen in injured atherosclerotic arteries (hypercholesterolaemic rabbits) using HSV-tk/ganciclovir (Simari et al., 1996, Steg et al., 1997). Another group used adenovirus to deliver cytosine deaminase to balloon-injured rabbit femoral arteries. This converts co-administered parenteral 5-fluorocytosine to the cytotoxic 5-fluorouracil. Again, a significant reduction in NIH was achieved (Harrell et al., 1997).

A further approach to prevent proliferation of VSMCs in neointimal lesions is to inhibit regulators of the cell cycle. Retinoblastoma protein (Rb) is a regulator of DNA transcription. Its phosphorylation releases bound transcription factors such as DNA elongation factor (E2F) allowing progression through the cell cycle. Chang et al used adenovirus to deliver a mutant form of nonphosphorylatable Rb to injured rat carotid and porcine femoral arteries suppressing neointimal formation (Chang et al., 1995b). Other groups achieved a similar effect using adenoviral overexpression of human (full length and truncated) Rb (Smith et al., 1997b) and a related protein RB2/p130 (Claudio et al., 1999) in the rat carotid model.

p21, a cyclin-dependent kinase (cdk) inhibitor, is an important regulator of the cell cycle and a potent inhibitor of VSMC proliferation that arrests cells in G1 through inhibition of cdks and proliferating cell nuclear antigen (PCNA). Adenoviral delivery *in vivo* to rat and pig balloon-injury models reduced NIH effectively (Chang et al., 1995a, Yang et al., 1996, Ueno et al., 1997a, Luo et al., 1999). Mitomycin C is an antibiotic known to display antiproliferative effects in tumour cells. *In vitro* experiments showed that lower concentrations induced VSMC cell-cycle arrest in phase G2/M with associated increase in p21 expression. Perivascular delivery post balloon injury reduced NIH in rats (Granada et al., 2005). Overexpression of another cdk inhibitor, p27, using adenovirus in the rat reduced neointimal formation by inhibition of cdk2 function and cyclin A gene transcription (Chen et al., 1997). Adenoviral delivery of a "fusion gene" combining the active regions of p27 and p16 (another cell cycle inhibitor) to injured rabbit carotid and porcine coronary vessels significantly reduced intimal thickening (Tsui et al., 2001). Viral transfer of the tumor suppressor p53 has been shown to inhibit neointimal formation in rabbit and rat restenosis models (Yonemitsu et al., 1998, Scheinman et al., 1999).

Antisense decoy oligodesoxynucleotide (ODN) therapy targeting cell cycle regulators has been extensively studied and shown potential clinical utility. The selected targets all play important roles in VSMC progression from phase G0/G1 and resultant proliferation. Successful reduction in neointimal formation has been obtained in restenosis models by targeting c-myb (Simons et al., 1992), c-myc (Shi et al., 1994), cdc2/PCNA (Morishita et al., 1993), cdk2 (Morishita et al., 1994), and bcl-x (Pollman et al., 1998). Both non-viral and viral methods of gene delivery were used. Mithramycin, an inhibitor of c-myc, was shown to be effective at reducing NIH when administered to rats undergoing carotid artery balloon injury (Chen et al., 1994).

As noted earlier, an important step in the development of neointima is the VSMC response to circulating mitogens that through interactions with the cell surface stimulate the nucleus to promote proliferation. This is mediated by a system of signal transducers within the cell. DNA vectors designed to inhibit ras (an intracellular signaling protein) delivered to balloon-injured rat carotid arteries via a pluronic gel resulted in a suppression of IH formation (Indolfi et al., 1995). Adenoviral delivery of mutant H-ras (Ueno et al., 1997b) and a G-protein inhibitor (Iaccarino et al., 1999) *in vivo* were also effective in rats. Antisense ODNs to A-Raf and C-Raf kinases administered to *in vitro* rat SMCs resulted in reduced serum-induced proliferation suggesting that they may also be involved in intracellular signaling and may be useful therapeutic targets (Cioffi et al., 1997).

Other groups have chosen to target transcription factors involved in VSMC proliferation and migration. Antisense ODN to the p65 subunit of nuclear factor-κB (NF- κB) inhibited *in vitro* VSMC proliferation and *in vivo* neointimal formation in rats (Autieri et al., 1995). A decoy ODN to E2F has been shown to markedly reduce neointimal formation in balloon-injured rat carotids (Morishita et al., 1995). Overexpression of transcription factor gax using adenovirus was shown to induce G0/G1 cell cycle arrest in VSMCs *in vitro*. This appeared to be due to upregulation of p21. Viral delivery to rat carotid (Smith et al., 1997a) and rabbit iliac (Maillard et al., 1997) injury models significantly reduced NIH. GATA-6 is another transcription factor that, like gax, is downregulated in dedifferentiated compared to contractile VSMCs. Adenoviral overexpression in the rat model incurred a similar reduction in NIH (Mano et al., 1999). Using a different carotid artery ligation model of restenosis in the rat, perivascular antisense ODN targeting early growth response factor (Egr-1) was shown to suppress neointimal formation (Lowe et al., 2002). The same group also used adenovirus-mediated overexpression of an injury-inducible transcription factor Yin Yang 1 to reduce NIH in balloon-injured rat and collar injured rabbit carotids. The authors reported that this was mediated by effects on p21 and p53 (Santiago et al., 2007).

Cytokines and growth factors represent further attractive targets in the restenosis cascade. Local delivery of adenovirus expressing β-interferon reduced neointimal formation in injured porcine iliofemoral arteries (Stephan et al., 1997). Basic fibroblast growth factor (bFGF) and platelet derived growth factor (PDGF) are well recognized as being important in neointimal formation. Antisense bFGF delivered via adenovirus (Hanna et al., 1997), direct perivascular delivery of antisense ODN to PDGF-BB (Sirois et al., 1997) and adenoviral transfer of a PDGF-BB antagonist (Deguchi et al., 1999) all produced reduced intimal thickening in rats. Another group used this PDGF antagonist to reduce neointimal formation in a different way. They found that perivascular delivery to injured arteries reduced the migration of adventitial fibroblasts, another important component of post-angioplasty remodeling (Mallawaarachchi et al., 2006). Yang et al used polymeric nanoparticles as a novel method of gene delivery to target the inflammatory chemokine monocyte chemoattractant protein (MCP)-1. This method was effective at reducing NIH in both a rabbit restenosis and VGD model (Yang et al., 2008).

Induction of apoptosis in VSMCs programmed to proliferate following vascular injury is another potential therapeutic approach to restenosis. One group used adenovirus to overexpress Fas ligand (FasL), an inducer of apoptosis, in injured rat carotids. A significant reduction in NIH was obtained. They also looked at the issue of immunity to

adenovirus by showing that AdFasL maintained its ability to suppress neointimal formation despite immunological priming, whereas Ad delivery of p21 did not (Sata et al., 1998, Luo et al., 1999).

Reactive oxygen species such as superoxide (O_2^-), hydrogen peroxide (H_2O_2) and hydroxyl radicals (OH^-) have been shown to be potential mediators of VSMC proliferation. They act through direct cell damage, induction of proinflammatory gene expression and by forming peroxynitrite ($ONOO^-$) wihich catabolises NO (Griendling et al., 2000). Qian *et al* developed a Hantavirus glycoprotein pseudotyped lentivirus and used it to overexpress the antioxidant SOD3 in balloon injured rabbit CAs. A significant reduction in NIH resulted with no evidence of off-target organ transgene expression or significant toxicity evident (Qian et al., 2006). This retargeting approach to a lentiviral vector produced much more efficient VSMC and EC transduction than unmodified lentivirus or Ad5 and certainly holds potential going forward.

1.4.1.4 Extracellular Matrix Formation

Extracellular matrix (ECM) degradation is an important component of neointima formation as it allows SMC migration. It is controlled *in vivo* by matrix metalloproteinases (MMPs) and their endogenous inhibitors, tissue inhibitor of metalloproteinases (TIMPs) (Baker, 2002). MMPs have been found to be elevated in multiple models of vascular injury and there has been considerable interest in the potential therapeutic gain in overexpressing TIMPs. Inhibition of neointimal formation was first shown in *ex vivo* human saphenous vein grafts following adenoviral delivery of TIMP-1 (George et al., 1998b). *In vivo* experiments were performed by Eefting et al, who used a novel non-viral delivery model in mice. They injected the gene of interest into the calf muscles of APOE*3Leiden hypercholesterolaemic donor mice and administered electroporation. The following day caval veins were harvested and grafted to the carotid artery of another mouse. Administration of TIMP-1 combined with the amino terminal fragment (ATF) of urokinase (involved in plasminogen activator proteolyis) resulted in reduced vein graft thickening and increased lumenal area, with a more marked effect than TIMP-1 alone (Eefting et al., 2010a). In a further study they added bovine pancreas trypsin inhibitor (BPTI), a potent protease inhibitor, to the TIMP-1.ATF complex and demonstrated a further significant reduction in thickening (Eefting et al., 2010b).

Overexpression of TIMP-2 by Ad5-mediated gene transfer successfully inhibited neointimal formation in *in vitro* and *in vivo* rodent models (Cheng et al., 1998) and also in a human SVG *in vitro* culture model (George et al., 1998a). When applied to a porcine VGD model however, no effect was demonstrated (George et al., 2000). This is likely due to the inability of TIMP-2 to bind to ECM or promote apoptosis of SMC (unlike TIMP-3). TIMP-3 has been shown to reduce neointimal formation in pig grafts using *ex vivo* adenoviral gene delivery (George et al., 2000, George et al., 2011) and non-viral ultrasound enhanced plasmid delivery (Akowuah et al., 2005) approaches. This reduction in vein graft intimal thickening was sustained at 3 months of follow-up suggesting potential long-term efficacy despite only a single incubation with the Ad vector (George et al., 2011).

Overexpression of TIMP-3 in human VSMC *in vitro*, by a lentiviral vector, efficiently reduced migration and induced a pro-apoptotic effect (Dishart et al., 2003). This approach could have potential for clinical suppression of NIH but requires further assessment in *in-vivo* models. TIMP-3 is felt to be effective due to its ability to promote apoptosis in and inhibit migration of SMCs in addition to ECM degradation (Baker et al., 1998).

These pre-clinical results are encouraging and the manipulation of ECM formation merits further testing in human controlled trials to see if it is an effective approach for limiting ISR or VGD.

1.4.1.5 Endothelialisation

An intact endothelium is important for control of VSMC proliferation and prevention of thrombus deposition (Van Belle et al., 1997b). Denudation of the endothelium during balloon angioplasty or stent deployment is unavoidable and represents an important factor in the development of neointima. This has led to studies exploring the potential role of vascular endothelial growth factors (VEGFs), a group of endothelium specific mitogens in the control of re-endothelialization after vascular injury. Isner's group were the first to report accelerated endothelialization associated with reduced neointimal formation in balloon-injured rabbit femoral arteries receiving recombinant $VEGF_{165}$ (Asahara et al., 1996). The same group then investigated the ability of $rhVEGF_{165}$ to promote endothelialization of a stent and limit ISR in rabbits. A significant reduction in intimal growth within the stented vessels, as well as a reduction in mural thrombus, compared to controls was reported (Van Belle et al., 1997a). At a similar time Yla-Herttuala's group

reported suppressed intimal thickening via plasmid-mediated delivery of VEGF to the adventia of a rabbit carotid collar model. It should be noted that in this study the endothelium is intact as the injury stimulus is extravascular. They were able to abolish the protective effect of VEGF using co-administration of L-NG-Nitroarginine methyl ester, a nitric oxide (NO) synthase inhibitor. The authors reported that VEGF suppressed VSMC proliferation by a mechanism involving endothelial NO production (Laitinen et al., 1997). The same group subsequently reported similar reductions in intimal thickening using intravascular adenovirus-mediated delivery of VEGF-C and VEGF-D isoforms to balloon-denuded rabbit aortas (Hiltunen et al., 2000a, Rutanen et al., 2005).

Conversely, other investigators have suggested that VEGFs may promote the development of restenotic lesions. Ruef et al found increased expression of VEGF in the neointima and media of balloon-injured baboon aortas with *in vitro* evidence of VEGF overexpression induced by reactive oxygen species, suggesting a potential role in neointimal development (Ruef et al., 1997). Consistent with this another group reported increased expression of VEGF, fms-like tyrosine kinase (flt)-1 and PDGF in neointimal VSMCs, macrophages and peri-stent endothelial cells following stent delivery to porcine coronary arteries. They suggested that VEGF promoted ISR through angiogenic and chemotactic properties as well as through synergy with PDGF (Shibata et al., 2001). These differing results led the Kuopio group to return to the rabbit carotid collar model and use adenovirus to deliver the six members of the VEGF family (VEGF-A, -B, -C, -D, -E and PIGF) known at that point. These isoforms are grouped according to the VEGF receptor they bind to and each differs in both molecular weight and biological properties. Isoforms A and D have strong angiogenic effects whilst B is less angiogenic and C primarily produces lymphangiogenesis with some angiogenic effects (Bhardwaj et al., 2003, Cao et al., 1998, Rissanen et al., 2003). VEGF-A and PIGF however have been shown to influence VSMC migration (Ishida et al., 2001). Isoforms A, D and $D^{\Delta N \Delta C}$ (a proteolytically processed mature form of VEGF-D) all increased NIH (Bhardwaj et al., 2005). A significant increase in levels of MMP-2 and MMP-9 was noted in these arteries. The authors concluded that factors including endothelial integrity, site and method of gene delivery, dose and even model used could all influence the role of VEGFs. Evidence suggests that any positive effect in terms of NIH suppression using VEGFs would be produced by re-endothelialisation. In the rabbit collar model the endothelium is intact, a potential reason why a different effect may have been observed to the early rabbit stent models. In Bhardwaj's study, high concentrations of VEGFs were produced in the adventitia and this resulted in significant angiogenesis and VSMC proliferation and migration. There is

therefore the potential that lower concentrations of VEGF could have a different biological effect with implications for the mode of delivery used (e.g. non-viral vs. viral). Lastly, with a difference seen between stented rabbit and pig arteries, significant species differences may play a role. These are all important considerations for progression to clinical studies from pre-clinical studies.

Lastly, the role of nitric oxide in preventing NIH has been a focus of study. Viral liposome delivery of endothelial NOS (eNOS) significantly reduced intimal thickening in the rat restenosis model (von der Leyen et al., 1995). Retroviral seeding of SMC expressing eNOS into injured rat arteries was another approach that resulted in suppression of NIH (Chen et al., 1998). Adenoviral delivery of eNOS to rodent, rabbit and porcine models also significantly reduced NIH (Sato et al., 2000, Janssens et al., 1998, Varenne et al., 1998, Kullo et al., 1997). The relatively more efficient inducible form of NOS (iNOS) was shown to significantly reduce intimal thickening in balloon-injured rat carotid and porcine iliac vessels using much lower doses of adenovirus than normally required (Shears et al., 1998).

1.4.2 Development of Gene Therapy Vectors

The development of optimal gene delivery for the vasculature has been an area of intense research, however the optimal vector remains somewhat elusive. The optimal delivery vector for vascular tissue should be efficient in transducing target vascular cells with minimal transduction of non-target cells, have low toxicity and immunogenicity and allow sufficient longevity of transgene expression so that an adequate and sustained clinical response can be obtained (Baker, 2002). Several vectors have been used in both preclinical and clinical studies, each with pros and cons, and much effort has been expended trying to optimize efficiency and safety.

1.4.2.1 Non-viral Vectors

Non-viral vectors have been extensively used in early trials of cardiovascular gene therapy (Yla-Herttuala and Martin, 2000, Isner, 2002). Many different forms of non-viral gene transfer have been tested including “naked” plasmid DNA, cationic liposomes, DNA-polycation complexes, decoy or antisense oligodeoxynucleotides (ODNs) and small interfering RNAs (siRNAs). Although easy to produce, and with minimal biosafety risks, non-viral vectors generally offer a low efficiency of cell transduction and transient effect due to intracellular degradation (Kratlian and Hajjar, 2012). Some studies have used adjunctive methods to improve transduction efficiency such as ultrasound mediation (Akowuah et al., 2005) and electroporation (Eefting et al., 2010a). Non-viral gene transfer methods are not subjected to the same regulatory issues facing viral vectors, and this remains a significant advantage. However, even with adjunctive methods it is unlikely that clinically effective transduction can be achieved in the human vasculature using non-viral vectors, therefore, their role in VGD and ISR remains limited currently.

1.4.2.2 Retroviruses

The first experiments showing effective *in-vivo* gene transfer to the vascular system were published over 20 years ago (Nabel et al., 1989). These demonstrated effective delivery and seeding of endothelial cells expressing a retrovirally transduced reporter gene into porcine iliofemoral vessels and were the catalyst for the field of vascular gene therapy. Retroviruses are RNA viruses whose viral genome inserts into the host chromosome. This provides stable transgene expression but raises safety concerns regarding insertional mutagenesis. Several patients who received retroviral gene therapy in a clinical trial to treat

X-linked severe combined immunodeficiency syndrome developed evidence of malignancy (Hacein-Bey-Abina et al., 2003). Furthermore, retroviral vectors produce poor transduction of non-dividing cells limiting efficacy in the vasculature. In one small clinical trial a retroviral vector was used to express the low-density lipoprotein receptor in *ex-vivo* hepatocytes which were then autologously transplanted into patients with familial hypercholesterolaemia (Grossman et al., 1994). Some reductions in circulating low-density lipoprotein levels were observed, however, these were short lived due to unstable transgene expression. Retroviral vectors are therefore generally not utilised for CVD gene therapies and research interest has shifted to different vector systems.

1.4.2.3 Adenoviruses

Adenoviruses (Ad) are the most frequently used vector in gene therapy clinical trials (23.5% of all trials, http://www.abedia.com/wiley/vectors.php). Ads are non-enveloped double-stranded DNA viruses. There are 57 known human serotypes divided into seven species (A-G). They can, in general, be relatively easily engineered to be replication-deficient, produced in high viral titres at clinical grade and do not integrate into the host genome meaning insertional mutagenesis is not a concern. They efficiently transduce dividing and quiescent cells although their broad cell tropism means they carry a risk of off target effects. They are also highly immunogenic with transduced cells being eliminated reasonably rapidly through cytotoxic T-cell mediated clearance (Yang et al., 1994). This results in a transient *in-vivo* gene expression which peaks at 7-14 days and is generally lost by 28 days (Guzman et al., 1993, Kass-Eisler et al., 1993). Although this may be too short a duration for some therapeutic applications it may be suitable in certain scenarios, possibly including vein graft failure and the acute complications following PCI. The serotype Ad species C serotype 5 (Ad5) is the most commonly used in experimental and clinical studies. This virus is reliant on the coxsackie and adenovirus receptor (CAR), a 46 kDa transmembrane receptor, for cell transduction (Bergelson et al., 1997, Kirby et al., 2000). Further interaction of the Ad5 with cellular integrins mediates capsid internalization (Wickham et al., 1993). While CAR is abundantly expressed on hepatocytes, expression on endothelial cells (ECs) is low and is absent on vascular smooth muscle cells (VSMCs), reducing Ad5 transduction efficiency unless high doses of vectors are used. Moreover, clinical efficacy of Ad5-based vectors is hampered by pre-existing immunity (neutralizing antibodies) and high affinity interactions with cellular and non-cellular blood factors (Coughlan et al., 2010). These interactions result in rapid clearance of the virus from the circulation and sequestration in the liver, limiting *in-vivo* targeting efficiency and resulting

in dose-limiting hepatotoxicity, thus suppressing clinical potential to-date. Ad5 cellular uptake mechanisms are summarized in Figure 1.3.

In vitro experiments indicate that primary cell tethering involves the Ad5 fiber knob domain engaging CAR for all species besides B-species viruses, which use alternate receptors, predominately CD46 (Bergelson et al., 1997, Gaggar et al., 2003, Wang et al., 2010b). Subsequent studies by Roelvink *et al* defined a number of amino acids located on the fiber knob domain that can prevent CAR binding *in vitro* (Roelvink et al., 1998). However, the introduction of mutations within the fiber knob domain that abrogate CAR binding and infectivity *in vitro* has no discernible effect on Ad5 biodistribution and transduction profiles *in vivo* following intravenous delivery (Alemany and Curiel, 2001, Nicol et al., 2004). These results were somewhat surprising, since it had been widely assumed that a large component of the hepatic sequestration of Ad vectors was mediated by the high level of CAR-expression on hepatocytes. Subsequent findings by a number of independent groups have shown that direct interactions between the viral capsid of several adenoviral serotypes and various blood factors including complement-4 binding protein, Factor IX, VII, protein C, but predominantly Factor X, can mediate hepatocyte transduction via heparan sulphate proteoglycans (HSPGs) (Kalyuzhniy et al., 2008, Parker et al., 2006, Shashkova et al., 2008, Shayakhmetov et al., 2005a, Shayakhmetov et al., 2005b, Vigant et al., 2008, Waddington et al., 2008).

These interactions with circulating blood factors have proven to be important in explaining why adenoviral vectors have not yet reached their full potential as *in-vivo* gene delivery vectors. Aside from Factor X-mediated liver gene transfer, when delivered intravascularly Ad5 has been shown to bind directly to platelets. These resultant platelet-virus aggregates are then degraded by the reticuloendothelial system, further impairing transduction efficiency (Stone et al., 2007a). This, along with activation of the complement system contributes to the development of thrombocytopenia, commonly seen following *in-vivo* Ad5 administration (Kiang et al., 2006). Interactions with neutrophils and monocytes and hemagglutination following vector binding with erythrocytes (shown to express CAR in humans, but not mice) have all also been implicated in limiting the efficacy of *in-vivo* adenoviral gene delivery (Lyons et al., 2006, Seiradake et al., 2009).

To avoid these interactions and improve the clinical potential of Ad-based therapeutics, particularly with regard to vascular gene therapy, research effort has focused on vector "retargeting and detargeting" strategies. *Detargeting* involves modification or shielding of

the main viral capsid proteins (hexon, penton base and fiber) that mediate interactions with native cell receptors (CAR/integrins/HSPGs) and circulating coagulation factors. Modification of the fiber knob domain, to abrogate CAR binding, could also reduce the potential toxicity caused by hemagglutination following binding of erythrocytes (Carlisle et al., 2009). Alongside genetic modification, chemical alteration of the viral capsid is another approach to allow vector detargeting. This typically involves the use of polymers to "shield" the capsid from undesirable *in-vivo* interactions with native receptors, coagulation factors or neutralizing antibodies. By removing these interactions and thus preventing or significantly reducing unwanted viral sequestration and removal, a much improved bioavailability can be obtained and toxicity reduced. An Ad5 vector, coated with the multivalent polymer poly[N-(2-hydroxypropyl)methacrylamide], showed a 100-fold reduction in liver transduction following *iv* injection in mice (Green et al., 2004). This vector showed a 42% increase in circulating plasma levels, compared to an unmodified vector, at 30 minutes post injection confirming increased blood persistence. There was also evidence of reduced hepatotoxicity with circulating liver enzyme levels being comparable to untreated controls. A downside to the detargeting approach is that transduction efficiency can be reduced as the capsid may be shielded from the target tissue of interest also, a problem retargeting looks to address.

These previously described physiological barriers and counter strategies are particularly important in relation to the systemic delivery of adenoviral vectors. They merit consideration however, as virus "escape" into the circulation following catheter-mediated local delivery to the vasculature can be substantial (Hiltunen et al., 2000b). Of potentially greater importance, with regard to the local delivery approaches relevant to the prevention of VGD or ISR, are strategies focused on optimising the uptake of viral particles by target vascular cells. *Retargeting* focuses on genetic or chemical modification of the vector (e.g. through alteration of the fiber or use of monoclonal antibodies) to improve transduction of a specific tissue, such as VSMC or EC (Coughlan et al., 2010). This targeting of a specific tissue type would allow improved efficacy for a given dose of vector, reducing off-target effects and dose-related toxicity. Modification of an Ad5 vector to target vascular ECs using the fms-like tyrosine kinase receptor-1 promoter was shown to increase transduction levels 7-fold in *ex-vivo* rat aortas (Work et al., 2004b). This was associated with a significant reduction in liver transduction. Similarly, Reynolds *et al* used a bispecific antibody retargeting approach to create an Ad5 vector directed to angiotensin-converting enzyme (ACE) (Reynolds et al., 2000). ACE is preferentially expressed on pulmonary capillary EC, and this approach resulted in a 20-fold increase in lung vasculature

transduction with an 80% reduction in off-target liver transgene expression *in-vivo* in rats. By combining the insertion of the vascular-targeted peptide SIGYPLP with fiber mutations blocking CAR binding, Nicklin *et al* developed an Ad5 vector displaying efficient and selective tropism for vascular EC *in vitro* (Nicklin et al., 2001b). Particularly relevant to VGD and ISR, targeting peptides such as RGD4C, EYHHYNK and GETRAPL, when incorporated into the fiber HI loop, have been shown to enhance Ad5 uptake into VSMC *in vitro* and intact vein graft tissue *ex vivo* 10-100 fold (Work et al., 2004a, Nicklin et al., 2000). A further potential approach involves combining traditional retargeting strategies with rare serotype pseudotyping (Bradshaw and Baker, 2012). Rare and non-human serotype vectors, with low seroprevalence, often display increased transduction efficiency of cells that do not display CAR through their use of alternate receptors (Teigler et al., 2012). Ad5 vectors can be pseudotyped with fibres from these rare serotypes, thus conferring high-affinity binding to alternate receptors such as CD46 which is highly expressed on the surface of vascular cells (Larochelle et al., 2008). For example, significantly improved targeting of the cardiac vasculature *in vivo* in rats was obtained by insertion of a vascular-targeted peptide (DDTRHWG) into the HI loop of an Ad5 vector pseudotyped with a fiber protein from a rare serotype (Ad19p) virus (Nicol et al., 2009). In clinical cancer studies, “oncolytic” vectors modified to enhance tumour transduction have shown potential clinical effectiveness with up to 61% of patients exhibiting evidence of anti-tumour activity (Nokisalmi et al., 2010, Pesonen et al., 2010).

Optimal design of viral vectors must also include strategies to evade the host immune system. Activation of the innate immune response by either the vector or transgene, leads to an acute inflammatory response, resulting in a rapid release of various pro-inflammatory cytokines and chemokines (1-6 h post injection) which leads to a rapid clearance of the virus from the circulation. The clinical importance of the innate immune response to adenoviral vectors was reinforced by the unfortunate death of a young patient in a non-vascular clinical trial (Raper et al., 2003). These initial events prime the adaptive immune response, which mediates a more selective (specific) response (Liu and Muruve, 2003, Worgall et al., 1997). It is estimated that up to 97% of the population have neutralizing antibodies against type C Ads, including the commonly studied Ad5, contributing to a lack of efficacy thus far in clinical trials (Nayak and Herzog, 2010). Specifically, high dose intravascular administration of Ad vectors has been found to induce high levels of cytokines, tumour necrosis factor α, interleukin-6, interleukin-12, interferon γ, interleukin-1 and the chemokines, regulated on activation, normal T cell expressed and secreted (RANTES) and monocyte chemoattractant protein-1 (Di Paolo et al., 2009, Hartman et al.,

2008, Alba et al., 2010). The precise origins of these pro-inflammatory mediators *in vivo* in humans is not known, however numerous studies have implicated macrophages (particularly liver Kupffer cells) and endothelial cells (Thaci et al., 2011). Certainly in rodent models, Kupffer cells have been shown to rapidly scavenge and remove Ad5 vectors from the circulation (Lieber et al., 1997) and contribute to the inflammatory response through release of cytokines and chemokines (Shayakhmetov et al., 2005b). This inflammatory response results in increased vector related toxicity and contributes to the extensive liver pathology that has been observed with the administration of Ad5 *in-vivo* (Lieber et al., 1997). Again, retargeting and detargeting approaches are being employed to circumvent these issues with immune responses (Nayak and Herzog, 2010, Ahi et al., 2011, Thaci et al., 2011).

A further approach to the issue of vector-induced immunogenicity has been the development of third-generation or "helper-dependent" Ad vectors. These Ads have had all viral genes removed from the genome resulting in minimal immunogenicity and prolonged transgene expression (Jozkowicz and Dulak, 2005). This removal of viral coding sequences prevents the production of viral proteins in infected cells. Therefore significant cytotoxic T-cell reactions do not occur and an adaptive immune response is not promoted (Vetrini and Ng, 2010). Helper-dependent Ad have been shown to be effective in gene transfer to the liver (Oka et al., 2001) and the vasculature (Wen et al., 2004, Flynn et al., 2010, Jiang et al., 2011) but remain untested in human clinical trials.

Taken together, the above interactions highlight the difficulty of using first generation adenoviruses in the setting of in-stent restenosis, where the virus is exposed to blood cells and serum proteins even if attached to a stent or delivered locally to the site of stent deployment. However, first generation Ad vectors do have proven efficacy in the setting of pre-clinical vein graft disease (George et al., 2011) where the virus is incubated with the target tissue (saphenous vein segment) for a period of 30 minutes *ex vivo* before flushing and engraftment. This opportunity to treat the target tissue *ex vivo* and wash out any unbound virus reduces the potential of adverse events and off-target effects.

Figure 1-3 Cellular uptake mechanisms of Adenovirus serotype 5 viral vectors

Following local delivery, the cellular uptake of the Ad5 vector is mediated by a primary interaction of the fiber knob with cell surface coxsackie and adenovirus receptors (CAR). Ensuing engagement of membrane α_v integrins by the Ad5 penton base protein leads to endocytosis of the viral particle. Following intravascular delivery, liver sequestration and hepatocyte uptake of Ad5 virons results from a nanomolar-affinity interaction between circulating coagulation factor X and viral hexon proteins. Immune cell-mediated phagocytosis also occurs following both local and systemic delivery. Taken from Bradshaw and Baker, Vascular Pharmacology. 2013; 58(3):174-181.

1.4.2.4 Adeno-associated Viruses

Adeno-associated viruses (AAVs) are from the family of parvoviruses and have broad ranging potential as gene therapy vectors (Tilemann et al., 2012). They are not associated with pathology in humans (Flotte and Carter, 1995). Their main advantages are a lack of toxicity *in vivo* and the ability to infect non-dividing cells (Monahan and Samulski, 2000). They display excellent long-term gene expression without excessive insertion into the host genome (Heistad, 2006). Disadvantages include limited space for cloning (<5kb) and also the potential for humoral immune response related to vector-specific antibodies and pre-existing immunity in the population (Monahan and Samulski, 2000). Multiple serotypes exist (11 identified to-date) with differences in organ biodistribution and expression profiles (Karvinen and Yla-Herttuala, 2010). Serotypes 1/6/8 and 9, for example, have been shown to mediate high transduction efficiency in cardiomyocytes (Pacak et al., 2006, Palomeque et al., 2007, Gregorevic et al., 2004).

Strong cardiomyocyte transduction in animal models using recombinant AAV vectors led to their use in the first human clinical trial of congestive heart failure, the CUPID trial (Jessup et al., 2011). Using a single intracoronary injection of an AAV1 vector expressing sarcoplasmic reticulum Ca2+-ATPase, the investigators showed that the treatment was safe and well-tolerated. This phase IIa trial also suggested treatment efficacy with improvements in clinical variables, heart failure biomarkers and imaging parameters in the high dose group. These results are encouraging and follow-up trials are awaited with interest.

With respect to vascular gene therapy, focus has been on improving the relatively poor gene transfer to ECs and VSMCs by AAV. Modification of AAV-2 serotype with the peptide SIGYPLP resulted in enhanced transduction of ECs (Nicklin et al., 2001a). As in Ad5, modification of AAV-2 with EYH increases selective transduction of VSMCs (Work et al., 2004a). *In vivo* delivery to rat aortas suggested that serotypes 1 and 5 may be superior to AAV2 for gene therapy to ECs and VSMCs (Chen et al., 2005). Insertion of an integrin-targeting peptide into the capsid of AAV1 enhanced transduction of human umbilical vein ECs and human saphenous vein ECs (Stachler and Bartlett, 2006). Further work has shown that serotypes 7 and 8 are very poor at transducing ECs due to sensitivity to proteasomal activity (Denby et al., 2005). While modifying capsid proteins is one approach to targeting the vasculature, pseudotyping AAV2 transgene cassettes in

combination with capsids from other serotypes may allow more efficient vectors to be produced (Lebherz et al., 2004). Finally, *in vivo* biopanning using phage display libraries can be used to identify peptides allowing modification of AAV2 and specific targeting to a particular vascular bed (Work et al., 2006).

While AAV vectors now appear to hold the most potential for cardiac gene transfer, it is as yet unclear whether retargeted vectors will be able to provide sufficient transduction efficiency in vascular cells to make them the vector of choice for clinical trials in ISR or VGD. If this, as well as circulating neutralizing antibodies, can be overcome however, their improved safety profile compared with Ad vectors certainly would make them attractive options.

1.4.2.5 Lentiviruses

Lentiviruses are from the retrovirus family and vectors can be derived from human immunodeficiency virus-1 (HIV-1). Unlike other retroviruses these vectors can transduce quiescent and dividing cells and are efficient at transfecting vascular cells as well as offering long-lasting transgene expression and low immunogenicity. Effective transduction of both ECs and VSMCs by a third-generation vesicular stomatis virus glycoprotein (VSV-G) pseudotyped lentiviral system was achieved *in vitro* (Dishart et al., 2003). Cefai *et al* displayed superior transduction of human coronary ECs and VSMCs *in vitro* and rat carotid arteries *in vivo* using a similar lentiviral vector, compared with Ad5 (Cefai et al., 2005). Effective therapeutic vascular gene transfer using lentiviral vectors has been shown in pre-clinical models of VGD and ISR hinting at their potential for use in the clinical settings and these will be discussed later (Qian et al., 2006, Dishart et al., 2003).

Disadvantages of the lentivirus include difficulty in producing vectors at titres suitable for clinical testing and also the potential for insertional mutagenesis, although clinical data to-date with HIV-based lentiviruses has not shown vector-induced mutagenesis.

To combat this theoretical risk of oncogenesis non-integrating lentiviral vectors have been developed. These have been shown to provide stable transgene expression *in vitro* (Vargas et al., 2004) and *in vivo* (Yanez-Munoz et al., 2006, Philippe et al., 2006). The incorporation of a mutated integrase gene allows the viral genome to remain episomal resulting in transient gene expression in dividing cells and long-term gene expression in quiescent cells. The potential of these vectors for vascular gene therapy remains to be

explored and depends on their ability to sustain transgene expression for a sufficient length of time, a critical factor when considering vasculoproliferative disorders.

1.4.3 Delivery of a Therapeutic Vector to the Target Tissue

1.4.3.1 Stent Models

With the expanding and widespread clinical use of stents the development of true preclinical ISR, rather than vessel injury, models has become of increasing relevance. The use of a coated stent to deliver gene therapy is attractive as it is site-specific, potentially helping to avoid the distal spread of therapeutic agents and viral vectors, thus minimising systemic toxic effects. The first progress in the field of gene therapy to prevent ISR was made by Dichek et al, who successfully seeded stainless steel stents with sheep endothelial cells that had been modified to express markers using retroviral gene transfer (Dichek et al., 1989). Much later the efficiency of this process was improved using endothelial cells expressing VEGF (Koren et al., 2006). The first successful use of a "gene-eluting stent" *in-vivo* was performed in a pig coronary angioplasty model. The stent polymer eluted plasmid DNA for green fluorescent protein (GFP) allowing detection of arterial transfection (Klugherz et al., 2000). The same group also reported successful transfection of porcine coronary arteries using a collagen coated stent with covalently-bonded monoclonal antibodies to adenovirus. This allowed binding of adenoviral particles to the stent allowing a degree of controlled site-specific local release (Klugherz et al., 2002). Another group used a different approach, seeding SMC harvested from porcine jugular veins onto fibronectin-coated stents, transducing them to express GFP and inserting them into porcine coronary arteries (Panetta et al., 2002).

Adding to the controversy surrounding the role of VEGF, Walter et al inserted human VEGF-2 plasmid coated polymer stents into the iliac arteries of normocholesterolemic and hypercholesterolemic rabbits. In their study VEGF accelerated endothelialisation compared to control stents (98% vs. 79% endothelial cover at 10 days) and also inhibited NIH as assessed by intravascular ultrasound with an 87% increase in lumenal cross-sectional area and a 54% reduction in cross-sectional narrowing (Walter et al., 2004). In a similar study however, it had been reported that VEGF-eluting stents tested in a rabbit model significantly reduced thrombosis but did not promote endothelialization or reduce NIH (Swanson et al., 2003). It is possible that differences in stent types used (polymer coated with plasmid DNA vs. radiolabelled absorption of VEGF) could explain the differences seen in these rabbit iliac studies.

Unsurprisingly, with such noted similarities in their pathologies, many targets thought to have potential in vein graft failure have also been tested in stent models. Johnson et al coated stents with an adenovirus expressing TIMP-3 and applied them to porcine coronary arteries (Johnson et al., 2005). A 40% reduction in neointimal area compared to bare metal stents at 28 days was conferred. Stents coated with a biocompatible polymer expressing 7ND-MCP-1 reduced neointimal area in rabbits (~60% reduction at 28 days post-stenting) and monkeys (25-30% reduction out to 6 months) (Egashira et al., 2007). This provides evidence that long-term clinical benefit may be achievable with the use of a gene-eluting stent.

The above studies have all used polymer coated stents to elute the genes of therapeutic interest, much in the same way that DES deliver their active compound. This polymer component however has been shown to cause a local inflammatory response which contributes to delayed healing and late complications such as thrombosis (van der Giessen et al., 1996, Garg and Serruys, 2010a). Levy's group in Philadelphia has therefore investigated alternatives to polymer coatings. The first method tested was gene delivery via bisphosphonate binding to the metallic stent surface. Following *in vitro* optimization they delivered Ad expressing iNOS to a rat carotid stenting model achieving a significant reduction in NIH (Fishbein et al., 2006). Furthermore, to enable better control of vector stability and delivery kinetics they developed a synthetic complex allowing adenoviral particles to reversibly bind to the stent through a hydrolysable ester bond. Again this method achieved a reduction in NIH using AdiNOS in the rat (Fishbein et al., 2008).

Not all attempts to manipulate growth factors have been successful. Adenoviral delivery of an antagonist to TGF-β, shown to be effective in reducing ECM formation in the VGD models, did not reduce stent-induced NIH in porcine coronaries despite a small decrease in ECM deposition. It did appear to increase vascular inflammation leading the authors to conclude that it may have a detrimental effect on lesion progression (Chung et al., 2010).

These encouraging results in some pre-clinical models of restenosis have been demonstrated despite overall low percentages (typically <10%) of transduced VSMC at the site of treatment (Sharif et al., 2006).

1.4.3.2 Thrombosis

Although rare, stent thrombosis remains an important complication of PCI. Best assessments of risk with DES suggest an ongoing incidence of 0.3-0.6% per annum with a mortality rate of 10-30% (Garg and Serruys, 2010b). A significant reduction in risk has been obtained by improvement in stent technology and methods of assessing adequate deployment as well as the use of prolonged dual anti-platelet therapy. Incomplete stent strut endothelialisation and polymer-induced inflammation have been heavily implicated in the aetiology of stent thrombosis. The potential of a gene-eluting stent to accelerate endothelialisation, thereby reducing the potential for thrombosis as well as inhibiting NIH makes it an intuitive competitor for the DES. To maximise effect however, delivery would have to be as biocompatible as possible, both from the perspective of any polymer used to bind the vector to the stent, as well as the delivery vector/transgene of choice. As previously discussed in the vectors section, local inflammation is a recognised issue. Although new-generation vectors may markedly reduce this in terms of systemic effects once delivered to the patient, even low-grade local inflammation may be enough to contribute to stent thrombosis. This approach requires testing in suitable preclinical models to identify safety and efficacy before moving on to randomized, controlled clinical trials with long term follow-up.

1.5 Human Perspectives and Clinical Trials

1.5.1 In-stent Restenosis

Other research began to investigate the safety and feasibility of intracoronary gene transfer in humans. A small initial study involved 15 patients undergoing percutaneous transluminal coronary angioplasty (PTCA) plus/minus stent delivery for stable symptomatic coronary artery disease. VEGF plasmid/liposome was delivered using a perfusion-infusion catheter post balloon angioplasty but prior to stent insertion. Of the 10 patients randomised to receive VEGF, 9 received stents. The procedure was well tolerated with no significant adverse effects. However, no difference in restenosis rates were seen at follow-up angiography 6-months later. (Laitinen et al., 2000).

This was followed by a Phase II study called the Kuopio Angiogenesis Trial (KAT) (Hedman et al., 2003). This was a randomized, placebo-controlled, double-blind study involving 103 patients with symptomatic coronary disease. Gene-delivery was performed using a perfusion-infusion catheter post-balloon angioplasty but pre-stenting. This time, however, patients were randomised to VEGF-expressing adenovirus ($2x10^{10}$ plaque forming units, n=37), double the dose of VEGF plasmid/liposome used in the previous study (n=28) or Ringer's lactate as control (n=38). Other than transient pyrexia in those receiving VEGF, and an elevation in serum C-reactive protein (CRP, a marker of inflammation) in those receiving Ad, no significant adverse effects attributable to gene therapy were identified. However, at 6-months follow-up using quantitative angiography there was no difference in minimal lumen diameter or percent of diameter stenosis (markers of ISR) between the groups. The authors did note an improvement in myocardial perfusion in the Ad-VEGF treated group and hypothesized that this may be due to VEGF-induced angiogenesis.

At a similar time to the KAT, the ITALICS trial was performed at the Thoraxcenter in Rotterdam (Kutryk et al., 2002). In this randomized, placebo-controlled, double-blind study 85 patients with symptomatic single-vessel coronary disease were assigned to placebo (physiologic saline) or antisense-ODN to the cell-cycle regulator c-myc. The gene therapy was delivered using a local-delivery catheter post-stent insertion. The dose of antisense ODN delivered was based on results from pre-clinical studies and pre-existing safety/efficacy data. Follow-up was again at 6 months but in this trial intravascular ultrasound (IVUS) as well as quantitative angiography was used. When results were

analysed no differences were seen in the rates of restenosis, degree of lumenal loss or clinical outcomes.

A few other small clinical ISR studies exist including AVAIL (antisense oligomer to c-myc post-PCI, n=44) (Kipshidze et al., 2007) and REGENT I Extension (iNOS lipoplex post-PCI, n=30) (von der Leyen et al., 2011). Both these studies suggested safety and feasibility of their compounds but were not powered for efficacy. ISR clinical trials are summarised in Table 1.2.

The KAT trial aside, all studies to-date looking at gene therapy in ISR have used non-viral transduction methods. As histological analysis cannot be performed in these live patients, we are only able to hypothesise about the degree of cell transduction obtained. Based on what is known from pre-clinical studies, and with the perfusion catheters used, it is highly unlikely that these non-viral methods were able to provide sufficient cell transduction during delivery and following restoration of coronary blood flow, to provide a measureable clinical reduction in ISR. The study numbers were also low as these were Phase I studies, not designed to adequately assess efficacy. They did, however, show safety and feasibility of their approach. The KAT, the only Phase II trial, used an Adenoviral vector expressing VEGF in the hope of promoting re-endothelialisation. Again, through rigorous assessment this study showed that the process was safe, and well tolerated. Reasons for lack of efficacy likely include, poor transduction efficiency in VSMCs with first-generation Ad vectors (due to lack of CAR expression), presence of neutralising antibodies to the vector and interaction with circulating blood components (e.g. Factor X) as previously discussed.

Ongoing developments in viral vector design and biocompatible polymers that can stably and measurable express a vector/gene of interest provide an avenue of continued hope for the role of gene therapy in preventing ISR. Although stent technology and associated clinical outcomes continue to improve (Bangalore et al., 2012), preclinical studies suggest that gene therapy with a safe and stable vector expressing endogenous proteins that restore normal vessel physiology can be an intuitive alternative to cytotoxic drugs for the prevention of stent complications.

Table 1-2 Clinical trials of gene therapy for the prevention of in-stent restenosis

Trial	N	Gene	Effect on ISR markers	Adverse Effects	Ref
(Unnamed)	15	VEGF P/L	Nil	Transient rise in CRP	Laitinen et al, 2000
Kuopio Angiogenesis Trial (KAT)	103	VEGF-AdV VEGF P/L	No effect on ISR Increase in myocardial perfusion in VEGF-AdV group	Pyrexia CRP rise	Hedman et al, 2003
ITALICS	85	c-myc antisense-ODN	Nil	Nil	Kutryk et al, 2002
AVAIL	44	c-myc antisense oligomer	Nil	Nil	Kipshidze et al, 2007
REGENT I Extension	30	iNOS lipoplex	Nil	Nil	von der Leyen et al, 2011

1.6 MicroRNA

As previously discussed, vascular injury following stent delivery results in endothelial dysfunction, activation of inflammatory pathways, the proliferation and migration of smooth muscle cells, accumulation of neointima and the development of in-stent restenosis (Clowes et al., 1986, Gordon et al., 1993, Karas et al., 1992, Mitra and Agrawal, 2006, Jukema et al., 2012). The role of microRNAs (miRs) in the maintenance of EC and VSMC homeostasis and also the negative remodelling following vascular injury is an area of intense research. Increasingly, there is significant interest in the potential therapeutic role that modulation of these novel regulatory molecules may play.

1.6.1 MicroRNA Processing and Function

MiRs are a group of highly conserved, short (20-25 nucleotides), non-coding ribonucleic acids that act to control gene expression at a posttranscriptional level (Lee et al., 1993, Bartel, 2004). This is accomplished through translational repression or mRNA decay (Zhao and Srivastava, 2007) and has lead to them being described as an “efficient molecular switch” (Abdellatif, 2012). They have been shown to be increasingly important in the modulation of various biological functions in animals, plants and unicellular eukaryotes, are tissue specific and developmentally regulated. Their abnormal expression is known to cause developemental abnormalities and be important in the process of human disease, importantly cancer and disorders of the cardiovascular system (Thum et al., 2007, Calin and Croce, 2006, Kloosterman and Plasterk, 2006).

1.6.1.1 MicroRNA Biogenesis

The mechanism for the formation of miRs is evolutionarily conserved. MiRs are encoded in the genome and initial transcription by the enzyme RNA Polymerase II creates long precursor molecules called primary microRNAs (pri-miRs) that are hundreds to thousands of nucleotides long and 5′-capped and 3′-polyadenylated in a similar way to messenger RNA (mRNA) (Lee et al., 2004). Within the nucleus, endonucleolytic cleavage of these pri-miRs occurs, mediated by the RNase III enzyme Drosha, producing ~60-100 nucleotide hairpin-shaped precursor microRNAs (pre-miRs) (Lee et al., 2003, Gregory et al., 2004, Denli et al., 2004). Under the control of the nuclear export factor exportin 5 these pre-miRs are exported out of the nucleus and into the cytoplasm (Bohnsack et al., 2004). Within the cytoplasm a second cleavage occurs, this time mediate by the RNase III enzyme

Dicer, forming a mature miRNA/miRNA* double-stranded duplex ~22 nucleotides in length (Lee et al., 2002). This duplex miRNA undergoes incorporation into the RNA-induced silencing complex (RISC) with the mature strand remaining part of the RISC while the passenger miRNA* strand is thought to be degraded, although this is increasingly less clear (Flynt and Lai, 2008). The combination of RISC with mature miRNA then allows association predominately with the 3′-untranslated (3′UTR) region of target genes (Flynt and Lai, 2008). It acts as a negative regulator of gene expression by promoting mRNA degradation and/or translational inhibition depending on the degree of complementarity involved (Valencia-Sanchez et al., 2006). The imperfect nature of the miR:mRNA base pairing means that a single miR can target tens to hundreds of distinct mRNAs (Baek et al., 2008, Friedman et al., 2009, Selbach et al., 2008). The biogenesis pathway is summarised in Figure 1.4.

Although typically it is through association with the 3′UTR that a miR regulates gene expression, it has been shown that base pairing can occur with the 5′UTR, exons or regulatory DNA sequences (Valencia-Sanchez et al., 2006). Complementarity between nucleotides 2 through 8 of the miRNA ("seed" region) appears to be essential for 3′UTR binding. This is why miRs with high sequence homology and identical seed regions are grouped into "families" likely to target similar sets of mRNAs (Lewis et al., 2005). To-date over a thousand miRs have been identified within the human genome, each of which could potentially target hundreds of mRNAs showing the depth of gene regulation involved (van Rooij, 2011, van Rooij, 2012). The majority of 3′UTRs contain binding sites for many individual miRs giving potential for cooperative interactions. Additional complexity is introduced with the potential for positive or negative feedback loops as the targets of many miRs can in turn modulate the expression of additional miRs. Furthermore, genetically clustered and cotranscribed miRs can often be expressed at different levels due to sequence-specific posttranscriptional maturation (Davis et al., 2008).

Thus miRs elicit critical changes in expression of genes important in many biological functions including developmental timing, cell differentiation, proliferation and death and also metabolism (Bushati and Cohen, 2007, Grosshans and Filipowicz, 2008, Kloosterman and Plasterk, 2006).

Figure 1-4 The microRNA biogenesis pathway

MicroRNAs (miRs) are encoded in the genome and transcribed by RNA Pol II to form long pri-miRNAs that are 5′-capped and 3′-polyadenylated. In the nucleus, pri-miRNAs undergo initial cropping by Drosha to form ~60–100 nt pre-miRNAs. These pre-miRNAs are exported to the cytoplasm by exportin V and undergo second cropping by Dicer to form the mature miRNA/miRNA* duplex. The miRNA/miRNA* duplex is subsequently separated and only the ~22 nt miRNA strand stably associates with the RISC complex. The RISC complex, loaded with miRNA, then directs translational inhibition or promotes degradation of mRNAs containing partially complementary miRNA recognition sequences often located in the 3′UTR. Taken from Davis-Dusenbery and Hata, J Biochem. 2010;148:381–392.

1.6.2 MicroRNAs in the vasculature

Several miRs have been shown to play key roles in establishing smooth muscle and endothelial cell fate and tissue homeostasis (Small and Olson, 2011, McDonald et al., 2011b). For example, a number of groups have shown in mice that SMC-specific deficiency in Dicer results in embryonic lethality due to defective blood vessel formation (Albinsson et al., 2011, Albinsson et al., 2010, Pan et al., 2011). Multiple miRs are now implicated in the complex regulation of the phenotype of cell types involved in vascular remodelling and the development of ISR (Figure 1.5). A list of miRs currently implicated in ISR and their proposed biological effects is given in Table 1.3.

Table 1-3 MicroRNAs implicated in the vessel response to injury and development of neointimal hyperplasia

MicroRNA	Regulation after vascular injury	Target Cell	Biological effect	Molecular Targets	Key References
miR-21	Upregulation	VSMC	Pro-synthetic *or* pro-contractile	PTEN, PDCD4	Ji et al, 2007;
miR-133a	Downregulation	VSMC	Pro-contractile	SP-1, Moesin	Torella et al, 2011;
miR-143	Downregulation	VSMC	Pro-contractile	ELK1, FRA1	Fujita et al, 2008; Horita et al, 2011; Cordes et al, 2009; Hergenreider, et al 2012;
miR-145	Downregulation	VSMC	Pro-contractile	ACE, KLF4/5, CALMK, MRTF	Cheng et al, 2009; Boettger et al, 2009; Xin et al, 2009; Davis-Dusenbery et al, 2011;
miR-146a	Upregulation	VSMC	Pro-synthetic	KLF4	Sun et al, 2011;
miR-221	Upregulation	VSMC	Pro-synthetic	C-KIT, p27, p57	Davis et al, 2009; Liu et al, 2011;
miR-92a	Unclear	EC	Cell adhesion and interactions	ITG-α	Bonauer et al, 2009; Iaconetti et al, 2012;
miR-126	Unclear	EC	Cell adhesion, interactions, proliferation, migration, apoptosis and EPC recruitment	VCAM-1, KLF2/VEGFR-2, CXCL12	Kuhnert et al, 2008; Wang et al, 2008;
miR-155	Upregulated	Macrophages ?VSMC	Inflammatory response, unclear role in ISR	Yet to be established	Nazari-Jahantigh et al, 2012; Wei et al, 2013;

Figure 1-5 MicroRNAs implicated in the vessel injury response, vascular remodelling, and angiogenesis

Purple and green shaded regions indicate microRNAs with “pro-angiogenic” and “anti-angiogenic” characteristics, respectively. SMCs – smooth muscle cells; ECs – endothelial cells; ACE - angiotensin converting enzyme; SuFu - suppressor of fused (Fus-1); Shh - sonic hedgehog; HGS - Hepatocyte growth factor-regulated tyrosine kinase substrate; IGF - insulin-like growth factor; ITGA5 - integrin-α5; PIK3R2 - phosphoinositol-3 kinase regulatory subunit 2 (p85β); PTEN - phosphatase and tensin homolog; Spred-1 - sprouty-related EVH domain-containing protein-1; VCAM-1 - vascular cell adhesion molecule. Taken from Small et al, Circulation. 2010 March 2; 121(8): 1022–1032

1.6.2.1 Complex role of miR-21 in restenosis

MiR-21 is transcribed from within the coding gene TMEM49 (vacuole membrane protein) on chromosome 17 and was first described as an "oncomir" due to its high level of expression in various cancers (Bonci, 2010). It has subsequently been shown to play an important role in the proliferation of VSMC in response to injury (Ji et al., 2007), atherosclerosis (Raitoharju et al., 2011), EC response to shear stress (Kuehbacher et al., 2007, Voellenkle et al., 2012, Weber et al., 2010b, Zhou et al., 2011) and the development of pulmonary hypertension (Parikh et al., 2012, Yang et al., 2012).

Initial work by Ji *et al*, showed that following balloon injury expression levels of miR-21 in rat carotid arteries were increased over 5-fold (Ji et al., 2007). Downregulation of miR-21 using a locally delivered antisense oligonucleotide significantly reduced neointima formation in the same model. This was supported by the observation that the expression level of miR-21 was significantly higher in dedifferentiated (serum cultured) rat VSMC than freshly isolated differentiated cells. The authors demonstrated that their observed effects on neointima formation were mediated, at least in part, by suppression of phosphatase and tensin homolog and upregulation of Bcl-2 (Ji et al., 2007). PTEN is a tumour suppressor gene with known antiproliferative effects while Bcl-2 is an oncogene involved in promoting cell survival and proliferation (Matsumoto and Hwang, 2007). In a separate study, Yang *et al*, validated that miR-21 expression was upregulated in dedifferentiated VSMC and in ligated mouse carotid arteries (Yang et al., 2011). In their *in-vitro* model, the authors showed that miR-21 overexpression repressed the transcription factor specificity protein-1 leading to the down-regulation of cystathionine gamma-lyase, an enzyme responsible for producing hydrogen sulphide. This reduced H_2S production contributes to stimulation of VSMC proliferation and reduced expression of differentiation markers.

Conversely, however, when pulmonary VSMCs were differentiated using TGF-β and BMPs the expression of miR-21 was increased at a post-transcriptional level through the promotion of pri-miR-21 processing by SMAD protein binding to Drosha (Davis et al., 2008). In this model the authors argued that miR-21 downregulates PDCD4 which acts as a negative regulator of VSMC contractile genes.

1.6.2.2 MiR-143/145

The VSMC associated miR-143/miR-145 gene cluster has been implicated as being important in the regulation of SMC contractility and stress response following vascular injury (Small et al., 2010, O'Sullivan et al., 2011, Robinson and Baker, 2012). These highly conserved, bicistronic miRs lie close together on chromosome 5 (Boettger et al., 2009, Cordes et al., 2009, Quintavalle et al., 2010). Both miRs are highly expressed in VSMC, particularly within the walls of the aorta and coronary arteries in mice (Boettger et al., 2009, Cheng et al., 2009, Cordes et al., 2009, Elia et al., 2009, Xin et al., 2009).

Initial *in-vitro* studies revealed that overexpression of miR-145 increases the expression of VSMC differentiation marker genes including smooth muscle alpha-actin (α-SMA), calponin and myosin heavy chain (MHC) (Cheng et al., 2009). When treated with miR-145 the VSMC maintained a differentiated phenotype, while miR-145 inhibitor decreased levels of these differentiation marker genes (Cheng et al., 2009). Further work supported these findings with evidence of a strong regulatory effect exerted by miR-143/145 on VSMC differentiation (Cordes et al., 2009). Studies performed using *in-vivo* rodent models and utilising miR-143/miR-145 knockout animals demonstrated a reduction in miR-143 and miR-145 expression following acute vascular injury (Xin et al., 2009, Elia et al., 2009, Boettger et al., 2009, Quintavalle et al., 2010). Furthermore, inhibition of neointimal development and promotion of contractile gene expression was achieved by miR-143 and miR-145 abrogation. Although miR-143/145 KO mice were found to be hypotensive, with abnormally thin vessel walls due to a reduction in contractile VSMC, and a concurrent increase in synthetic VSMCs they were however viable and fertile with no gross macroscopic defects (Boettger et al., 2009, Xin et al., 2009, Elia et al., 2009). This suggested that although fundamental for VSMC homeostasis *in-vivo* these miRs were not essential for development.

The effects of the miR-143/miR-145 cluster on VSMC phenotype are mediated by diverse and complex signalling pathways. These are summarised in Figure 1.6. Serum response factor (SRF) and its cofactors myocardin and myocardin-related transcription factors (MRTFs) are key regulators in VSMC differentiation and de-differentiation (Miano et al., 2007). SRF acts by binding to CArG-box elements within the promoter regions of contractile genes thus promoting gene expression (Miano et al., 2007). This results in

Figure 1-6 Summary of signalling pathways mediating effects of miR-143/miR-145 cluster on VSMC phenotype

KLF2 binds to putative KLF2-binding site in the miR-143/miR-145 promoter activating transcription, which leads to enrichment of miR-143/miR-145 in microvesicles that can be transferred to vascular smooth muscle cells. TGF-β promotes the binding of SMADs to SBEs in the miR-143/miR-145 and myocardin promoters, thereby increasing miR-143/miR-145 transcription both directly and indirectly through increasing myocardin–SRF interaction. TGF-β also promotes myocardin expression through a p38MAPK-dependent pathway. BMP4 promotes nuclear translocation of MRTF-A increasing its interaction with SRF and promotes miR-143/miR-145 transcription through the CArG box upstream of miR-143/miR-145 cluster. Jag-1 promotes the nuclear translocation of the NotchICD which forms a complex with CBF1 activating a CBF1-binding site in the upstream of miR-143/miR-145. MiR-143 reduces miR-21 availability by negative regulation of FRA-1 leading to increase in PTEN expression. Mature miR-143 and miR-145 promote the expression of SMC marker genes and negatively regulate the transcription factors which promote proliferation and migration. BMP4 - bone morphogenetic protein 4; KLF2 - Kruppel-like factor 2; NotchICD - Notch intracellular domain; SBEs - SMAD-binding elements; SMC - smooth muscle cell; SRF - serum response factor. Taken from Robinson and Baker, Curr Opin Lipidol. 2012 Oct;23(5):405-11.

activation of miR-143 and miR-145 transcription (Cordes et al., 2009, Xin et al., 2009). Further contribution is provided by signalling molecules TGF-β and BMP4 which promote miR-143 and miR-145 expression by acting on myocardin (via both p38MAPK and SMAD-dependant pathways) and MRTF-A respectively (Davis-Dusenbery et al., 2011, Long and Miano, 2011). It is worth noting that these signalling pathways act independently. A further, SRF-independent pathway has been suggested to play a part in miR-143 and miR-145 regulation. In *in-vitro* studies the activation and nuclear translocation of Notch receptors by Jagged-1 led to an increase in miR-143/miR-145 expression via formation of a complex with the transcriptional regulator CBF1 and subsequent SMAD-mediated CArG activation. (Boucher et al., 2011). This activation of Notch receptors promotes expression of VSMC contractile proteins calponin, α-SMA and SM22α, which are found to be reduced in cells treated with inhibitors of both miR-143 and miR-145 (Boucher et al., 2011).

As previously discussed, miR-21 has been implicated in the regulation of VSMC proliferation through suppression of the anti-proliferative PTEN. SRF promotion of miR-143 expression has been shown to indirectly decrease transcription of miR-21 via negative regulation of FRA-1, the net effect being an increase in PTEN levels (Fujita et al., 2008, Horita et al., 2011).

Mature miR-143 and miR-145 act by promoting the expression of VSMC marker genes and negative regulation of transcription factors involved in VSMC proliferation and migration (Rangrez et al., 2011). Krueppel-like factor 4 (KLF4) and Krueppel-like factor 5 (KLF5) have been shown to be key targets of miR-145 (Cordes et al., 2009, Xin et al., 2009, Cheng et al., 2009). These factors act as transcriptional repressors, playing a role in the regulation of VSMC phenotype by inhibiting proliferation and downregulating VSMC differentiation marker genes, notably α-SMA and myocardin (Garvey et al., 2010). Adenovirus-mediated restoration of miR-145 levels in rat carotid arteries subjected to balloon-injury was shown to reduce neointima formation through the promotion of myocardin secondary to KLF5 suppression (Cheng et al., 2009).

Lastly, both miR-143 and miR-145 have been implicated in the paracrine regulation of VSMC phenotype by endothelial cells (Hergenreider et al., 2012). Krueppel-like factor 2 (KLF2) is a transcription factor induced in endothelial cells following injury. When overexpressed in *in-vitro* ECs it results in enrichment of extracellular microvesicles with miR-143 and miR-145. When placed in co-culture with VSMCs these microvesicles

induced downregulation of KLF4 and also Ets LiKe gene 1 (ELK1) a transcription factor targeted by miR-143 with an inhibitory effect on VSMC differentiation (Hergenreider et al., 2012, Cordes et al., 2009). Additionally, injection of microvesicles taken from KLF2-transduced ECs into fat fed ApoE$^{-/-}$ mice, reduced atherosclerotoic lesion area (Hergenreider et al., 2012). Taken together these results support functional miR transfer between ECs and VSMCs highlighting the importance of endothelial integrity in maintaining a contractile VSMC phenotype and the role miRs may play in this.

These important *in-vitro* and *in-vivo* studies show that miR-143 and miR-145 expression is potentially very important in the regulation of VSMC phenotype through manipulation of key regulators of contractile gene expression. These models argue that miR-143/miR-145 mediated downregulation of proproloferative and promigratory targerts is a key "molecular switch" in the maintenance of a contractile differentiated VSMC phenotype *in-vivo* that is lost following acute vascular injury and therefore may be a key modifiable factor in the development of ISR.

1.6.2.3 MiR-221

miR-221, a non-VSMC specific antiangiogenic oncomir, positively regulates SMC proliferation through modulation of cell-cycle regulators (McDonald et al., 2011b, Small et al., 2010). It is upregulated in VSMCs in response to platelet-derived growth factor beta (PDGF-β) and acts to reduce SMC differentiation by down-regulation of cKit and increase SMC proliferation by suppressing p27Kip1 and p57Kip2, two important cell cycle suppressors (Davis, Hilyard et al. 2009; Liu, Cheng et al. 2009; Liu, Cheng et al. 2011). In similarity to miR-21, Ji *et al* showed a moderate elevation in miR-221 expression following carotid artery angioplasty in the rat (Ji et al., 2007).

1.6.2.4 miR-92a and miR-126

Although not directly associated with VSMCs these EC-specific miRs have been shown to be important in the maintenance of vascular integrity and angiogenesis (McDonald et al., 2011b, Small et al., 2010). Depletion of miR-126 in mice results in vascular leakage and haemorrhage with impaired wound healing and angiogenesis (Kuhnert et al., 2008, Wang et al., 2008).

miR-92a is also EC-enriched and shown to be upregulated following ischaemia with an apparent role as a negative regulator of vessel growth (Bonauer et al., 2009). In murine models of limb ischaemia and myocardial infarction, antagomir knockdown resulted in improved tissue recovery secondary to accelerated vessel growth (Bonauer et al., 2009). Using an *in-vivo* model of rat carotid artery balloon injury and stent delivery, Iaconetti *et al,* achieved enhanced re-endothelialization and reduced neointimal formation using an antagomir to miR-92a (Iaconetti et al., 2012). This lead the authors to hypothesise that inhibition of miR-92a held potential as a therapeutic strategy to improve endothelial regeneration and reduce restenosis after vascular injury (Iaconetti et al., 2012).

1.6.2.5 miR-146a

Following balloon angioplasty to the carotid artery in rats it was shown that levels of miR-146 were elevated 2-3 fold (Ji et al., 2007). This was not further investigated in this study, however. Subsequently, it was shown that miR-146a may have a role in promoting VSMC proliferation *in-vitro* and vascular neointimal hyperplasia *in-vivo* (Sun et al., 2011). This effect appeared to be mediated by a negative feedback loop involving miR-146a and KLF4. Interestingly, KLF4 was shown to compete with KLF5 to bind to and regulate the miR-146a promoter resulting in opposing effects on miR-146a expression levels (decreasing and increasing respectively). By using both gain- and loss-of-function approaches, the authors found that miR-146a promoted VSMC proliferation *in-vitro*. Also, transfection of antisense miR-146a oligonucleotide into balloon-injured rat carotid arteries markedly decreased neointimal hyperplasia (Sun et al., 2011).

The miR-146a/b family has also been implicated in the negative regulation of inflammation both in human peripheral blood monocytes following exposure to atherogenic stimuli (Chen et al., 2009) and also alveolar epithelial cells following exposure to cytokines (Perry et al., 2008). Overexpression of miR-146a was shown to reduce inflammatory cytokine release from dendritic cells subjected to an acute stimulus while antagomirs to miR-146a increased inflammatory cytokine secretion (Chen et al., 2011). In a chronic model of pulmonary inflammation miR-146a levels were reduced (Sato et al., 2010). This potential role in the inflammatory response for a miR also implicated in neointimal formation is interesting in view of the previously discussed role for inflammation in both ISR and stent thrombosis.

1.6.2.6 miR-155

miR-155 has been shown to be expressed in VSMC, ECs and primarily activated macrophages as well as being upregulated in human atherosclerotic lesions (O'Connell et al., 2007, Raitoharju et al., 2011). In the setting of ISR the recruitment of monocytes to the vessel wall and subsequent differentiation into macrophages is a crucial component of the inflammatory response that occurs during vessel remodelling (Wei et al., 2013). During this proinflammatory activation of macrophages, miR-155 has been shown to be upregulated and seen to exert a variety of pro and anti-inflammatory effects (Nazari-Jahantigh et al., 2012). Whether it has any role in the development of restenotic lesions or regulation of VSMC phenotype awaits clarification.

1.6.2.7 miR-133a

miR-133a is abundantly expressed within the heart and plays a key role in both development and maintenance of cardiac and skeletal muscle (Care et al., 2007, Liu and Olson, 2010). There is also some evidence that it may play a role in VSMC phenotypic switch. In an elegant study, Torella *et al* revealed that miR-133a is negatively regulated by PDGF (an established promoter of VSMC proliferation) and that overexpression *in-vitro* inhibits both VSMC proliferation and Sp-1 (a promoter of KLF4) induction by PDGF (Torella et al., 2011). Using an *in-vivo* model of balloon-injured rat carotid arteries the authors showed that adenoviral overexpression of miR-133a resulted in reduced cell proliferation markers, prevented upregulation of Sp-1 and provided a significant (~60%) reduction in neointimal formation (Torella et al., 2011). Lastly they showed that silencing of miR-133a using an antagomir approach augmented intimal lesion formation suggesting that this pathway merits further investigation with regards to prevention of ISR.

1.7 HYPOTHESIS

The principle aim of this thesis was to investigate the potential of vascular gene therapy in the prevention of coronary in-stent restenosis, as an alternative to the current pharmacological approach of DES. It was hypothesized that a viral vector could be used to effectively deliver a therapeutic transgene to a porcine model of coronary in-stent restenosis and achieve a measurable reduction in neointimal hyperplasia. This hypothesis was tested *in vivo* using both a local delivery catheter approach and also the coating of a metal stent with viral vector using a thermoreversible gel.

It is becomingly increasing evident that microRNAs play an important regulatory role in the maintenance of VSMC and EC homeostasis and that their dysregulation may play an important role in the development of neointimal hyperplasia and hold potential for therapeutic modulation. This remains to be tested in a large animal model of coronary stent delivery. It was hypothesized that miRs implicated in the development and regulation of NIH in rodent models of vascular injury would show similar patterns of dynamic dysregulation in a porcine model of coronary stent delivery. This hypothesis was tested using an *in vitro* model of VSMC proliferation and migration, and qRT-PCR and *in-situ* hybridization approaches in the *in vivo* porcine model.

Lastly, miRs have been shown to be present, stably, in the circulation leading to interest in their potential use as cardiovascular biomarkers. This was assessed in the serum of patients undergoing CABG surgery. RNA was extracted from serum and dynamic expression of miRs determined using qRT-PCR. Correlation analysis was performed with classical biomarkers and perioperative factors. It was hypothesized that a panel of cardiovascular miRs showing measurable and consistent changes in expression would be identified allowing future correlation with clinical outcome in patients undergoing CABG surgery.

2 Materials & Methods

2.1 CHEMICALS

All chemicals, unless otherwise stated, were obtained from Sigma-Aldrich (Poole, UK). All cell-culture reagents were obtained from Gibco (Paisley, UK) unless otherwise stated. Dulbecco's calcium and magnesium free phosphate buffered saline (PBS) was obtained from Lonza (Basal, Switzerland).

2.2 CELL LINES

Primary Human Coronary Artery Smooth Muscle Cells (HCASMC) were obtained from PromoCell GmbH (Heidelberg, Germany).

Surplus human saphenous vein tissue was obtained with informed consent from patients undergoing CABG at the Golden Jubilee National Hospital. All procedures had local ethical approval (Research Ethical Committee number: 06/S0703/110 and 12/NW/0036) and experimental procedures conformed to the principles outlined in the Declaration of Helsinki. Primary Human Saphenous Vein Smooth Muscle Cells (HSVSMC) were isolated from medial explants.

For adenovirus production, human embryonic kidney cell line (293) cells were used. The transformed human embryonic kidney cell line (293T) was used for lentiviral production.

2.3 TISSUE AND CELL CULTURE

All experiments involving tissue and cell culture were performed under sterile conditions using biological safety class II vertical laminar flow cabinets. Cell lines were grown as a monolayer in 150 cm^2 tissue culture flasks, maintained in appropriate cell culture media and incubated at 37^oC in a 5% CO_2 atmosphere incubator. Both HCASMC and HSVSMC were maintained in Smooth Muscle Cell Growth Medium 2 (PromoCell, Heidelberg, Germany) supplemented with 15% foetal bovine serum (PAA laboratories, UK), 2 mM L-Glutamine (Invitrogen, Paisley, UK), 50 μg/ml penicillin (Invitrogen) and 50 μg/ml streptomycin (Invitrogen).

For the 293 and 293T cell-lines, cells were maintained in Dulbecco's Modified Eagle's Medium (DMEM) supplemented with 10% foetal bovine serum, 2 mM L-Glutamine, 50 μg/ml penicillin and 50 μg/ml streptomycin

Both *in-vitro* and *ex-vivo* experiments involving viral vectors were performed in a dedicated tissue culture laboratory with separate incubators to avoid cross-contamination.

2.3.1 Preparation of smooth muscle cells from saphenous vein explants

Saphenous vein explants were transported to the institute in culture medium immediately following completion of surgery by courier. Vessel segments were transferred to a large glass petridish containing sylgard and culture medium. The vein segment was cut longitudinally and pinned out using 25G hypodermic needles. The EC layer was removed by gently rubbing the inner vessel wall with the plunger from a 2ml syringe. Using a disposable blade the medial layer was scored at 1cm intervals. Using forceps the VSMC layer was then removed in squares and transferred to a separate petridish containing culture media. Following recovery, all VSMC layers were placed onto the white ceramic disc of a chopping table and chopped into approx. $1mm^2$ segments. These segments were washed from the chopping disc into a 50ml falcon tube containing culture medium. After allowing the VSMC segments to sink to the bottom of the tube, the culture media was siphoned off using a 20ml syringe with quill. The remaining cells were washed twice with 20ml of culture medium then transferred to a $25cm^2$ tissue culture flask with 5ml of fresh culture medium. Cells were incubated overnight then managed as per maintenance of established cell lines.

2.3.2 Maintenance of established cell lines

Cells were grown as a monolayer and the media replaced every 3-4 days. Cells were routinely passaged at approximately 80% confluence to prevent overgrowth and loss of surface contact in culture flasks. To passage, cells were washed twice in PBS and incubated with 5ml of trypsin-ethylenediamine tetra-acetic acid (trypsin-EDTA, Gibco, Paisley, UK) for 5 min at 37^oC or until the majority of cells had detached from the flask surface. The action of trypsin-EDTA was then attenuated by the addition of 5ml culture medium. Cells were pelleted by centrifugation at 1500rpm for 5 min. Media/trypsin-EDTA were poured off and the pellet re-suspended in culture media for further passaging or

plating. Before plating cells were counted using a haemocytometer (Hausser Scientific, PA, USA) to allow calculation of the required seeding density.

2.3.3 Cryopreservation and recovery of cultured cell lines

For cryopreservation cells were harvested as described in section 2.3.2. The cell pellet from an ~80% confluent 150cm^2 culture flask was re-suspended in 2ml culture media supplemented with 10% dimethyl sulphoxide (DMSO). This cell suspension was then aliquoted into a cryopreservation vial and cooled at a constant -1^{o}C/min to -80^{o}C using isopropanol. Frozen vials were then transferred to liquid nitrogen tanks and stored at -196^{o}C indefinitely.

Cell recovery was achieved by rapid thawing in a water bath at 37^{o}C, followed by drop-wise addition of 10ml pre-warmed culture media to allow for slow change in the osmotic gradient. Cells were pelleted by 1500rpm centrifugation for 5 min and resuspended in culture media before addition to a 25cm^2 culture flask. Following overnight incubation, the medium was changed and cells were managed as per section 2.3.2.

2.4 PRODUCTION OF VIRAL VECTORS

2.4.1 Recombinant Ad5 production

The AdGFP vector used in Chapter 3 is a recombinant Adenovirus species C serotype 5 expressing enhanced GFP from the CMV promoter. This RAd-eGFP vector was previously generated in-house as described by Dishart *et al* and Nicklin *et al* (Nicklin et al., 2001b, Dishart et al., 2003).

High titre stocks were obtained through large-scale expansion of a plaque pure stock of AdGFP in 293 cells. Cells were grown to approximately 80% confluence as previously described and then infected with virus using a multiplicity of infection of 1 plaque forming unit (pfu) per cell. After 3 to 4 days incubation the cytopathic effect of the virus caused the cells to detach from the base of the culture flask and the media/cell suspension was collected. Cell harvesting was achieved by centrifugation at 2000rpm for 10min. The supernatant was removed and the cell pellet re-suspended in 8ml PBS. To remove excess non-viral proteins, 8ml Arklone P (trichlorotrifluoroethane) was added and mixed by gentle inversion. This mixture was then centrifuged at 3000rpm for 15 min. The top aqueous layer containing the virus was removed and stored at -80^{o}C.

2.4.2 AdGFP purification through caesium chloride gradient

Sterilised (70% Ethanol/30% sterile dH_2O) clear 14ml ultracentrifuge tubes (Beckman Coulter, London, UK) were placed in a tube rack. A caesium chloride (CsCl) gradient was produced by adding, in order, 2.5ml of CsCl with a concentration of 1.45g/ml, 3ml of CsCl with a concentration of 1.32g/ml and 2ml of 40% glycerol. Care was taken not to mix the layers. The crude Ad5 stock from section 2.4.1 was then added and the remaining volume of the tube filled with PBS.

Tubes were transferred to a Sorvall Discovery 90 rotor container (Sorvall Centrifuges, Connecticut, USA) and ultracentrifuged at 25,000rpm for 1.5h at 4^{o}C with maximum acceleration and zero deceleration. This creates a distinct opalescent band of virus situated between the two CsCl layers. The virus is removed by carefully piercing the tube below the band using a 21G needle and removing the band in the minimal volume possible while taking care not to disrupt the other layers. This extracted virus is carefully added to a SlideA-Lyzer dialysis cassette with a molecular weight cut-off of 10,000 Da (Perbio

Science, Cramlington, UK). The virus was dialysed against 0.01M Tris pH 8.0 and 0.001M EDTA (2L volume), first for 2h then overnight in fresh buffer and finally for a further 2h in fresh buffer supplemented with 10% (v/v) glycerol. Purified virus was finally extracted from the cassette and stored at -80^{o}C in 50µl aliquots.

2.4.3 Virus titration by end-point dilution assay

Initially 293 cells were seeded to approximately 60% confluence in a 96-well plate. Ten-fold serial dilutions of virus stock were made using PBS and then added to the plate with ten replicates of each titration (100µl/well). Following overnight incubation the media was replaced with 200µl culture medium. Media was replaced every 2-3 days and wells were examined for cytopathic effects using a microscope. The development of cytopathic effects represented infection and once apparent the well was "marked-off" and the media no longer replaced. Following 8 days incubation the number of wells containing plaques were counted. From these, the titre of the adenoviral stocks in pfu/ml can be obtained as follows:

- The proportionate difference = (%positive above 50% - 50%) / (%positive above 50% - % positive below 50%)

- Log ID_{50} (infectivity dose) = log dilution above 50% + (proportionate distance x -1) x dilution factor

- $TCID_{50}$ (tissue culture infectivity dose) = $1/ID_{50}$

- $TCID_{50}$/100µl x dilution factor (10) = $TCID_{50}$/mL

- 1 $TCID_{50}$/ml = 0.7pfu

2.4.4 Quantification of virus particles

Virus particle titre was determined using the protein content of the virus stock. This was established using the Micro bicinchoninic (BCA) Protein Assay Kit (Thermo Fisher Scientific, IL, USA). Bovine serum albumin (BSA) standards at concentrations of 200, 40, 20, 10, 5, 2.5, 1 and 0.5µg/ml were prepared in PBS and 150µl of each pipetted in duplicate into a 96-well plate. A blank control of 150µl PBS was used. 1, 3 and 5µl of the virus stock was then added in duplicate and made up to 150µl with PBS. A working

reagent comprising 25 parts reagent A, 24 parts reagent B and 1 part reagent C from the kit was then prepared and 150µl added to each well. The plate was then covered and incubated at 37^{oC} for 2h. After cooling to room temperature levels of absorbance at 570nm are measured using a plate reader. The values from the blank control (background) are subtracted from all samples and standards. A standard curve was then created allowing the amount of protein present in each virus to be established. The virus particle number can then be calculated using the formula 1µg protein = $1x10^9$ viral particles.

2.4.5 Recombinant Ad5 expressing LacZ

All experiments in this thesis involving AdLacZ used a high grade commercial virus RAd 35 (Baylor College of Medicine Vector Development Lab, TX, USA). This Ad5 vector expresses β-galactosidase, a hydrolase enzyme coded by the gene lacZ from its CMV promoter. All virus used (*in-vitro* and *in-vivo)* came from the same production batch and had titres of $4.7x10^{12}$ particles/ml and $2.5x10^{11}$ pfu/ml.

2.4.6 Production of Lentivirus expressing eGFP

The second-generation lentiviral vector expressing enhanced GFP used in Chapter 3 had previously been developed in-house (Dishart et al., 2003). It utilises a lentiviral construct plasmid encoding the marker gene, enhanced green fluorescent protein (eGFP), (pHR'SIN-cPPT-SFFV-eGFP-WPRE) under the control of the spleen focus forming virus (SFFV) promoter, pseudotyped with the vesicular stomatitis virus glycoprotein (VSV-g) expressed by the pMD.G2 plasmid and the lentivirus packaging plasmid containing the wildtype integrase gene (pCMV delta R8.74) (Demaison et al., 2002, Yanez-Munoz et al., 2006).

This vector was produced in low passage 293T cells by standard triple transfection with a vector construct, envelope plasmid (pVSV-G) and packaging plasmid (Int 8.74). Low passage 293T cells were seeded ($12x10^6$/T175 flask) and incubated overnight at 37^oC. Into 5ml of OptiMEM (Life Technologies, CA, USA), 50µg of vector construct, 17.5µg of envelope plasmid and 32.5µg of packaging plasmid were added and then sterilized by filtration through a 0.22µm filter. In a separate tube, 1µl of 10mM polyethylenimine (PEI) was added to 5ml OptiMEM and sterile filtered. Both solutions were then combined and incubated at room temperature for 20min. After washing with OptiMEM I reduced serum media with Glutamax I to remove any remaining serum, 10ml of the transfection mixture was added to each T175 flask and incubated at 37^oC for 4 hours in 5% CO_2. The

transfection mixture was then removed and replaced with 20ml fresh DMEM media and returned to the incubator. The virus-containing supernatant was collected 48h later and filtered in a 0.22μm filter unit before being stored at 4^{o}C. Fresh DMEM (10ml) was added to the flasks and the final supernatant collected, filtered and added to the first batch at 72h.

2.4.7 Concentration of Lentivirus

A Beckman Optima L-80 XP Ultracentrifuge (Beckman Coulter Ltd, Buckinghamshire, UK) was pre-cooled to 4^{o}C using the vacuum setting. Six 15ml ultra-clear centrifuge tubes were sterilised in ethanol and 15ml of the previously collected and sterilised virus-containing supernatant was added to each. The tubes were loaded into the SW-32.1 Ti rotor system (Beckman Coulter) and ultracentrifuged at 23,000rpm for 2h at 4^{o}C (maximum acceleration, 9 deceleration). The supernatant was immediately removed, care being taken not to disturb the virus pellet and the tubes were refilled with remaining supernatant from section 2.4.6 and re-centrifuged until complete. After the final spin and removal of supernatant, 100μl of OptiMEM I reduced serum media with Glutamax I, was added to each tube followed by 20min incubation on ice. After thorough pipette resuspension the tubes were pooled and then aliquoted (5μl aliquots) before freezing at -80^{o}C.

2.4.8 Calculation of virus titre in 293T cells

Firstly, a 12-well plate was seeded with a 293T cells at a density of 5x10^{4}cells/well and incubated for 24h. The media was then removed and replaced with 1ml fresh supplemented DMEM (section 2.3). Serial dilutions (10^{-2}-10^{-6}) of the freeze-thawed lentiviral stock (section 2.4.7) were prepared and added to each well in duplicate (30μl then 100 μl). Following a 72h incubation (37^{o}C, 5%CO_2) the media was removed, each well was washed with 500μl PBS and then cells were re-suspended in 200μl PBS following detachment with a rubber policeman.

Viral DNA was extracted from each sample using the QIAamp DNA Mini Kit (QIAGEN, Limburg, Netherlands) according to manufacturer's instructions. The detached cells were transferred to 1.5ml eppendorfs and then 20μl of the broad-spectrum serine protease proteinase K added. This step is required to break down contaminating proteins present during DNA extraction. Next, 200μl of lysis buffer AL (SDS, EDTA and guanidine hydrochloride) was added before incubation at 56^{o}C for 10 min to achieve optimal lysis. SDS acts as a detergent, disrupting the phospholipids present in cell membranes and EDTA

chelates divalent metals (mainly magnesium and calcium) resulting in cell membrane destabilisation and cell lysis while also inhibiting DNases. Guanidine hydrochloride is a chaotropic salt that facilitates the absorption of DNA (but not RNA, polysaccharides, proteins etc) onto the silica-gel membrane in the QIAamp spin columns.

Following the addition of 200µl of 100% ethanol each sample was mixed by pulse-vortex and loaded into a QIAamp spin column. Samples were centrifuged at 6000g for 1 min to allow DNA absorption onto the silica membrane. Flow-through was discarded. The spin column was then washed with 500µl buffer AW1 (guanidine hydrochloride and ethanol) and centrifuged at 6000 x g for 1 min. A second wash of buffer AW2 (ethanol) was added and the samples centrifuged at 20,000 x g for 3 min to dry the columns. Each spin column was then placed in a clean eppendorf and 50µl sterile water added. After leaving to rest for 5 min to allow DNA elution, a final centrifuge step (6000 x g for 1min) was performed. This final elution step was repeated to maximise DNA yield and then DNA levels were measured using spectrophotometric quantification.

The lentivirus genomic copy number was quantifed in this extracted DNA by Taqman^{TM} quantitative real time PCR (qRT-PCR) according to a published protocol for late reverse transcriptase amplicon (Butler et al., 2001). Standard curves for quantification were prepared by serial dilution of lentiviral vector construct plasmid DNA of known concentrations (determined as above), based upon the following equations:

- Molecular weight of plasmid DNA = (Base Pairs) x (330 Daltons x 2 nucleotides / base pairs) = Daltons (1 Dalton = 1 g/mole)

- Weight of one copy of plasmid DNA (molecule) = g/mole / Avagadro's constant (molecules/mole) = g/molecule

- Copy number of plasmid DNA per ml of plasmid stock = Concentration of plasmid (g/ml) / g/molecule

- Initial dilution for top standard = Copy number of plasmid/ml / top standard required

- Convert to microlitres = 1000 / initial dilution factor for top standard = µl of plasmid DNA stock required for 1ml

For each 12.5µl reaction of the 384-well TaqMan™ plate the following was added:

- 6.25µl of 2 x TaqMan universal mastermix (contains AmpliTaq Gold DNA polymerase, dNTPs, passive reference and optimised buffer components).
- 3.125µl primer/probe mix
- 250ng DNA or 1µl plasmid DNA standard
- 2.125µl sterile water

Each standard and sample was run in triplicate. A non-template control (substitute 1µl sterile water for plasmid DNA), again in triplicate, was added to eliminate false positives.

The plate was run on an Applied Biosystems 7900HT fast real-time PCR system, under the following conditions: an initial incubation of 50°C for 2 min then an initial denaturing step of 95°C for 10 min, followed by 40 cycles of amplification consisting of denaturing (95°C, 15s) and annealing/extending (60°C, 1 min). The amount of real RT amplicons during each cycle were detected by measuring the increase in FAM fluorescence (quenched by TAMARA) with excitation at 540nm and emission at 570nm. Data acquisition was performed during the exponential phase.

The raw cycle number or cycle-threshold (Ct) for both standards and samples were exported from SDS v2.3 software (Applied Biosystems, Foster City, CA, USA) and exported into a spreadsheet. The standard curve of the measured standards was plotted using the formula $x = log(x)$ to form a linear regression and allow calculation of the equation of the line. Titre samples were then averaged across the triplicates and corrected using the equation of the line. Infectious viral units per ml (iu/ml) of each sample dilutent were calculated using the following sequential equations:

- Total DNA extracted = concentration of DNA (ng/µl) x volume of DNA eluted (µl)
- %Total DNA added to TaqMan = (250ng/total DNA extracted)x100
- Cell number used in qRT-PCR reaction = $(5x10^4)$ x (%Total DNA added/100)

- Amplicon copy number/cell = Corrected samples (from spreadsheet) / cell number used

- Infectious viral units / ml (iu/ml) = [(Dilution factor x 1000) / volume of virus added to plate (µl)] x copy number/cell

The mean of all sample diluents from the titre plate was taken to give a final titre and reported in iu/ml.

2.5 VIRUS TRANSDUCTIONS

These experiments were performed in Chapter 3 to test the ability of adenoviral and lentiviral vectors to transduce human VSMC.

2.5.1 Virus cell binding

Cells were seeded in a 12-well plate at a seeding density of $2x10^5$ cells / well and incubated overnight at 37^{o}C to achieve 70-80% confluence the following day. The cells were subsequently washed twice with PBS before being transferred to serum-free media. Viruses were diluted to the desired concentration using serum free media. For Ad5 transductions, concentrations were calculated in viral particles /cell (vp/cell). Lentiviral vectors were diluted to the required MOI using the following equation:

Amount of viral stock required (μl) = (Number of cells x MOI needed) / iu/μl

All infection incubations were performed for 4h at 37^{o}C unless otherwise stated. Cells were washed twice in PBS to remove unbound virus then placed in fresh complete media and incubated for 48h before transgene expression was assessed by microscopy and transgene quantification.

For experiments involving RAd 35 transduction, cells were washed in phosphate buffered saline (PBS) and infected with 5000vp/cell of virus in the presence or absence of physiological concentrations (10μg/ml) of coagulation FX (Haematologic Technologies, Vermont, USA) and presence or absence of 15% Poloxamer 407 (BASF, Ludwigshafen, Germany) in serum-free media. Incubation times used were 1, 5, 10, 30 and 60mins, after which cells were washed twice with PBS, transferred into standard VSMC media and incubated for a further 48 hours at 37°C. Cells were harvested and lysed by freeze-thawing in 0.2% Triton-X100/PBS. All experiments were performed 3 separate times in triplicate.

2.5.2 Determination of Protein Concentration in Cell and Tissue Lysates

The amount of protein in cell lysates was determined using the micro bicinchoninic acid (BCA) assay kit (Pierce, Rockford, USA) as per manufacturer's instructions. Briefly, a

standard curve was generated using dilutions of BSA ranging from 25µl/ml to 2000µg/ml. 200µl of BCA working reagent (Reagent A:B, 49 parts:1 part dilution) was added to 25µl of cell or tissue lysate or standard in duplicate in a 96-well plate. The plate was covered to protect from light then incubated at 37^{o}C for 30 min. The absorbance was measured at 570nm on the Wallac VICTOR^{2} plate reader (Wallac, Turku, Finland).

2.5.3 GFP transgene quantification

After PBS washing, 50µl of 1 x Reporter Lysis Buffer was added. Cells were placed on ice and mechanically dislodged from the plate surface using a rubber policeman. A standard curve of recombinant GFP, ranging from 0.01 to 1µg/ml was produced and 100µl of each dilution was added in duplicate to a 96-well plate. 100µl of PBS was added in duplicate as a blank control. 20µl of each sample from section 2.5.1 was then added to a fresh well in duplicate 80µl 1 x Reporter Lysis Buffer was added. The plate was incubated at room temperature for 10 min before luminescence was measured using a Wallac VICTOR^{2} plate reader (Wallac). GFP activity was then normalised to the total protein content of the samples, measured by bicinchoninic acid assay (section 2.5.2) producing relative light units per milligram protein (RLU/mg protein).

2.5.4 B-galactosidase transgene quantification

Expression of β-galactosidase was quantifed using the Tropix Galacto-Light Assay Kit (Applied Biosystems, Foster City, CA, USA) as per the manufacturer's instructions. After removal of media, cells were rinsed with PBS. 1ml of lysis buffer (500ml PBS/1ml Triton-X) was added to each well of the 12-well plate and cells scraped with a rubber policeman. The plate was freeze/thawed and cell lysis was confirmed using microscopy. 10µl of each sample was transferred to a black 96-well plate and 70µl of Tropix Galacton Plus:Galacto-Light Diluent mix (1:100 dilution of Tropix Galacton Plus in 100mM NaH_2PO_4 and 1mM $MgCl_2$, pH 8) was added. Cells were covered in tinfoil to protect from light and incubated at room temperature for 1 hour. 100µl of Tropix Accelerator II was added to each well and incubated for 2 min. Luminescence was measured using a Wallac VICTOR^{2} plate reader (Wallac) as in section 2.5.2. β-galactosidase activity was normalised to total protein content of the samples, measured by bicinchoninic acid assay as before (section 2.5.2) giving results in relative light units per milligram protein (RLU/mg protein).

2.5.5 LacZ staining

Cells that had been transduced by RAd 35 were fixed for 10 minutes in 4% paraformaldehyde (PFA) at 4^{o}C. After 3xPBS washes (5 min) cells were then stained with sterile-filtered X-gal working solution- [(20ml): 1.54 ml 1M Na_2HPO_4, 0.46 ml 1M NaH_2PO_4, 26µl 1M $MgCl_2$, 1.2ml 50mM $K_3Fe(CN_6)$, 1.2ml 50mM $K_4Fe(CN_6)$, 1ml of 20mg/ml x-gal (dissolved in dimethyl formamide) and 14.574ml dH2O]. Cells were incubated at 37°C for 24 hours in the dark and were then washed twice in PBS (5 min) prior to imaging by microscopy (section 2.9).

2.6 HAEMAGGLUTINATION ASSAY

With regard to the use of a porcine model of ISR to test viral gene delivery it was important to establish any potential interaction between Ad5 and porcine erythrocytes. This was assessed using a haemagglutination assay performed according to previously published methods (Cichon et al., 2003, Nicol et al., 2004).

2.6.1 Preparation of erythrocytes

Blood was taken from pigs, by puncture of the pulmonary arteries at time of euthanasia using an 18G needle and 20ml syringe, and added to a 15ml falcon tube containing 140ul citrate phosphate dextrose (CPD) (Sigma) per ml of blood. Human blood was taken from healthy volunteers and treated the same. 8ml of Percoll (Sigma) solutions of 81%, 70%, and 55% (v/v) were prepared using HBSS pH7.2 (Gibco, Paisley, UK). For example, for 55% (v/v): 4.4ml Percoll was added to 3.6ml HBSS. Percoll gradients were then prepared in a 15ml Falcon tube with 2ml of 81% Percoll solution at the bottom and 2ml of 70% Percoll solution carefully added on top followed by 2ml 55% Percoll solution. 2ml of blood was then carefully pipetted on top of the gradient. The tubes were transferred to a centrifuge and spun at 3000rpm for 4 min and then at 2500rpm for 6 min. This forms a series of bands with the erythrocytes contained in the dense red band in the middle. The solution above the erythrocyte band was carefully removed before the erythrocyte band was then siphoned off using a P200 pipette and the volume recorded. To the erythrocytes, an equal volume of filtered 4% dextran (v/v) was added and the solution was mixed well and incubated for 6 min at room temperature. An equal amount of 2 % dextran (volume of erythrocytes + same added volume of 4% dextran) was then added and the suspension incubated for 30 min at 37^{o}C. The upper layer of dextran sedimentation was removed (the erythrocytes are now the lowest layer in the dextran sedimentation) and 5mls of PBS was added to re-suspend the erythrocytes. After further centrifugation at 865rpm for 8 min the cells were washed then re-suspended in 2mls of 55% Percoll. This suspension was applied to a fresh Percoll gradient and centrifuged as before. Finally, the erythrocyte band was removed and diluted to the required concentration (v/v) in PBS.

2.6.2 Haemagglutation Analysis

Virus solutions were diluted by 1/25, 1/50, 1/100, 1/200 in PBS. 50µl of the chosen erythrocyte solution was pipetted into each well of a concave bottomed 96-well plate.

Carefully, 50µl of a virus dilution was added doing each virus dilution in duplicate where possible. PBS was used instead of virus for uninfected control wells and a positive control for agglutination was added (1% Triton X-100 to lyse the RBCs). Plates were gently swirled to mix erythrocyte and virus solutions together and incubated at 37^{o}C for 2hrs to allow sedimentation. Plates were then graded as according to published criteria (Cichon et al., 2003). A red button shaped spot in centre of well = no haemagglutination, and a cloudy well with no spot = complete haemagglutination.

2.7 GENERAL MOLECULAR BIOLOGY TECHNIQUES

2.7.1 Vascular Smooth Muscle Cell Stimulation

This section, and 2.7.2 describe the methods used in Chapter 4 human *in vitro* experiments.

HCASMC were seeded at a density of 5x10^{4} cells per well in a 12-well plate using normal SMC media (see section 2.3) and incubated overnight at 37^{o}C to achieve ~80% confluency. The media was removed and cells washed once with PBS. To each well, 1ml of serum-free (0.1%) high-glucose DMEM was added and the plates incubated for a further 48h (quiescence) to induce a differentiated contractile state.

The cells were then stimulated to a dedifferentiated proliferative phenotype by replacing media with the following mitogens (in duplicate):

- No serum (serum-free DMEM) as an undifferentiated control
- 15% serum (in normal SMC media)
- PDGF-BB at 20ng/ml (stocks at 10µg/ml so 2µl added to 1ml media)
- IL-1α at 10ng/ml (stocks at 1µg/ml [made up in 0.1% BSA/PBS as per manufacturers instructions] so 10µl stock added to 1ml media)
- Combined PDGF_BB and IL-1α (at same concentrations as above)

- bFGF at 20ng/ml (stocks at 10µg/ml so 2µl added to 1ml media)

Each plate was then incubated at 37^{o}C for a variable duration of time dependant on the time-point being studied (1h, 5h, 18h or 24h). At the appropriate time point, cells were washed again with PBS and 700µl QIAzol (QIAGEN) added to allow cell harvesting and extraction of RNA.

2.7.2 Cell migration

HCASMC were seeded in 12-well plates and quiesced in 0.1% media for 48 hours as described in section 2.7.1. A previously described scratch assay was then used as this has been shown to effectively and simply mimic cell migration *in-vivo* (Liang et al., 2007). This method is based on the observation that, upon creation of a new artificial gap (a scratch or wound) on a confluent cell monolayer, the cells on the edges of the newly created gap will move together to close the scratch until new cell–cell contacts are established again. In this thesis, the purpose of this assay was not to directly measure the degree of migration obtained, but to promote a migratory cell phenotype and measure associated changes in microRNA expression. Direct quantification of the degree of migration was therefore not obtained and microscopy was only used to confirm the presence of cell migration at each time-point. A 200µl pipette tip was used to produce three evenly sized vertical scratches per well. Cells were then washed with PBS, placed in fresh media and returned to the incubator. Images were captured at 0, 6 and 16 hours post-scratch. At the appropriate time point, cells were washed again in PBS and harvested by the addition of 700µl QIAzol (QIAGEN) as in section 2.7.1.

2.7.3 RNA extraction

The following sections describe methods used in Chapter 4 for the quantification of miR both *in vitro* and *in vivo.*

2.7.3.1 Total RNA extraction from cells

RNaseZap (Ambion, TX, USA), a surface decontamination solution that destroys RNases on contact, was used to clean all apparatus and work surfaces. RNase-free filter tips were used in all experiments using RNA. Total RNA (including miRNA and small RNA fractions) was extracted from cells using the miRNeasy Mini Kit (QIAGEN) as per

manufacturer's instructions. Briefly, cells were harvested in QIAzol, transferred to RNase-free 1.5ml eppendorfs and 140µl of cholorform was added. The samples were mixed by 15s of vigorous shaking. Following a 2-3 min incubation at room temperature, the homogenate was centrifuged at 12,000 x g for 15 min at 4^{o}C. The upper aqueous phase was added to a new collection tube (care taken to avoid transfer of any interphase) and 1.5 volumes (usually ~525µl) of 100% ethanol added to ensure ideal binding conditions. The samples were then mixed thoroughly by pipetting and up to 700µl transferred into a RNeasy Mini filter column in a 2ml collection tube. After centrifugation at $\geq$ 8000 x g for 15 secs at room temperature the flow-through is discarded. This centrifugation allows the RNA to bind to the silica-gel membrane of the spin column. This spin is repeated until all of the sample (in aliquots of up to 700µl) has passed through the membrane. At this point, on-column DNAse treatment was performed using the RNase-Free DNase Set (QIAGEN) as per the manufacturer's instruction. Briefly, 350µL of buffer RWT was added to the column and centrifuged for 15 secs at 8000 x g to wash. The flow-through was again discarded. 10µL of DNAse I stock solution was added to 70µL of buffer RDD in a clean eppendorf and mixed by gentle inversion. This DNase I incubation mix was then pipetted directly onto the RNeasy Mini spin column membrane and incubated on ice for 15 min. A further wash step, adding 350µL of buffer RWT into the column and centrifuging for 15s at 8000 x g was then performed and the flow-through discarded. Returning to the protocol, two further wash steps using 500µL of buffer RPE with spins of 8000 x g for 15s and 2 min respectively are followed by elution of the RNA into 30µl of RNase-free water in a fresh collection tube (1.5ml eppendorf). The eluted RNA was passed through the spin column again to increase the RNA yield. The quantity of total RNA in each sample was quantified by NanoDrop^{TM} (ND-1000 spectrophotometer [Labtech International, Ringmer, UK).

2.7.3.2 Total RNA extraction from tissue

RNA extraction from porcine tissue was perfomed using the above method with some modifications. Frozen vessels were disrupted under liquid nitrogen in a pestle and mortar. Any stent present was removed at this point using careful dissection. The arterial fragments were homogenized (Polytron, Switzerland) in a bijou containing 1400µl of QIAzol (Qiagen) with intermittent cooling of the sample on ice. The homogeniser blade had been cleaned with 3% H_2O_2 for 30 mins before and after use and then washed with Nuclease free water prior to use. Once completely homogenized, the sample was left to incubate for 5 min at room temperature before the addition of 280µl of cholorform and thorough

mixing. From this point on the method followed was as documented above for extraction from cells.

2.7.4 cDNA synthesis

For miRNA expression analysis, cDNA was synthesized from total RNA using stem-loop reverse transcription primers and RT kit (Applied Biosystems, Foster City, CA, USA). Each reaction utilises an RT primer specific to an individual miR. The RT product therefore contains single-stranded cDNA complimentary to the miR of interest only. Total RNA was diluted into aliquots at 2ng/µl concentration using RNase-free water. RT was performed in a 96-well PCR plate (Thermo Scientific) and is prepared on ice. Each well contains 2.5µl of total RNA (5ng) in addition to the following: 0.075µl of 100mM dNTP mix (with dTTP), 0.5µl MultiScribe^{TM} Reverse Transcriptase (50U/µl), 0.75µl 10x RT buffer, 0.1µl RNase Inhibitor (20U/µl), 2.08µl Nuclease-free water and 1.5µl of specific miR (or endogenous control) primer. The plate was then mixed by gentle centrifugation and run on a PCR block. Thermal cycling conditions were 16^{o}C for 30 min (to allow for primer annealing), 42^{o}C for 30 min (to allow for cDNA synthesis) then finally 85^{o}C for 5 min to stop the cDNA synthesis reaction and to destroy any DNase activity. Plates were then stored at -20^{o}C until required for qRT-PCR.

2.7.5 Quantitative Real Time Polymerase Chain Reaction

TaqMan^{TM} qRT-PCR (Applied Biosystems, ABI Prism, 7900HT Sequence Detection System) was used to quantify the relative concentration of miRNA present in all experiments (cells and tissues) in this thesis. This quantitative process is based on the detection of a fluorescent signal produced proportionately during amplification of a PCR product. During the target amplification step, the AmpliTaq Gold DNA polymerase amplifies target cDNA synthesized from the RNA sample (section 2.7.4) using sequence-specific primers. The subsequent cleavage of TaqMan probes releases fluorescent signals. The amount of fluorescence released during the amplification cycle is proportional to the amount of product generated in each cycle and can be measured directly. When PCR amplification is in the exponential phase then data is acquired. qRT-PCR was performed using TaqMan Universal Master Mix II with TaqMan miR/endogenous control expression probes (Applied Biosystems) according to the manufacurer's instructions. Reactions were performed using 384-well PCR plates and optical lids. Each well contained 5µl TaqMan Master Mix, 0.5µl miR-specific probe, 3.835µl nuclease-free water and 0.67µl of RT

product (section 2.7.4). Reactions were performed in triplicate and plates were set up on ice. 3 extra wells for each probe were added to the plate (with 0.67µl nuclease-free water instead of cDNA) as negative template control. Expression was normalized to miR-199a-3p or RNU-48 for pig and human samples respectively. The plates were run using the TaqMan detection system under the following cycle conditions: 40 cycles of 95^{o}C for 15s (amplification) then 60^{o}C for 1 min (annealing). Delta(d)-Ct values were determined by subtracting the Ct of the appropriate endogenous control from the Ct of the miR in question. A reference sample is determined and the ddCt calculated by subtracting the reference value from each sample. The RQ is then determined by raising ddCT to power of -2 and raising negative ddCT to power of 2 (Schmittgen and Livak, 2008).

2.8 HISTOLOGY

2.8.1 Stent Electrolysis

For morphometric and in-situ hybridisation analysis of stented segments of porcine arterial tissue, removal of the stent with preservation of vessel architecture was a key consideration. As discussed in Chapter 3, the common method of resin embedding and rotary saw sectioning is time consuming, expensive and allows only limited analysis (Rippstein et al., 2006). The experiments in this thesis utilised a method of stent dissolution previously published by Bradshaw *et al* to circumvent these issues (Bradshaw et al., 2009, Samra et al., 2010). This process utilises the reverse of methods routinely used in industrial electroplating where a differential voltage is applied to two metallic objects placed in a mildly acidic salt solution. The result is that metal ions dissolve from the object with the more positive voltage and either from complexes in solution or diffuse through the solution to deposit onto the object with the more negative voltage. The assembled apparatus for stent dissolution is shown in Figure 2.1 (Panels A-B). Two holes were made through the lid of a 5ml bijou using a 14G needle. A 22G needle was blunted and passed through one hole to allow passage of a stilette (taken from an angioplasty balloon). An electrical wire was used to attach the stilette to the positive terminal of a 10V power supply. A copper wire was attached to a metallic washer placed at the bottom of the bijou, passed up through the second hole in the bijou lid and attached to the negative terminal of the power supply by electrical wire.

One end of the fixed stented segment was dissected to expose stent struts. These were attached to the stilette by moulding the end to interweave through them. The bijou was then filled with 5% citric acid containing 5% (w/v) NaCl. The volume of solution was adjusted so that the lower end of the stent was submerged but the stilette/stent connection lay above the fluid level. The voltage source was then turned on to 5V (Current 1-2mA). The flow of ions from the positive to the negative terminal signifying stent dissolution is shown in Figure 2.1 Panel B. Completion was signalled by the corrosion of the stent to stilette connection. After completion the tissue was carefully sectioned using a scalpel. An arterial segment free of stent is shown in Figure 2.1 Panel C. Typically, small fragments of un-dissolved stent were left and these were carefully removed using a dissecting microscope and forceps (Figure 2.1 Panel D). The arterial segments could then undergo conventional histological techniques as described in section 2.8.3 onwards.

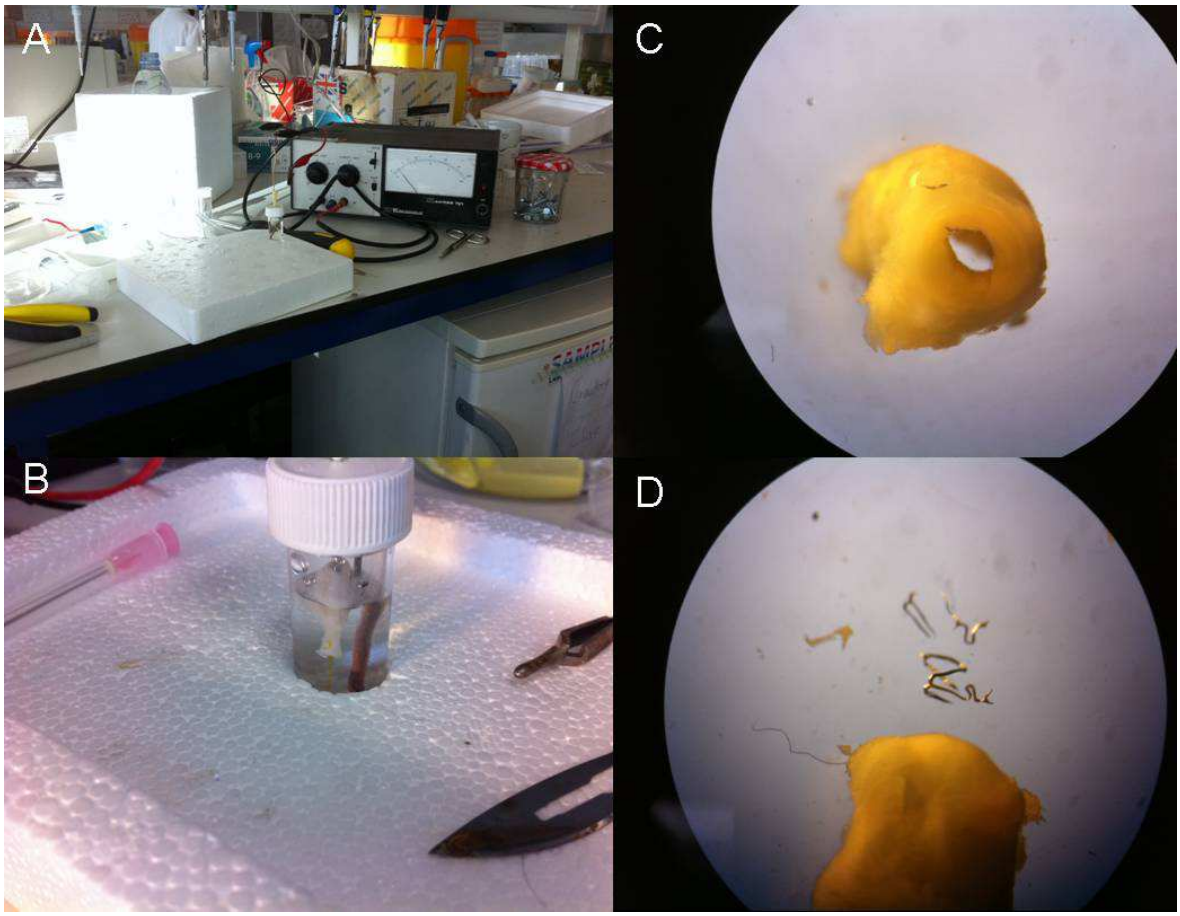

Figure 2-1 Stent dissolution using electrolysis method

Assembled apparatus for stent electrolysis (A) with close-up of a dissolving stent (B). Movement of ions in solution can be seen as linear yellow discolouration emerging from the lower aspect of the tissue. *En-face* sectioned arterial segment following stent removal by electrolysis showing absence of stent struts in the vessel wall (C). Residual stent fragments carefully removed with forceps (D).

2.8.2 En-face β-galactosidase staining

Excised vessel segments that had been treated with RAd 35 (expressing LacZ) were fixed in 2% paraformaldehyde at 4^{o}C for 5 hours. Each vessel was carefully opened *en-face* using a scalpel, with care taken to minimise any disruption to tissue architecture, and pinned onto a glass petridish containing sylgard. Samples were then immersed in X-gal working solution (section 2.5.5) for 24 hours at 37^{o}C. Arteries were then washed 3 times with PBS and analysed for β-galactosidase expression using microscopy.

2.8.3 Paraffin processing

Following tissue fixation in 4% paraformaldehyde for 5 hours at 4^{o}C, arterial samples were washed in PBS, transversely sectioned as required using a scalpel and placed into individual labelled cassettes. Tissues were then processed routinely in an enclosed tissue processor (Shandon Excelsior, Thermo Scientific) and dehydrated through a serial alcohol gradient and xylene before embedding in paraffin wax ready for subsequent histological analysis:

1. 70% (v/v) Ethanol	30 min	10^{o}C
2. 95% (v/v) Ethanol	1h	30^{o}C
3. 100% (v/v) Ethanol (1)	1h	30^{o}C
4. 100% (v/v) Ethanol (2)	1h	30^{o}C
5. 100% (v/v) Ethanol (3)	1h	30^{o}C
6. 100% (v/v) Ethanol (4)	1h	30^{o}C
7. 100% (v/v) Ethanol (5)	1h 30min	30^{o}C
8. 50% (v/v) Ethanol/50% Xylene (v/v)	1h 30min	30^{o}C
9. Xylene (1)	1h	30^{o}C
10. Xylene (2)	1h 30min	30^{o}C

11. Paraffin wax (1)	30min	62°C
12. Paraffin wax (2)	1h 30min	62°C
13. Paraffin wax (3)	2h	62°C
14. Paraffin wax (4)	2h	62°C

The arterial segments were then embedded in a block of paraffin wax. These were allowed to set by placing on a cooling block once the segment had been placed end-on to allow transverse sections to be cut.

2.8.4 Tissue Sectioning

Prior to sectioning, the paraffin wax blocks containing arterial segments were pre-cooled on a cooling block for a minimum of 30 min to aid acquisition of sections. Blocks were pared until one full face of tissue could be cut then serial 3μm (for IHC or H&E staining) or 6μm (for ISH) sections of paraffin embedded tissue were obtained through the whole segment using a rotary microtome (RM2235, Leica). Sections were placed onto the surface of a water bath containing nuclease-free water at 50°C and separated with forceps to allow collection onto poly-L-lysine coated slides (Starfrost® Adhesive Microscope Slides). All slides were placed in an oven at 60°C overnight to fix the section to the slide surface and melt surrounding paraffin wax.

2.8.5 Haematoxylin and Eosin Staining

Haematoxylin and Eosin (H&E) histological staining is routinely performed to assess morphological detail. The basic dye haematoxylin stains acidic structures, such as nuclei and rough endoplasmic reticulum (due to high content of DNA and RNA respectively), a dark purplish blue. Eosin is an acidic dye that stains basic structures (mainly cell cytoplasm) pink or pinkish red.

To remove wax from slides they were immersed twice in Histoclear (National Diagnostics) for 5 min. Rehydration was performed in graded alcohols (100%, 95% and 70% Ethanol for 5 min each) then running water for 5 min.

Slides were then added to Haematoxylin in a staining jar for 2 minutes before being washed in running water. They were subsequently added to Eosin in a separate staing jar for 2 minutes before being dehydrated in a second set of graded alcohols (70%, 95% and 100% for 5 min each) and cleared in Histoclear (2 x 5min) before mounting with coverslips using Histomount mounting medium (National Diagnostics).

2.8.6 Immunohistochemistry (IHC)

2.8.6.1 Antigen retrival

Formalin tissue fixation forms protein cross links that can mask antigenic sites within tissue specimens. Antigen retrieval methods break these cross-links therefore unmasking antigens to allow binding processes to be performed. A sodium citrate buffer (10mM Sodium Citrate, 0.05% Tween 20, pH 6.0) was prepared and heated in a microwave to a temperature of 95-100^{o}C. Deparaffinized and rehydrated slides (section 2.8.4) were immersed in the buffer, covered in cling-film, and returned to the microwave for 5 min at high power. The antigen retrieval solution was then topped up and microwaved for a further 5 min at high power. The solution was left to cool for 10 min to allow antigens to fold correctly and then returned to running tap water prior to the next step.

2.8.6.2 Quenching

Quenching is performed by inhibiting endogenous peroxidase using hydrogen peroxide. Slides were incubated for 10 min in 3% (v/v) H_2O_2 before being washed with PBS (3x 5 min).

2.8.6.3 Antibody binding

IHC was performed using fluorescent secondary antibodies. Sections were first placed in a blocking solution (20% v/v goat serum in PBS) for 30 min at room temperature in a humidified chamber to prevent sections drying out. The serum used is from the species in which the secondary biotinylated antibody has been raised and blocks the sites where non-specific binding would occur between the primary antibody and the tissue section. Excess serum was carefully removed before washing in PBS. Sections were then incubated overnight at 4˚C in a humidified chamber with the appropriate primary antibody and equivalent strength isotype matched IgG negative control diluted in blocking solution. For

detection of eGFP, a mouse monoclonal antibody to GFP (Abcam, Cambridge, UK) was used at a final concentration of 25μg/ml in blocking solution. A mouse anti-human mAb against α-smooth muscle actin (Sigma) at 82μg/ml in 1% (wt/vol) BSA in PBS and a mouse anti-rat mAb against PCNA (Abcam) at 0.5μg/ml in PBS were also used in experiments in this thesis. Slides were then washed 3 times for 5 min in PBS before addition of the biotinylated goat anti-mouse secondary antibody (Dako, Cambridge, UK) diluted 1:300 in 3% (v/v) goat serum in PBS and incubation for 1h at room temperature. Optimal visualisation of staining was achieved using 3',3'-diaminobenzidine tetrahydrochloride dihydrate and hydrogen peroxide. Sections were counter-stained with haematoxylin.

2.8.7 In-situ hybridisation

In-situ hybridization (ISH) is a well-developed method for visualising gene expression and localisation in specific tissues and cell types. It uses a labelled complementary DNA or RNA strand (i.e., probe) to localize a specific DNA or RNA sequence in a portion or section of tissue. The protocol used in this thesis is optimised to detect individual miRs using specific double-DIG-labelled LNA^{TM} probes (Exiquon, Vedbaek, Denmark) as per the manufacturer's description, with some modification (Jorgensen et al., 2010, Tesch et al., 2006). Probe chemistry is summarized in Figure 2.2.

Figure 2-2 *In-situ* hybridization for microRNA

Following microRNA demasking using Proteinase-K, double-DIG-labeled LNA™ probes hybridize to the microRNA sequence. The digoxigenins can then be recognized by a specific anti-DIG antibody that is directly conjugated with the enzyme Alkaline Phosphatase (AP). AP converts the soluble substrates 4-nitro-blue tetrazolium (NBT) and 5-bromo-4-chloro-3'-indolylphosphate (BCIP) into a water and alcohol insoluble dark-blue NBT-BCIP precipitate. [Taken from Exiquon miRCURY LNATM microRNA ISH Optimisation Kit (FFPE) Instruction manual v1.3 (Nov 2010)].

2.8.7.1 Preparation

All solutions, where possible, were treated with diethyl pyrocarbonate (DEPC) to prevent RNase contamination. As with all RNA work, surfaces and equipment were treated with RNaseZap (Ambion). Formalin-fixed paraffin embedded sections (6μm) were incubated at 60^{o}C in an oven overnight. Samples were cleared and hydrated through histoclear and graded ethanol as follows:

- 2 x 10 min Histoclear
- 2 x 10 min 100% Ethanol
- 1 x 5 min 90% Ethanol
- 1 x 5 min 90% Ethanol
- 1 x 1 min DEPC-treated water

2.8.7.2 Unmasking and Deproteinating Sections

All solutions were made with, and all washes performed with, DEPC-treated PBS unless otherwise stated. Slides were placed in freshly prepared 0.1% DEPC (200ul DEPC in 200mL of distilled water) for 1hr with stirrer then unmasked with 10mM sodium citrate (pH6) in a microwave for 10-12 min at 800W. After cooling on ice for 10 mins, slides were immersed in 0.2M HCL for 20mins then washed twice for 5 min each. Slides were immersed in 0.3% Triton-X for 10 mins followed by 3 x 5 min washes. Proteinase K treatment was performed with prewarmed (37^{o}C) 10µg/ml proteinase K (Sigma-Aldrich) added to the sections and incubation in a humidified chamber for maximum 20 minutes at 37^{o}C. This step was reduced to 15 min for miR-21. Slides were then rinsed in DEPC-treated PBS before being immersed in 0.2% glycine, washed (5 min) and then fixed with 4% paraformaldehyde for 10 min on ice. Finally, slides were washed 3 times (5 min each).

2.8.7.3 Hybridisation

Hybridisation with 40 nM double digoxigenin-labelled miR-21, miR-143, miR-145 or scrambled control probes (Exiqon, Vedbaek, Denmark) was carried out with hybridisation temperatures of 55˚C for miR-21, 60˚C for miR-143 and miR-145 and 57˚C for the scramble control probe. 50-100µl of hybridisation buffer [25ml: 12.5ml deionised formamide, 5ml 20x SSC buffer, 1.25ml 50x Denhart's solution, 5ml (2.5mg/ml) salmon sperm, 1.5ml (10mg/ml) yeast, 250µl of 2.5% SDS, 500µl of 10% DIG blocking reagent and 4.5ml DEPC-treated water] was added to each section. Slides were placed in a humidified RNase-free box and incubated at the appropriate hybridisation temperature for 1 hour. The probe was diluted to a final concentration of 40mM in hybridisation buffer and sparingly added to sections before covering with DEPC-treated coverslips. Slides were

hybridised overnight at the appropriate hybridisation temperature in humidified RNase-free boxes.

2.8.7.4 Stringency washing

The following day, coverslips were gently removed in a container of 5xSSC at room temperature before the slides were transferred to a staining rack. Slides were washed in 1xSSC at hybridisation temperature for 20 min, 0.2xSSC at hybridisation temp for 20 min, 0.2xSSC at room temperature for 5 min with gentle agitation on a shaking plate and finally in PBS at room temperature for 5 min with gentle agitation.

2.8.7.5 Immunological detection

After completion of wash steps, sections were covered with blocking buffer (0.5% blocking reagent [Roche, 10% (w/v) in 100mM maleic acid:150mM NaCl buffer], 10% heat-inactivated goat serum [70^{o}C for 30 min prior to use], 0.1% Tween, 1x DEPC-treated PBS) and incubated for 1 hour at room temperature. Anti-DIG-AP Fab fragments (Roche, Basel, Switzerland) and BM purple AP substrate (Roche) were used for detection (Figure 2.2). Anti-DIG-AP Fab fragments were diluted 1:500 in blocking reagent and added to sections which were then incubated overnight at 4^{o}C in a humidified chamber. Slides were then washed for 3x5min in PBS with 0.05% Tween 20 (a detergent) before a final 5 min wash in AP buffer (100mM Tris HCL pH9.5, 100mM NaCl, 0.1% Tween 20).

2.8.7.6 Colour solution

NBT/BCIP solution (Roche) was prepared in DEPC-treated water as per the manufacturer's instructions with addition of tetramisole hydrochloride (2mM final concentration) and applied to cover each section. Slides were placed into humidified trays, covered with tinfoil to protect from light and left to incubate at room temperature for between 1-3 days. Colour solution was topped up every couple of days as required. Slides were observed using microscopy regularly for staining. Once colour staining had appeared slides were washed 3x5 min in PBS with 0.05% Tween 20 then mounted with aqueous mounting solution and edges fixed with clear nail varnish. Imaging was performed as described in section 2.9.

2.9 MICROSCOPE IMAGING

All images were captured using a BX41 optical microscope (Olympus Optical Co Ltd) with Cool Snap MP3 camera (Media Cybernetics, Wokingham, UK) and Q Capture Pro software (Qimaging, Surrey, BC Canada). Measurements were taken using Image Pro-Plus® Analyzer 7.0 (Media Cybernetics).

2.9.1 Morphometric analysis

Morphometric analysis was performed on formalin-fixed arterial segments subjected to stent dissolution through electrolysis and H&E staining. Borders were manually traced for lumen area and area circumscribed by the internal elastic lamina. The neointimal area was calculated from the internal elastic laminal area minus the lumen area. Results are expressed as the mean value for each treatment group.

2.10 EX-VIVO METHODS

2.10.1 Delivery of adenovirus to ex-vivo porcine coronary arteries using the Clearway™ RX Therapeutic Perfusion Catheter

The Clearway™ RX (Atrium Medical, New Hampshire, USA) is a semi-compliant microporous polytetrafluoroethylene (PTFE) balloon perfusion catheter. It is delivered on a monorail platform over a standard 0.014" coronary wire and fully inflates at low pressure (1-4 atm). The balloon material has a microporous structure of tortuous channels allowing an infused agent to weep out in a controlled manner along the whole length of the balloon coating its entire surface (Fig 2.3). This prevents the vessel trauma seen to be caused by jets of drug being eluted at high pressure with early porous balloon devices. The low pressure inflation of the device allows the balloon to occlude the vessel preventing the therapeutic agent from being lost in the circulation and allowing direct contact with the vessel intima without trauma from stretching of the vessel (Saraf et al., 2008).

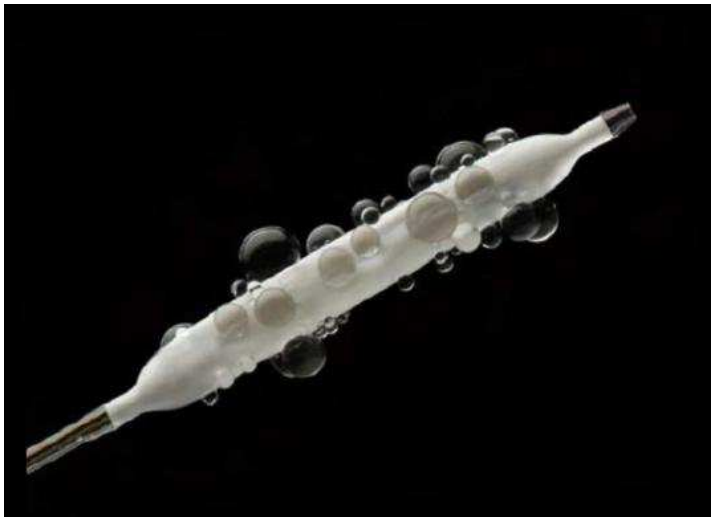

Figure 2-3 Clearway™ RX Therapeutic Perfusion Catheter (Atrium Medical)

To assess the potential of the Clearway™ RX for viral gene delivery it was tested in *ex-vivo* porcine coronary arteries (n=3). Previously untreated animals were sacrificed and the heart removed as described in section 2.11.3.8. Intact 40mm segments of proximal to mid LAD (for viral delivery) and RCA (untreated control) were carefully dissected from the myocardium and transferred to sterile PBS on ice. Viral delivery was performed under sterile conditions in a biological safety class II vertical laminar flow cabinet. Arterial

segments were transferred to a large glass petridish containing sylgard and fixed using 21G needles. A longitudinal incision of 3-4mm was made in the proximal portion of the vessel using a scalpel to allow direct access to the lumen. The Clearway RX catheter was prepped using PBS as per manufacturer's instructions. The balloon was then introduced to the lumen through the incision and positioned at an appropriate distal site. A total of 300µl of AdGFP ($1.157x10^{12}$ particles/ml, $1.51x10^{10}$ pfu/ml) diluted to 1ml in PBS (Final concentration $4.53x10^{9}$ pfu/ml) was infused at low pressure (4atm) over approximately 5 minutes using a 10ml MicroMate pressure-control syringe (Sigma-Aldrich). Apposition of the inflated balloon with the vessel wall was confirmed visually. The vessel was then flushed with PBS to mimic return of circulatory flow. The treated segment (20mm) of vessel was placed in 10% DMEM culture medium and incubated for 24 hours at $37^{o}C$ before fixation, histological processing and antibody staining (section 2.8).

2.11 *IN*-VIVO METHODS

2.11.1 Ethics and Legislation

All animal procedures were performed in accordance with Home Office Guidance and the Animals (Scientific Procedures) Act 1986. All experimental procedures were performed under the project licence PPL 60/3410, held by Dr Simon Kennedy and the personal licence 60/11896, held by Dr Keith E. Robertson. All animals received humane care according to the European Convention on Animal Care. Procedures involving the use of ionising radiation were performed in accordance with the Department of Health Ionising Radiation (Medical Exposure) Regulations 2000 (IRMER).

2.11.2 Animals and Environment

Male large-white/Landrace pigs (20-24kg, 10 weeks old) were bred and supplied by a single producer (SAC Commercial Ltd, Edinburgh, UK) and used in all experiments. All animals were maintained and procedures performed in the Biological Procedures Unit of the University of Strathclyde, Glasgow. In accordance with local guidelines, animals received a minimum of 7 days acclimatisation in the unit before any procedures were performed. All animals were housed under controlled environmental conditions on a 12-hour light/dark cycle, with free access to water and twice-daily feeding.

2.11.3 Coronary Angiography Procedural Technique

2.11.3.1 General Considerations

All procedures were performed in a dedicated operating theatre under sterile conditions. A mobile image intensifier with a C-arm provided fluoroscopy (Siremobil 4N, Siemens, Germany). Continuous single-lead ECG, invasive blood-pressure, oxygen saturation, temperature and expired CO_2 monitoring was utilised. A monophasic direct-current external defibrillator was present in theatre at all times. Standard theatre set-up and monitoring is shown in Figure 2.4.

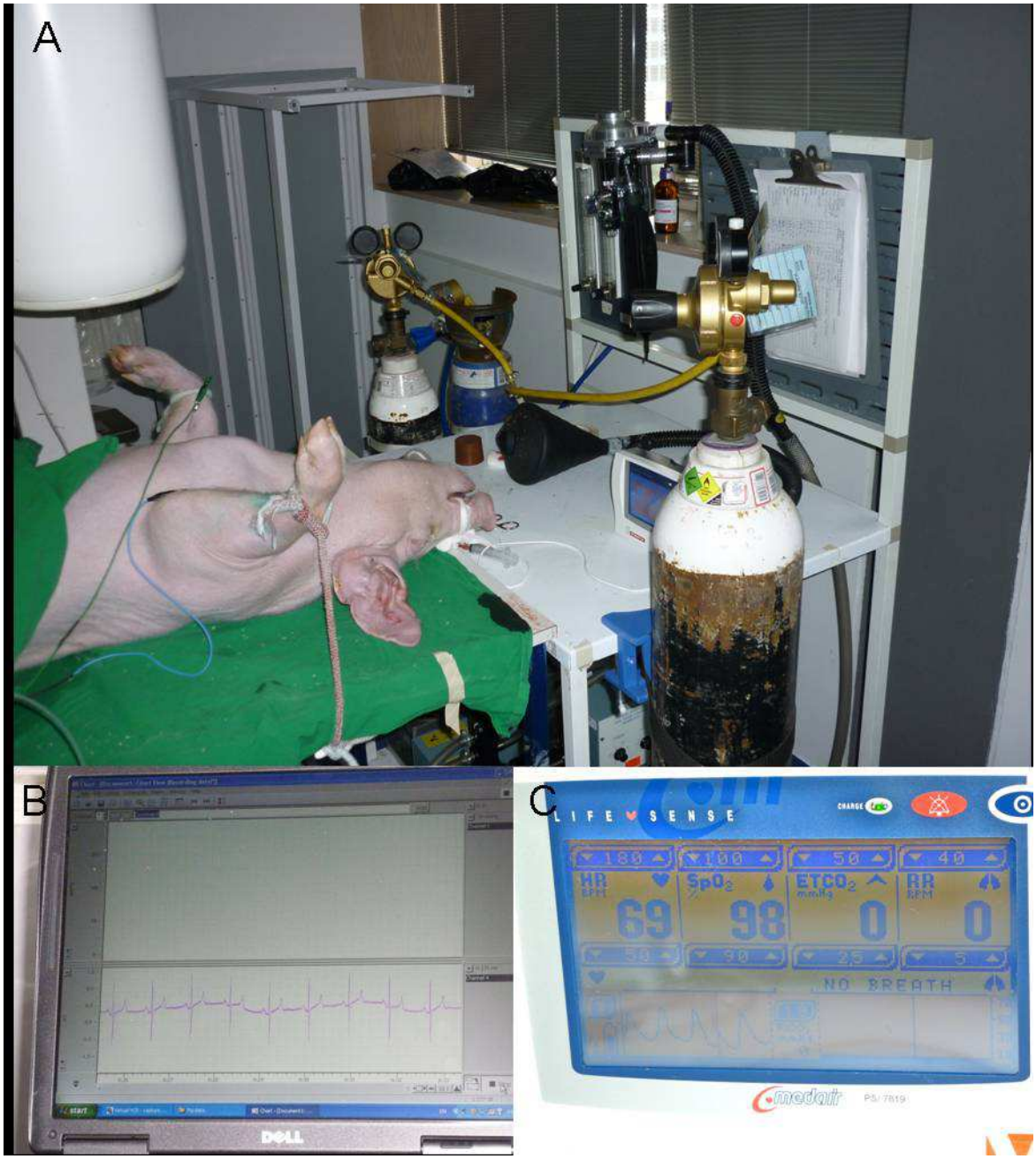

Figure 2-4 Theatre set-up for coronary angiography

Intubated pig in dorsal recumbancy on theatre table (A). C-arm can be seen in the top-left corner with trolley containing Boyle's machine and ventilator at the head of the table. Invasive BP and single-lead ECG monitoring (B) and oxygen saturations (C) were used in all animals.

2.11.3.2 Periprocedural pharmacotherapy

Pigs receiving coronary stents were premedicated with aspirin (150mg PO, Teva, Leeeds, UK) and clopidogrel (150mg PO, Sanofi-Aventis, Guildford, UK) the day prior to surgery. On the day of surgery, all animals received a further 75mg of each agent and this was continued every second day until sacrifice. The tablets were crushed and mixed in with the animals chow. Following anaesthesia (section 2.11.3.3), all animals received analgesia (0.15mg IM buprenorphine, Alstoe Ltd, York, UK) and antibiotics (300mg IM ampicillin, IntervetUK Ltd, Walton, UK) to cover the perioprocedural period. As discussed in Chapter 3, following initial procedural difficulties, an anti-arrhythmic cocktail of amiodarone (75mg IV, Sanofi-Aventis) and lidocaine hydrocholoride (50mg IV, Taro Pharmaceuticals, Ireland) was administered following the onset of stable anaesthesia. A standard dose of anticoagulation (3000Units IV heparin) was administered to all animals following insertion of the arterial sheath.

2.11.3.3 Anaesthesia

All procedures were performed under general anaesthesia. Animals were sedated by an injection of tiletamine/zolazepam (100mg Zoletil IM, Virbac, Suffolk, UK) prior to transfer to the theatre. Gas induction of anaesthesia utilising 4% isoflurane (Abbott Laboratories Ltd, Maidenhead, UK) in oxygen (7 l/min) and nitrous oxide (2 l/min) via a snout mask was used to allow placement of subcutaneous ECG monitoring probes, administration of premedication and IV access using a 20G cannula in a large ear vein. To facilitate endotracheal intubation, propofol (30mg Rapinovet IV, Schering-Plough, Welwyn Garden City, UK) was administered. Pigs were intubated in a supine position using a long straight-bladed Magill laryngoscope and a lubricated 6F endotracheal tube introduced through the vocal cords under direct vision. Gas maintenance of anaesthesia was routine using 2% isoflurane in oxygen/nitrous as above. Maintenance IV normal saline was used and the animals temperature monitored using a rectal probe and heating mat (VetTech Solutions Ltd, UK). Following anaesthesia, animals were placed into dorsal recumbency.

2.11.3.4 Arterial access

Arterial access was obtained via a cut-down approach to the left femoral artery. The left groin was sterilised using povidone-iodine solution and the surgical field prepared with sterile drapes. The femoral artery was approached through a 6cm transverse incision in the cranio-medial aspect of the groin. The artery was identified and exposed using blunt dissection, care taken to identify and separate artery from the vein (usually bellow) and small femoral nerve. Once the artery was freed from its surrounding fascia, proximal and distal suture ties were applied to the exposed artery and the distal suture tied tightly (Figure 2.5). A loose single loop was placed in the proximal suture and the ends secured in artery forceps, in case quick haemostasis was required. Arterial entry was obtained using a modified Seldinger technique. The artery was punctured with the needle from a human transradial artery access kit (Arrow® International UK Ltd, Middlesex). The 0.025 inch soft tipped guidewire was introduced nto the arterial lumen and the needle was removed and the 6F radial sheath inserted over the wire. The wire and dilator were removed and the sheath was flushed with heparinised saline. The sheath was then secured to the skin with a suture (Figure 2.5).

2.11.3.5 Coronary catheterization

A selection of standard, human, 6F coronary guide catheters were available for all procedures. Common shapes used included Judkins left (JL3.5) and right (JR4), or Amplatz right (AR1) and left (AL1). These were advanced up the descending aorta and around the aortic arch before being introduced to the coronary ostia using a standard 0.035” guidewire under fluoroscopy (in the majority of cases in an AP projection). If coronary engagement proved difficult then a little RAO (for the LMS) or LAO (for the RCA) tilt was used. Catheter position was confirmed, and coronary angiography performed, by selective injection of radiographic contrast (Omnipaque 140, GE Healthcare, Bucks, UK). For angiography, the catheter was attached via a Y connector with O-ring valve to a 3 port manifold, connected to an electronic pressure transducer, heparinised saline flush and a luer-lock 10 ml syringe attached to the distal end for intra-arterial injection of contrast.

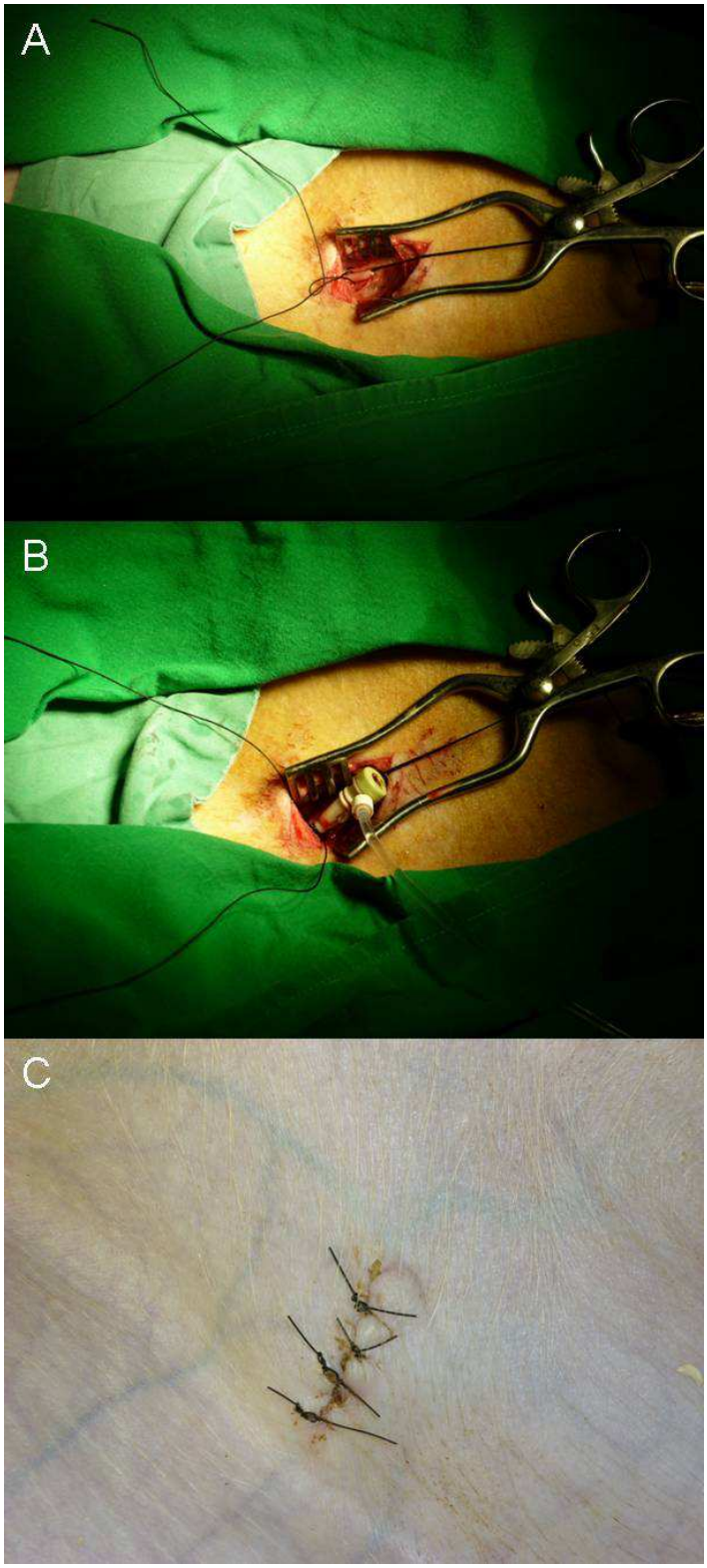

Figure 2-5 Arterial Access

After sterile preparation, an incision is made in the left groin and isolation of the femoral artery performed by blunt dissection. Distal ligation is performed using a suture and a loose tie placed proximally to allow rapid haemostasis (A). A 6F radial sheath is introduced to the vessel using a modified Seldinger technique. At the end of the procedure the artery is ligated to achieve haemostasis and the wound closed in three layers (C).

2.11.3.6 Closure

After removal of the guide catheter post-procedure, the proximal suture was tightened around the sheath which was then withdrawn. The artery is therefore ligated to achieve haemostasis. The wound was then closed in 2 deep layers using absorbable sutures (Dexon™ II, Covidien Ltd, Dublin, Ireland) and a subcutaneous continuous buried layer (Ethilon®, Ethicon Inc, NJ, USA) (Figure 2.5).

2.11.3.7 Recovery

Animals were extubated and recovered from anaesthesia under direct supervision in the theatre. Once awake, animals were returned to their enclosure and received a normal diet, with supplementation of antiplatelets as described above if coronary stents were implanted.

2.11.3.8 Animal sacrifice

Animals were sedated with 200mg IM tiletamine/zolazepam (Zoletil, Virbac). Following cannulation of a large ear vein, an IV bolus of pentobarbital (100mg/kg, Merial, Harlow, UK) was administered. Access to the thoracic cavity was obtained via midline sternotomy using a bone cutter and rib retractors. The visceral and parietal pericardium was stripped from the cardiac surface and the heart mobilised. Traction was applied to the heart, avoiding pressure on areas with coronary stents if present, and the great vessels cut with scissors to allow removal of the whole heart from the thoracic cavity. The coronary arteries were carefully and immediately dissected out from the cardiac surface. Vessel processing and analysis was performed as described in the relevant sections.

2.11.4 Coronary Stent Model

The procedure of balloon delivery and stent deployment is identical to that used in humans in the clinical catheterization laboratory (Figure 2.6). Once the appropriate coronary ostium was selected using a guide catheter a standard 0.014” coronary guidewire was introduced and passed to the distal portion of the vessel to be treated. The stent was passed to the appropriate region over the guidewire using the monorail technique and expanded to the required pressure using an indeflator (Boston Scientific, MA, USA) filled with 50% radiographic contrast/50% normal saline. Following deployment, all equipment was removed from the vessel and repeat angiography performed to exclude complications.

Coronary artery spasm was seen commonly and in most cases responded to an intracoronary bolus of glyceryl trinitrate (100-200μg, Hameln Pharmaceuticals Ltd, Gloucester, UK) delivered via the guide catheter.

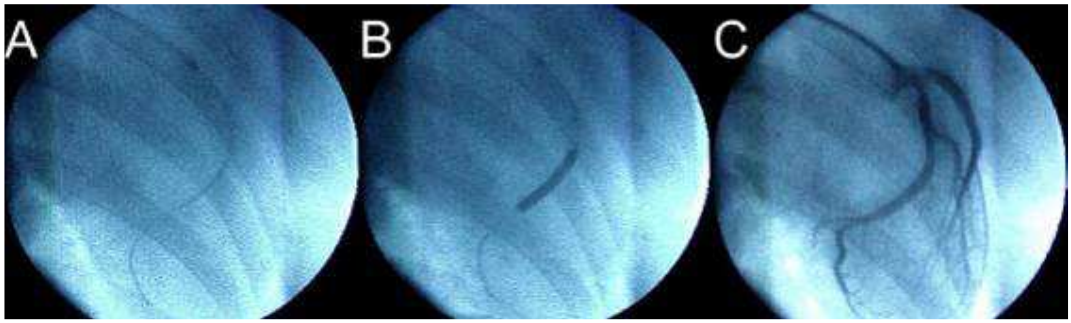

Figure 2-6 Stent delivery to porcine Left Anterior Descending (LAD) artery

Following catheter engagement of the left main coronary artery (LMS) a guide-wire is passed to the distal LAD (A). The stent is introduced by monorail and inflated in the mid-vessel at a stent:vessel ratio of 1.2:1 (B). Final angiogram showing vessel patency and adequate stent overexpansion (C). All projections are right anterior oblique.

2.11.5 Development of in-stent restenosis

The porcine model of ISR is well established and provides reliable neointimal development at 28 days following stent implantation to healthy porcine arteries (Schwartz et al., 1992, Schwartz et al., 1990). It is achieved by controlled stent overexpansion to a stent:artery ratio of 1.2:1 (as assessed visually by angiography) and was used in all experiments in this thesis. Balloon inflation was performed for 30 seconds. The proximal to mid portion of a given vessel was generally chosen for stent delivery as this was most commonly the area of appropriate size to allow stent overexpansion. Once the luminal diameter had been assessed visually, the stent was deployed at the appropriate pressure (usually 8-14atm) to achieve 1.2:1 over-sizing. Sufficient injury was confirmed by angiography.

2.11.6 Local delivery of viral vectors

2.11.6.1 Development of Model and Initial Problems

The initial planned experiments involved two groups of three animals. Each animal was to receive a bare-metal stent (Multi-Link Vision, 3.0x15mm, Abbott Vascular, USA) to 2 of the 3 major epicardial coronary arteries, with the third left untreated as a control. The first group were then to receive RAd 35 expressing Lac Z and the second AdGFP and pHR SIN lentivirus, delievered via a 3.0x15mm Clearway^{TM} RX catheter.

Unfortunately, the first 4 animals suffered intra-procedural death secondary to cardiac dysrhythmia. All deaths occurred during initial angiography or following delivery of the stents. None had received any virus.

This led to a review of the model and changes to the experimental protocol which are discussed in detail in Chapter 3. Intra-procedural mortality was subsequently much improved throughout the rest of the *in-vivo* work performed.

2.11.6.2 Viral Gene Delivery using Clearway™ RX and GENIE™

The Clearway™ RX (Atrium Medical) semi-compliant microporous polytetrafluoroethylene (PTFE) balloon perfusion catheter is described in section 2.10.1. The GENIE™ (Acrostak, Winterthur, Switzerland) local drug delivery system is a balloon catheter consisting of proximal and distal occlusive balloons with a non-dilatating central segment that forms a reservoir. When a suitably sized device is placed over a stented segment of artery the reservoir fully covers the stent. The distal balloon has holes that directly infuse a therapeutic agent coaxially in a proximal direction. This allows the therapeutic agent to be held within the reservoir, while the occlusive segments are inflated, without directing any jets towards the vessel wall (Figure 2.7-2.8). This has been used to successfully deliver paclitaxel to stented arteries in both pre-clinical *in-vivo* (Dommke et al., 2007) and clinical settings (Herdeg et al., 2009). Like the Clearway, it operates on a monorail exchange platform.

Figure 2-7 GENIE™ local drug delivery system

Schematic taken from **www.acrostak.com**. The perfusion balloon is mounted on a monorail platform for delivery to the required vessel segment over a standard coronary guidewire (1). A therapeutic agent is perfused through a distal port at low pressure, which inflates occlusive proximal and distal segments (2). Holes in distal balloon allow therapeutic agent to be delivered coaxially (3) and fill a reservoir created between the distal and proximal balloons (4). A fully deployed GENIE with reservoir filled with therapeutic agent (5).

All local delivery experiments were performed in animals that had received Multi-Link Vision BMS (Abbott Vascular) as described in section 2.11.4. After removal of the stent-delivery balloon the coronary wire was left in position with the tip in the distal vessel. The local delivery device was then exchanged onto the wire using the monorail technique and guided to the stented segment under fluoroscopic guidance. Both devices display radio-

opaque markers to allow accurate positioning. The chosen viral vector was then delivered at the appropriate pressure (1-4atm) using a 10ml MicroMate pressure-control syringe (Sigma-Aldrich) (Figure 2.9). Following completion of viral delivery the devices were deflated and all equipment removed through the guide catheter. Repeat angiography was performed using selective injection of radiographic contrast to confirm vessel patency and exclude complications. Animals were recovered as previously described and sacrificed at 7 days post-procedure.

Figure 2-8 GENIE^{TM} local drug delivery system

Coaxial delivery of blue ink from holes in distal balloon shown in a water bath (A). Schematic showing a deployed GENIE with occlusive inflation of distal and proximal balloons and a previously delivered coronary stent positioned within the device reservoir (B). (Taken from Dommke *et al*, Thromb Haemost 2007; 98: 674–680).

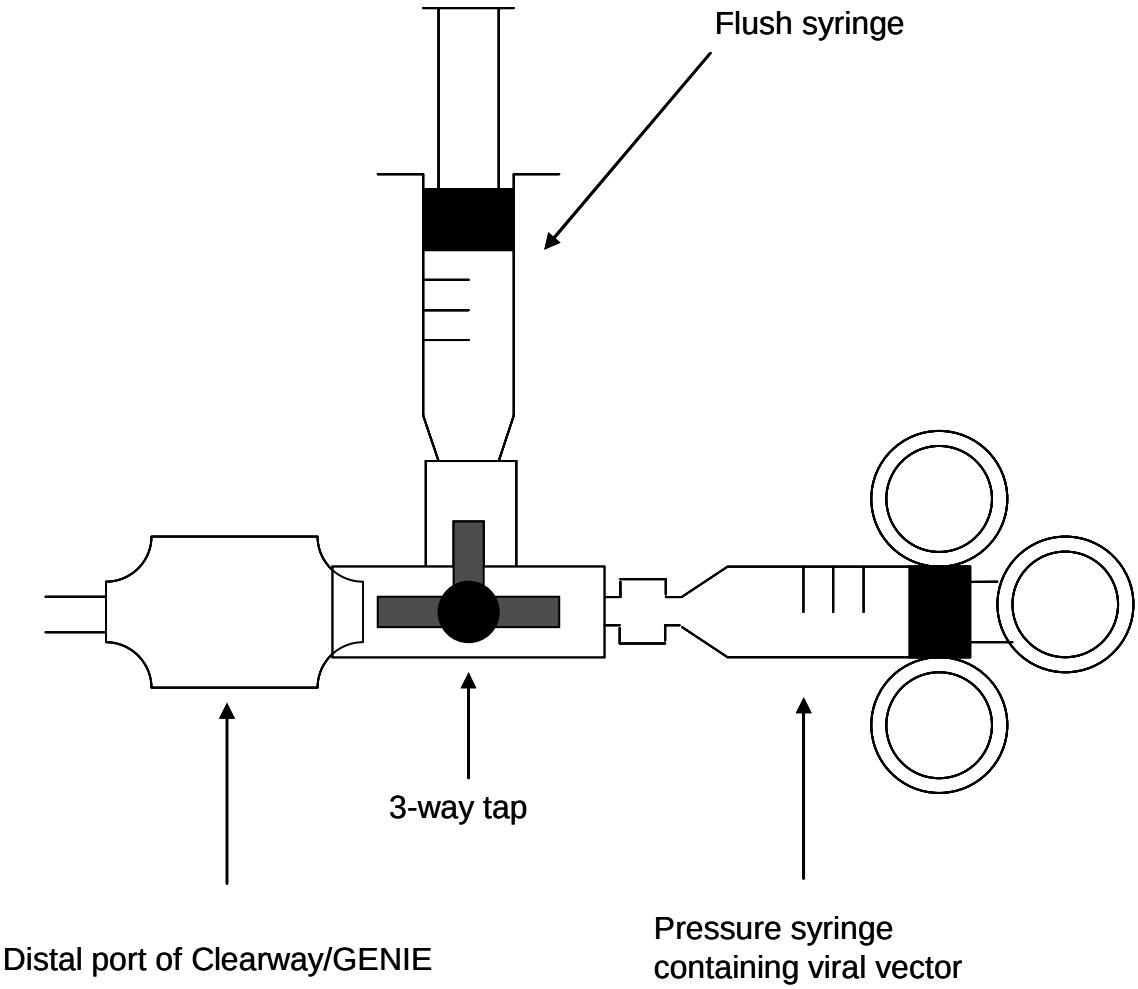

Figure 2-9 Schematic for delivery of viral vector using a pressure syringe

Controlled viral vector delivery was obtained by using a MicroMate (Sigma-Aldrich) pressure syringe connected to a three way tap. A flush syringe containing normal saline (0.9%) was attached to the upper limb of the three-way tap to allow continued controlled inflation following delivery of the virus, for the required duration of time.

2.11.7 Stent-based delivery of viral vectors

2.11.7.1 Poloxamer 407

Poloxamer 407 (Lutrol F127, BASF, Levallois, France) is a biocompatible polyoxyethyl-polyoxypropyl block co-polymer used in pharmacology to create sustained release gels (Figure 2.10). These are used in a variety of clinical settings e.g. in anti-inflammatory indomethacin preparations (Kabanov et al., 2005). It is readily water soluble and has the capability to form thermo-reversible gels, the rheological properties of which are concentration dependant (BASF Data Sheet). In a solution of 15% concentration, poloxamer 407 will be a liquid at 4^{o}C and a viscous gel at body temperature (Feldman et al., 1997) (Figure 2.11).

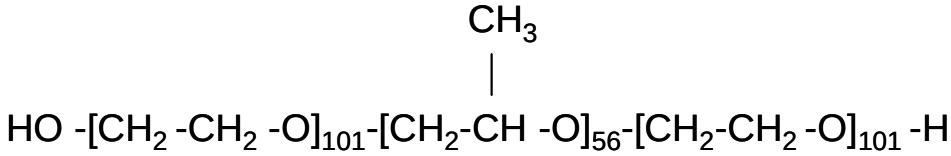

Figure 2-10 Chemical structure of Poloxamer 407 (BASF)

Poloxamer 407 gel was prepared using the "cold process" described by the manufacturer (BASF Lutrol F-Grades Technical Information, April 2010). A 15% (w/v) solution was used in all experiments in this thesis. Briefly, the required amount of sterile water was pre-cooled to 4^{o}C in a beaker. This was then placed on a magnetic stirring plate in a cold room (4^{o}C). 15g of Poloxamer 407 powder was added per 100ml of water. The solution was then covered and left to stir overnight until all the powder had dissolved. It was stored at 4^{o}C (in a liquid state) until ready to use.

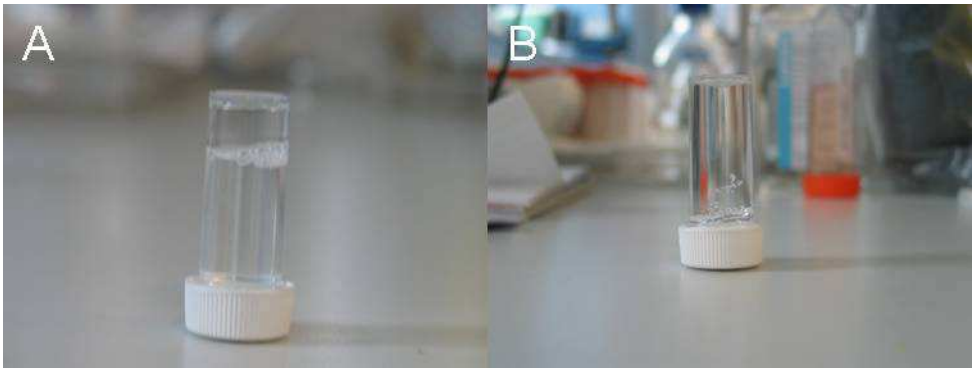

Figure 2-11 Poloxamer 407 as a thermo-reversible gel

Poloxamer 407 (BASF) as a liquid at 4^{o}C (A) and a viscous gel at 37^{o}C (B).

2.11.7.2 Yukon stent system

The Yukon stent platform (Translumina, Hechingen, Germany) is a pre-mounted, sandblasted 316L stainless steel microporous stent designed for on-site stent coating with rapamycin or sirolimus without the obligate use of a polymer (Wessely et al., 2005, Watt et al., 2013). The microporous surface allows for abluminal application of a therapeutic agent and a degree of delayed elution (Figure 2.12).

2.11.7.3 Stent preparation and delivery

All stents used in this experiment were Yukon 3.0x16mm BMS (Translumina). All virus used was the RAd 35 adenovirus expressing LacZ ($2.5x10^{11}$ pfu/ml) as previously described. Six animals were used for this experiment and each received a single Yukon stent (one spray coated, one manually coated and one with air dried virus only) to all 3 main epicardial coronary arteries. Stent implantation and viral doses are summarised in Chapter 3, Table 3.3. For the first 3 animals a viral dose of $5x10^{9}$ pfu/stent was used. For the second 3 animals a dose of $5x10^{10}$ pfu/stent was used. As documented in Table 3.3, the appropriate dose of virus was thawed on ice then thoroughly mixed with the appropriate volume of cold poloxamer 407 (4^{o}C). This solution was kept at 4^{o}C until required.

The Translumina stent coating process is summarised in Figure 2.12 and was performed as per manufacturer's instructions with some modifications. The disposable cartridge containing the stent was placed into the coating device and a 1ml drug reservoir containing the cooled virus/poloxamer solution connected. After input of the appropriate stent length, the coating process was initialised by advancement of the reservoir into a mobile positional

ring containing 3 jet units. This allows for uniform coating of the stent surface. Coating was driven by pressurised air at 1.4bar. Following completion of the spray cycle, the cartridge was removed from the coating device and placed in an oven for 30 min at 37^{o}C to allow the poloxamer 407 to form a viscous gel. Following incubation the stent was removed from the cartridge ready for implantation.

For manually coated stents the Yukon was removed from its cartridge and the virus/poloxamer solution was applied to the abluminal suface as uniformly as possible using a sterile (autoclaved), fine paintbrush. Following application the stents were incubated at 37^{o}C for 30 min prior to implantation.

For air dried stents, the Yukon was removed from its cartridge and the appropriate volume of virus applied directly to the abluminal surface, as uniformly as possible, using a Gilson P20 or P200 pipette (Gilson Scientific Ltd, Luton, UK). No poloxamer 407 was included. The stent was then left to dry at room temperature for 10 min prior to implantation.

All stents were delivered over a 0.014” coronary guidewire as previously described. Stents were positioned at appropriate vessel segments for a 1.2:1 overexpansion and deployed using an indeflator (9-12atm, nominal pressure for Yukon 9atm). Balloons were inflated for 30 seconds. After removal of all equipment from the vessel, angiography was performed as previously described to ensure vessel patency and exclude complications. Animals were sacrificed at day 7 post-procedure. Stented arterial segments were carefully dissected and opened en-face for β-galactosidase staining. Samples of lung, liver, spleen and myocardium distal to the site of each stent were removed at the time of euthanasia for assessment of distal organ transduction.

Figure 2-12 Yukon® stent system (Translumina)

Scanned electron micrograph image of microporous abluminal surface of the Yukon stent system (A) (Taken from **www.translumina.de**). Theatre set-up for porcine Yukon experiments with spray-coating machine on the left (connected to pressurised air system) and oven for post-application incubation on right (B). Schematic describing stent cartridge and spray coating mechanism (C) (Taken from Wessely *et al*, Arterioscler Thromb Vasc Biol. 2005 Apr;25(4):748-53).

2.11.8 MicroRNA expression in neointima

For this experiment, 3.0x15mm Vision Multi-Link (Abbott Vascular) bare-metal stents were delivered randomly to two of the three main coronary arteries (3 groups, n=4/group, 2 stents/animal). For the 4th group (n=4, 2 stents/animal), Endeavour (Medtronic, Minneapolis, MN, USA) drug-eluting stents were used. The stent to artery ratio was 1.2:1 as before. The pigs receiving BMS were euthanized at 0 (n=4), 7 (n=4) and 28 days (n=4) post-procedure. The pigs receiving DES were euthanized at 28 days. After careful dissection of the stented segment (and unstented control vessel), the excised vessels were divided into 2 parts at the centre of the stent, with half being snap frozen in liquid nitrogen for RNA extraction and half fixed in 4% paraformaldehyde (5 hours) for histological analysis. After being snap frozen, arteries for RNA extraction were stored in 10x volumes of pre-chilled (-80^{o}C) RNA*later*-ICE (Ambion Inc) to maintain RNA integrity during the RNA tissue extraction process (section 2.7.3.2). The tissue in RNA*later*-ICE was incubated at -20^{o}C for 16-24h to allow tissue permeation, before being stored at -80^{o}C until RNA extraction.

2.11.8.1 Optical coherence tomography

Following the realisation that it was not possible to achieve dissolution of the Endeavour DES stent using electrolysis, all 28 day samples (BMS and DES, 2 groups, n=4/group, 2 stents/animal) were analysed *ex-vivo* using a C7 Dragonfly OCT catheter (St Jude Medical, MN, USA). Formalin-fixed arterial segments were placed in a container with PBS. The OCT catheter was passed into the arterial lumen using direct vision and a pullback run through the whole vessel segment performed. Obtained images were analysed using ImageJ software (NIH Imaging, http://rsbweb.nih.gov/ij). Neointimal thickness (defined as the minimum distance between each strut and the lumen) was determined at each strut site and calculated as a mean for each stented coronary segment.

2.12 MICRORNA LEVELS IN CABG PATIENTS

2.12.1 Study Population

Twenty-two patients undergoing CABG at a single centre (Prince of Wales Hospital, Hong Kong) were prospectively recruited. Written informed consent was obtained in all cases and the study was approved by the ethical committee of the Chinese University of Hong Kong. Patient baseline characteristics and key features of intra- and post-operative course were recorded. One patient (Patient 13) was excluded from all analysis due to a complicated peri-operative course. Serum samples for RNA extraction were obtained pre-op (PO) and at days 1 (POD1) and 5 (POD5) post-op as follows: peripheral whole blood was sampled by venepuncture and allowed to clot for 10 minutes at room temperature before centrifugation at 4000rpm for 10 minutes. Serum (supernatant) was removed and stored in RNase free tubes at -80^{o}C. Serum C-reactive protein (CRP), cardiac isoform of troponin T (cTnT), urea, creatinine, albumin, total billirubin, alkaline phosphatase (ALP) and alanine transaminase/glutamic pyruvic transaminase (ALT/GPT) levels were also measured at all time points as part of normal clinical care. All patients received standardised warm (37^{o}C) blood cardioplegia with no cooling during cardiopulmonary bypass.

2.12.2 RNA isolation

Total RNA, including the miRNA component, was isolated from serum using a trizol-based miR isolation protocol (Fichtlscherer et al., 2010, De Rosa et al., 2011). Prior to isolation, serum samples were thawed at 37^{o}C in a water bath. 250µl of serum was added to 700µl TRI Reagent BD (Sigma-Aldrich, Poole, U.K.), a blood derivate specific trizol compound, and incubated for 5 minutes at room temperature. At this point 5 µl of 5 nM Syn-cel-miR-39 miScript miRNA Mimic (QIAGEN) was added to each sample. After the addition of 140µl of chloroform, each sample was mixed for 15s using a vortex and incubated for a further 2-3 min at room temperature. Total RNA was extracted from the homogenate using the miRNeasy Mini Kit (QIAGEN) as previously described (section 2.7.3.1). On column DNase I digestion is not required when using serum samples (as the trizol and RNeasy kits effectively remove most of the trace amounts of DNA in blood

components) and this step was therefore replaced with a 700µl buffer RWT wash and centrifugation at 8000 x g for 15s.

2.12.3 Quantitative real time polymerase chain reaction (qRT-PCR)

Following spectrophotometric quantification (Nano Drop, Thermo Scientific, Inc.), RNA was diluted to 2ng/µl before reverse transcription (5ng total RNA) using the Taqman microRNA Reverse Transcription kit and miR-specific primers (Applied Biosystems), as described in section 2.7.4. MiR levels were determined by qRT-PCR using Taqman assay kits for the corresponding miR and the 7900HT Fast Real-Time PCR system (Applied Biosystems), as described in section 2.7.5. Threshold cycle (Ct) values were obtained using the automatic baseline setting.

2.12.4 Data Analysis and Normalisation

To-date no established housekeeping miR for serum has been validated, therefore Ct values were normalised to a spiked-in nonhuman recombinant miR (Caenorhabditis elegans cel-miR-39) as previously described (Mitchell et al., 2008). Cel-miR-39 was chosen because of its lack of sequence homology to human miRNAs and previously determined absence of empiric hybridization to human miRNA probes on miRNA microarrays (Mitchell et al., 2008). The molar concentration of cel-miR-39 to be spiked-in has been derived empirically to produce Ct values comparable to those of moderately abundant miRNAs (e.g., miR-16) measured in human plasma and serum. For comparison, miR expression levels are given as fold-change (RQ – Relative Quantity) from pre-operative levels, versus cel-miR-39, calculated using the $2^{-\Delta\Delta Ct}$ method (Schmittgen and Livak, 2008). To ensure findings were robust, analysis was repeated for all miRs using the "standardization to the mean of all measured miRs" approach (Zampetaki et al., 2012a).

2.13 STATISTICAL ANALYSIS

2.13.1 Software

All data in this thesis were analysed using GraphPad Prism 4 (GraphPad Software Inc., San Diego, CA, USA.).

2.13.2 In Vitro

All *in-vitro* results are expressed as mean ± standard error of the mean (± SEM). *In-vitro* experiments were performed in triplicate on at least three independent occasions and analysis was by unpaired Student's t test. In the case of multiple comparisons, a one-way analysis of variance (ANOVA) with Tukey's post-hoc correction was used. P-values $p<0.05$ after post-analysis were considered statistically significant.

2.13.3 In-vivo

Comparisons between groups were made using a one-way ANOVA with Tukey's post-hoc correction. P-values $p<0.05$ after post-analysis were considered statistically significant.

2.13.4 MicroRNAs in CABG patients

Significance of any temporal change in miR levels was assessed by repeated measures analysis of variance (ANOVA) with a Tukey post-test, or a Friedman test with Dunn's multiple comparison if a normality test was failed. Pearson correlation was used to compare changes in levels of miRs ($\Delta\Delta Ct$) to rise in serum cTnT and CRP after logarithmic transformation. A value of $p<0.05$ was considered statistically significant.

3 Local Delivery of Viral Vectors in a Porcine Coronary Stent Model

3.1 INTRODUCTION

As discussed in Chapter 1, gene-therapy remains a potential alternative to the use of pharmacotherapy for the prevention of coronary in-stent restenosis. The stent-eluted antiproliferative agents currently utilised, in addition to inhibiting proliferation of VSMC, have also been shown to impair endothelial cell proliferation resulting in delayed recovery of the endothelial cell layer and delayed healing (Farb et al., 2001). This impaired endothelialisation manifests clinically as late ST (due to exposed stent struts) and increased severity of intimal disease (as an intact endothelium is important in maintaining VSMC in their differentiated state). A “gene-eluting” stent platform is an intriguing concept, with the potential to allow delivery of a site-specific therapy tailored to target specific stages of the pathological process (VSMC dedifferentiation) while maintaining or promoting positive vessel healing (e.g. re-endothelialisation).

The initial aim of this chapter was to manufacture then test adenoviral and lentiviral vectors in *in-vitro* and *ex-vivo* models to assess their suitability for use in intra-coronary viral gene delivery.

Second, was to establish a large animal model of vessel injury and coronary stent implantation suitable for use in testing viral-mediated gene delivery.

The final aim was to deliver therapeutic vectors to this model, using commercially available delivery catheters, and assess the potential of this technique in the prevention of ISR.

3.2 RESULTS

3.2.1 Manufacture and testing of Viral Vectors

3.2.1.1 Transduction of Human Saphenous Vein Smooth Muscle Cells Using an Adenovirus expressing Green Fluorescent Protein

As proof of concept before moving to *ex-vivo* and *in-vivo* gene delivery, cultured HSVSMC were transduced in culture using an Ad5 vector expressing GFP. Significantly detectable levels of GFP expression were only obtained following exposure to higher doses of Ad (≥5000 vp/cell) (Figure 3.1). Representative images of cells transduced with AdGFP are shown in Figure 3.3 Panels A-C.

3.2.1.2 Transduction of Human Saphenous Vein Smooth Muscle Cells Using a Lentiviral Vector expressing Green Fluorescent Protein

The same cultured HSVSMC were also transduced with a second-generation lentiviral vector expressing GFP. Significant levels of cell transduction were obtained at ratios as low as 5 MOI (Figure 3.2 – 3.3). This is consistent with previously observed work showing that lentiviral vectors are more efficient at transducing VSMC than unmodified Ad5-based vectors (Dishart et al., 2003).

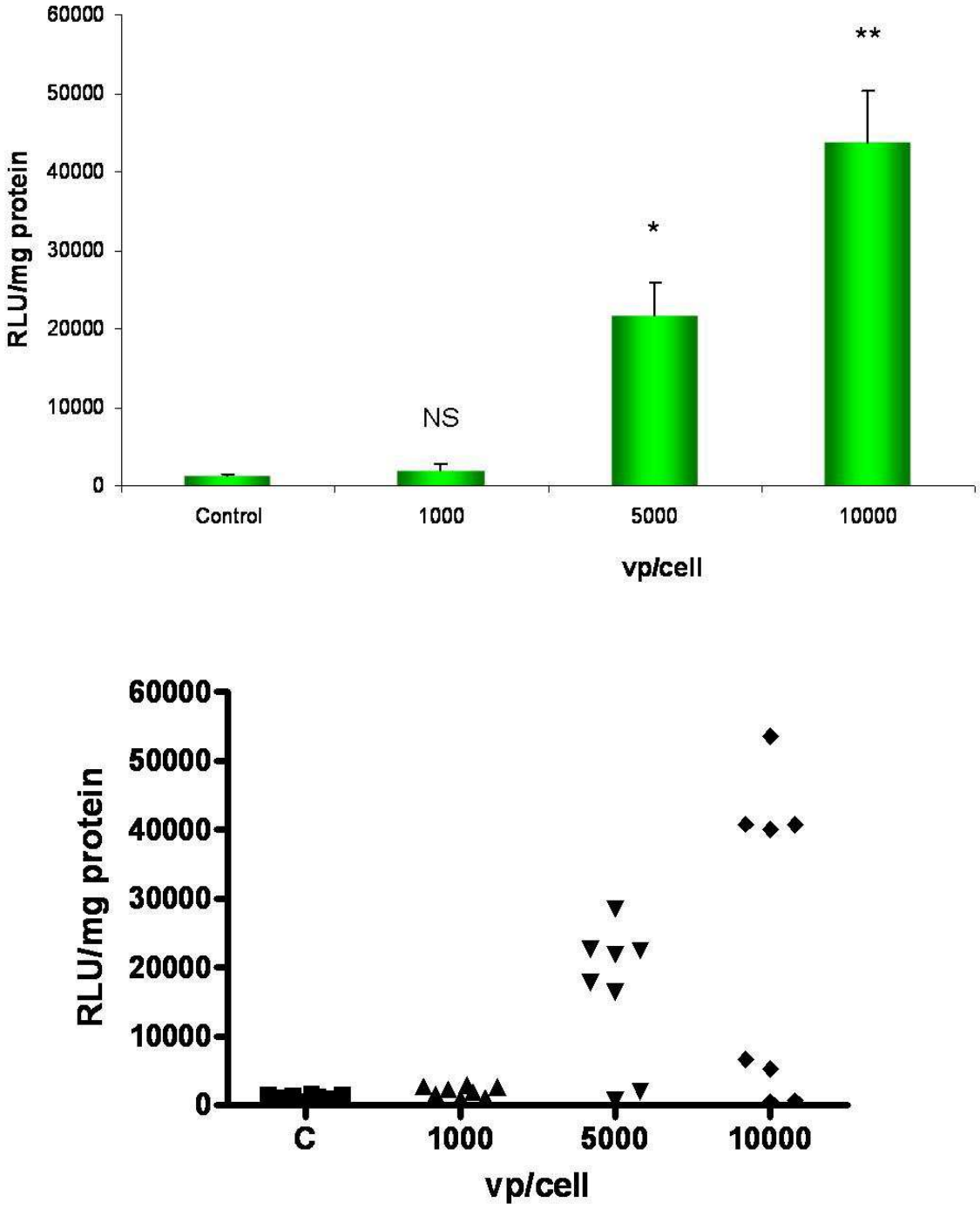

Figure 3-1 Transduction of VSMC with Ad5 expressing eGFP

Viral transduction of Human Saphenous Vein Smooth Muscle Cells (HSVSMC) *in-vitro* using adenovirus expressing GFP. GFP activity is assessed by luminescence and results expressed as relative light units (RLU) normalised to total protein content (mg) (Mean $\pm$ SEM). * $p<0.05$ **$p<0.01$ NS = non-significant. Bottom panel shows scatter plot of RLU values.

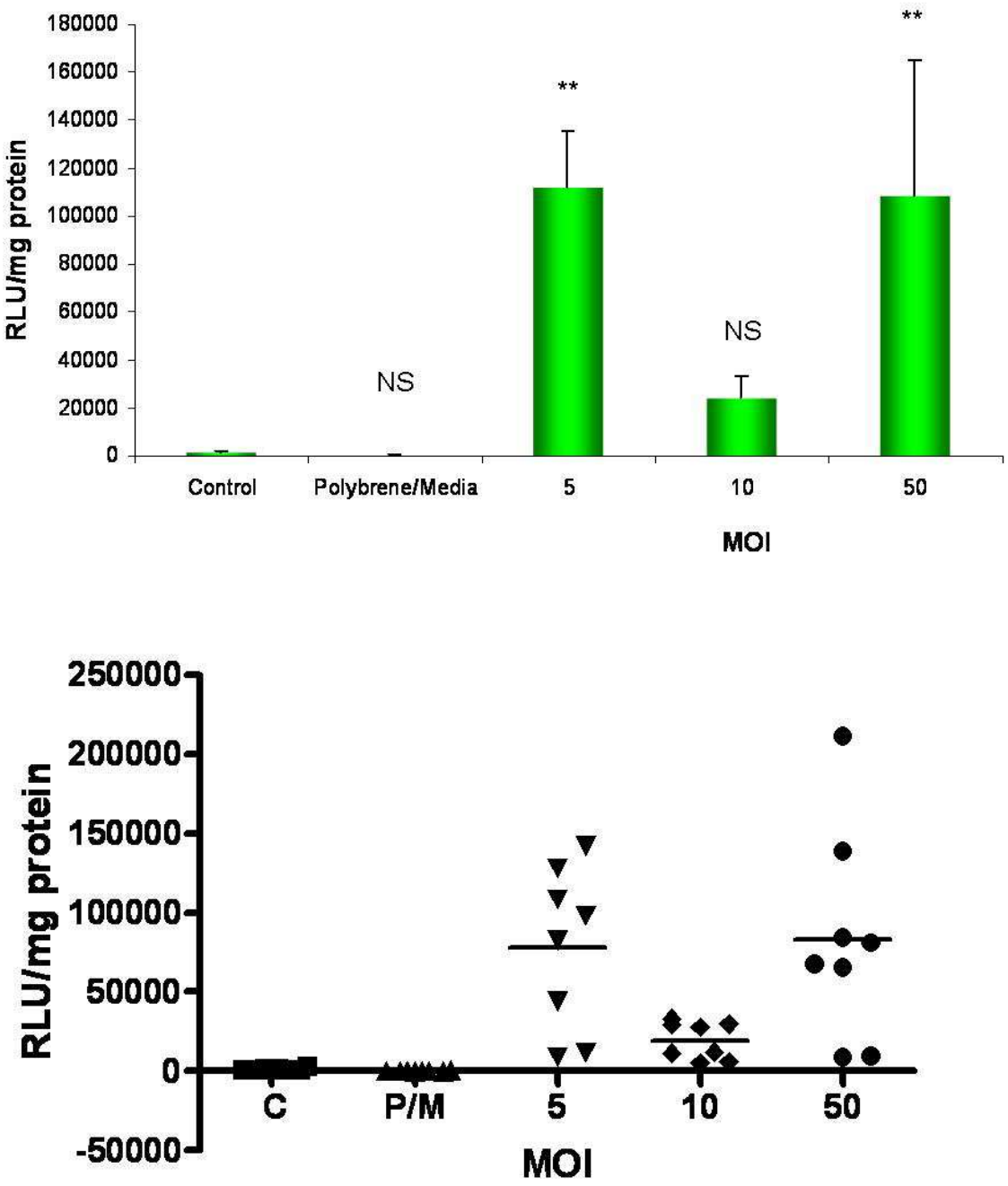

Figure 3-2 Transduction of VSMC with SFFV lentivirus expressing eGFP

Viral transduction of Human Saphenous Vein Smooth Muscle Cells (HSVSMC) in-vitro using lentivirus expressing GFP. Confluent HSVSMC were incubated with the appropriate concentration of virus for 4h at 37^{o}C. GFP activity is assessed by luminescence and results expressed as relative light units (RLU) normalised to total protein content (mg) (Mean + SEM). * $p<0.05$ **$p<0.01$ NS = non-significant. MOI = multiplicity of infection. Bottom panel shows scatter plot of RLU values. Significant levels of cell transduction were obtained at ratios as low as 5 MOI consistent with previous findings that lentiviral vectors are more efficient at transducing VSMC than unmodified Ad5-based vectors.

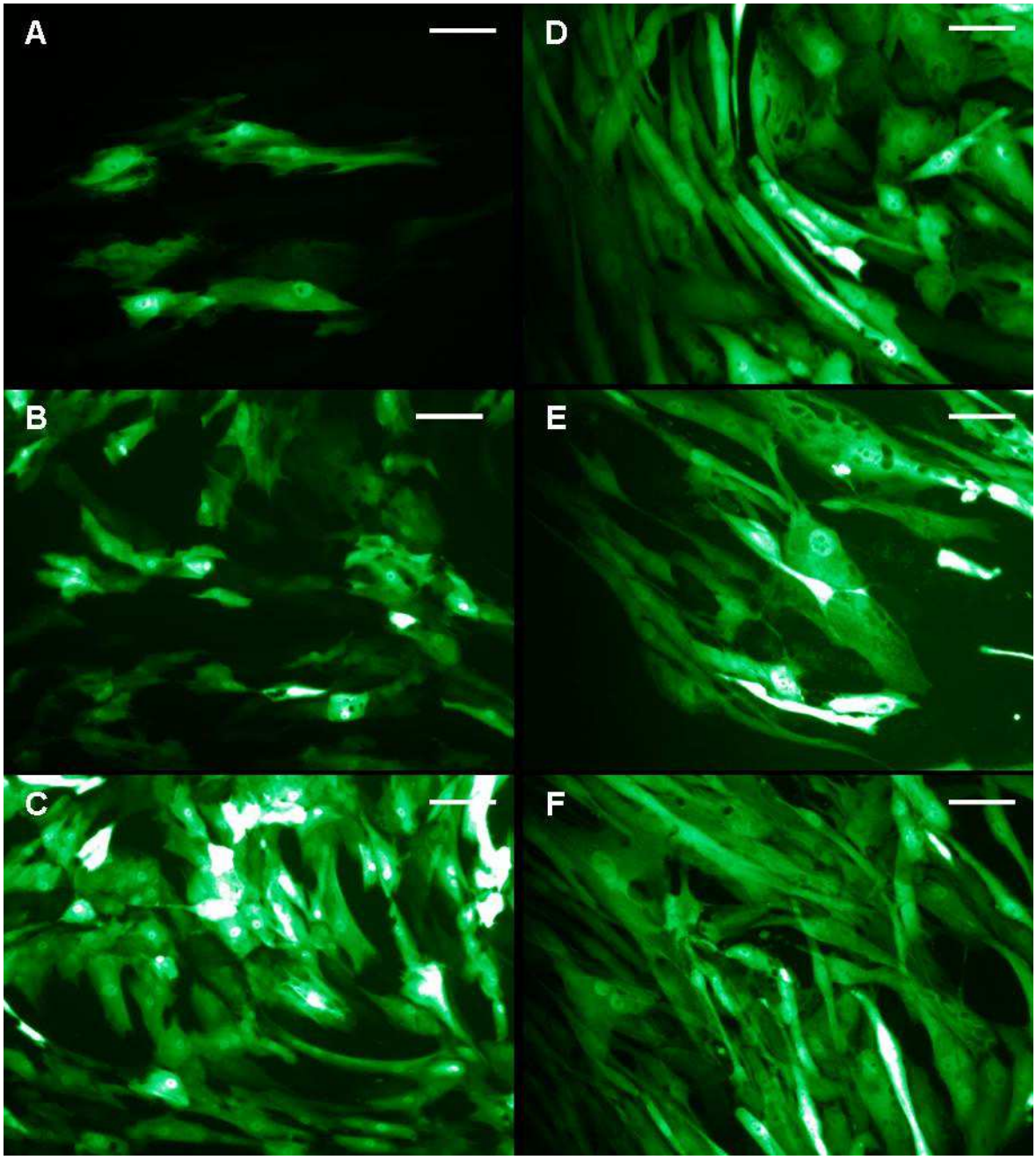

Figure 3-3 Viral transduction of human smooth muscle cells

Representative images of HSVSMC transduced with AdGFP at doses of 1000 vp/cell (A), 5000 vp/cell (B) and 10,000 vp/cell (C) and SFFV lentivirus at MOI 5 (D), MOI 10 (E) and MOI 50 (F). All images are at x40 magnification. Scale bars represent 50μm.

3.2.2 Haemagglutination

As discussed in Chapter 1, an important factor limiting the effectiveness of Ad5 as a gene-therapy vector *in-vivo* in humans is CAR-mediated interaction with erythrocytes. Expression of CAR by erythrocytes has been shown to vary between species with high levels in humans and rats and low levels in mice. With regard to the use of a porcine model of ISR to test viral gene delivery it was important to establish any potential interaction between Ad5 and porcine erythrocytes. This was assessed using a haemagglutination assay (Cichon et al., 2003). Multiple plates were run with varying concentrations of porcine erythrocyte solution (1%, 3%, 5%, 10% and 15%) to establish the optimal amount for analysis. For final analysis concentrations of 8% and 15% pig erythrocytes and 2% human erythrocytes were chosen. PBS was used as a negative control and 1% Trition X-100 as a positive control (to lyse RBCs). Four dilutions of unmodified Ad5 CMV Lac Z (1/25, 1/50, 1/100 and 1/200) were applied to the erythrocyte pellets. This was compared to equal dilutions of AdKO1, an Ad5 vector with a known CAR-ablating mutation as a further control (Nicol et al., 2004). This experiment was repeated on 3 separate occasions. Human erythrocytes showed haemagglutination at all concentrations of Ad5 CMV LacZ but none when exposed to the KO1 virus (Fig 3.4). Porcine erythrocytes displayed no evidence of haemagglutination with either virus. This therefore suggests that CAR-mediated interaction with erythrocytes will not occur *in-vivo* when Ad5 is delivered intravascularly to the pig.

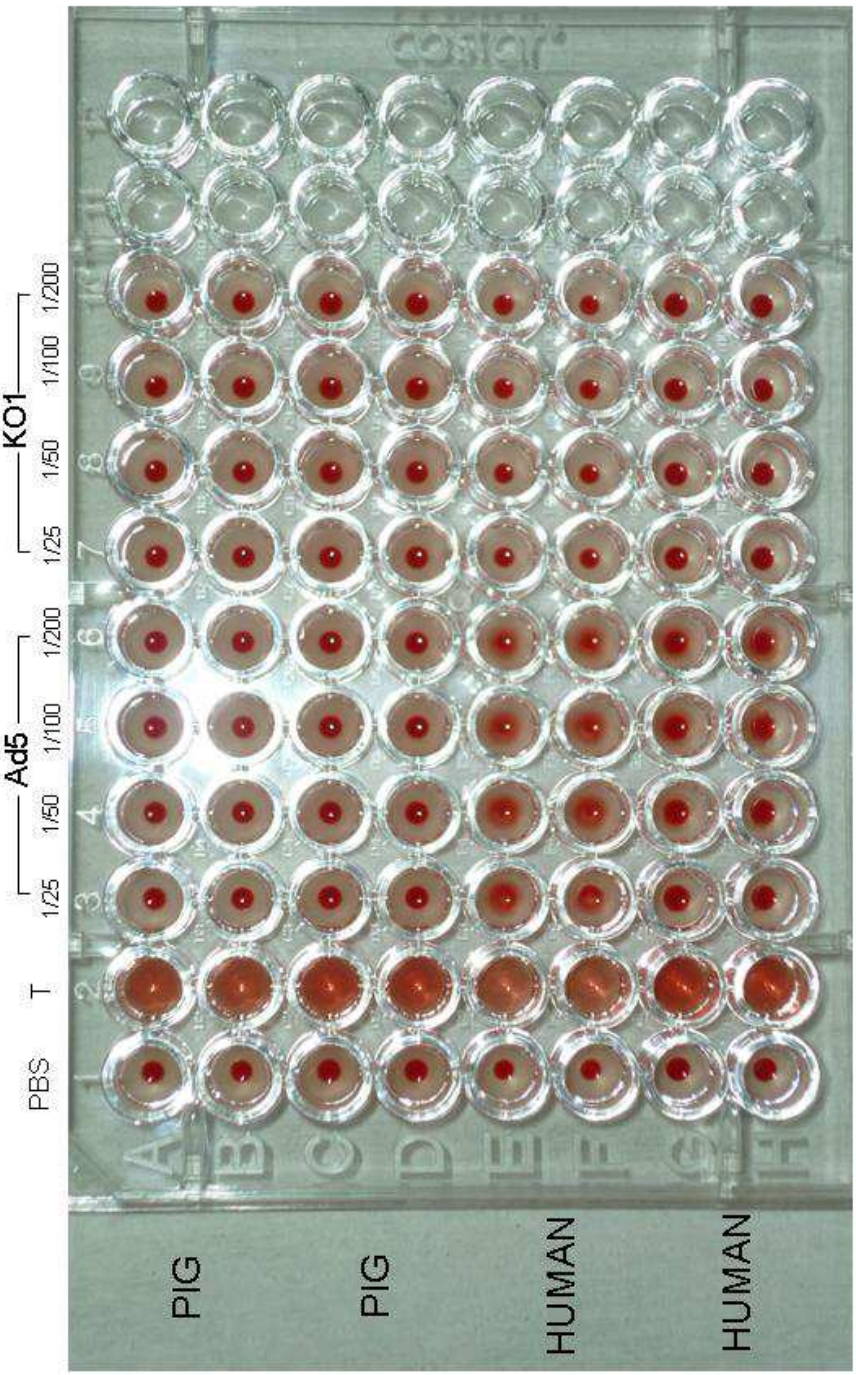

Figure 3-4 Haemagglutination Assay

Rows A-B contain 8% porcine erythrocyte solution, rows C-D 15% porcine erythrocyte solution and rows E-H 2% human erythrocyte solution. PBS added as negative control. T = 1% Triton X-100 as positive control. Porcine erythrocytes show no evidence of haemagglutination with unmodified Ad5 or Ad5 with CAR-ablating mutation. Human erythrocytes show evidence of cell lysis with all dilutions of unmodified Ad5 consistent with erythrocyte binding (haemagglutination).

3.2.3 Delivery of adenoviral vector to ex-vivo porcine coronary arteries using the Clearway™ RX Therapeutic Perfusion Catheter

Prior to progression to the *in-vivo* model it was important to test the performance of the initial local delivery system in an *ex-vivo* model.

3.2.3.1 Adenovirus expressing Green Fluorescent Protein

In arteries incubated with antibody to GFP, immunohistochemical staining was present circumferentially throughout the media in the treated segements (Figure 3.5 Panels B,D,F). This staining was absent in treated arteries exposed to IgG negative control (Figure 3.5 Panels A,C,E).

3.2.3.2 Adenovirus expressing LacZ

To make the process of histological analysis following vector delivery more straightforward it was felt that AdLacZ (RAd 35) could be used instead of AdGFP to allow en-face staining with β-galactosidase rather than having to use monoclonal antibodies. The above experiment was repeated, this time using 500μl of RAd 35 ($4.7x10^{12}$ particles/ml, $2.5x10^{11}$ pfu/ml) diluted to 1ml in PBS (Final concentration $1.25x10^{11}$ pfu/ml). Following 24h culture the vessels were opened *en-face* and stained with β-galactosidase. Again results were consistent with successful transduction of the vessel wall (Figure 3.6) however, in this experiment the majority of the staining appeared to be adventitial rather than medial (Figure 3.6 Panel C).

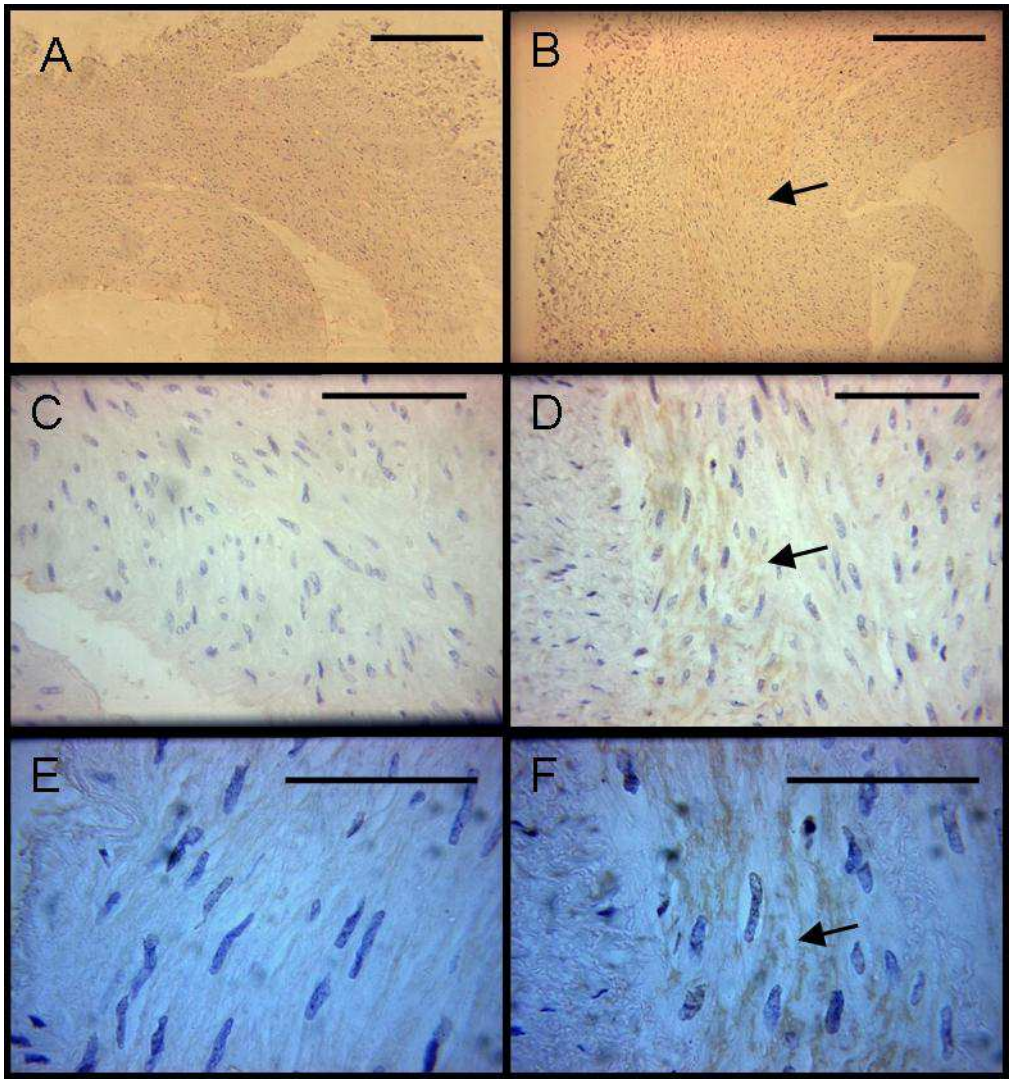

Figure 3-5 AdGFP delivery via Clearway RX to *ex-vivo* porcine arteries

All panels are from arteries treated with $4.53x10^9$pfu AdGFP virus. Sections were formalin-fixed then sectioned at 3µm. Immunohistochemical staining performed using fluorescent secondary antibodies. Panels A,C,E with treated with IgG1 negative control antibody. Panels B,D,F treated with antibody against GFP (1/250). Arrows show areas of 3',3'-diaminobenzidine staining consistent with viral transduction within the vessel media. Panels A&B, x10 magnification, Scale bar = 300µm. Panels C&D, x20 magnification, Scale bar = 100µm. Panels E&F, x40 magnification, Scale bar = 50µm.

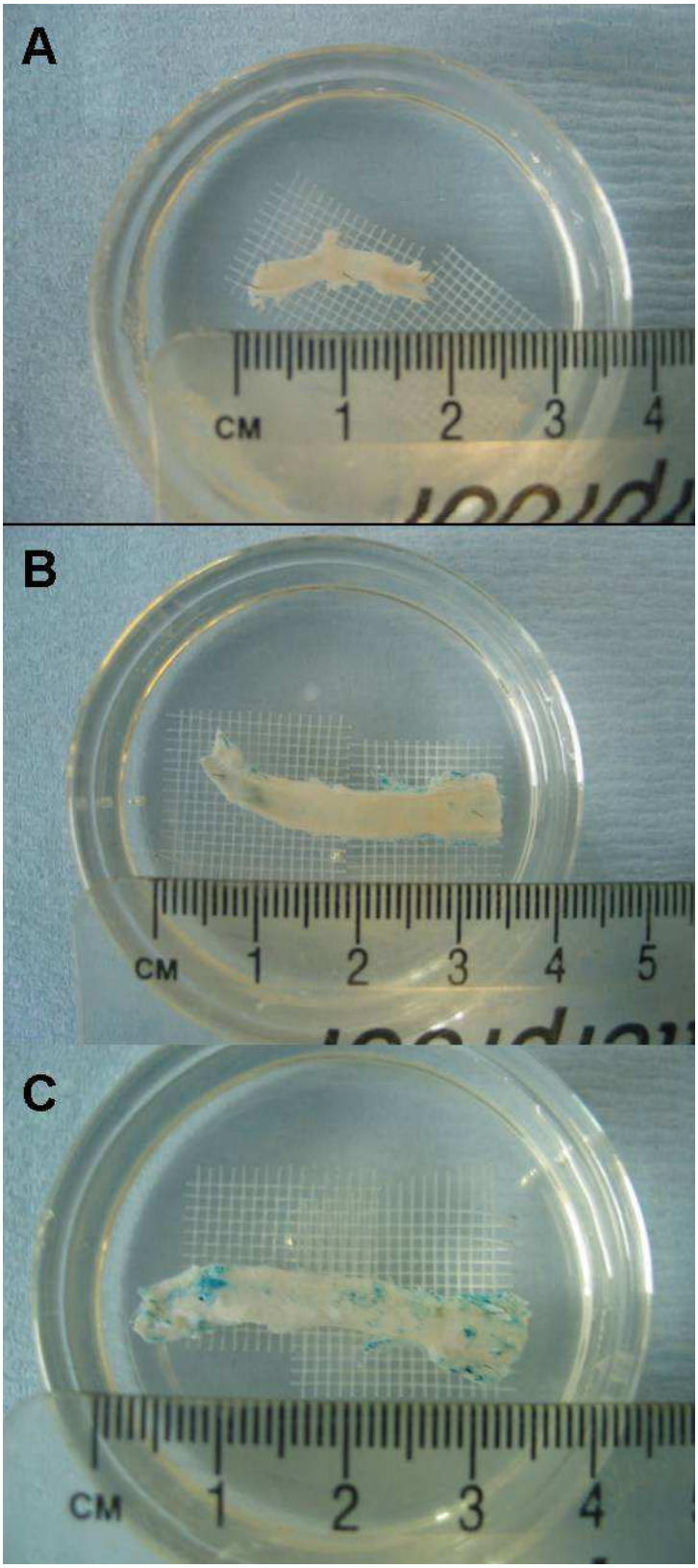

Figure 3-6 AdLacZ delivery via Clearway RX to ex-vivo porcine arteries

Each artery received $1.25x10^{11}$pfu of RAd 35 adenovirus expressing LacZ. After fixation, arteries were opened *en face* and incubated with X-gal working solution for 24 hours. Panel A shows untreated control artery. Panel B shows a segment of treated artery opened *en face* with the lumenal surface visible. Panel C shows the same segment as C turned round to reveal the adventitial surface of the vessel. The blue colour represents β-galactosidase staining on adventitial surface consistent with successful viral transduction of the vessel wall.

3.2.4 Local Delivery of Viral Vectors in a Porcine model of Intracoronary Stenting

3.2.4.1 Viral Gene Delivery using Clearway^{TM} RX

As described in Chapter 2, initial problems with high animal mortality (4 of 6 animals) were encountered. The remaining 2 animals underwent stent insertion and viral gene delivery without complication. Each animal received a Multi-Link Vision 3.0x15mm BMS (Abbott Vascular) to both the RCA and LAD with the LCx used as an unstented control. The first stented segment received $1x10^{10}$ pfu of RAd 35 (40μl) and the second $5x10^{10}$ pfu (200μl). The diluted viral solution (1ml in PBS) was delivered at low pressure as previously described (Chapter 2 Figure 2.9). After viral delivery the animals were recovered then euthanized at 7 days post-delivery as previously described. Excised stented arterial segments were stained with β-galactosidase. A low level of superficial β-galactosidase staining was seen in stented segments but not control vessels following removal of the X-gal solution (Figure 3.7). Based on prior experience of using β-galactosidase staining in SVG incubated with Ad expressing LacZ (George et al., 2000) this was not felt to represent a clinically relevant level of viral gene transfer.

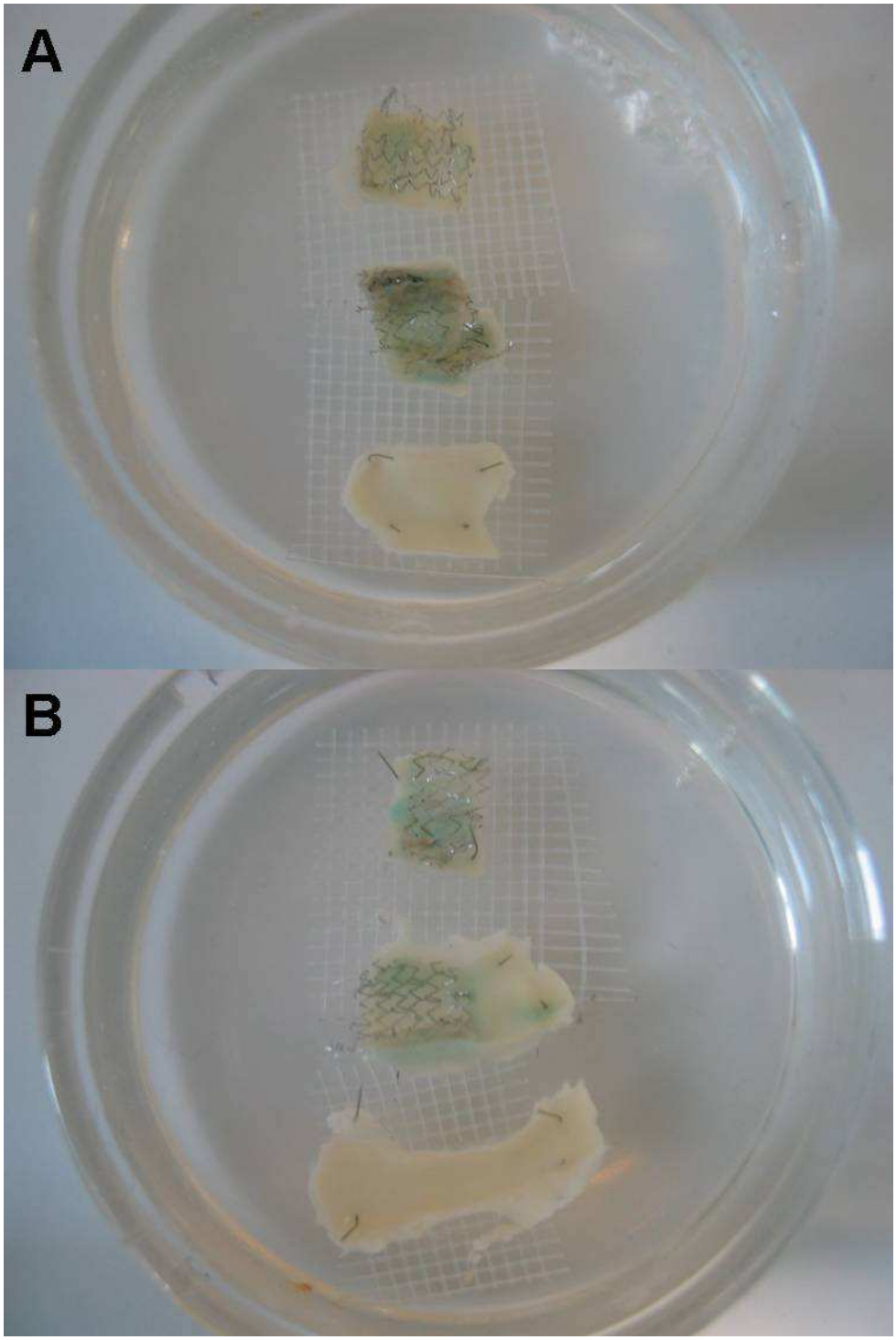

Figure 3-7 Delivery of AdLacZ to stented porcine coronary arteries using Clearway RX

In-vivo Delivery of AdLacZ (RAd35) via Clearway Rx (n=2 animals). Each animal received 2 Multi-Link Vision 3.0x15mm BMS with subsequent local viral vector delivery using the Clearway RX perfusion catheter. Euthanasia at 7 days post-viral delivery. Following fixation, arteries were opened *en-face* and stained with X-gal working solution. Panel A (Pig 1) from top to bottom RCA ($1x10^{10}$ pfu virus), LAD ($5x10^{10}$ pfu virus), LCx (unstented control). Panel B (Pig 2) from top to bottom RCA ($1x10^{10}$ pfu virus), LAD ($5x10^{10}$ pfu virus), LCx (unstented control). Low-grade staining only in treated vessels, not consistent with significant viral transduction.

3.2.4.2 Viral Gene Delivery using GENIE™

It was hypothesized that the GENIE™ (Acrostak) could be a more effective device for delivery of an adenoviral vector to the pig as its reservoir may have been better suited to keeping the virus in contact with the stented segment of arterial wall.

As gene delivery to two stented vessels per pig had proven to be time consuming with the Clearway™ and to simplify the experiment, we chose to deliver a single 3.5x15mm BMS to each animal. Six pigs were used. Again RAd 35 expressing LacZ was the preferred vector ($2.5x10^{11}$ pfu/ml). This was diluted to 5ml in PBS giving a final concentration of $2.5x10^{10}$ pfu/ml. Despite a constant inflation pressure of 2atm the time taken to deliver the 5ml of viral solution was variable with a mean of 2.75+/-0.89 mins, and range of between 1 and 6 mins (Figure 3.8, Table 3.2). The total inflation times achieved with heparinised saline flush delivered at 2atm were also variable with a mean of 7.08+/-1.88 mins and range of between 3 and 15 minutes (Figure 3.8, Table 3.2). The procedure was not well tolerated with 50% of the animals suffering complications of varying severity (Table 3.2).

All pigs were sacrificed at 7 days post-procedure. Stented segments were processed as described in Chapter 2. All stented vessels were patent at the time of euthanasia. No β-galactosidase staining was observed in any of the stented arterial segments (Figure 3.9).

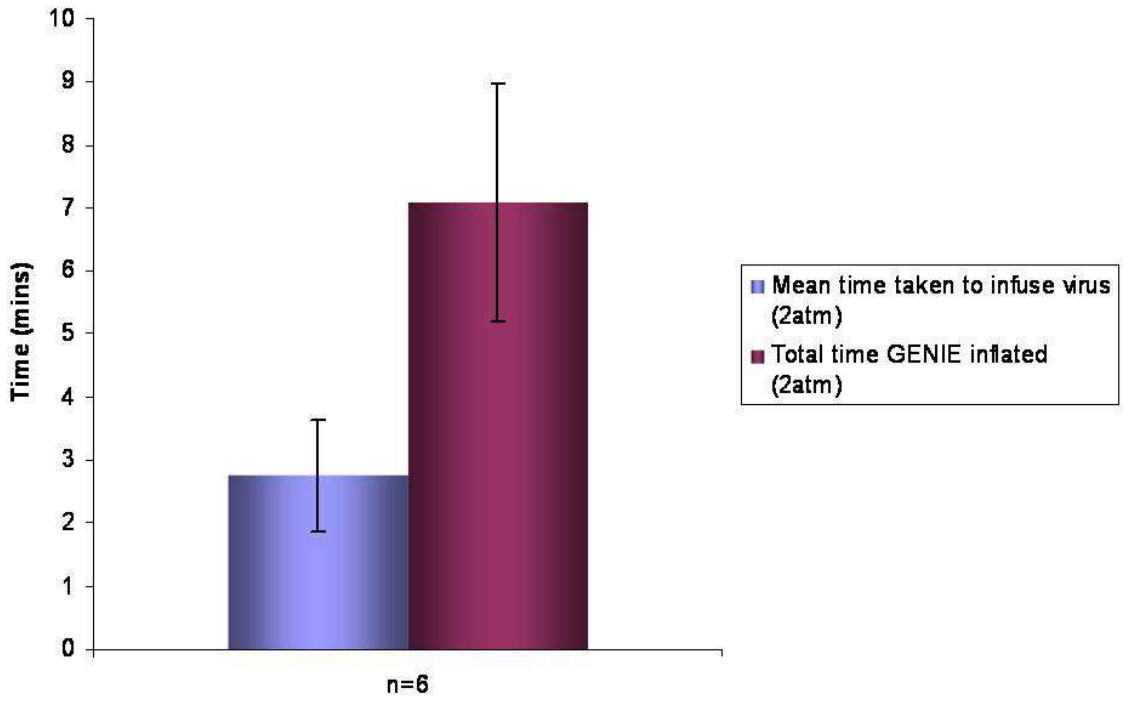

Figure 3-8 Time taken to deliver viral vector and total inflation times for GENIE™

Mean time to infuse 5ml virus at 2atm = 2.75 + 0.89 mins. Mean total GENIE inflation time = 7.08 + 1.88 mins.

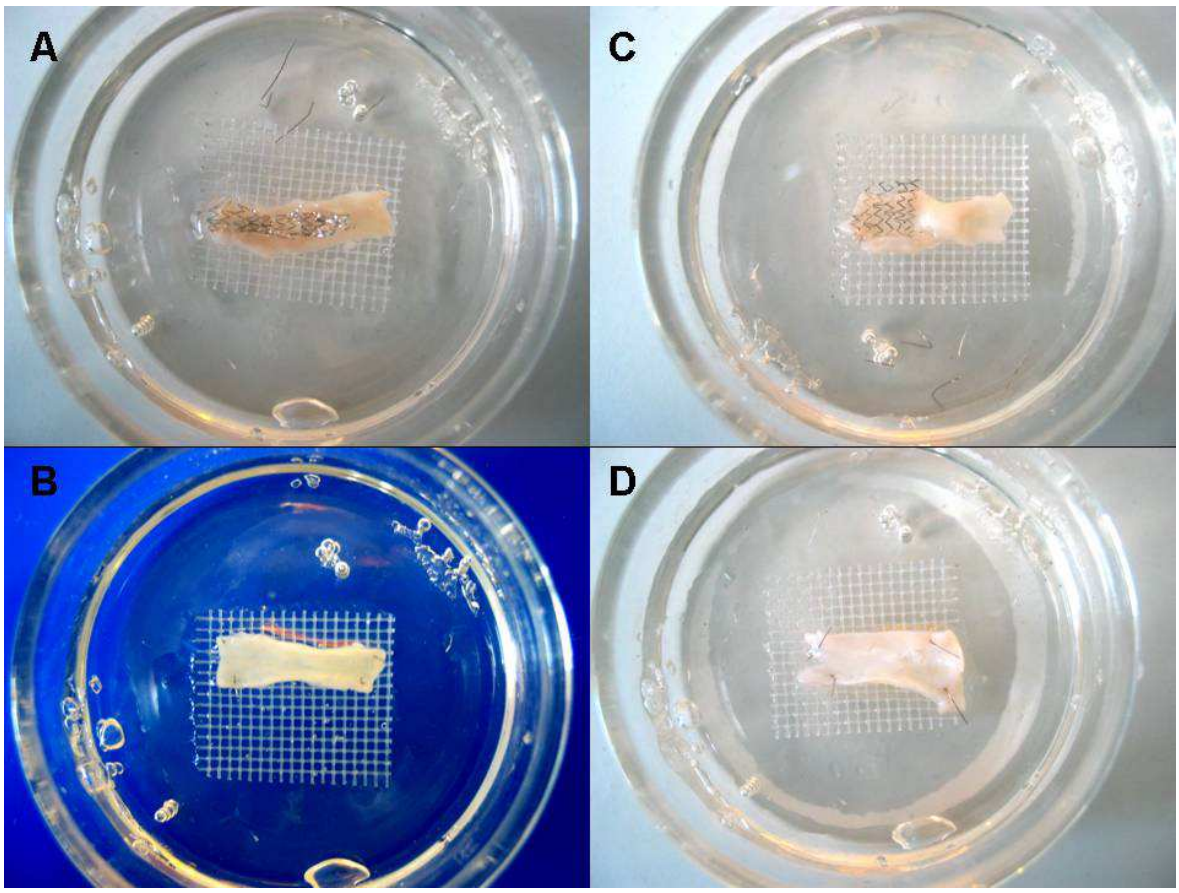

Figure 3-9 Delivery of AdLacZ to stented porcine coronary arteries using GENIE™

In-vivo RAd 35 delivery via GENIE™ local delivery catheter (n=6). All animals received a single Multi-link Vision 3.5x15mm BMS. 500µl of RAd 35 at 2.5 x 10^{11} pfu/ml ($4.7x10^{12}$ particles/ml) was diluted in PBS a to final volume of 5ml (Final concentration $2.5x10^{10}$ pfu/ml) and delivered via a GENIE™ perfusion catheter at a constant pressure of 2 atm. Animals were euthanized at 7 days post-delivery. Upon harvesting arteries were fixed in 2% PFA for 5 hours before being immersed in X-gal stain for 24h at 37°C. Representative images from Pig 1004 (A&B) and Pig 1006 (C&D). Panels A&C show stented vessels with viral delivery. Panels B&D unstented control vessels. No β-galactosidase staining visible in treated arteries or controls.

Table 3-1 Viral vector delivery to the porcine model with GENIE catheter

All stents are Multi-link Vision (Abbott Vascular). 3.5x20mm GENIE used for all animals. Inflation pressure 2atm. VDT – viral delivery time.

Pig	Stent	Vessel	Virus conc (5ml total vol.)	VDT (mins)	Total Inflation Time (mins)	Complications
1001	3.5x15mm	RCA	$2.5x10^{10}$ pfu/ml	1	15	Nil
1002	3.5x15mm	LCx	$2.5x10^{10}$ pfu/ml	5	5	Occlusive stent thrombosis →VT → VF → Death
1003	3.5x15mm	LCx	$2.5x10^{10}$ pfu/ml	6	6	VF → resuscitated
1004	3.5x15mm	LAD	$2.5x10^{10}$ pfu/ml	1	3	Nil
1005	3.5x15mm	LAD	$2.5x10^{10}$ pfu/ml	1.5	3.5	Multiple VE's → settled with IV Amiodarone
1006	3.5x15mm	RCA	$2.5x10^{10}$ pfu/ml	2	10	Nil

3.2.5 Stent-based delivery of viral vectors

Results from the above experiments investigating local delivery of adenoviral vectors were clearly disappointing. The Clearway RX and GENIE represented the only local delivery catheters that could be sourced. Previous devices used in both clinical drug delivery *in-vivo* and pre-clinical gene therapy studies such as the Dispatch catheter (Lincoff et al., 1994) or Infiltrator balloon (Barath et al., 1997) are no longer commercially available and could not be obtained through parent companies. We therefore returned to the literature to investigate the possibility of creating our own gene-eluting stent.

3.2.5.1 Poloxamer 407

As previously discussed, clinical utility currently favours use of a stent based platform for gene therapy. It was hypothesised that we could combine the coatable properties of the Yukon stent system with the improved transduction efficiency provided by poloxamer 407 and create an Ad5 eluting stent platform for delivery to the porcine model.

3.2.5.2 Effect of Poloxamer 407 on transduction of HCASMC *in-vitro*

Prior to moving to *in-vivo* experiments the effect of poloxamer 407 on the transduction efficiency of RAd 35 when applied to HCASMC in culture was evaluated (n=3). Based on previous work in our laboratory (Bradshaw, Parker *et al*; unpublished) we used a viral dose of 5000 vp/cell as higher doses have been shown to induce cell toxicity during longer incubation times. The primary aim was to see if the addition of a 15% poloxamer 407 gel reduced the time taken for significant cell transduction. Cells were exposed to virus, virus + 15% poloxamer gel, virus + coagulation FX (10 μg/ml) and virus + poloxamer + FX. Incubation times were 1, 5, 10, 30 and 60mins. Previous work in our laboratory has shown that the addition of coagulation FX at doses comparable to that in the human circulation (10 μg/ml) to unmodified Ad5 vectors can increase transduction efficiency through utilisation of the HSPG pathway (Bradshaw, Parker *et al*; unpublished). This was therefore used as a positive control.

Addition of 15% poloxamer 407 did not increase the transduction efficiency of HCASMC compared with RAd 35 virus alone (Figure 3.10-3.13). As expected, addition of FX consistently increased transduction efficiency compared with RAd 35 alone. This was not significant at 30 mins due to cell toxicity secondary to an experimental error. At 30 mins, the combination of RAD35, poloxamer and FX was significantly increased even in comparison to RAd 35+FX (Figure 3.10). By 60 minutes these differences were attenuated across most conditions due to cell toxicity (Figure 3.11-3.13).

These results support the potential role of poloxamer gel as a viral delivery reservoir, acting to maintain a high pericellular viral concentration.

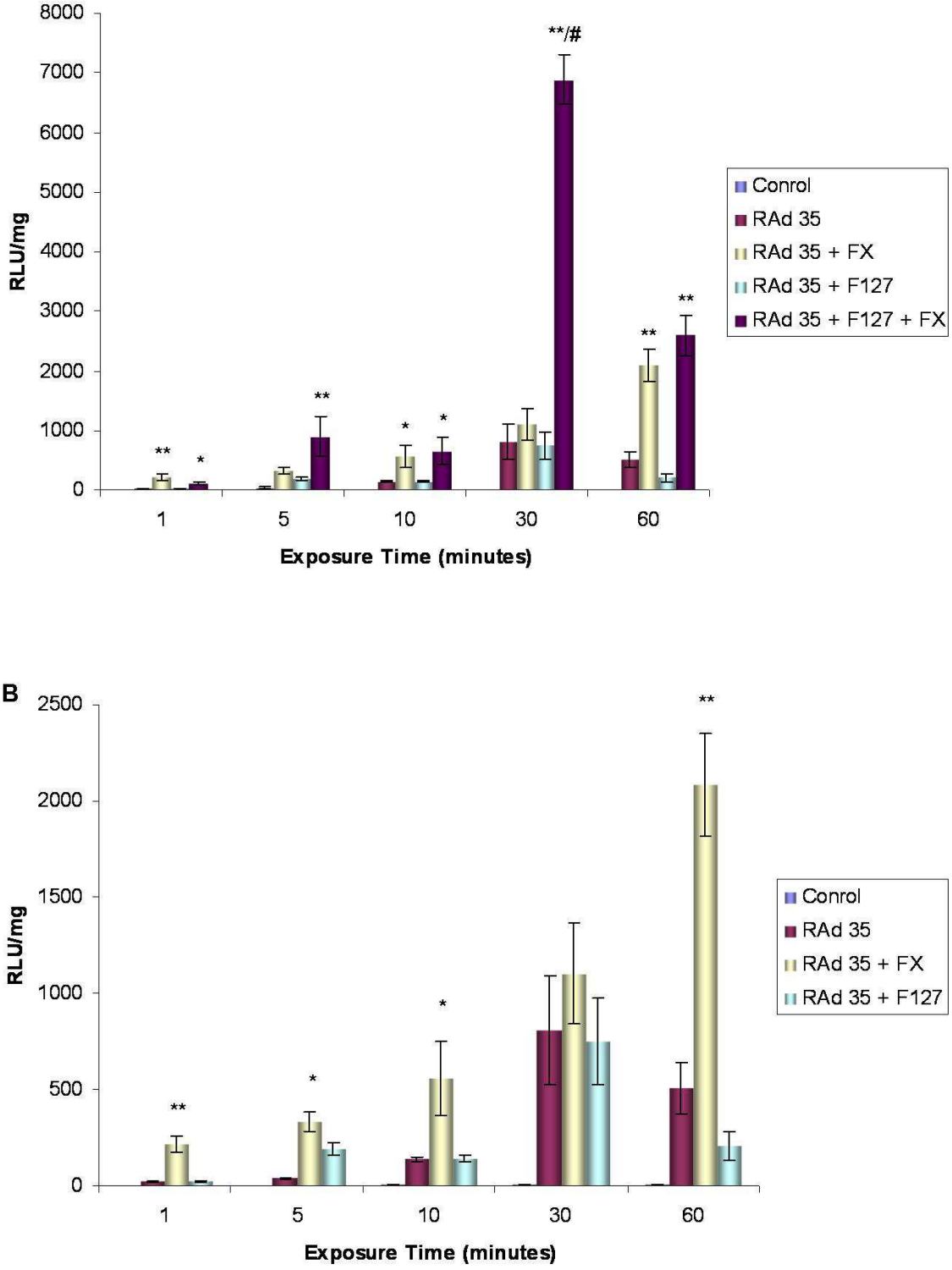

Figure 3-10 Effect of Poloxamer 407 on transduction of HCASMC by AdLacZ

HCASMC (n=3) transduced *in-vitro* with RAd 35 (AdLacZ) at 5000vp/cell for varying exposure durations and in the presence or absence of Poloxamer 407 (F127) or coagulation factor X (FX) (A). Panel B shows same graph as A with RAd35 + F127 + FX excluded. B-galactosidase activity assessed using luminescence and results expressed as mean relative light units/mg total protein content $\pm$ SEM. * = $p<0.05$ vs. RAd 35, ** = $p<0.01$ vs. RAd 35, # = $p<0.05$ vs. RAd 35+FX as determined by ANOVA with Tukey post-analysis for multiple comparisons.

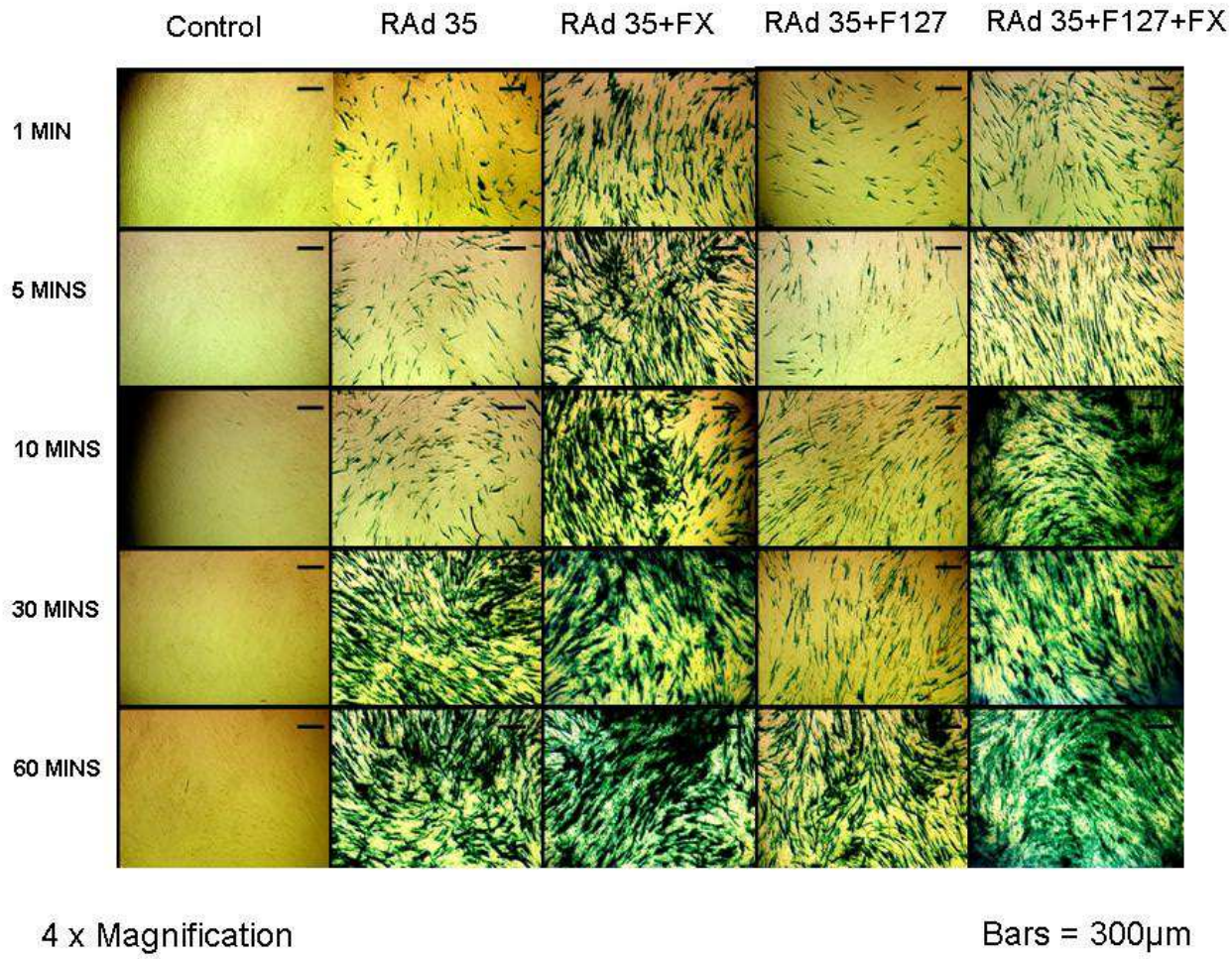

Figure 3-11 Representative images of β-galactosidase expression in HCASMC transduced with AdLacZ +/- Poloxamer 407

RAd 35 = AdLacZ. F127 = Poloxamer 407. FX = Coagulation factor X. Times indicate duration of cell exposure to virus. x4 magnification. Scale bars = 300µm.

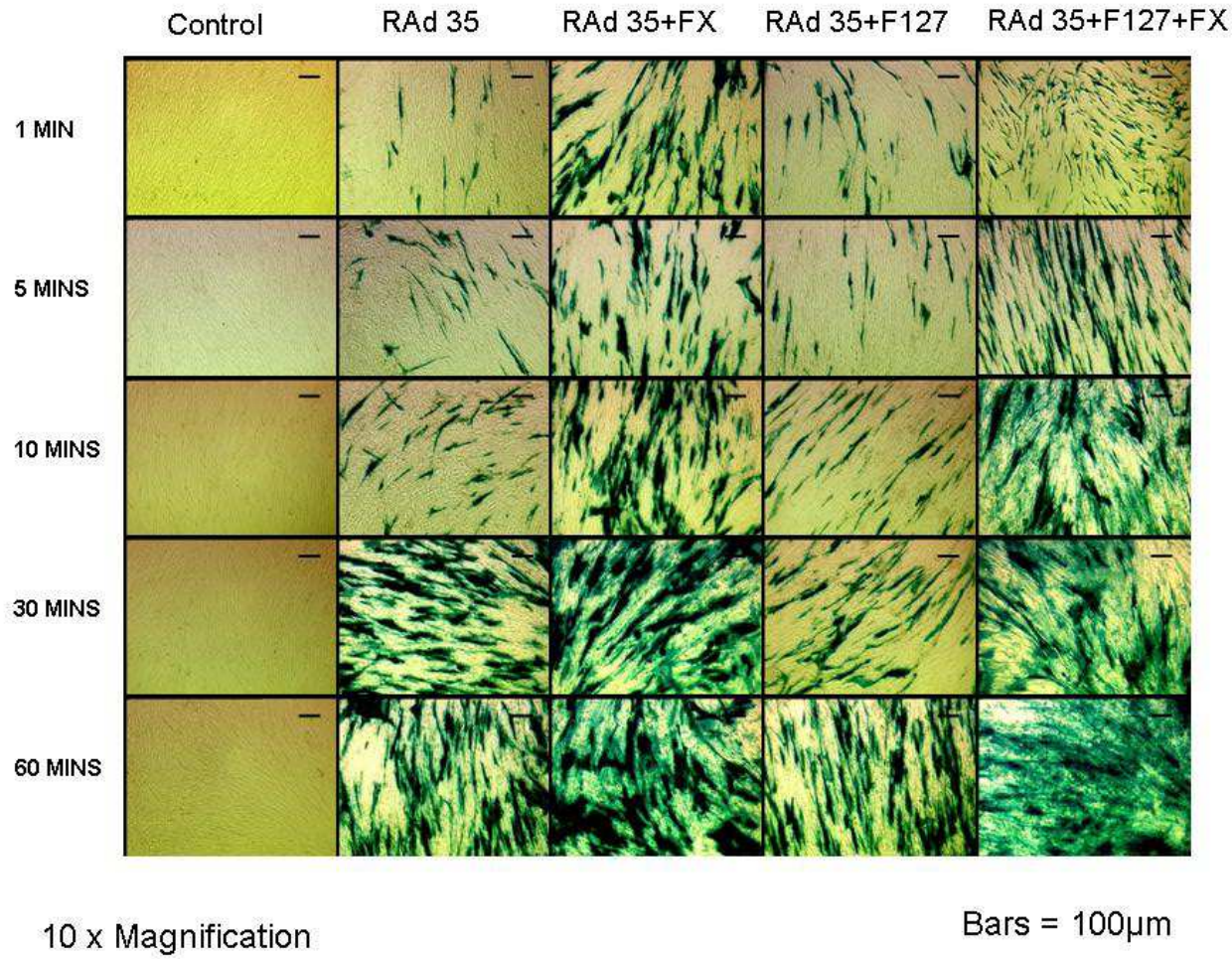

Figure 3-12 Representative images of β-galactosidase expression in HCASMC transduced with AdLacZ +/- Poloxamer 407

RAd 35 = AdLacZ. F127 = Poloxamer 407. FX = Coagulation factor X. Times indicate duration of cell exposure to virus. x10 magnification. Scale bars = 100µm.

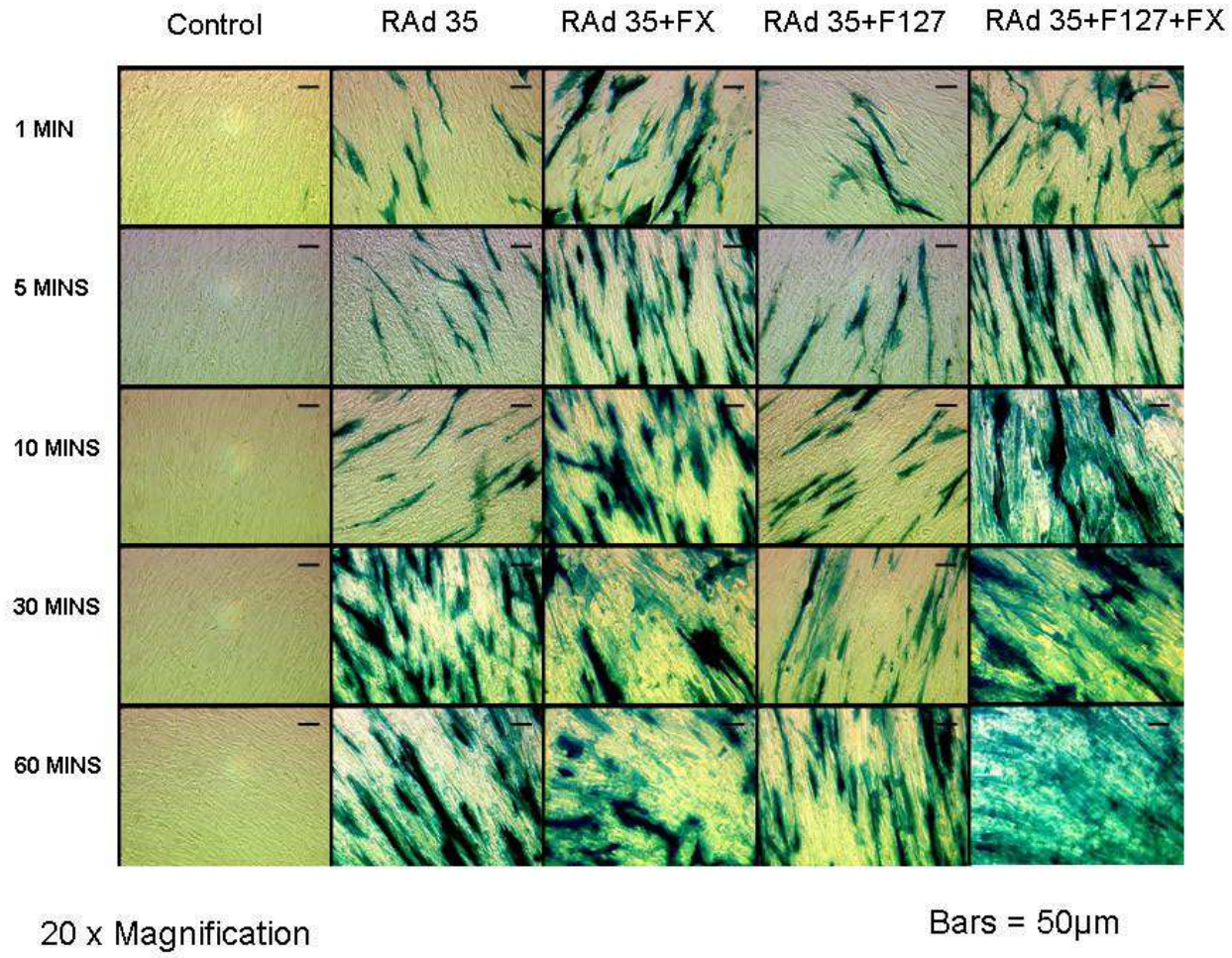

Figure 3-13 Representative images of β-galactosidase expression in HCASMC transduced with AdLacZ +/- Poloxamer 407

RAd 35 = AdLacZ. F127 = Poloxamer 407. FX = Coagulation factor X. Times indicate duration of cell exposure to virus. x20 magnification. Scale bars = 50µm.

3.2.5.3 Delivery of RAd 35 stents

This experiment was performed in 6 animals (Table 3.3). Stents were prepared as described in chapter 2. Each pig received 3 stents: 1 spray coated with RAd35 in 15% poloxamer 407, 1 with manually applied RAd35 in 15% poloxamer 407 and 1 air dried virus without poloxamer. The first three animals received a viral dose of $5x10^9$ pfu/stent, consistent with previously published *in-vivo* work (Table 3.3) (Van Belle et al., 1998). The second group of three animals received a higher dose of $5x10^{10}$ pfu/stent (Table 3.3). All stents were Yukon 3.0x16mm and deployed as described in chapter 2. Representative deployment of a Yukon stent into the RCA is shown in Figure 3.14 Panel A).

The procedure was generally well tolerated. Pig 1009 vomited and clinically aspirated at the time of intubation. Oxygen saturations were maintained at 98% throughout the procedure. Recovery from anaesthesia was more prolonged than normal but no problems were detected with close observation post-procedure and the animal made a full recovery. The Pigs were sacrificed at 7 days post-procedure. Figure 3.14 Panel B shows a representative oversized Yukon in the LCx coronary artery at time of euthanasia.

When the stented vessels were harvested all were patent except the Cx from pig 1009 (a stent with manually applied virus and poloxamer) which was thrombosed. No gross evidence of myocardial infarction was seen on examination of the myocardium supplied by this vessel and the pig had displayed no ill effects prior to euthanasia.

Following incubation with X-gal solution there was no β-galactosidase staining visible in any of the stent groups at either viral dose (Figure 3.15). This suggests that there had been no effective transfer of LacZ to the arterial wall. Staining of samples of liver, lung and spleen however showed marked presence of β-galactosidase consistent with distal organ sequestration of virus as seen in previous animal models following *in-vivo* delivery of unmodified Ad5 (Figure 3.16). These findings were consistent across all studied animals. No β-galactosidase staining was identified in samples of myocardium taken from the left ventricle distal to the deployed stents (Figure 3.16 Panel D).

Table 3-2 Delivery of RAd35 using Poloxamer 407-coated stents

*Air Dried stents did not receive 15% Poloxamer 407 gel. Virus and Poloxamer were pre-mixed at 4°C and stored on ice. RAd 35 – $2.5x10^{11}$ pfu/ml (20µl = $5x10^{9}$ pfu, 200 µl = $5x10^{10}$ pfu). Yukon 3.0x16mm were used in all animals (9-12atm, nominal pressure 9atm). 30s balloon inflations used.

	Vessel				
Pig	**Coated**	**Painted**	**Air Dried**	**Virus (µl)**	**Poloxamer 407***
1007	RCA	Cx	LAD	20	180
1008	RCA	LAD	Cx	20	180
1009	RCA	Cx	LAD	20	180
1010	LAD	RCA	Cx	200	800
1011	RCA	Cx	LAD	200	800
1012	Cx	LAD	RCA	200	800

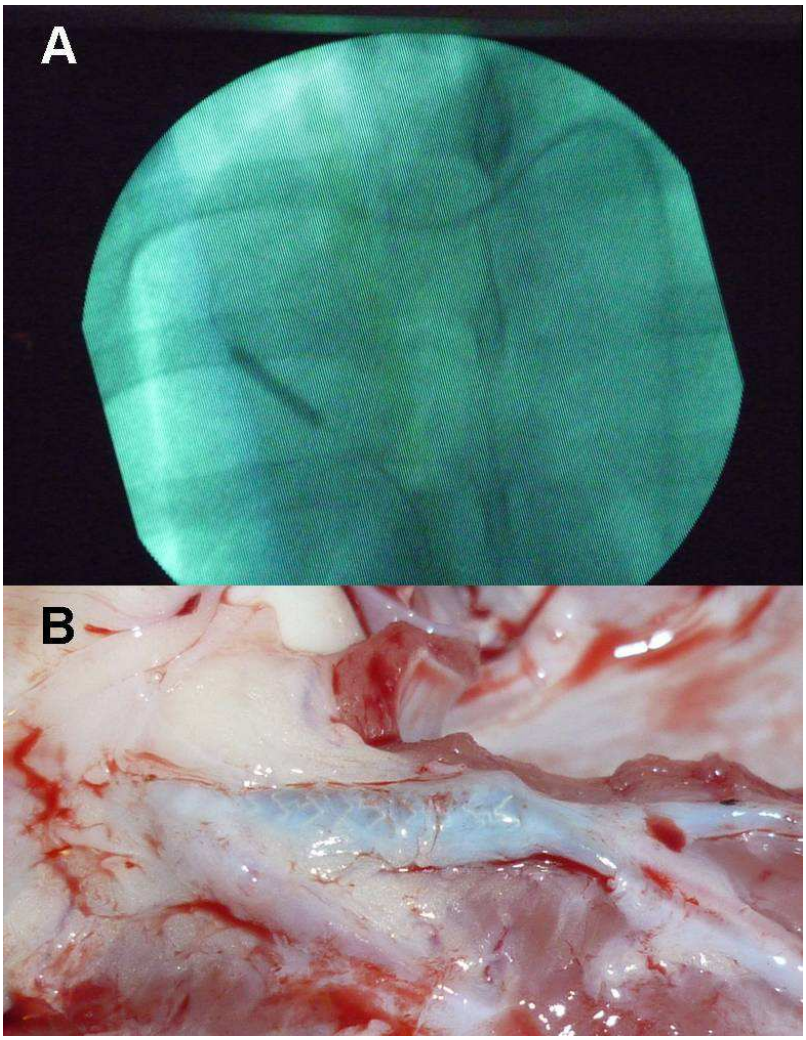

Figure 3-14 Deployment of Yukon stent system in the porcine model

Representative angiogram (PA projection) of Yukon 3.0x16mm stent being deployed in the RCA (A). *In-situ* Yukon stent within the LCx artery of a pig at time of euthanasia (B).

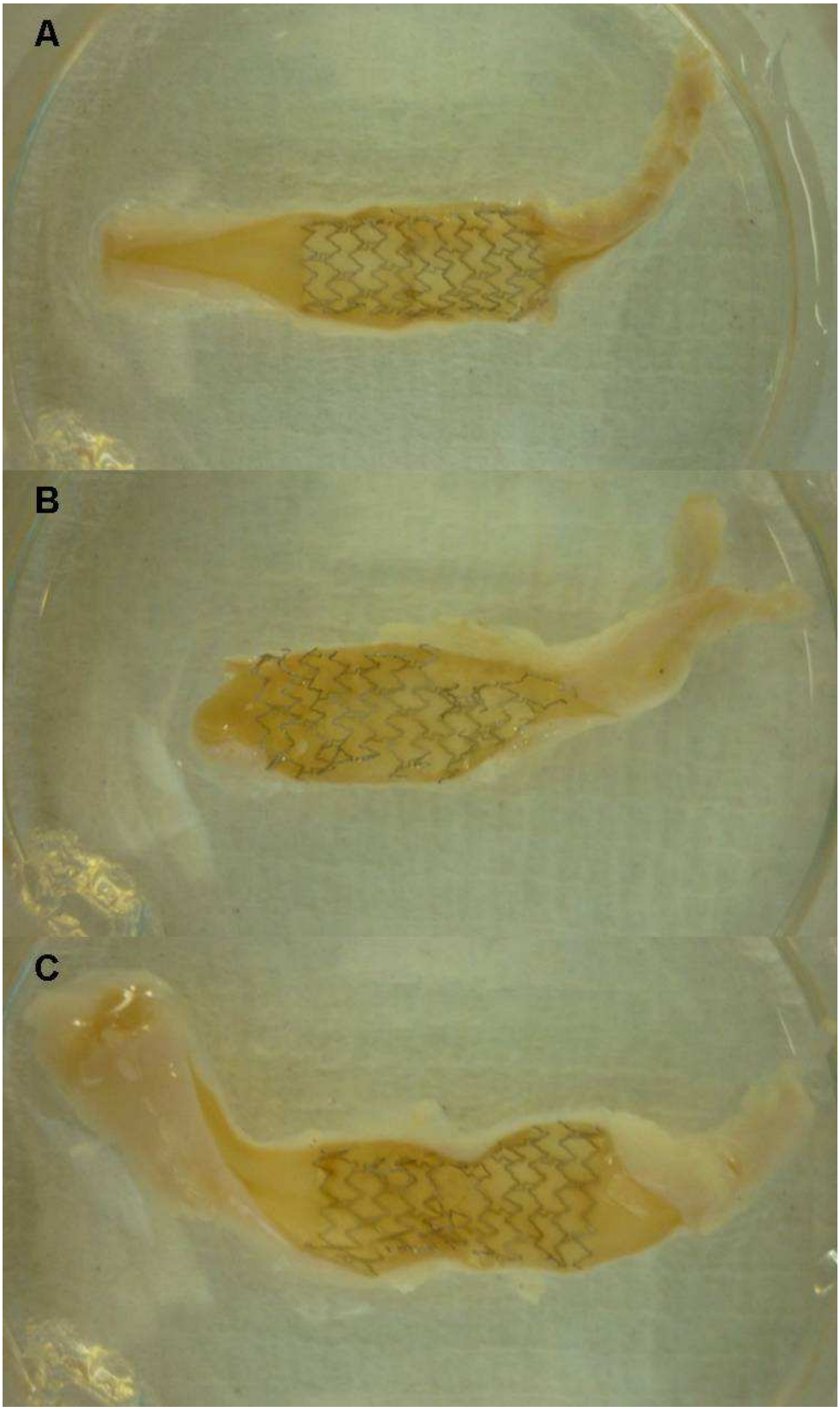

Figure 3-15 Delivery of Yukon stents coated with RAd 35

Representative photographs from Pig 1011. Animal received 3 Yukon stents – Panel A = RCA (Sprayed). Panel B = Cx (Manually applied). Panel C = LAD (Air dried, no poloxamer 407). Viral dose/stent = $5x10^{10}$pfu AdLacZ). No evidence of β-galactosidase staining, following incubation with X-gal working solution, with any coating method. This indicates a failure to achieve significant viral delivery to the vessel wall.

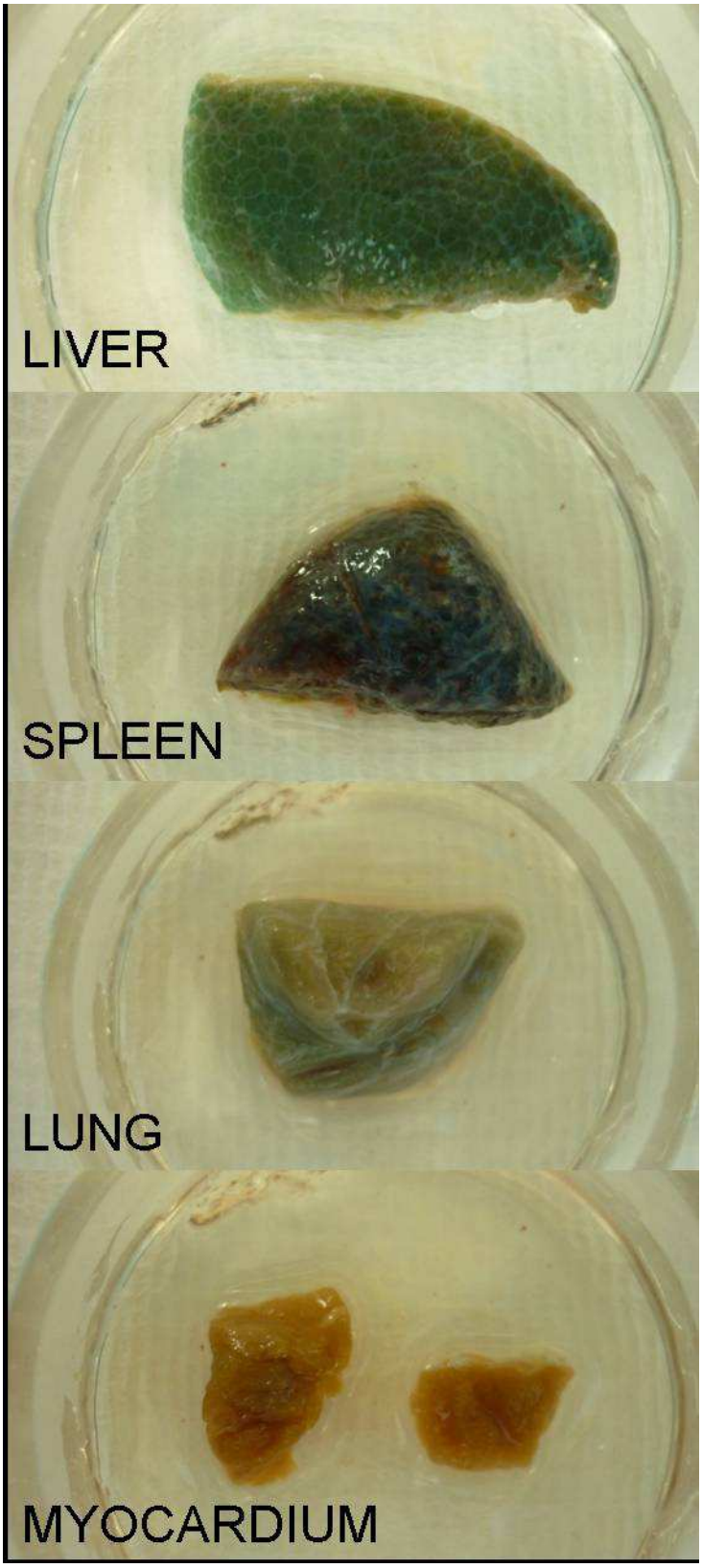

Figure 3-16 Distal organ sequestration of AdLacZ

Representative images from same animal as in Figure 3.15 (Pig 1011). Viral dose $5x10^{10}$pfu AdLacZ per stent. Tissues were formalin-fixed and incubated in X-gal working solution for 24h at 37^{o}C. β-galactosidase staining is present in the liver, spleen and lung consistent with distal organ sequestration of virus. No β-galactosidase activity was present in myocardial samples taken distally to the deployed Yukon stent (RCA). These results were consistent across all animals.

3.3 DISCUSSION

The experiments in this chapter failed to achieve the initial stated aim of successful viral gene delivery to the arterial wall *in-vivo* using local delivery methods. It was therefore not possible to progress to the testing of potential therapeutic vectors with a view to the inhibition of ISR. However, the aim of successfully setting up and reproducibly testing a large-animal model of both stent deployment and local delivery of a vector suitable for future experimental use was achieved.

The pre-clinical restenosis model chosen for the evaluation of vascular gene therapy in this chapter was the porcine model of coronary injury. The undiseased coronary arteries of domestic crossbred swine respond similarly to those in humans following injury, with reliable development of neointima at 28 days following stent implantation (Schwartz et al., 1990, Schwartz et al., 1992, Schwartz et al., 2004). Current consensus group guidelines recommend juvenile normocholesterolaemic domestic cross-bred farm swine or the adult miniature pig as the preclinical models of choice for investigating new stent technologies or novel treatments for ISR (Schwartz et al., 2002). Swine with either familial or diet-induced hypercholesterolaemia are available and do develop advanced atherosclerosis with lesions resembling those in humans, replete with a necrotic core and thin fibrous cap (Granada et al., 2009, Thim et al., 2010). They are, however, impractical for the majority of preclinical studies as the atherosclerotic lesions can take several years to fully develop, resulting in animals that weigh in excess of 200kg (Granada et al., 2009). As well as being time consuming this results in the addition of considerable cost due to animal upkeep and welfare. Furthermore, considerable inter-animal biological variability exists within these models and it remains unclear how closely they truly mimic the human chronic atherosclerotic process (Williams et al., 2012).

In the weight range 30-50kg the heart and coronary arteries of the undiseased domestic pig approximate in both size and anatomical structure to the adult human (Crick et al., 1998). Coronary artery distribution is essentially analogous to that in humans with the LMS arising from the left coronary cusp and bifurcating into the LAD, which runs anteriorly in the interventricular groove, and LCx, running posterolaterally in the atrioventricular groove (Weaver et al., 1986). Similarly the RCA arises from the right coronary cusp and when dominant (~80% of animals) supplies the posterior descending artery which runs in the posterior interventricular groove (Weaver et al., 1986). Differences do arise in cardiac orientation with the more midline position of the porcine heart and its retrosternal apex

resulting from the anteroposterior oval shape of the thorax (as opposed to the lateral ovoid shape in humans) (Crick et al., 1998). This does result in some practical considerations as angiographic views differ slightly when compared to standard human projections (Williams et al., 2012).

When reviewed in 2007, it was noted that adenoviral vectors were the most commonly used gene delivery vector in clinical trials (24.7% of all trials) up to that point (Edelstein et al., 2007). The majority of these trials used vectors based on Ad species C serotype 5 (Bradshaw and Baker, 2012). It was therefore appropriate to manufacture and assess the transduction efficiency of an Ad5 vector *in-vitro* in human VSMC, the ultimate target cell for the prevention of ISR. In keeping with previously published results (and as discussed in Chapter 1) significant transduction could only be obtained at higher viral concentrations. It was the initial plan for the experiments in this chapter to use a second-generation lentiviral vector expressing GFP in the *in-vivo* porcine model. As predicted our manufactured vector was able to efficiently transduce human VSMC *in-vivo* at low viral doses. Concurrent work in our institution had evaluated and identified efficient gene transfer to human VSMC using both integrase-competent and integrase-deficient lentiviral vectors and resultant inhibition of cell proliferation and migration through the delivery of the regulatory protein Nogo-B (Chick et al., 2012). Unfortunately production of suitable titres of lentiviral vector in the laboratory at the required amount proved to be extremely time consuming (3 weeks for a viral preparation to produce enough vector for use in 2-3 animals) and prohibitively expensive. A decision was therefore made to revert to use of Ad5 vectors initially, which can be manufactured at appropriate titres and volumes much more easily, while developing the porcine model and testing local delivery catheters.

Having made the decision to initially test Ad5 vectors it was important to establish the extent of CAR-mediated interaction that could occur with circulating erythrocytes when introduced to the *in-vivo* porcine model. Similarly to in murine models, no haemagglutination with porcine erythrocytes was noted following incubation with the Ad5 vector. This would however, have had to be taken into account should any future therapeutic benefit have been obtained in the porcine model.

Several local delivery catheters had previously been developed and used for the purpose of initially local drug delivery, then ultimately, delivery of viral gene therapy vectors (Lincoff et al., 1994, Barath et al., 1997). However, not only had they generally failed to achieve efficient, reliable or reproducible gene delivery, none remain commercially available

(Sharif et al., 2004). It was important to source suitable alternatives as when the project was first designed it had been planned to use the Dispatch catheter system (Tahlil et al., 1997). The Clearway RX system was at the time a novel and recently available perfusion catheter designed to deliver intracoronary antiplatelet therapy directly to culprit lesions without resultant vessel trauma (Saraf et al., 2008). Its ability to slowly elute a therapeutic solution, and provide occlusive direct contact with the vessel wall at low inflation pressure suggested potential utility as a delivery catheter for a gene therapy vector.

To test its utility it was first used to deliver both Ad5 expressing GFP then Ad5 expressing LacZ to *ex-vivo* segements of porcine coronary artery. Experimental conditions were set to as closely mimic *in-vivo* conditions as possible. Initial results were encouraging with evidence of successful viral transduction of the vessel wall obtained using both vectors.

Translation to the *in-vivo* porcine model was to prove initially problematic as 4 of the initial 6 animals suffered from intra-procedural dysrhythmic death. The fifth also suffered from a dysrhythmia but was successfully resuscitated. There appeared to be no clear procedural reason for this. Appropriate antiplatelet therapy with aspirin and clopidogrel had been administered with animals receiving a 150mg loading dose of each on the preprocedural day and 75mg of each on the day of the procedure. They were also adequately anticoagulated with 3000iU of heparin administered intravenously at the start of the procedure. It has been noted that peri-procedural mortality is higher in the porcine model than for human procedures with published guidelines stating acceptable rates of <15% early mortality and <25% overall mortality for a complete study (Schwartz et al., 2002). It is noted, however, that these rates are somewhat high and that this level of animal loss suggests a problem with either the device/agent being tested or general method and technique (Schwartz et al., 2002). More recent procedural guidance has suggested that while some deaths will be related to the experimental nature of testing new technologies, it is likely that a significant proportion are due to poor technique or inexperienced operators, and therefore potentially avoidable (Williams et al., 2012). These experienced investigators report a mortality of <1% at their institution.

All of the deaths in this initial group occurred before the introduction of virus and therefore could not be explained by this. At this point the experiment was paused and advice sought from our institutional vet, veterinary anaesthetists from the University of Glasgow Vet School and also from investigators at another institution with considerable experience in the use of this experimental model. It was noted that all of the animals came from the same

litter. Two potential explanations were put forward. It has been noted that pigs can be genetically susceptible to malignant hyperthermia (known as Porcine Stress Syndrome) and that this can be induced by inhalational anaesthetics or nitrous oxide. This is known to be common in pigs due to inbreeding and is invariably fatal (Williams et al., 2012). All of our animals were receiving a combination of isoflurane and nitrous oxide as maintenance anaesthesia. At this point temperature monitoring was not in place. The second possible explanation is that, again due to inbreeding, pigs can be susceptible to dysrhythmia secondary to cardiac channelopathies or Long QT syndrome (Dr Julian Gunn, University of Sheffield, Personal communication). The single-lead ECG tracings were retrospectively reviewed for all the dead animals. While the QT segments did not appear to be relatively prolonged, no reference range for a "normal" pig QT interval exists in the literature therefore this was difficult to quantify.

Based on this, several alterations were made to the experimental protocol. Use of a rectal temperature probe with continuous monitoring and an attached heated mat to maintain a core temperature of 37^{o}C was introduced. A decision was also made to administer prophylactic IV antiarrhythmic therapy at the beginning of the procedure. A regimen of amiodarone 75mg and lignocaine 50mg given as IV bolus at the start of the procedure was introduced. Although this can carry additional risk as both agents can also be proarrhythmic it was felt to be an appropriate strategy. From this point until the end of the experiments, no malignant hyperthermia or arrhythmic death occurred. The single animal that died in a later experiment suffered acute stent thrombosis.

Using the Clearway RX to deliver two concentrations of Ad5 expressing LacZ ($1x10^{10}$pfu and $5x10^{10}$pfu) to porcine coronary arteries previously treated with a BMS did not result in significant viral transduction of the arterial wall as assessed by β-galactosidase staining. The most likely explanation for this is that the Clearway RX was unable to provide a long enough duration of virus contact with the vessel wall. The virus was diluted to a final volume of 1ml. It was felt that to dilute the Ad5 vector in a larger volume than this (with resultant drop in viral concentration) would significantly impair effective transduction. Therefore the duration of viral delivery was short – with 1ml delivered at a pressure of 2atm – at less than 60 seconds. To keep the balloon inflated in the hope that virus would be kept in contact with the vessel for longer, 0.9% saline solution was infused through a three-way tap after all the virus had been injected, at a pressure of 1atm. This likely contributed to washing the virus into the circulation however. Once the perfusion balloon was deflated, coronary blood flow restored which completed the wash out of the virus. To have a

constant viral infusion at an effective concentration would have resulted in a massive overall dose exposing the animal to a considerable risk of toxicity.

The only other commercially available perfusion catheter that could be sourced was the GENIE drug delivery device. The design of this catheter, with its reservoir that could theoretically hold a concentrated virus solution in contact with the vessel wall for longer than the Clearway RX was felt to be a potentially viable alternative. Again no significant vessel transduction could be obtained using Ad5 LacZ. Using a high grade viral vector it was felt suitable to dilute to 5ml final volume giving a concentration of $2.5x10^{10}$ pfu/ml. In pre-clinical studies of paclitaxel to porcine coronary arteries a volume range of 2.9 +/- 1.6ml was delivered over 120seconds (Dommke et al., 2007). Despite using a constant delivery pressure of 2atm and a fixed volume of 5ml, the viral delivery time achieved was variable at 2.75+/-0.89mins (Range 1-6 minutes). Again balloon inflation was maintained using an indeflator filled with 0.9% saline maintained at 2atm connected to the GENIE device via a three-way tap to avoid balloon deflation after delivery of the virus solution was complete. This provided a mean balloon inflation time of 7.08+/-1.88 minutes. Again, unavoidably, this may have resulted in a degree of virus wash-out. The variability in perfusion/inflation time despite constant pressure and volume is likely explained by slight variations in vessel diameter as this was determined by visual assessment.

Although an improvement compared with the Clearway RX, a mean incubation time of 7 minutes before restoration of coronary flow is still not enough to provide measurable *in-vivo* VSMC transduction using unmodified Ad5 vectors. This was confirmed by the *in-vitro* transduction of HCASMC. The incubation (inflation) time achieved was limited due to poor tolerance of the procedure by the animals as 50% (3 animals) suffered from complications occurring at the time of GENIE inflation. The pigs used in standard pre-clinical models are juvenile, healthy animals that have minimal pre-existing coronary collateral flow (Maxwell et al., 1987, White et al., 1992). They therefore lack ischaemic preconditioning and are susceptible to complications with more prolonged balloon inflation.

In conclusion, these findings suggest that there is little clinical utility in the use of unmodified Ad5 vectors for viral gene delivery to the vasculature, post-stent delivery *in-vivo,* using currently available occlusive local delivery catheters with subsequent restoration of coronary flow.

The modern clinical setting favours the use of a stent platform to deliver therapeutic agents targeted at reducing ISR. Although results in pre-clinical models have been encouraging it has proven difficult to stably attach a given delivery vector to a metal platform and allow controlled and efficacious elution *in-vivo*. Methods used have become increasingly complex, ranging from the use of positively charged polymer coatings to "bind" more negatively charged viral particles (Johnson et al., 2005) to complex synthetic binding strategies (Fishbein et al., 2008). The final experiments in this chapter pursued a simpler approach.

In previously reported pre-clinical studies, the biocompatible polyoxyethyl-polyoxypropyl block co-polymer poloxamer 407 has been shown to increase VSMC transduction *in-vitro* and *in-vivo* with adenoviral and lentiviral vectors (Dishart et al., 2003, Feldman et al., 1997, Maillard et al., 2000, March et al., 1995, Van Belle et al., 1998). March *et al* identified a greater than 10-fold increase in VSMC transduction *in-vitro* when Ad expressing LacZ was combined with a 15% poloxamer 407 solution (March et al., 1995). They hypothesised that the poloxamer gel acted as a delivery reservoir for the virus and improved gene delivery by maintaining a high pericellular viral concentration. It has also been suggested that interactions between the poloxamer gel and cell membrane can facilitate cellular uptake of Ad (Cho et al., 2000). Subsequently, Feldman *et al* used a 15% poloxamer gel to improve the transduction efficiency of a similar Ad5 vector when delivered to balloon-injured rat carotid arteries *in-vivo* (Feldman et al., 1997). Furthermore, they showed that, importantly, using the poloxamer gel reduced the required incubation time without compromising the transduction efficiency. No specific tissue toxicity was observed, consistent with prior reports (Johnston and Miller, 1985). Using a channel balloon local delivery catheter, the same group identified a 3- to 15-fold increase in transduction efficiency when delivered to non-stented rabbit iliac arteries and a 7-fold increase when delivered prior to stent insertion (Van Belle et al., 1998). Their method allowed a reduction in transduction time from 30 to 5 minutes with minimal reduction in efficiency. The use of poloxamer gel did not significantly compromise vessel patency (thrombotic occlusion was rare) in these studies and prior work had shown that the gel disappears over 1-2hours *in-vivo* (Simons et al., 1992).

Review of the literature did not suggest that this approach had been taken any further. Certainly the above results were encouraging in that a poloxamer gel/Ad5 combination could be an attractive way to achieve effective local biological effects with shorter transduction times. It should be noted however, that in all of the above *in-vivo* studies

vessel blood flow was ceased during the incubation period, either by temporary vessel ligation or balloon occlusion. This is an important factor when considering the translation of results to a coronary artery model, where as previously described, prolonged flow occlusion can be problematic.

A strategy was therefore devised using the thermoreversible properties of poloxamer 407 and utility of the spray-coatable Yukon stent system (Mehilli et al., 2006) to create an Ad5 LacZ-eluting stent platform with a transient biocompatible polymer predicted to last 1-2 hours in the circulation (Simons et al., 1992).

This approach again proved unsuccessful with no evidence of effective viral transduction of the arterial wall. In keeping with previous *in-vivo* studies, it became clear that the virus had sequestrated to non-target organs, namely the liver, spleen and lung. No evidence of viral transduction was seen within the myocardium. As discussed in chapter 1 this occurs due to Ad5 interaction with components of the circulating blood stream, principally coagulation factor X (Coughlan et al., 2010, Bradshaw and Baker, 2012). It had been hoped that the poloxamer 407 would overcome this effect, however it is highly water soluble and therefore likely dissolved in the circulation during positioning and deployment of the coated Yukon stents. With previous *in-vivo* models there had always been a short period of stasis when the poloxamer/virus mix was introduced to the target vasculature before restoration of circulating blood flow. This is clearly not possible in the coronary circulation with a percutaneously delivered device. Success of current DES technology utilises the liphophilic properties of the antiproliferative agents to influence drug absorption into the arterial wall as opposed to being dissolved and lost in the circulation (Garg et al., 2013). The lack of lipophilicity and marked aqueous solubility of poloxamer 407 clearly inhibits its effectiveness in this setting.

In summary, despite initial procedural issues a reproducible model of porcine stent implantation suitable for the evaluation of vascular gene therapy was developed. However, successful transduction of the stented arterial wall using unmodified Ad5 vectors could not be achieved using two commercially available delivery catheters or a stent platform coated with a biocompatible thermoreversible gel polymer. In view of the disappointing nature of these results and the costs involved in using this pre-clinical model, it was felt that further development of suitable viral vectors and alternative delivery methods was required. Both of these approaches are being investigated within our institution and will be further

discussed in chapter 6. However, both fell out-with the time frame available for completion of this PhD.

The focus of this project therefore switched to the potential role of microRNAs in the development of ISR and the evaluation of their manipulation as a potential therapeutic option using the porcine model of intracoronary stent delivery. This will be discussed in the following chapter.

4 Role of MicroRNAs in a Porcine model of In-stent Restenosis

4.1 Introduction

It was the aim of this chapter to investigate and validate expression levels of miRs thought to be important in the maintenance of vascular function and development of ISR and with potential for downstream therapeutic modulation. It was hypothesised that expression patterns of regulatory miRs in the vasculature would alter in response to stent-induced injury.

Firstly, *in-vitro* experiments were performed using human coronary artery smooth muscle cells (HCASMC), the principle cell type involved in the formation of neointimal lesions. Expression levels of miRs implicated in the control of VSMC phenotype were assessed in HCASMC stimulated to a proliferative phenotype by classical mitogens and to a migratory phenotype using a wounding assay.

Secondly, all previously reported studies in this area have used *in-vitro* or *in-vivo* rodent models of vascular injury. A more clinically relevant large animal (porcine) model of in-stent restenosis was therefore utilised to assess the expression levels of miRs previously reported to play a role in VSMC regulation as well as novel targets. *In-situ* hybridization was used to co-localise dysregulated miRs within neointimal lesions to establish potential targets for future therapeutic modulation.

4.2 Results

4.2.1 Changes in microRNA expression levels as HCASMCs proliferate

Through the use of miRNA microarray and confirmation using qRT-PCR and Northern Blot analysis, Ji *et al*, identified 11 miRs that were significantly dysregulated in rat carotid arteries following balloon injury (Ji et al., 2007). MiRs-21, -146, -214 and -352 were all upregulated following vascular injury while miRs-125a, -125b, -133a, -143, -145, -347 and -365 were significantly downregulated. We wished to establish the importance of these miRs in a human *in-vitro* model. Confluent HCASMC were incubated with serum-free media for 48 hours to induce a differentiated contractile state. The cells were then stimulated to dedifferentiate to a proliferative phenotype by incubation with classical mitogens (Newby and George, 1993): 15% FCS, PDGF, IL-1α, PDGF and IL-1α in combination and bFGF. RNA was extracted from the cells at various time points namely 1, 5, 18 and 24 hours. Expression levels of miRs at each time point were established using qRT-PCR and comparison made to differentiated cells held in serum free media for an identical length of incubation.

The expression level of miR-21 was increased 2.5-3 fold at 1 hour when stimulated by FCS, PDGF or PDGF+IL-1α (Figure 4.4). Interestingly, levels had returned to baseline by 5 hours. IL-1α in isolation and bFGF had no significant effect on miR-21 levels. Levels of mIR-146a were increased by stimulation with FCS and remained elevated out to 18 hours (Figure 4.5). In isolation PDGF had no effect, and IL-1α only increased levels at 18 hours, however, in combination miR-146a expression was increased 2.5 fold at 1 hour, 5.5 fold at 5 hours and 4 fold at 18 hours (Figure 4.5). Only a marginal effect was seen using bFGF with a 2 fold increase at 18 hours only. Expression levels of miR-146b, however, were unaffected by mitogen stimulation at the measured time points (Figure 4.6). MiR-365 expression levels were increased between 3-6 fold by all mitogens at 1 hour, again returning to baseline by 5 hours (Figure 4.7). Levels of miR-221 (Figure 4.8), miR-143/145 (Figure 4.9) and miR-133a (Figure 4.10) were unchaged compared with differentiated cells at all time points.

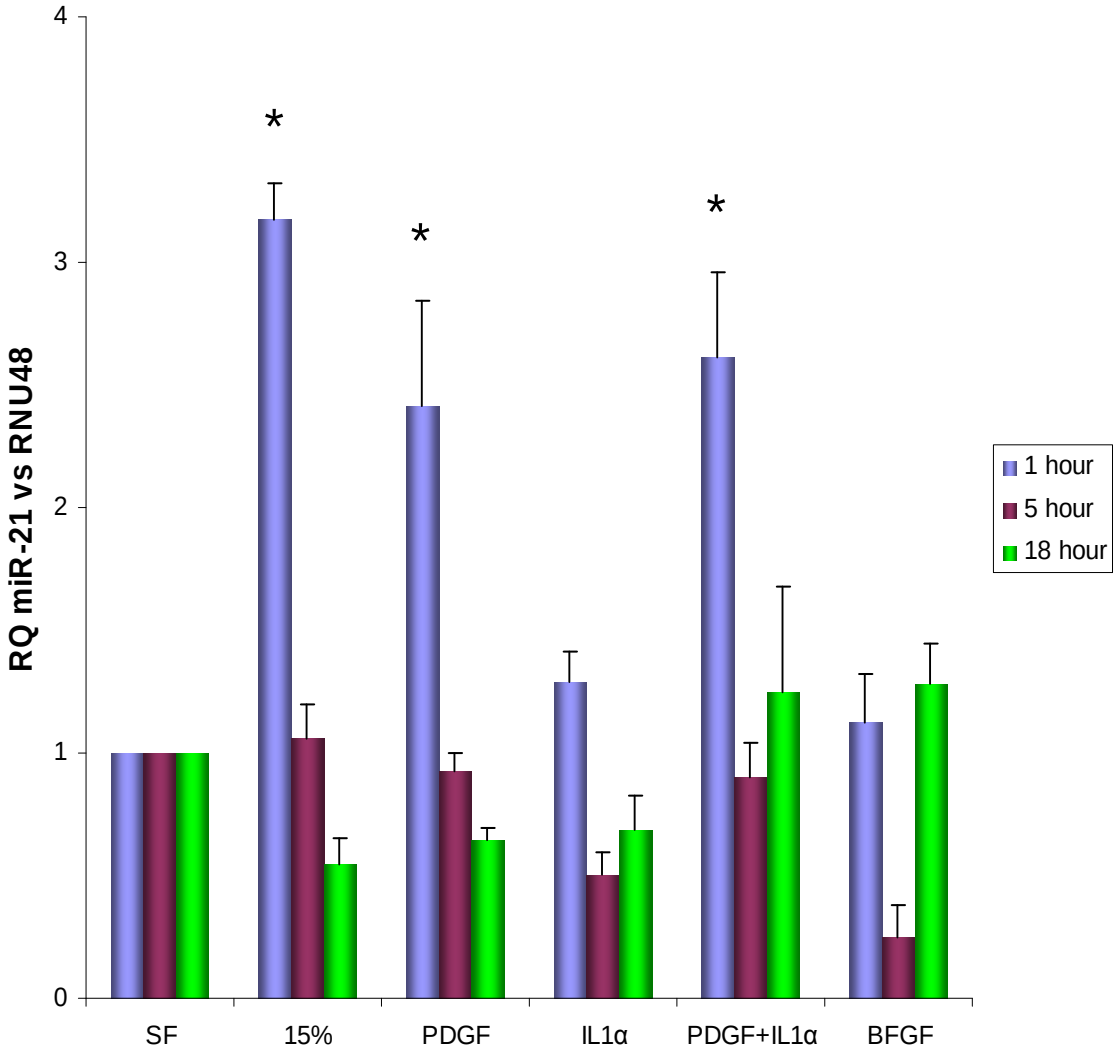

Figure 4-1 Change in expression level of miR-21 with HCASMC phenotypic switch

In vitro human coronary artery smooth muscle cells (HCASMC) were incubated with serum free media to induce a differentiated contractile state. Cells then underwent mitogen-mediated stimulation to a dedifferentiated proliferative phenotype. RNA was extracted from cells at each time point and miR-21 expression determined using qRT-PCR with RNU48 as an endogenous control. All comparisons made to control (differentiated) cells held in serum-free (0.1%) media for an identical length of time. Results displayed as Relative Quantity (RQ) $\pm$ RQmax calculated using the $2^{-\Delta\Delta Ct}$ method. * = $p<0.01$, # = $p<0.05$, No symbol = no significant change, One-way ANOVA with Tukey post-correction. SF – serum free media. 15% = SMC media with 15% serum. PDGF – Platelet derived growth factor. IL1α – interleukin-1α. BFGF – basic fibroblast growth factor.

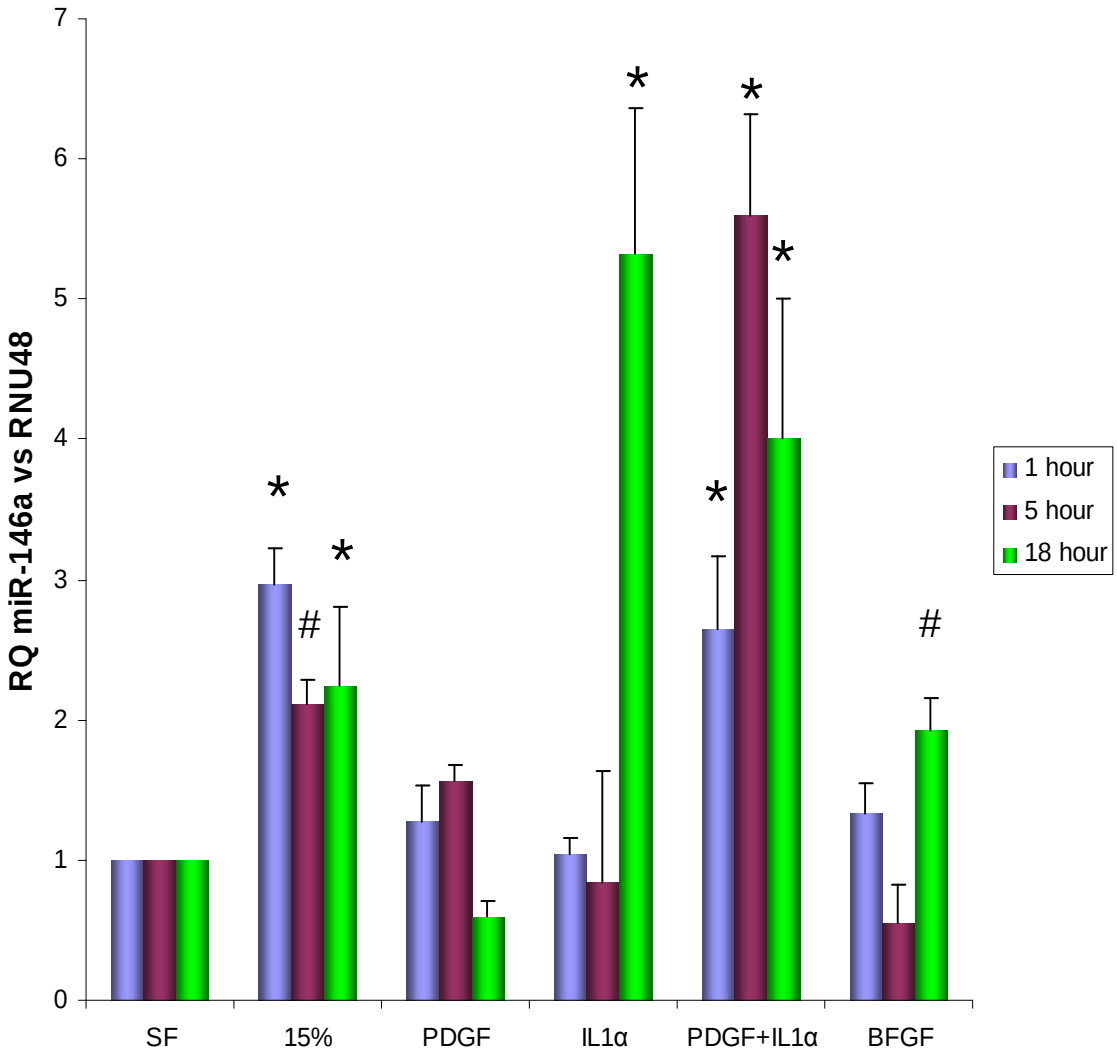

Figure 4-2 Change in expression level of miR-146a with HCASMC phenotypic switch

In vitro human coronary artery smooth muscle cells (HCASMC) were incubated with serum free media to induce a differentiated contractile state. Cells then underwent mitogen-mediated stimulation to a dedifferentiated proliferative phenotype. RNA was extracted from cells at each time point and miR-146a expression determined using qRT-PCR with RNU48 as an endogenous control. All comparisons made to control (differentiated) cells held in serum-free (0.1%) media for an identical length of time. Results displayed as Relative Quantity (RQ) $\pm$ RQmax calculated using the $2^{-\Delta\Delta Ct}$ method. * = $p<0.01$, # = $p<0.05$, No symbol = no significant change, One-way ANOVA with Tukey post-correction. SF – serum free media. 15% = SMC media with 15% serum. PDGF – Platelet derived growth factor. IL1α – interleukin-1α. BFGF – basic fibroblast growth factor.

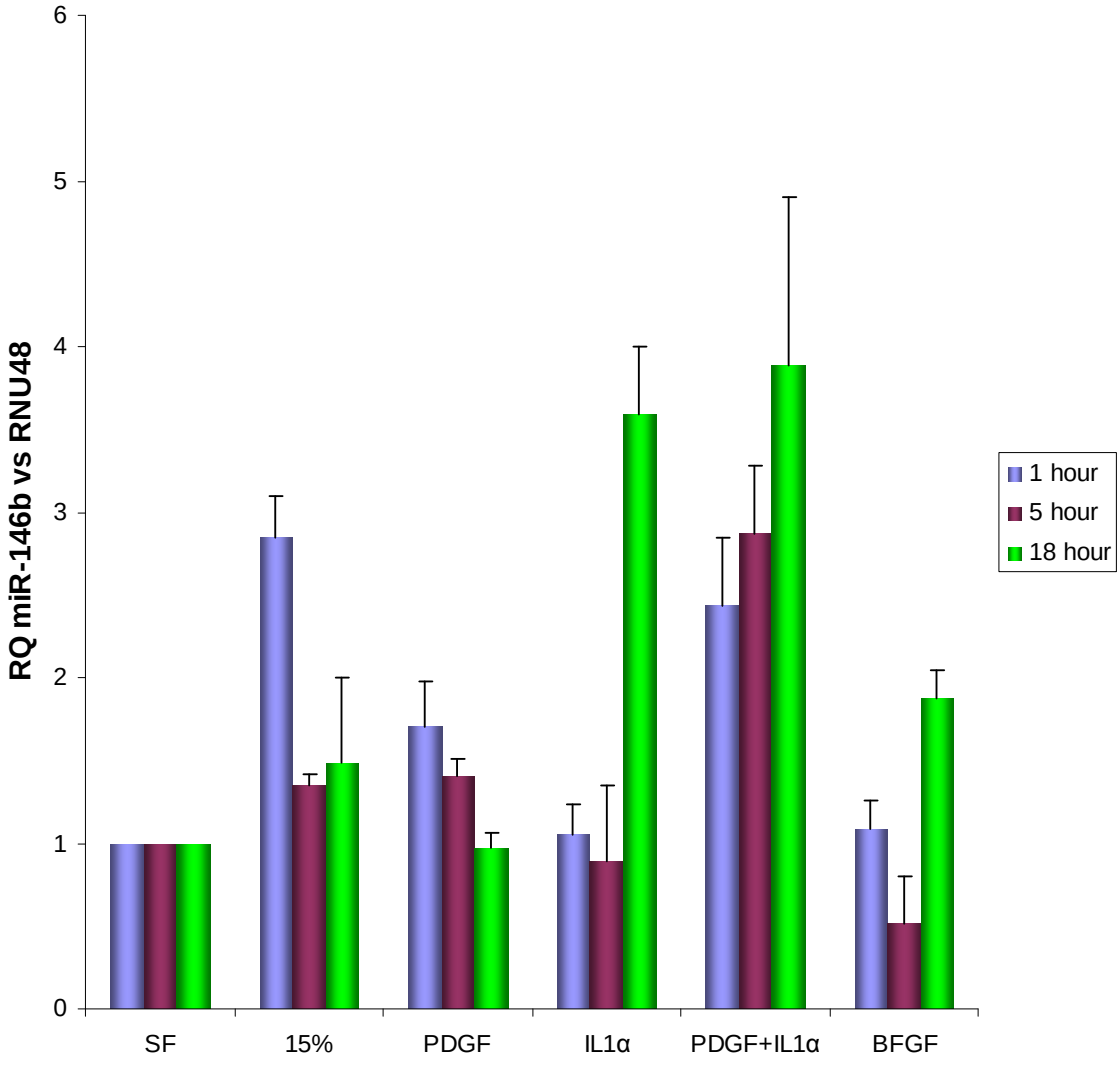

Figure 4-3 Expression level of miR-146b with HCASMC phenotypic switch

In vitro human coronary artery smooth muscle cells (HCASMC) were incubated with serum free media to induce a differentiated contractile state. Cells then underwent mitogen-mediated stimulation to a dedifferentiated proliferative phenotype. RNA was extracted from cells at each time point and miR-146b expression determined using qRT-PCR with RNU48 as an endogenous control. All comparisons made to control (differentiated) cells held in serum-free (0.1%) media for an identical length of time. Results displayed as Relative Quantity (RQ) $\pm$ RQmax calculated using the $2^{-\Delta\Delta Ct}$ method. No significant change in expression level was identified at any time point compared to differentiated cells (One-way ANOVA with Tukey post-correction). SF – serum free media. 15% = SMC media with 15% serum. PDGF – Platelet derived growth factor. IL1α – interleukin-1α. BFGF – basic fibroblast growth factor.

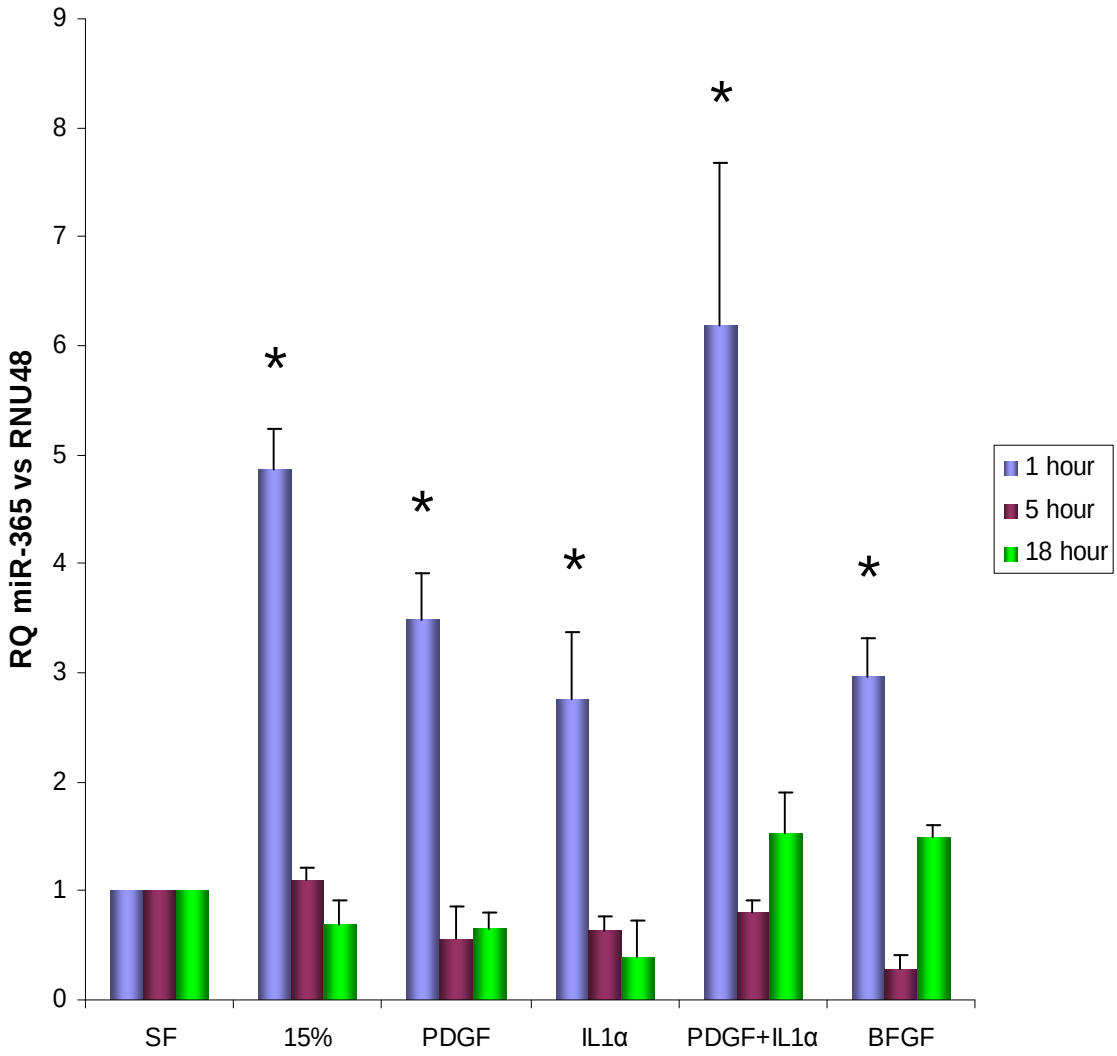

Figure 4-4 Change in expression level of miR-365 with HCASMC phenotypic switch

In vitro human coronary artery smooth muscle cells (HCASMC) were incubated with serum free media to induce a differentiated contractile state. Cells then underwent mitogen-mediated stimulation to a dedifferentiated proliferative phenotype. RNA was extracted from cells at each time point and miR-365 expression determined using qRT-PCR with RNU48 as an endogenous control. All comparisons made to control (differentiated) cells held in serum-free (0.1%) media for an identical length of time. Results displayed as Relative Quantity (RQ) $\pm$ RQmax calculated using the $2^{-\Delta\Delta Ct}$ method. * = $p<0.01$, # = $p<0.05$, No symbol = no significant change, One-way ANOVA with Tukey post-correction. SF – serum free media. 15% = SMC media with 15% serum. PDGF – Platelet derived growth factor. IL1α – interleukin-1α. BFGF – basic fibroblast growth factor.

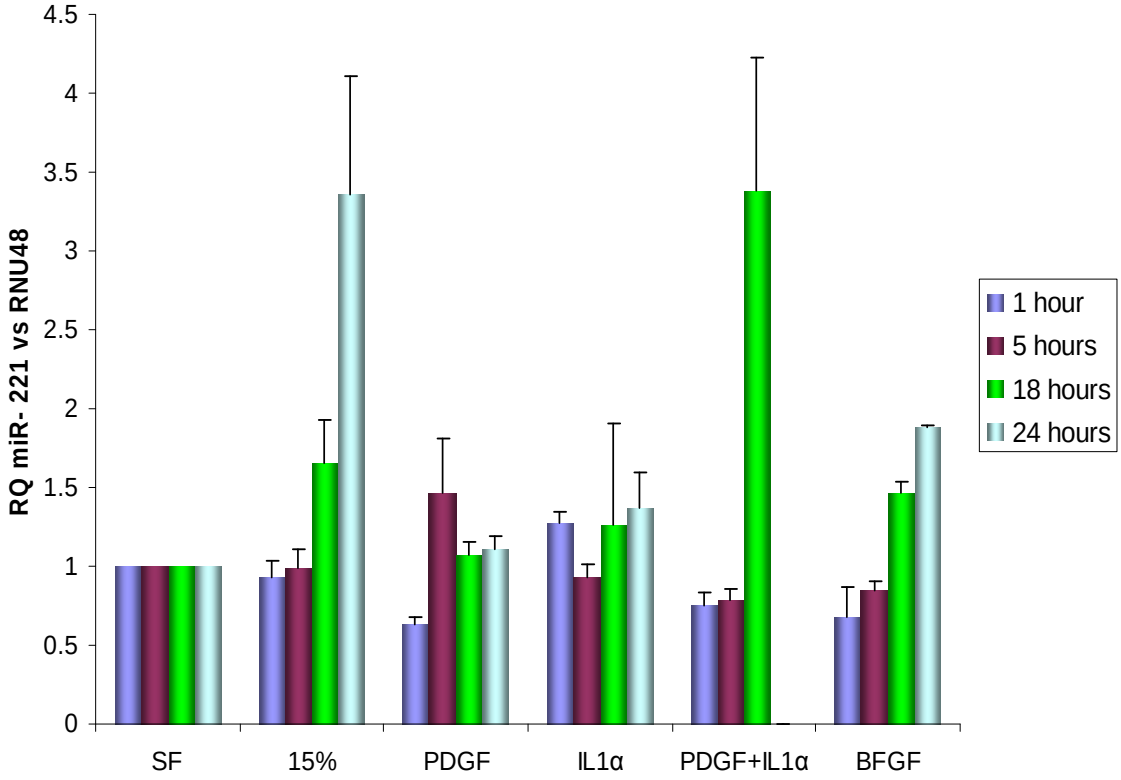

Figure 4-5 Expression level of miR-221 with HCASMC phenotypic switch

In vitro human coronary artery smooth muscle cells (HCASMC) were incubated with serum free media to induce a differentiated contractile state. Cells then underwent mitogen-mediated stimulation to a dedifferentiated proliferative phenotype. RNA was extracted from cells at each time point and miR-221 expression determined using qRT-PCR with RNU48 as an endogenous control. All comparisons made to control (differentiated) cells held in serum-free (0.1%) media for an identical length of time. Results displayed as Relative Quantity (RQ) $\pm$ RQmax calculated using the $2^{-\Delta\Delta Ct}$ method. No significant change in expression level was identified at any time point compared to differentiated cells (One-way ANOVA with Tukey post-correction). SF – serum free media. 15% = SMC media with 15% serum. PDGF – Platelet derived growth factor. IL1α – interleukin-1α. BFGF – basic fibroblast growth factor.

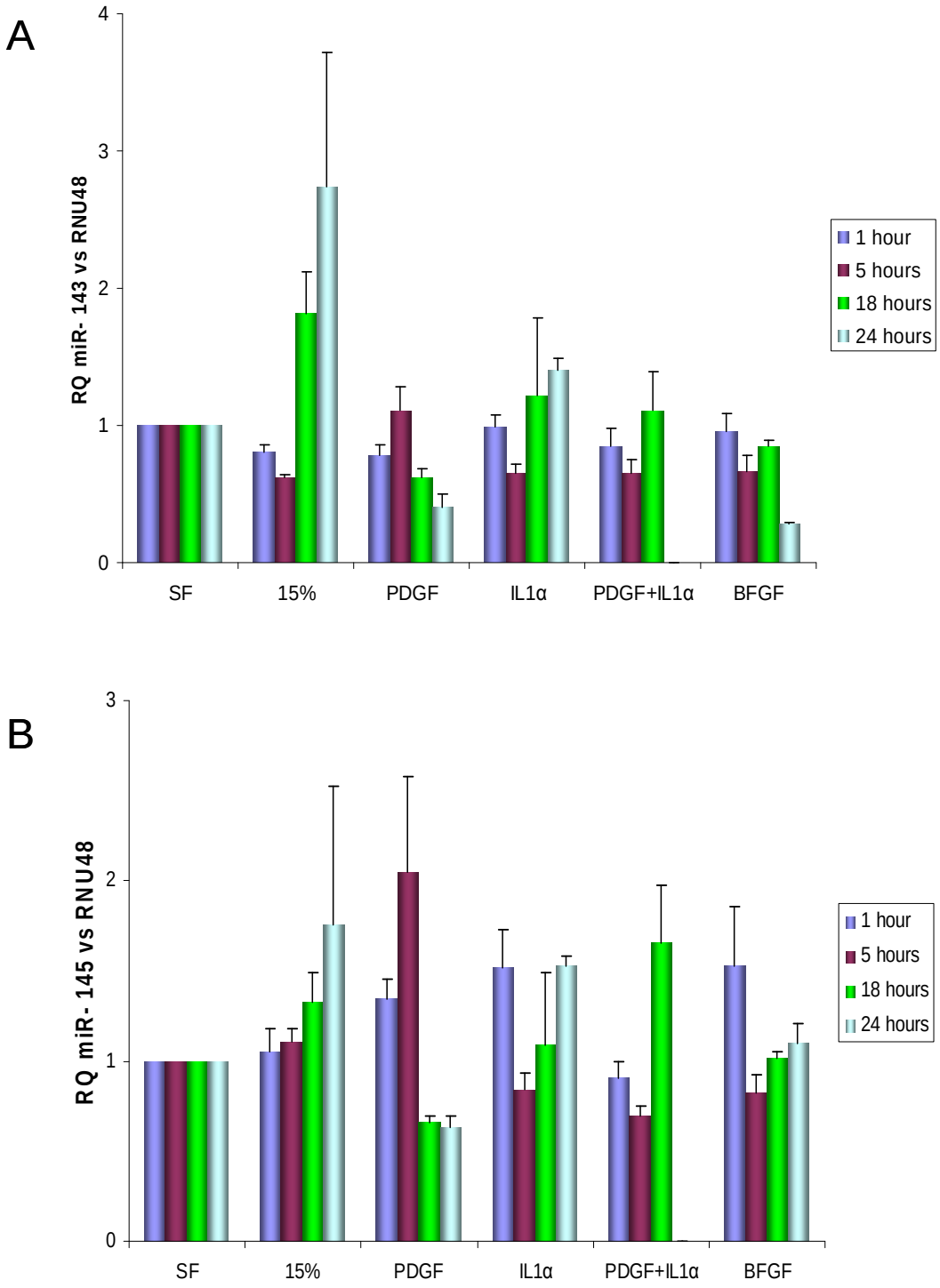

Figure 4-6 Expression level of miR-143 and miR-145 with HCASMC phenotypic switch

In vitro human coronary artery smooth muscle cells (HCASMC) were incubated with serum free media to induce a differentiated contractile state. Cells then underwent mitogen-mediated stimulation to a dedifferentiated proliferative phenotype. RNA was extracted from cells at each time point and miR-143 (Panel A) and miR-145 (Panel B) expression determined using qRT-PCR with RNU48 as an endogenous control. All comparisons made to control (differentiated) cells held in serum-free (0.1%) media for an identical length of time. Results displayed as Relative Quantity (RQ) $\pm$ RQmax calculated using the $2^{-\Delta\Delta Ct}$ method. No significant change in expression level was identified at any time point, for either miR, compared to differentiated cells (One-way ANOVA with Tukey post-correction). SF – serum free media. 15% = SMC media with 15% serum. PDGF – Platelet derived growth factor. IL1α – interleukin-1α. BFGF – basic fibroblast growth factor.

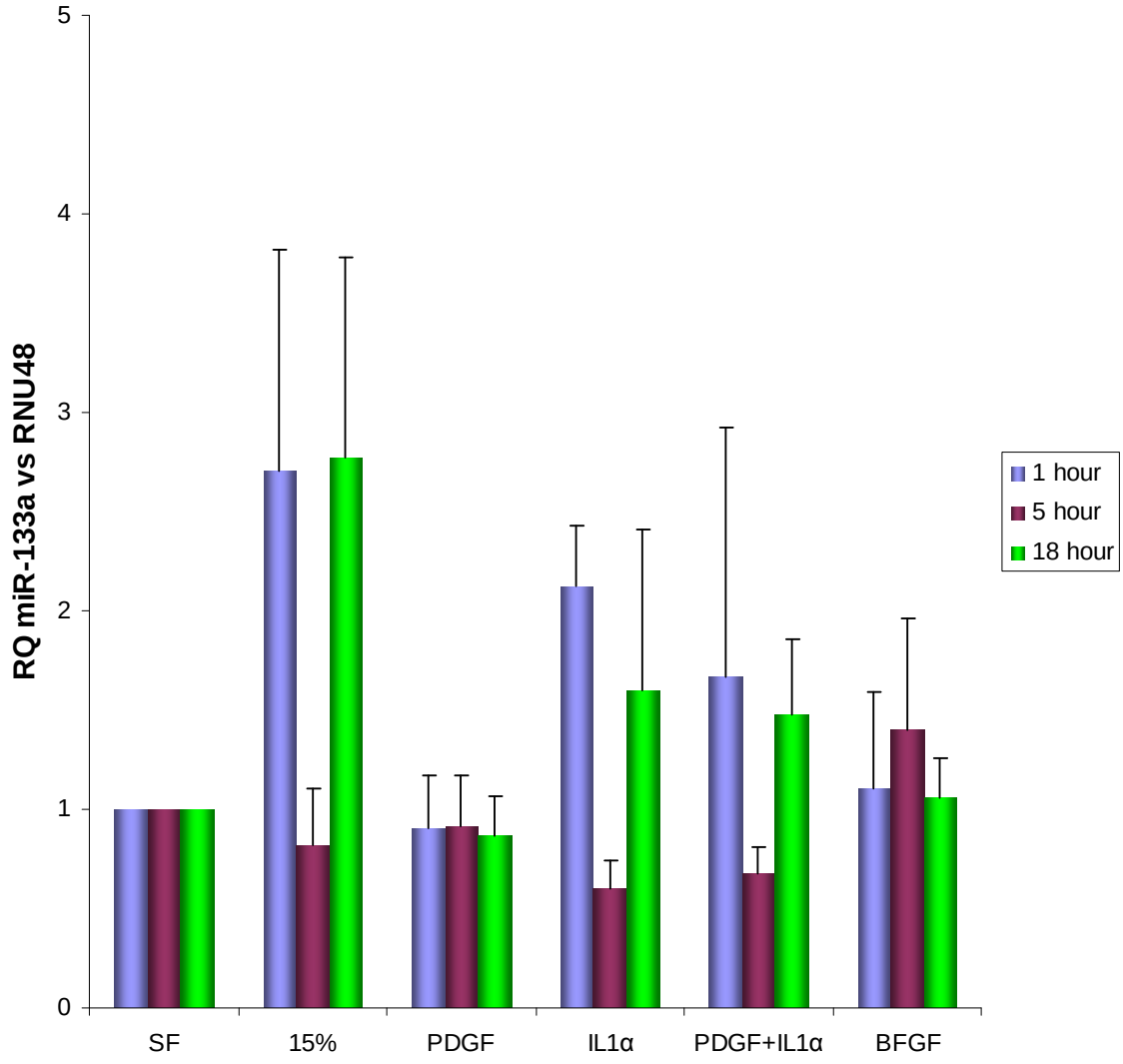

Figure 4-7 Expression level of miR-133a with HCASMC phenotypic switch

In vitro human coronary artery smooth muscle cells (HCASMC) were incubated with serum free media to induce a differentiated contractile state. Cells then underwent mitogen-mediated stimulation to a dedifferentiated proliferative phenotype. RNA was extracted from cells at each time point and miR-133a expression determined using qRT-PCR with RNU48 as an endogenous control. All comparisons made to control (differentiated) cells held in serum-free (0.1%) media for an identical length of time. Results displayed as Relative Quantity (RQ) $\pm$ RQmax calculated using the $2^{-\Delta\Delta Ct}$ method. No significant change in expression level was identified at any time point compared to differentiated cells (One-way ANOVA with Tukey post-correction). SF – serum free media. 15% = SMC media with 15% serum. PDGF – Platelet derived growth factor. IL1α – interleukin-1α. BFGF – basic fibroblast growth factor.

4.2.2 MicroRNA expression alters as HCASMC switch to a migratory phenotype

To establish a potential role for these vascular miRs in the de-differentiation of human VSMC to a migratory phenotype, a scratch assay was performed. Representative images of scratched cell monolayers, then subsequent cell migration to close the wound are shown in Figure 4.11. Expression of miR-21 was elevated 4.8 fold ($p<0.01$ vs. 0hrs) at 6 hours, before decreasing to 1.8 fold at 16 hours (Figure 4.12). Levels of miR-221 were elevated 2-fold at 6 hours, returning to baseline by 16 hours (Figure 4.12). Surprisingly, expression levels of miR-145 were also slightly elevated at 6 hours compared with cells at 0 hours (RQ 1.8, $p<0.01$ vs. control) but fell to 33% of initial levels at 16 hours (Figure 4.13). Expression levels of miR-143 were similarly elevated at 6 hours (RQ 1.77, $p<0.01$ vs. control) however returned to baseline at 16 hours with no evidence of any decrease in expression levels (Figure 4.13). Levels of miR-146a and -146b did not change across any time point (Figure 4.14).

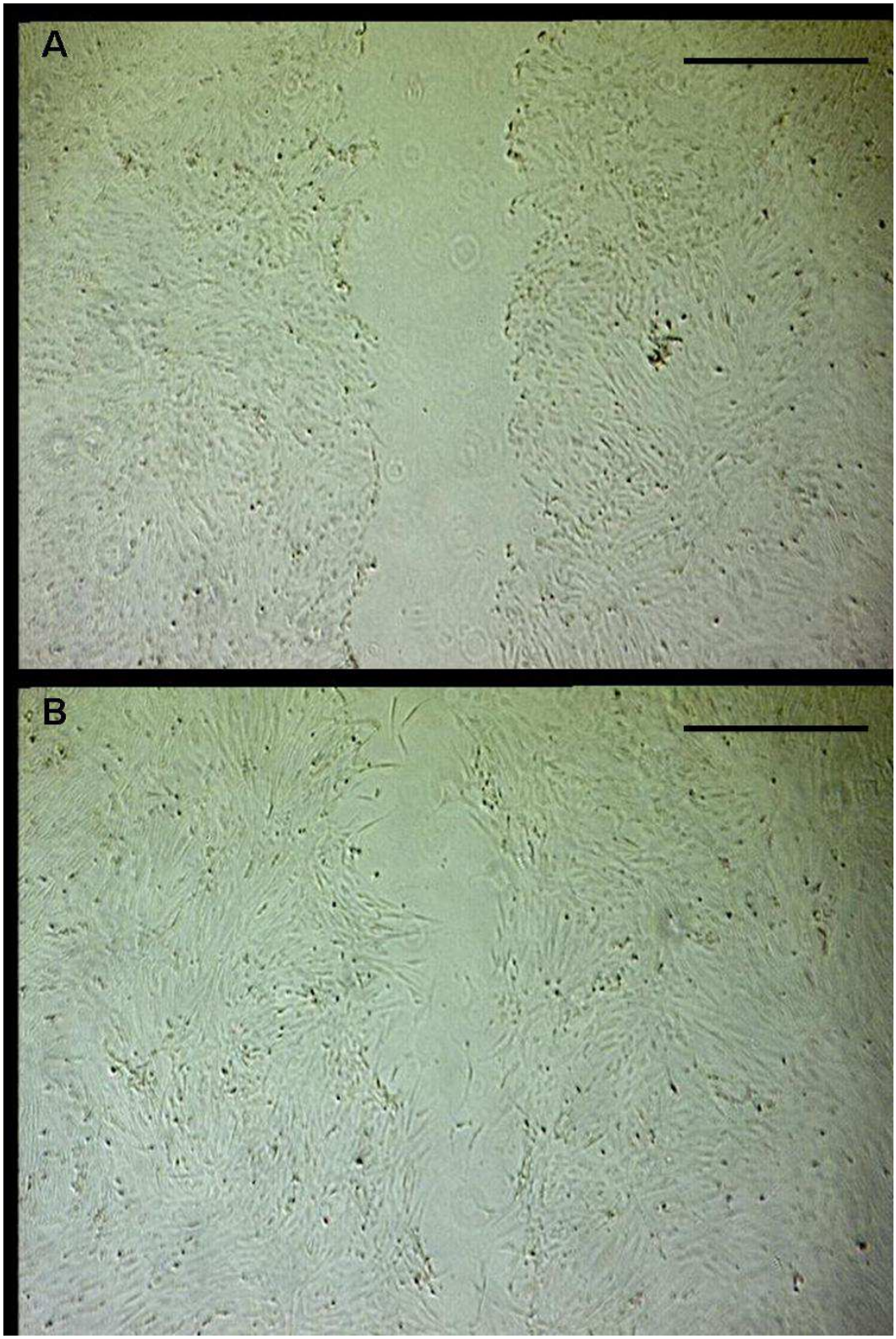

Figure 4-8 ***In vitro*** **scratch migration assay**

Representative images of a human coronary artery smooth muscle cell (HCASMC) monolayer during an *in vitro* scratch assay that mimics cell migration *in vivo*. Cells are quiesced to a differentiated phenotype before creation of an artificial wound or scratch. This promotes a migratory phenotype and cells will move together until new cell-cell contacts are made. Panel A shows cell layer at time of wounding with a 200µl pipette tip. Panel B shows same cells 18 hours later with evidence of cell migration closing the gap. Images at x4 magnification. Scale bar = 500µm.

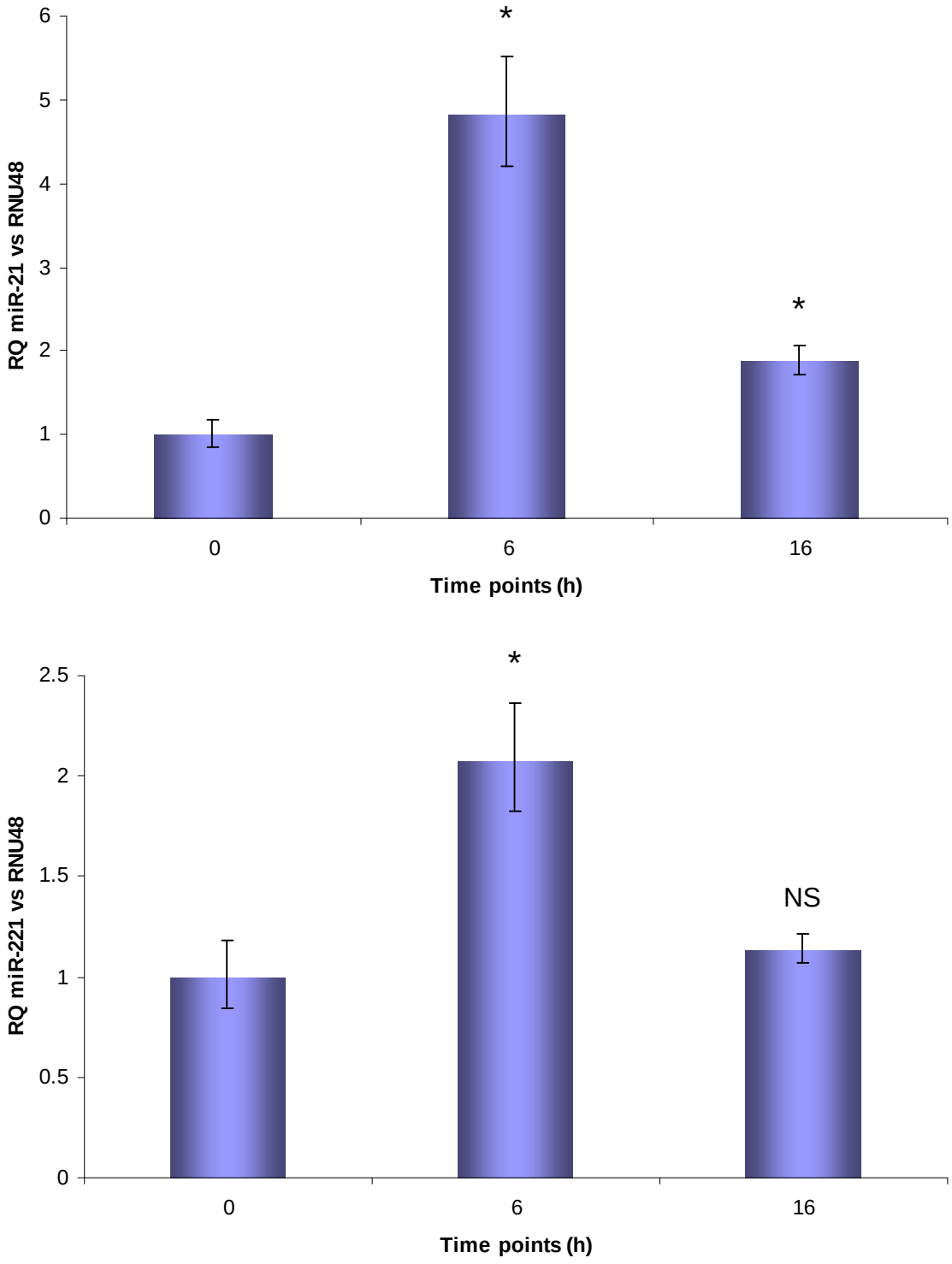

Figure 4-9 Change in expression level of miR-21 and miR-221 with HCASMC switch to a migratory phenotype

In vitro human coronary artery smooth muscle cells (HCASMC) were incubated with serum free media to induce a differentiated contractile state. Cells were then promoted to a migratory phenotype using a scratch assay technique. RNA was extracted from cells at each time point and miR-21 (Top panel) and miR-221 (Bottom panel) expression determined using qRT-PCR with RNU48 as an endogenous control. All comparisons made to control differentiated cells (at time point 0 - baseline). Results are displayed as Relative Quantity (RQ) $\pm$ RQmax calculated using the $2^{-\Delta\Delta Ct}$ method. * = $p<0.01$, NS = no significant change from baseline levels, One-way ANOVA with Tukey correction.

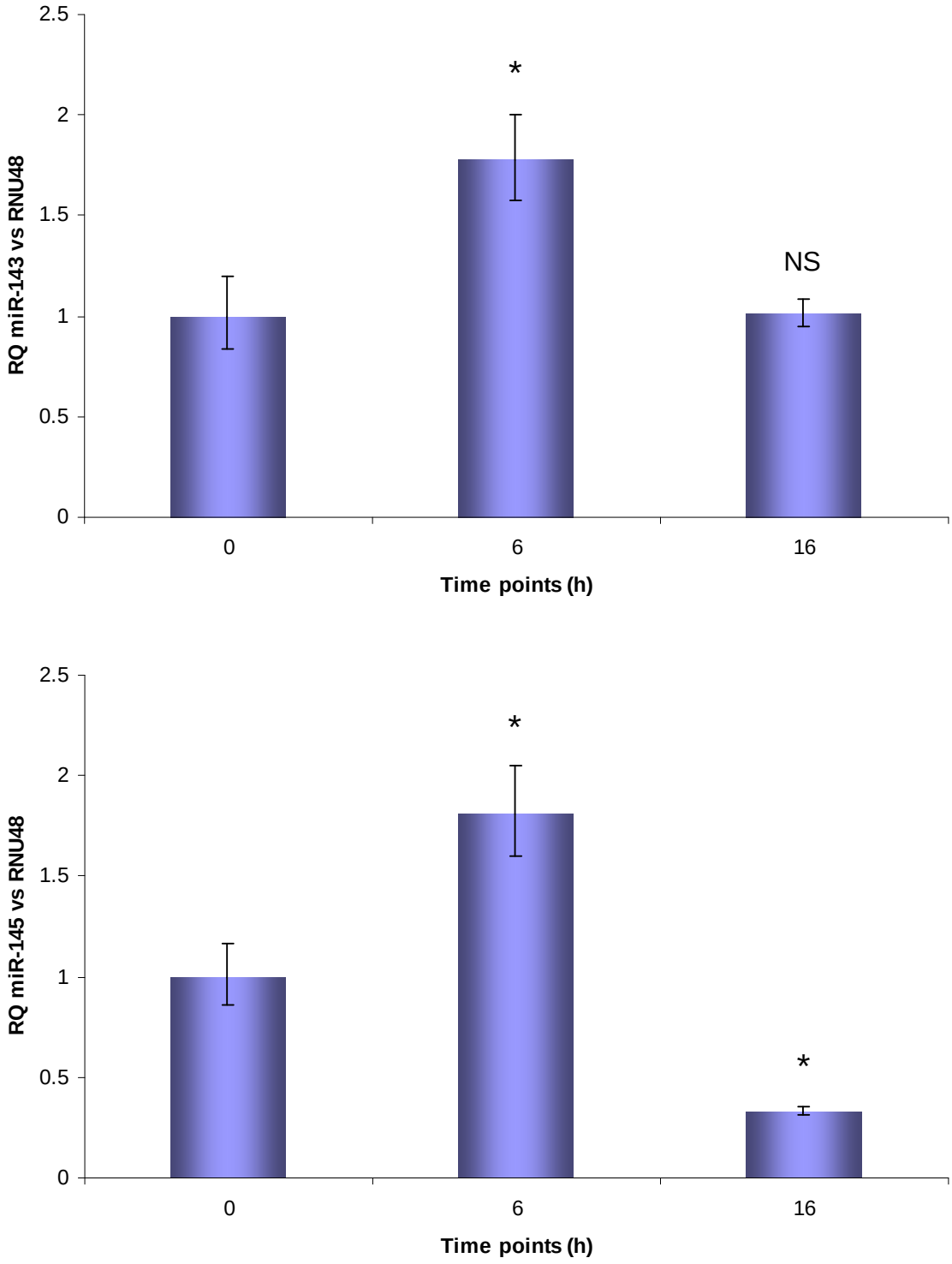

Figure 4-10 Change in expression level of miR-143 and miR-145 with HCASMC switch to a migratory phenotype

In vitro human coronary artery smooth muscle cells (HCASMC) were incubated with serum free media to induce a differentiated contractile state. Cells were then promoted to a migratory phenotype using a scratch assay technique. RNA was extracted from cells at each time point and miR-143 (Top panel) and miR-145 (Bottom panel) expression determined using qRT-PCR with RNU48 as an endogenous control. All comparisons made to control differentiated cells (at time point 0 - baseline). Results are displayed as Relative Quantity (RQ) $\pm$ RQmax calculated using the $2^{-\Delta\Delta Ct}$ method. * = $p<0.01$, NS = no significant change from baseline levels, One-way ANOVA with Tukey correction.

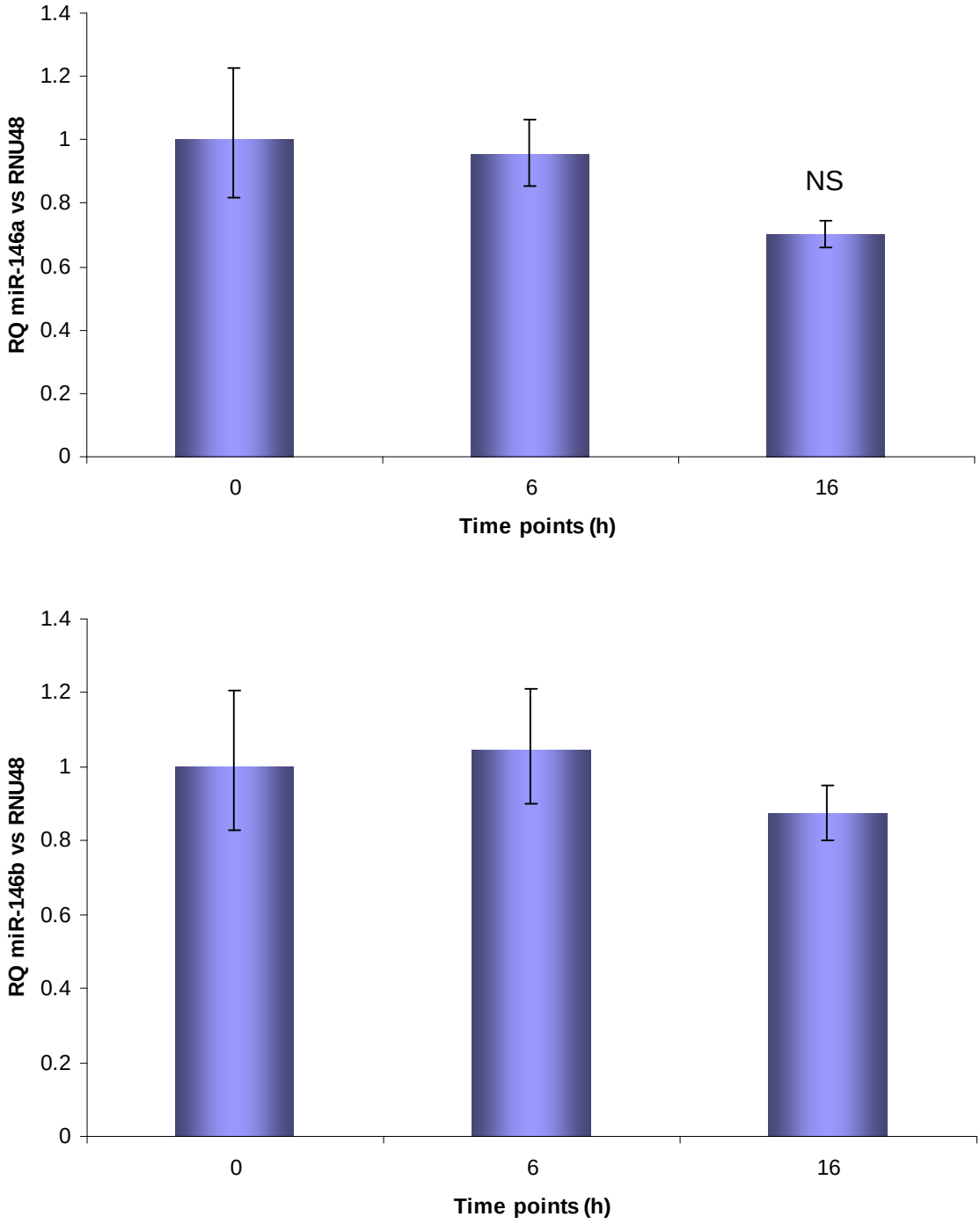

Figure 4-11 Expression level of miR-146a and miR-146b with HCASMC switch to a migratory phenotype

In vitro human coronary artery smooth muscle cells (HCASMC) were incubated with serum free media to induce a differentiated contractile state. Cells were then promoted to a migratory phenotype using a scratch assay technique. RNA was extracted from cells at each time point and miR-146a (Top panel) and miR-146b (Bottom panel) expression determined using qRT-PCR with RNU48 as an endogenous control. All comparisons made to control differentiated cells (at time point 0 - baseline). Results are displayed as Relative Quantity (RQ) $\pm$ RQmax calculated using the $2^{-\Delta\Delta Ct}$ method. No significant change from baseline levels was identified at any time point for either miR (One way ANOVA with Tukey post-correction).

4.2.3 In-vivo Porcine model of In-stent Restenosis

In order to investigate the potential role of miRs in the development of ISR a porcine model was utilised as described in Chapter 2. To ensure vessel injury and stimulate neointimal development an established method of stent overexpansion was utilised (Gunn et al., 2002, Ialenti et al., 2011). For this experiment, and in keeping with the age of pigs used, 3.0x15mm Vision Multi-Link (Abbott Vascular, Santa Clara, CA, USA) bare-metal stents were implanted in most animals (3 groups, n=4/group). For the 4th DES (28 days) group (n=4), Endeavour (Medtronic, Minneapolis, MN, USA) drug-eluting stents were used. The stent to artery ratio used was 1.2:1 as assessed visually during angiography. Practically therefore this meant that a 3.0x15mm stent was implanted in a segment of artery measuring 2.5mm using nominal pressure (9 atmospheres). This is reported as being effective in inducing significant neointimal formation at 28 days in the porcine model (Ialenti et al., 2011, Watt et al., 2013).

4.2.3.1 Histology

As shown in Figure 4.15 Panels A-D, significant neointimal formation was achieved in animals receiving BMS. The mean neointimal thickness obtained was 0.08 $\pm$ 0.01mm at 7 days and 0.22 $\pm$ 0.02mm at 28 days ($p<0.001$, 7 days vs. 28 days, Fig 4.28E).

However, it ultimately proved impossible to electrolyse the Endeavour DES using the equipment available. This was despite use of maximal voltage available (10V) for prolonged duration (up to 1 hour) and with attempted disruption of the stent polymer using a scalpel. Due to excessive tissue trauma and disruption in these samples (Figure 4.16 Panels F-G) no interpretable histology or *in-situ* hybridisation data was obtained from the animals who received DES.

It was, however, possible to obtain some virtual histology data, *ex-vivo* in these animals using an optical coherence tomography (OCT) catheter. The mean neointimal thickness, as obtained by OCT, measured at 0.51 $\pm$ 0.05mm in BMS at 28 days and 0.48 $\pm$ 0.26mm in DES at 28 days (Figure 4.16 Panels A-B). There was no significant difference detected between the two groups ($p=0.68$). In keeping with the different methods of measurement inherent to each technique, OCT was seen to overestimate mean neointimal thickness as compared to histological analysis (0.51 $\pm$ 0.05mm vs. 0.22 $\pm$ 0.02mm, $p<0.0001$, Figure 4.17).

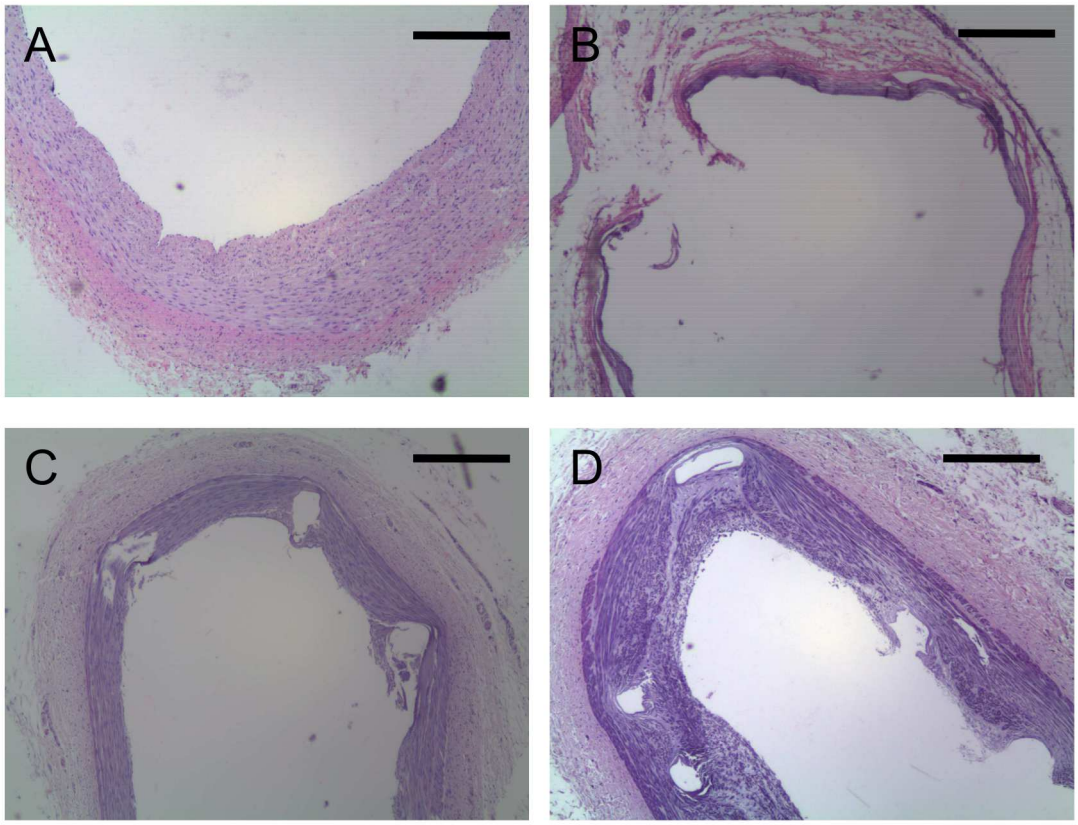

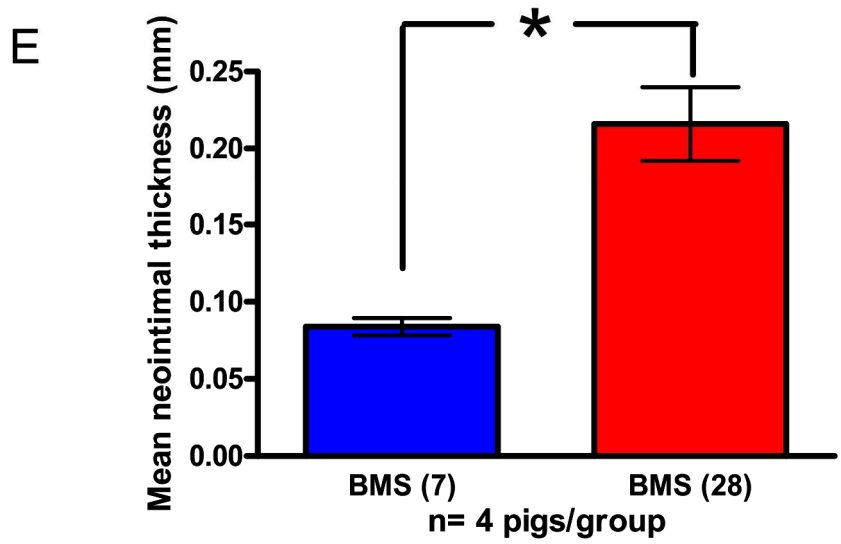

Figure 4-12 Morphometric analysis of porcine arteries treated with bare-metal stents

Measurement of mean neointimal thickness confirms development of significant neointimal hyperplasia at 28 days following the insertion of overexpanded (1.2:1) cobalt-chromium coronary stents (BMS). Panels A-D show representative photomicrographs, stained with haematoxylin and eosin, to allow morphometric analysis. Stents have been removed using electrolysis. Panel A – Control (Unstented vessel). Panel B – BMS (Day 0). Panel C – BMS (Day 7). Panel D – BMS (Day 28). Scale bars = 300μm. Panel E - Mean neointimal thickness. * = $p<0.0001$(Student's *t* test). Neointimal area = internal elastic laminal area minus the lumen area.

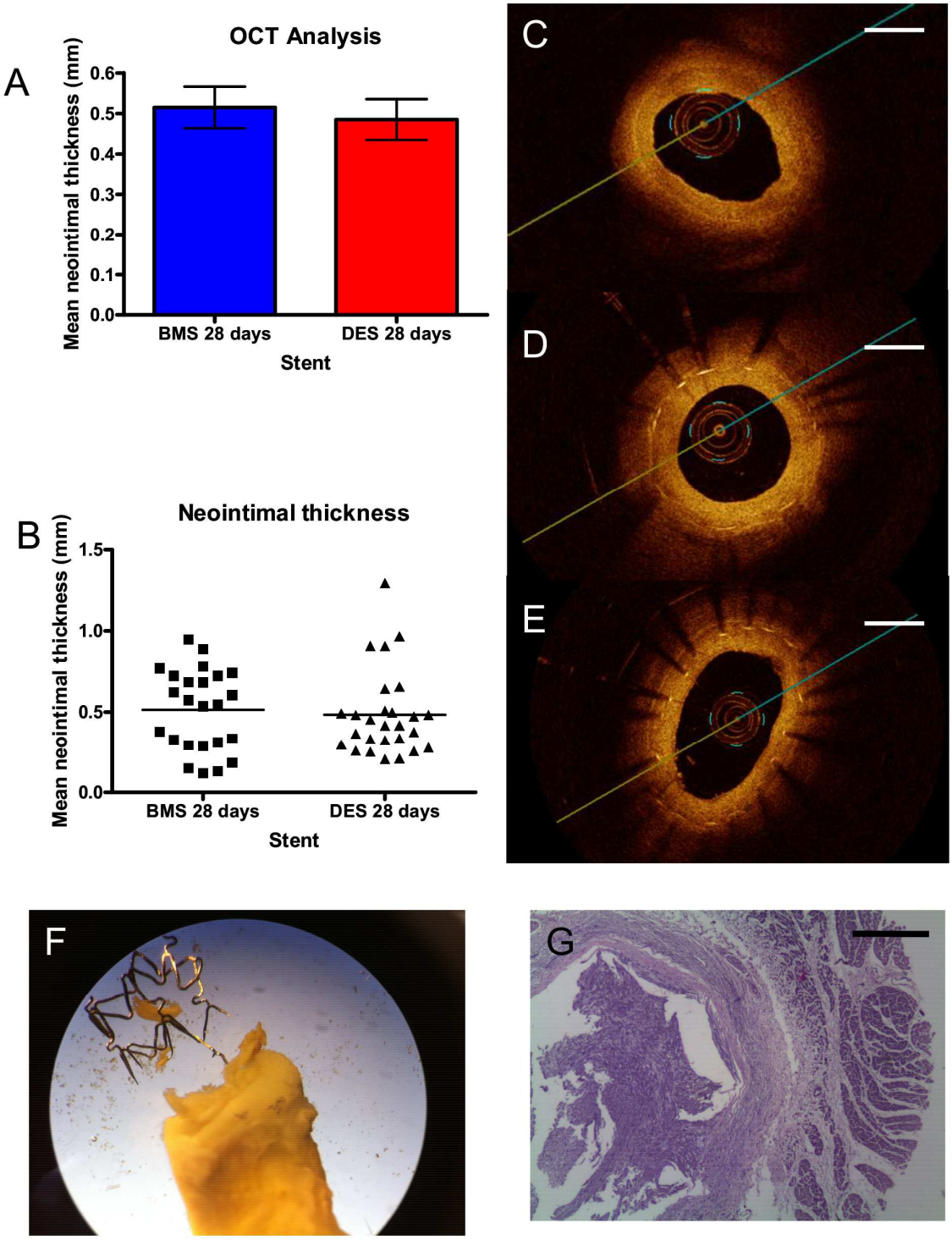

Figure 4-13 "Virtual" histology of BMS vs. DES at 28 days obtained using OCT

Mean neointimal thickness as, measured by optical coherence tomography (OCT) *ex vivo*, in pigs receiving bare-metal (BMS) or drug-eluting (DES) stents (n=4/group, 2 stents/animal). All measurements taken from animals euthanized at 28 days post-stent implantation. Panels A and B show no difference in the extent of neointimal hyperplasia induced by 1.2:1 overexpansion of cobalt-chromium BMS or zotarolimus eluting DES. p = 0.68 (Student's *t* test). Panels C-E show representative OCT images from unstented control artery, BMS at 28 days and DES at 28 days, respectively. Scale bar = 1mm. Panel F shows intact stent struts dissected from an artery implanted with DES despite being subjected to prolonged electrolysis (dissecting microscope view). Panel G is a representative H&E stained section from an artery implanted with DES showing the typical tissue disruption encountered when stent dissolution was attempted. x4 magnification. Scale bar = 300μm.

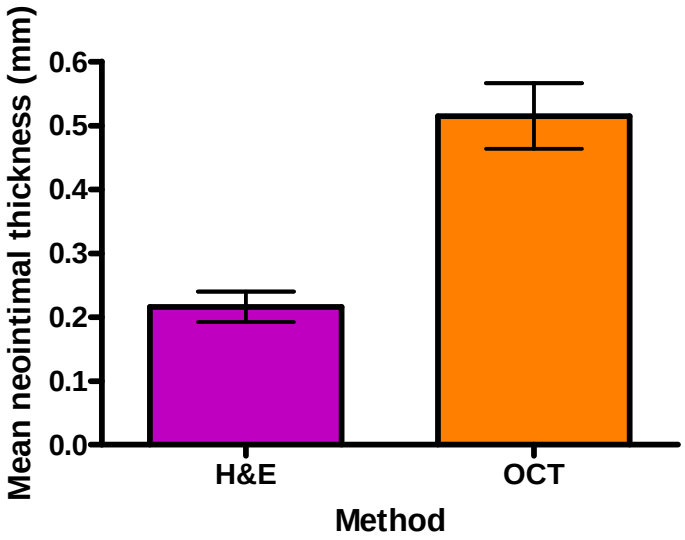

Figure 4-14 Comparison of neointimal area as measured by OCT and H&E morphometry

A comparison was made of neointimal thickness, as measured by morphometry in H&E stained sections, and optical coherence tomography in pigs implanted with BMS and euthanized at 28 days (n=4, 2 stents/animal). Following formalin-fixation arteries were assessed *ex vivo* with an OCT catheter before stent electrolysis, histological processing and H&E staining. For H&E sections, internal elastic laminal area is measured and then the lumen area is subtracted to give the mean neointimal thickness. For OCT, it was not possible to measure the IEL area due to loss of resolution following formalin-fixation. Therefore a tracing was made around the stent struts to give a stent area, from which the lumen area was subtracted. This results in a significant overestimation compared to classical histology ($p<0.0001$).

4.2.3.2 Choice of endogenous control

When using qRT-PCR techniques for characterisation of miR expression patterns in tissue, corrections must be made for differences between samples arising due to variations in RNA quality and quantity (de Kok et al., 2005, Stahlberg et al., 2004). These variations occur due to sample collection, amount of starting material, the method of RNA extraction and cDNA synthesis. To control these variations a normalisation to a suitable endogenous control gene (or genes) is performed. To be used as an endogenous control, gene expression must be constant and highly abundant across tissue and cell types. Suitable endogenous control genes for use in porcine vascular tissue have not yet been established. In a previous report, Gu *et al*, studied 47 different porcine tissues and showed that the most stable EC genes for use in normalization were *sus scrofa* ssc-miR-17, -103 and -107 with ssc-miR-17, -23a and -103 being most reliable in muscle tissue (Gu et al., 2011). Vascular muscle tissue was not used in their analysis.

To establish appropriate endogenous control genes for use in porcine models we analysed expression levels of apparently stable miRs in a TaqMan Low-Density microRNA microarray analysis of porcine vascular tissue (saphenous vein, carotid artery, SVG at 7 and 28 days) used in a separate study within our institution (McDonald et al., 2013). These results are summarised in Figure 4.18 and Table 4.2. Both miR-17 and miR-199a-3p appeared suitable and stable for use as endogenous controls in porcine vascular tissue with abundant expression, narrow confidence intervals and standard deviations of <1. For all following experiments, miR-199-3p was used to maintain consistency within the *in vivo* models utilised in our institution (McDonald et al., 2013).

Table 4-1 Mean cycle thresholds (Ct) of potential endogenous control microRNAs

	U6	miR-17	miR-23a	miR-23b	miR-103	miR-199a-3p
Mean Ct	15.37	16.39	29.30	24.45	21.77	17.04
Std. Deviation	0.6779	0.7327	2.993	2.845	1.172	0.9177
Std. Error	0.1384	0.1496	0.6241	0.5807	0.2391	0.1873
Lower 95% CI of mean	15.08	16.08	28.00	23.24	21.28	16.65
Upper 95% CI of mean	15.66	16.70	30.59	25.65	22.27	17.43

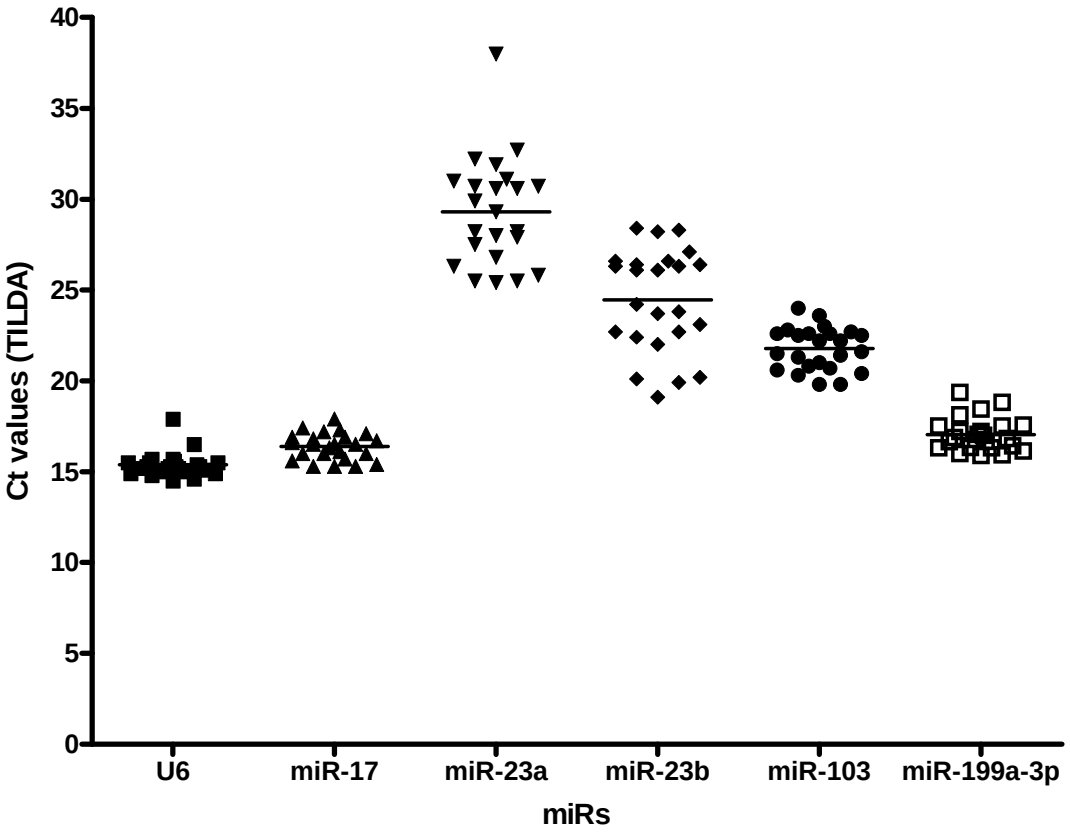

Figure 4-15 Scatter plots of raw Ct values for potential porcine endogenous controls

Ct values taken from TaqMan Low-Density microRNA microarray analysis of porcine vascular tissue (saphenous vein, carotid artery, and interposition saphenous vein grafts at 7 and 28 days) used in a separate study within our institution. U6 spliceosomal RNA, miR-17 and miR-199a-3p, show abundant expression, narrow confidence intervals and standard deviations of <1, suggesting suitability for use as endogenous controls in qRT-PCR analysis of porcine vascular tissue.

4.2.3.3 Expression of MiR-21/221

MiR-21 levels were upregulated at 7 and 28 days in arteries stented with both BMS and DES (Figure 4.19). At 7 days post BMS insertion there is a greater than 5-fold increase in expression which was maintained out to 28 days (RQ 3.8, $p<0.001$). No differences were seen between BMS and DES at 28 days ($p>0.05$). MiR-221 levels were elevated at Day 7 in the BMS group, returning to baseline at 28 days (Figure 4.19). No increase was observed at 28 days when a DES was used.

4.2.3.4 Expression of MiR-143/145

qRT-PCR analysis of miR-143 and miR-145 in stented vessels showed that expression levels of both were significantly down regulated at 7 and 28 days post stent implantation (Figure 4.20). Compared to unstented control vessels, miR-145 (but not miR-143) expression was down-regulated in vessels harvested immediately following stent insertion (Day 0) (Figure 4.20). Levels of miR-145 only were significantly lower in arteries receiving DES compared with BMS at 28 days (75% vs. 48% downregulation).

4.2.3.5 Other Vascular MicroRNAs

Analysis of other vascular associated miRs was performed in the stented vessels. Levels of miR-92a, miR-126, miR-155 and miR146a showed no change in expression compared with unstented control vessels (Figure 4.21 Panel A). Expression levels of miR-133a showed a statistically significant increase in vessels harvested immediately post stent insertion (RQ 5.6, $p<0.05$ vs. control) however had returned to baseline by Day 7 (Fig 4.21 Panel B).

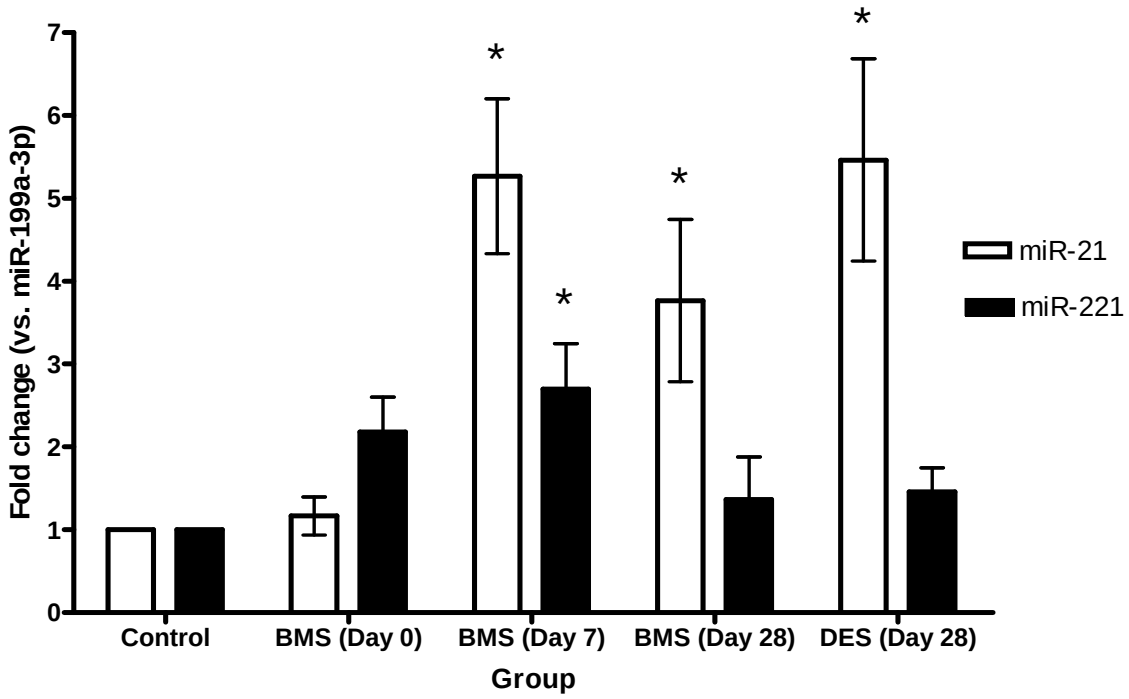

Figure 4-16 Expression levels of microRNAs upregulated in a porcine model of coronary in-stent restenosis

Pigs received standardized BMS (cobalt alloy) or DES (Zotarolimus-eluting) (n=4/group, 2 stents/animal) over-expanded at a ratio of 1.2:1 to induce neointimal hyperplasia. Animals were euthanized at 0, 7 or 28 days (BMS) and 28 days (DES). Total RNA was extracted from snap-frozen stented tissue. miR expression levels were determined by quantitative real-time polymerase chain reaction and normalized to miR-199a-3p. For comparison, miR expression levels are given as fold-change versus control vessels (unstented arteries) calculated using the $2^{-\Delta\Delta Ct}$ method. Significance was assessed by repeated measures ANOVA with a Tukey post-test. A value of $p<0.05$ was considered statistically significant. * = $p<0.001$

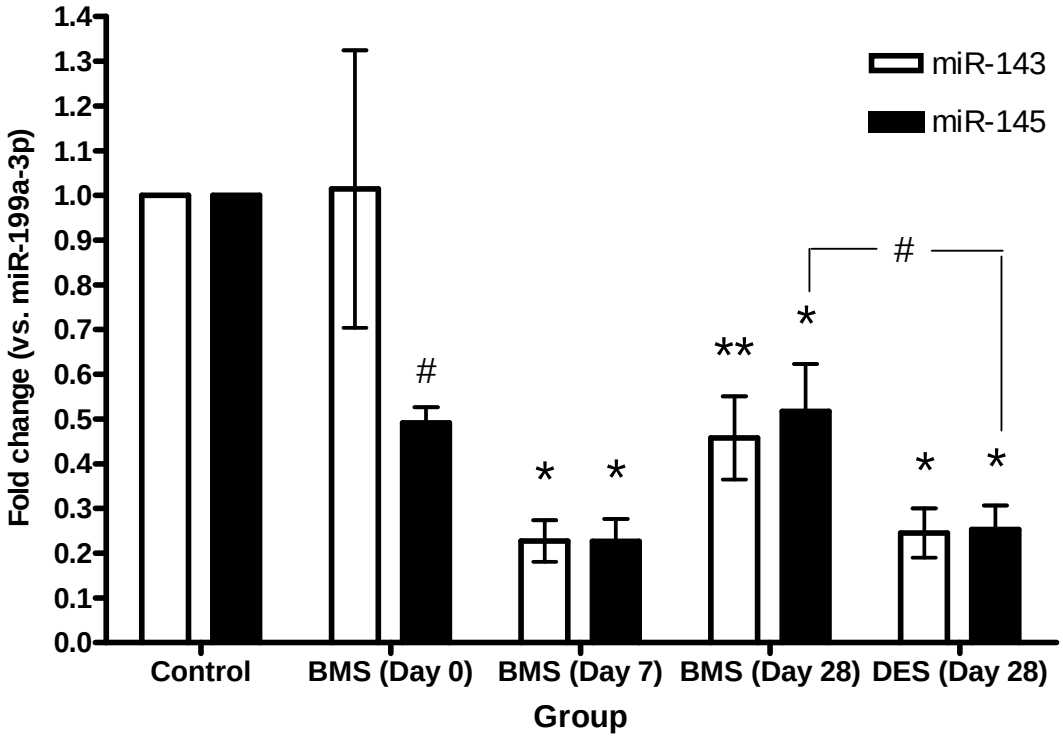

Figure 4-17 Expression levels of microRNAs downregulated in a porcine model of coronary in-stent restenosis

Pigs received standardized BMS (cobalt alloy) or DES (Zotarolimus-eluting) (n=4/group, 2 stents/animal) over-expanded at a ratio of 1.2:1 to induce neointimal hyperplasia. Animals were euthanized at 0, 7 or 28 days (BMS) and 28 days (DES). Total RNA was extracted from snap-frozen stented tissue. miR expression levels were determined by quantitative real-time polymerase chain reaction and normalized to miR-199a-3p. For comparison, miR expression levels are given as fold-change versus control vessels (unstented arteries) calculated using the $2^{-\Delta\Delta Ct}$ method. Significance was assessed by repeated measures ANOVA with a Tukey post-test. A value of $p<0.05$ was considered statistically significant. # = $p<0.05$, ** = $p<0.01$, * = $p<0.001$ (vs. unstented control unless otherwise indicated).

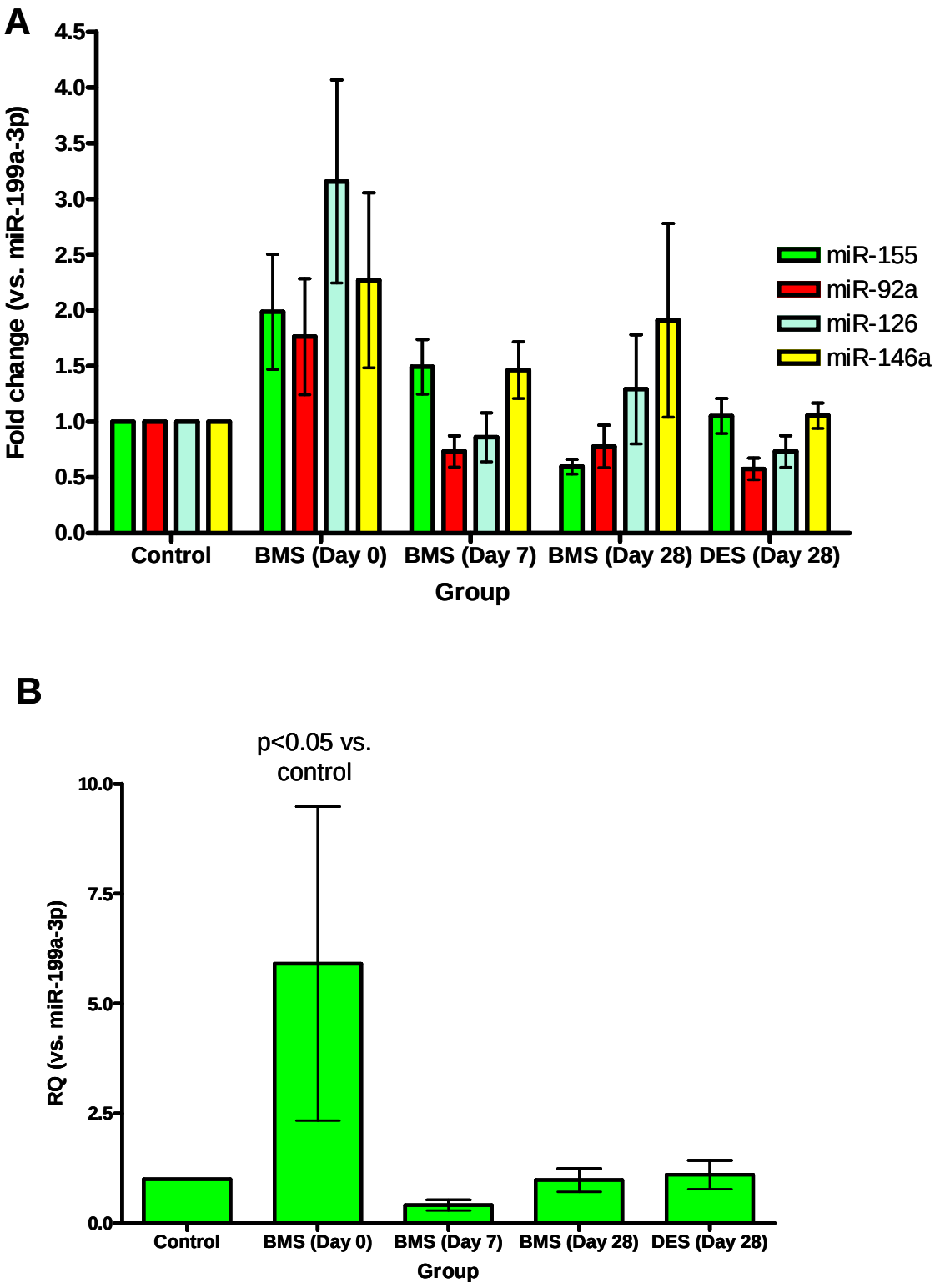

Figure 4-18 Expression profiles of vascular microRNAs not significantly altered in response to vessel injury and stent implantation in porcine model

Panel A - miRs with no change in expression levels. Panel B – miR-133a expression levels. Pigs received standardized BMS (cobalt alloy) or DES (Zotarolimus-eluting) (n=4/group, 2 stents/animal) over-expanded at a ratio of 1.2:1 to induce neointimal hyperplasia. Animals were euthanized at 0, 7 or 28 days (BMS) and 28 days (DES). Total RNA was extracted from snap-frozen stented tissue. miR expression levels were determined by qRT-PCR and normalized to miR-199a-3p with expression levels given as fold-change versus unstented control vessels calculated using the $2^{-\Delta\Delta Ct}$ method. Significance was assessed by repeated measures ANOVA with a Tukey post-test. A value of $p<0.05$ was considered statistically significant. All above comparisons – $p>0.05$ vs. unstented control except miR-133a Day 0 vs. control as indicated.

4.2.3.6 Localisation of miR-21

In-situ hybridisation (ISH) was used to localise the areas of increased miR-21 expression within the stented vessel wall. This proved challenging with initial significant tissue degradation occurring. By shortening the duration of tissue exposure to Proteinase K this was overcome, to a degree. Interpretation of the obtained images proved difficult due to persistent background staining in control samples exposed to a scrambled probe. However, despite these obstacles ISH revealed increased miR-21 expression in the neointima of vessels at Day 7 and Day 28 following BMS implantation, most notably around the stent struts (Fig 4.19). These findings were consistent with the qRT-PCR data. No interpretable data could be obtained from vessels receiving DES due to excessive tissue trauma caused by the electrolysis process in these samples.

4.2.3.7 Localisation of miR-143/145 expression in neointima

Again, ISH was used to further interrogate the expression of miR-143/145 in the vessel wall following stent deployment. Consistent with the qRT-PCR data, this revealed an immediate rapid loss of miR-145 from the vessel wall (Fig 4.20A). However, at 7 and 28 days post-BMS deployment both miRs were detectable in areas of neointima development (Fig 4.20A). At day 28, both miRs were also detectable in the vessel media (Fig 4.20A). Positive staining for α-SMA (Fig 4.20B) was localised to a similar region as miR-143/145 expression. These patterns suggest that although the global level of miR-143/145 expression detectable by qRT-PCR is down-regulated in response to vascular injury, expression of miR-143/145 emerges within the neointima and in the media at later time points.

Staining for proliferating cell nuclear antigen (PCNA) showed concordance in the neointima with areas of miR-143 and miR-145 expression, particularly around the stent struts (Fig 4.21). Of note, no PCNA staining was present in the vessel immediately post stent deployment (Fig 4.21). These results suggest that miR-143 and miR-145 are expressed in dedifferentiated VSMCs within the neointima.

Again, no interpretable data could be obtained from vessels treated with DES.

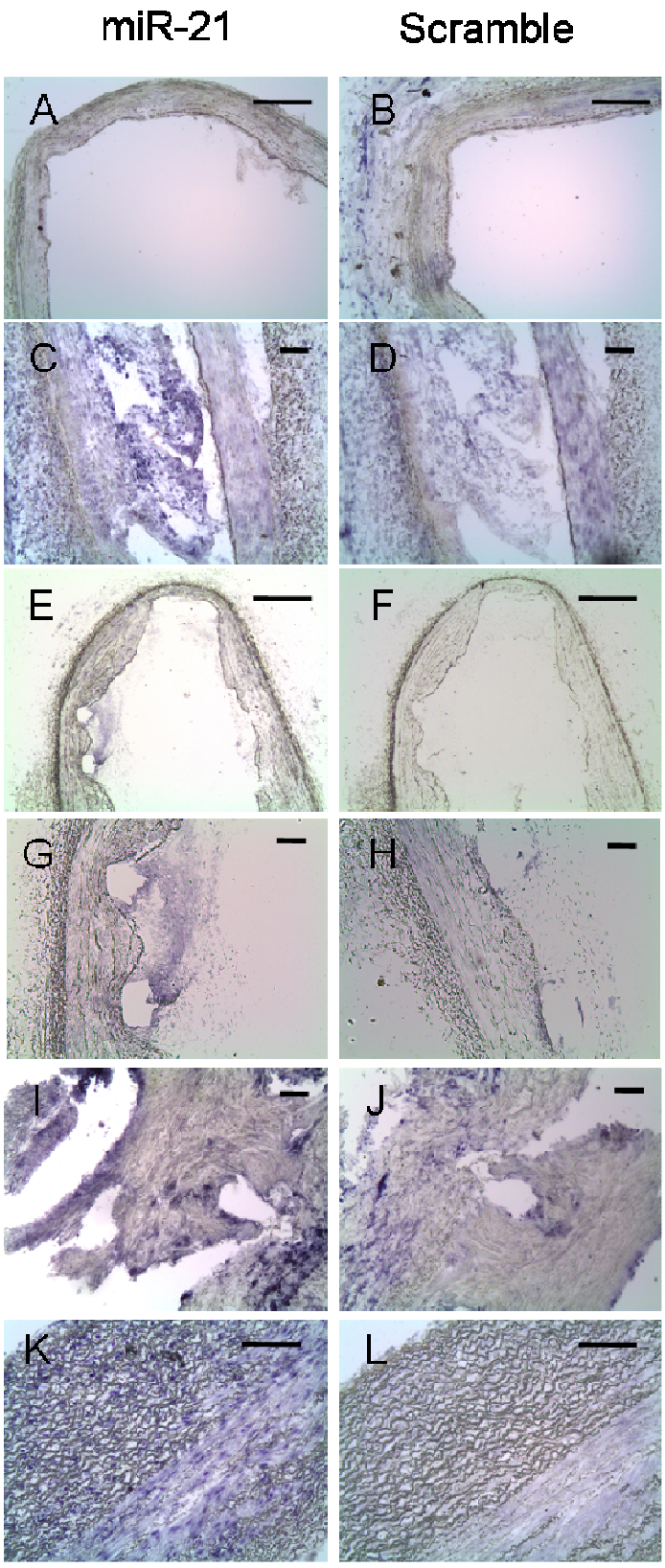

Figure 4-19 miR-21 localisation in stented porcine vessels

Pigs received BMS or DES (n=4/group, 2 stents/animal). Animals were euthanized 0, 7 or 28 days post procedure. Representative in situ hybridization (violet) images using miR-21 and scrambled probes. Panels A-B - Day 0 BMS (x4 magnification). Panels C-D - Day 7 BMS (x10 mag). Panels E-F - Day 28 BMS (x4mag). Panels G-H - Day 28 BMS (x10 mag). Panels I-J – Day 28 DES (x10 mag). Panels K-L - unstented control (x4 mag). Scale bars = 300μm for x4 magnification and 200μm for x10 magnification.

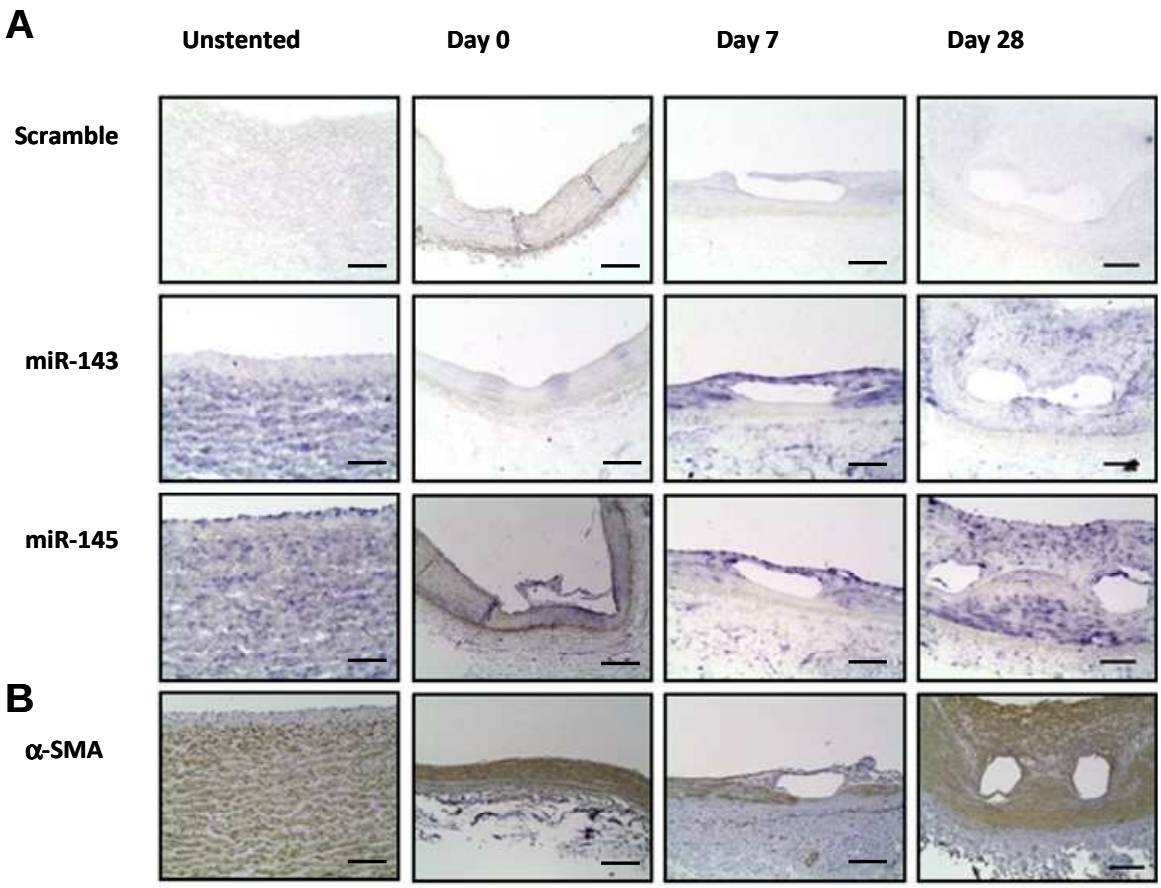

Figure 4-20 miR-143/miR-145 localisation in stented porcine vessels

Pigs received bare-metal stents (n=4/group, 2 stents/animal). Animals were sacrificed 0, 7 or 28 days post procedure. Panel A - Representative in situ hybridization (violet) images using scrambled, miR-143 or miR-145 probes in control unstented, day 0, day 7 and day 28 stented vessels. Panel B - Representative immunohistochemical staining of α-SMA in serial sections. Scale bar represents 100 µm.

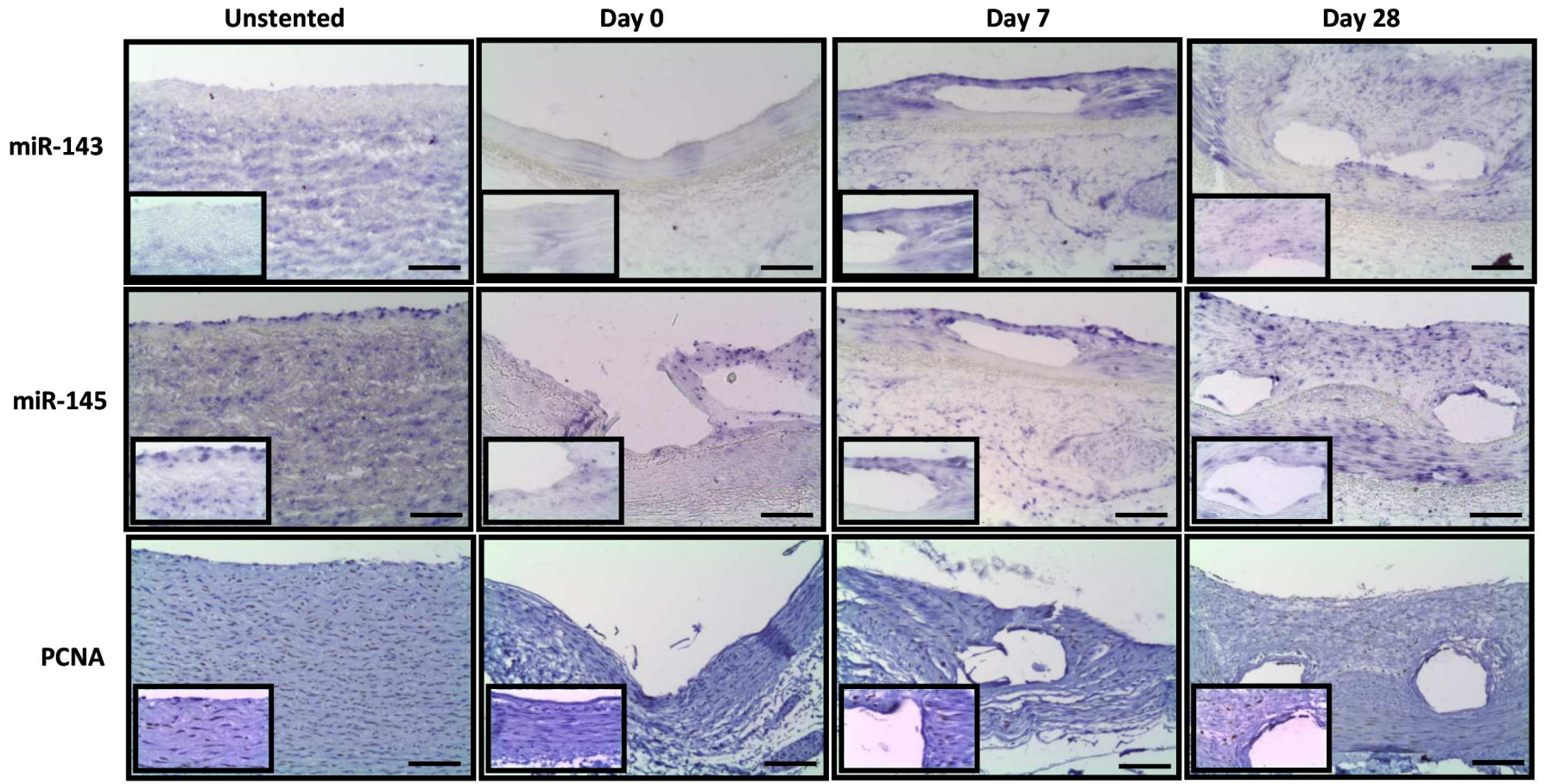

Figure 4-21 Immunolocalization of cells expressing miR-143 and miR-145 in stented porcine coronary arteries

Upper two rows show representative in situ hybridization (violet) images using miR-143 or miR-145 probes in control unstented, day 0, day 7 and day 28 stented (BMS) vessels. Lower panels show immunohistochemistry staining for proliferating cell nuclear antigens (PCNA) in serial sections. Scale bars represent 100μm.

4.2.3.8 Novel MicroRNAs Dysregulated in Restenosis

As discussed, the above investigated miRs have all been implicated in the development of restenosis in *in-vitro* or small animal *in-vivo* models. To identify potentially novel miRs that may be involved in the ISR pathway, we investigated a panel of miRs dysregulated, on microfluidic array analysis, in response to interpositional vein grafting in a porcine model utilised within our institution (McDonald et al., 2013). Verification was performed by qRT-PCR analysis in RNA samples from stented porcine coronary arteries (BMS and DES) as above.

Both the miR-142-3p and miR-142-5p stem loops showed promise, with early approximate 2-fold increases in expression immediately following BMS delivery and peaking at 5-6 fold at day 7 post stent implantation (Figure 4.25). This increase in expression was maintained out to 28 days (Figure 4.25). These findings paralleled changes seen in porcine vein grafts at 7 and 28 days post-engraftment (McDonald et al., 2013). Interestingly, arteries stented with DES did not show any change in miR-142-3p or miR-142-5p expression.

Expression levels of miR-23b showed a 46% reduction at day 7 following BMS implantation and had returned to baseline by day 28 (Figure 4.26 Panel A). No change was observed with DES at 28 days (Figure 4.26 Panel A). Levels of miR-30c were unchanged at day 7 post-BMS but then showed a marked (95%) reduction at day 28 (Figure 4.26 Panel B). At 28 days following DES delivery however, there was no change in expression (Figure 4.26 Panel B). Lastly, miR-99b expression levels were reduced by 45% at day 7 following BMS insertion, returning to baseline at day 28 while DES induced a more marked reduction of 60% at the 28 day time point (Figure 4.26 Panel C). These results were again consistent with the changes seen in response to vein engraftment at identical time points (Unpublished data).

Of the other investigated miRs: let-7a, miR-24, miR-29a, miR-29b, miR-195 and miR-197 none showed any change in expression levels following stent delivery in porcine coronary arteries (Figure 4.27).

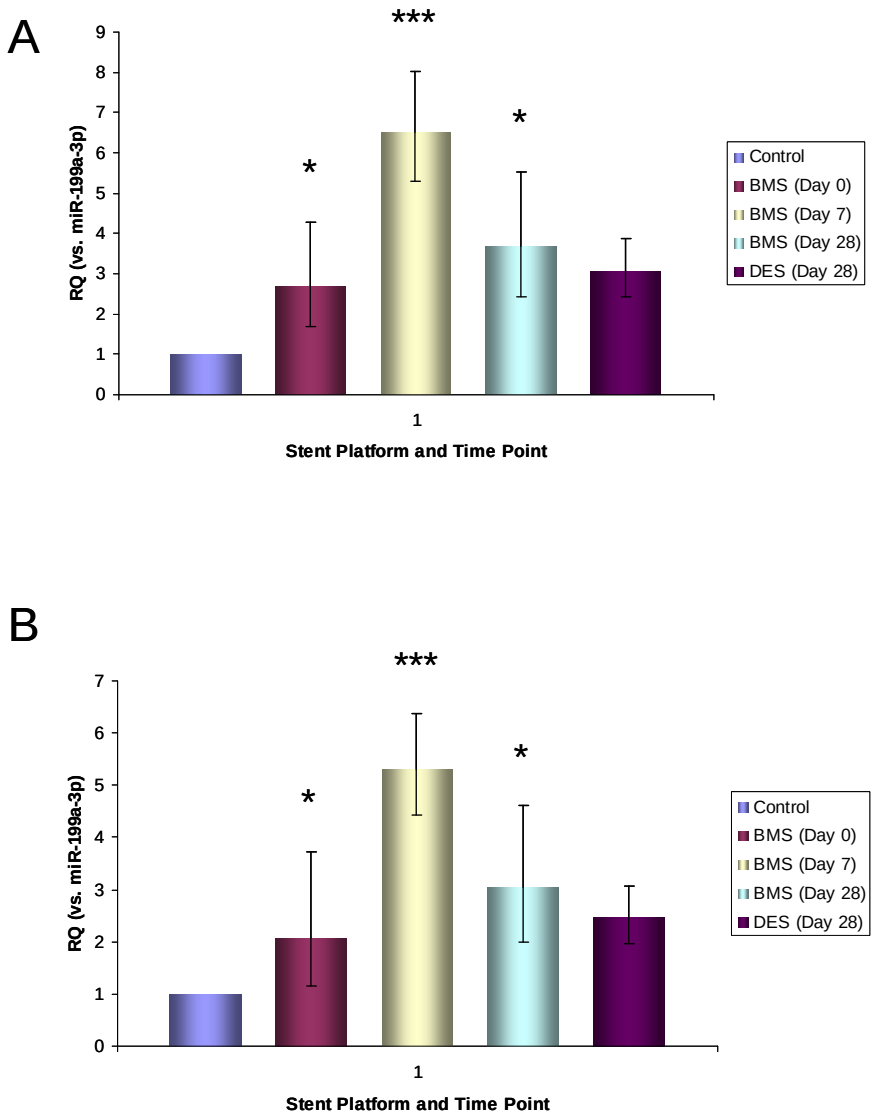

Figure 4-22 Change in expression of miR-142-3p and miR-142-5p in response to coronary stent insertion

Panel A – miR-142-3p. Panel B – miR-142-5p. Pigs received standardized BMS (cobalt alloy) or DES (Zotarolimus-eluting) (n=4/group, 2 stents/animal) over-expanded at a ratio of 1.2:1 to induce neointimal hyperplasia. Animals were euthanized at 0, 7 or 28 days (BMS) and 28 days (DES). Total RNA was extracted from snap-frozen stented tissue. miR expression levels were determined by quantitative real-time polymerase chain reaction and normalized to miR-199a-3p. For comparison, miR expression levels are given as fold-change (RQ) versus control vessels (unstented arteries) calculated using the $2^{-\Delta\Delta Ct}$ method. Significance was assessed by repeated measures ANOVA with a Tukey post-test. A value of $p<0.05$ was considered statistically significant. * = $p<0.05$, ** = $p<0.01$, *** = $p<0.001$.

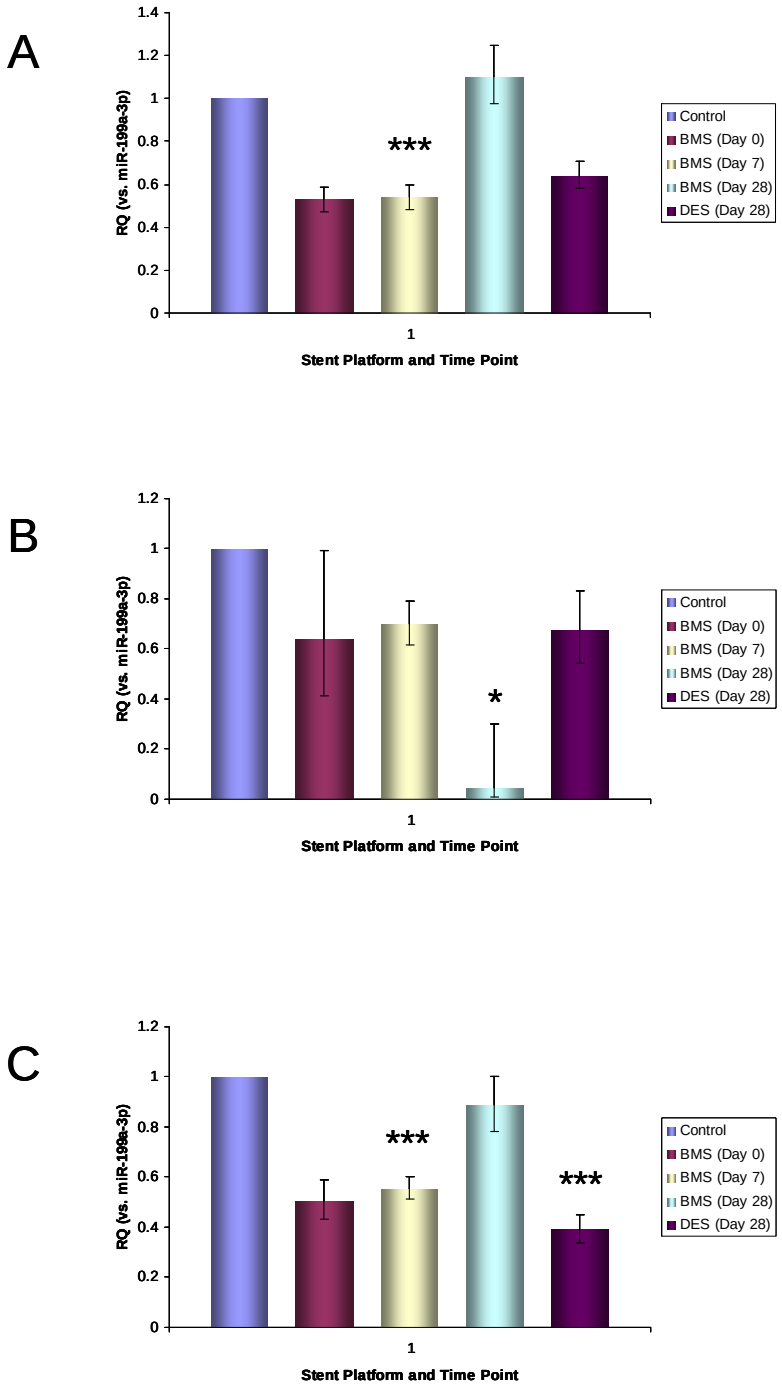

Figure 4-23 Other novel microRNAs dysregulated in porcine ISR model

Panel A – miR-23b. Panel B – miR-30c. Panel C – miR-99b. Pigs received standardized BMS (cobalt alloy) or DES (Zotarolimus-eluting) (n=4/group, 2 stents/animal) over-expanded at a ratio of 1.2:1 to induce neointimal hyperplasia. Animals were euthanized at 0, 7 or 28 days (BMS) and 28 days (DES). Total RNA was extracted from snap-frozen stented tissue. miR expression levels were determined by quantitative real-time polymerase chain reaction and normalized to miR-199a-3p. For comparison, miR expression levels are given as fold-change (RQ) versus control vessels (unstented arteries) calculated using the $2^{-\Delta\Delta Ct}$ method. Significance was assessed by repeated measures ANOVA with a Tukey post-test. A value of $p<0.05$ was considered statistically significant. * = $p<0.05$, ** = $p<0.01$, *** = $p<0.001$.

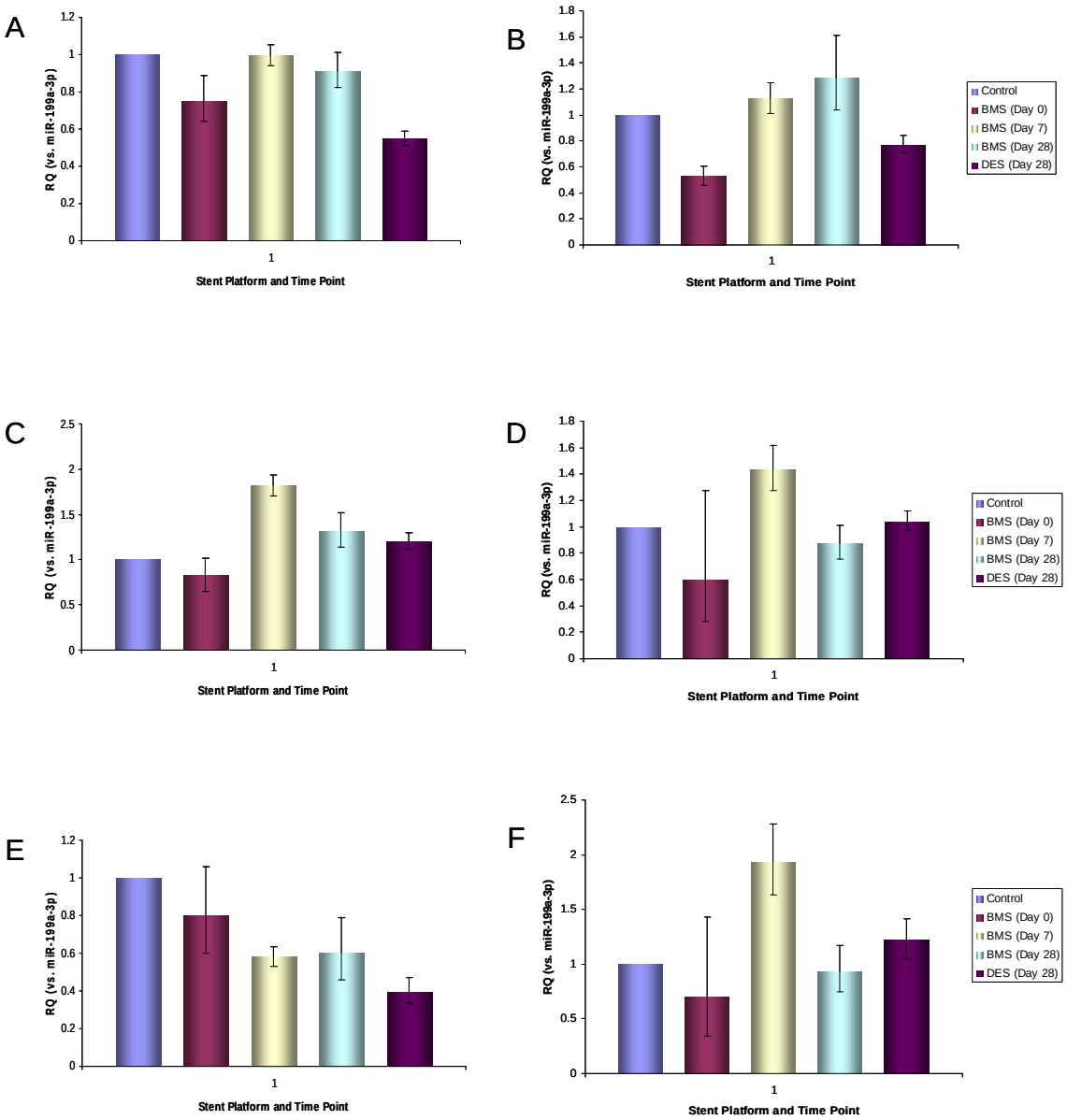

Figure 4-24 Investigated microRNAs with no change in expression in porcine ISR model

A – let 7e. B – miR-24. C – miR-29a. D – miR-29b. E – miR-195. F – miR-197. Pigs received standardized BMS (cobalt alloy) or DES (Zotarolimus-eluting) (n=4/group, 2 stents/animal) over-expanded at a ratio of 1.2:1 to induce neointimal hyperplasia. Animals were euthanized at 0, 7 or 28 days (BMS) and 28 days (DES). Total RNA was extracted from snap-frozen stented tissue. miR expression levels were determined by quantitative real-time polymerase chain reaction and normalized to miR-199a-3p. For comparison, miR expression levels are given as fold-change (RQ) versus control vessels (unstented arteries) calculated using the $2^{-\Delta\Delta Ct}$ method. Significance was assessed by repeated measures ANOVA with a Tukey post-test. $p>0.05$ for all comparisons.

4.3 Discussion

As previously discussed, vascular injury is a critical mediator of neointimal formation during the development of ISR. The mechanical injury induced by stent deployment and atherosclerotic plaque disruption results in the release of cytokines and growth factors that trigger an inflammatory cascade, VSMC proliferation and migration and the deposition of ECM. From a therapeutic perspective therefore, neointima formation and the "healing" process of re-endothelialisation remain important targets for preservation of stent patency (Dangas et al., 2010).

It is now well established that the de-differentiation of VSMC from a contractile to synthetic phenotype is integral to the progression of neointimal formation. De-differentiation results in accelerated cell proliferation and migration in combination with increased cytokine production and resultant excessive ECM deposition (Ip et al., 1990). This phenotypic switch is mediated by multiple key transcription factors including SRF, myocardin and the KLF protein family (Kawai-Kowase and Owens, 2007, Miano et al., 2007). Since the discovery of the key regulatory molecules, microRNAs, there has been a huge growth in studies investigating their importance in the regulation of VSMC gene expression and potential role in vascular physiology and pathologies. Due to the complex and multifactorial nature of ISR, miRs involved in both VSMC and EC function as well as the immune response may all be important in its progression.

To-date there have been multiple reports describing key miRs that are highly expressed within the vascular wall and importantly dysregulated following vascular injury (McDonald et al., 2011b, Wei et al., 2013). These models suggest that this dynamic regulation of specific miRs during the development of neointima following vascular injury is critical to the dedifferentiation of VSMC and process of reendothelialisation through interactions with key transcription factors. The majority of these published models, however, involve rodents (cell lines or in-vivo injury) with minimal data from human tissue and none from the established large animal models of stent delivery routinely used in the assessment of stent technology (Schwartz et al., 2004, Schwartz et al., 2002).

It was the purpose of this chapter therefore to further investigate the complex role of key vascular miRs in the development of restenosis following stent delivery using a novel porcine stent model and with a view to providing further insight into the potential for their therapeutic modulation in the setting of ISR.

As an initial approach it was felt to be important to attempt to investigate the role of these vascular miRs in human coronary artery smooth muscle cells using *in-vitro* models. When quiescent (differentiated) HCASMCs were stimulated to a de-differentiated proliferative phenotype using classical mitogen stimulation it was found that levels of miR-21, miR-146a and miR-365 were increased when compared to unstimulated control cells. This observed dysregulation in miR-21 and miR-146a levels was consistent with previously published findings and provides further strength to the argument that both miR-21 and miR-146a play a role in VSMC dedifferentiation. However, it is unclear from these results whether this observed miR dysregulation represents "cause" or "effect". Based on previous data it seems likely that these findings represent part of the mechanism controlling change in cell phenotype but could just be by-products and therefore be biomarkers for dedifferentiation. Under the above experimental conditions, miR-21 up-regulation appeared to be dependant on the presence of PDGF, whereas miR-146a was more consistently elevated when IL1α and PDGF were combined. It should be noted that under these experimental conditions serum contains a mix of mitogenic stimuli.

MiR-365 has not previously been identified as being involved in the regulation of VSMC phenotype. It has been implicated as an oncomir in human cancers including those of the lung and skin (Qi et al., 2012). Under the above conditions it showed consistent upregulation at 1 hour across all mitogen groups, before quickly returning to baseline, suggesting that it may be important in the early dedifferentiation process. However, unfortunately due to time constraints I was not able to follow this up in the *in-vivo* model. These findings are however interesting and certainly merit future investigation.

No evidence of dysregulation of miR-143, miR-145 or miR-221 levels was identified in this *in-vitro* model. There are multiple potential explanations for this finding. Principle is that *in-vitro* assays using isolated VSMC are simplistic and do not accurately reflect the complex nature of miR networks and particularly the cross-talk that occurs between cell types (e.g. EC, fibroblasts, immune cells) *in-vivo*. The choice of mitogens used will not accurately reflect the full range of stimuli that may result in VSMC dedifferentiation so it is entirely possible that the experimental protocol did not provide the right conditions to observe any dysregulation in these miRs. Also, with the defined time points used, it may be that earlier or later changes in miR expression were missed.

It is possible that certain miRs may be more related to promoting or regulating a migratory rather than proliferative phenotype therefore *in-vitro* experiments were performed using a

wound assay. Again both miR-21 and miR-221 were found to be upregulated in a pattern consistent with previously published results. Both miR-143 and miR-145 showed an initial small upregulation in expression that was unexpected, however following this miR-145 (but not miR-143) levels reduced significantly compared to control levels, consistent with previously published studies. No change in miR-146a levels were observed in this model of migration. Again, in interpreting these results the limitations described for the stimulation experiment apply.

To summarise the results from these *in-vitro* experiments it is reasonable to hypothesise that miR-21, miR-146a, miR-221 and miR-365 overexpression may contribute to the promotion of a dedifferentiated VSMC phenotype in the development of human neointimal lesions. The results for miR-143 and miR-145 were less clear however, but it was felt that based on results from rodent studies that they still merited further investigation *in-vivo*.

Although many *in-vivo* studies have been performed investigating the potential role of miRs in the development of neointima, they have predominately used balloon-injury to rat carotid arteries to induce NIH. There are many pathological similarities but also some differences between the lesions that develop following balloon injury and those that occur after stent implantation. Also, although evolutionarily conserved, species differences in the roles and importance of specific miRs likely exist. For these reasons the *in-vivo* experiments contained in this chapter were performed in the large animal porcine model of stent overexpansion. We believe that we are the first group to use this model to investigate the role of miRs in ISR.

Implantation of both bare-metal and drug-eluting coronary stents into porcine coronary arteries results in upregulation of miR-21 as assessed by qRT-PCR. This increase was shown to persist out to at least 28 days post-implantation. Furthermore, In-situ hybridisation demonstrated the abundant expression of miR-21 throughout the vessel wall with the highest level in the developing neointima. A particularly strong signal was identified in neointima directly adjacent to stent struts. These findings are similar to those seen in rodent arteries following balloon injury and support the hypothesized role of miR-21 in VSMC phenotypic modulation following vessel injury and the pathological development of ISR. Therapeutic modulation of miR-21 levels, e.g. by antisense-mediated knockdown, remains to be tested in a large animal model of stent delivery but has shown to be effective in reducing neointimal formation following balloon injury in rats (Ji et al., 2007) and is therefore an approach worthy of consideration. In addition, inhibition of miR-

21 has been suggested to attenuate fibrosis in a model of heart failure (Thum et al., 2008) and also improve the function of endothelial progenitor cells in patients with CAD (Fleissner et al., 2010). The inhibition of miR-21 could conceivably be a novel way to inhibit neointimal formation while also promoting re-endothelialisation *in-vivo* and thus reducing ISR and stent thrombosis in the clinical setting. However, it is a ubiquitous miR, expressed in multiple tissue types and performing complex roles. Therefore systemic delivery of a therapeutic agent could potentially create off-target safety issues (e.g. oncogenesis). Localised delivery via, for example, a stent-based platform could be one approach to overcome these issues.

Similarly, miR-221 expression levels were shown to be elevated following stent delivery at 7 days, although had returned to baseline by 28 days. Unfortunately, due to time and cost constraints I was not able to perform co-localisation experiments for this miR but these observations from the porcine model support the hypothesis that miR-221 contributes to VSMC phenotypic switch and merits further investigation.

Current understanding regarding the role of the miR-143/miR-145 cluster in the control of VSMC phenotype has mainly been extrapolated from *in-vitro* and *in-vivo* small-animal models. Consistently, these studies have suggested that miR-145, and to a lesser extent miR-143, are key to maintaining VSMC in a differentiated state. This regulatory ability is lost following acute vascular injury when expression levels are seen to fall, presumably as part of a mechanism to allow vessel healing. In the setting of acute vascular injury, restoration of miR-145 was shown to limit neointimal formation in rodents. Following coronary stent insertion in pigs, miR-143/miR-145 levels are dynamic and consistent with the published data show a global decrease in expression as measured by qRT-PCR. *In-situ* analysis, however, suggested that although there is a significant decrease in expression within the injured vessel as a whole, a high level of expression develops in the media and emerging neointima. This increase was localised to areas with an increased expression of αSMA suggesting a correspondence to increasing VSMC re-popularisation. It has been proposed that rather than being essential for differentiation, the miR-143/miR-145 cluster acts to prevent de-differentiation and loss of the contractile VSMC phenotype associated with a decrease in αSMA expression and an increase in proliferation (Elia et al., 2009). The results from the porcine vessels are contrary to this with high levels of both miR-143 and miR-145 present in the developing neointima and correlating strongly with SMC markers. These findings are consistent with other work performed in our laboratory

showing a similar picture in the neointima of vein grafts from both a porcine model and also pathological failed human grafts (MacDonald *et al*, Unpublished data).

The exact reasons for these discrepancies require clarification as there are clear important implications for future therapeutics. In-situ hybridisation immediately following stent delivery (Day 0) confirms early loss of miR-145 expression consistent with qRT-PCR findings. It then "returns" when neointima has formed at the later time points, although overall vessel levels remain low. It is possible that this overexpression is not pathological and represents miR transfer from regenerating ECs that is designed to "terminate" neointimal formation by returning VSMCs to a contractile phenotype and thus prevent complete vessel occlusion. This would certainly be consistent with the observed difference in levels of miR-145 when BMS and DES were compared at 28 days. It is possible that the well recognised effect of DES on re-endothelialisation results in reduction of extracellular miR-145 transport. It should be noted, however, that no significant difference in neointimal area, as assessed by OCT, was seen between BMS and DES at 28 days. Further mechanistic studies are clearly required to investigate the relevance of these findings. Interestingly, in the porcine model, the location of miR-145 expression (and to a lesser extent miR-143) in the developing neointima appeared to be in the nucleus. It may therefore represent an increase in the level of pri-miR within the cells, which is detectable using the in situ probes, but not using the qRT-PCR probes. This suggests that transcription of the cluster is actively occurring within cells of the developing neointima and additional studies are required to assess the dynamics of miR-143/miR-145 expression and maturation under this form of pathological stress. This may also go some way to explaining the lack of significant miR-143/mir-145 dysregulation seen in my earlier described *in vitro* experiments.

Based on prior studies, several groups have postulated that restoration of miR-143/miR-145 levels following vascular injury could be a novel way of preventing neointimal formation and therefore ISR. However, my results suggest that the opposite may be true, and that pursuing local inhibition of these microRNAs may be more effective in view of their abundant expression within neointimal VSMC. Interestingly, Xin *et al*, have described a reduction in neointima formation after ligation of the carotid artery in miR-145-null mice adding further weight to this argument (Xin et al., 2009).

I believe that both approaches merit further investigation and that future large animal studies should assess the effects of both promotion and inhibition of these microRNAs in the setting of ISR.

Following stent delivery to porcine coronary arteries there was no evidence of dysregulation in miRs-92a, -126, -146a or -155 as compared to control unstented vessels and assessed by qRT-PCR. Levels of miR-133a were found to be significantly elevated immediately following vessel injury but unchanged from control at all other time points. These findings suggest that these micoRNAs do not play a significant role in the development of ISR *in-vivo* following stent delivery to porcine vessels. The change in miR-133a immediately following injury could be explained as an immediate response to VSMC injury as part of a reparative process however with no difference at any other time point is unlikely to play a significant role in ongoing neointimal development and therefore was not felt to represent a significant target for modulation *in-vivo*. Both miR-92a and miR-126 have been suggested to play important roles in the response of endothelial cells to injury (Harris et al., 2008, Nicoli et al., 2010, Zernecke et al., 2009) and in cell-to-cell communication between EC and VSMC (Zernecke et al., 2009, Hergenreider et al., 2012). While clearly not directly key to the VSMC response to injury and phenotypic switch they may still hold therapeutic potential through the stimulation of endothelial regeneration (Iaconetti et al., 2012). More rapid and complete endothelial recovery would be hoped to reduce the risk of stent thrombosis and artificial overexpression of miR-126 or inhibition of miR-92a may inhibit ISR development even though levels are not directly altered following injury. Further experiments are clearly required to justify this approach, for which the porcine model of stent delivery is ideal.

Due to cost restrictions I was not able to perform microRNA profiling experiments (e.g. microarray) on the RNA extracted from porcine vessels treated with BMS or DES. This has previously been performed in a porcine model of interposition vein grafting and reported by our institution (McDonald et al., 2013). This model of vein-graft disease, vascular injury and intimal hyperplasia shares many pathological similarities to the stent model of neointimal ISR. I therefore investigated a series of novel miRs, not previously implicated in the response to vascular injury, but significantly dysregulated in engrafted porcine veins by performing qRT-PCR verification on RNA from the porcine stent model.

The most interesting results related to miR-142-3p and miR-142-5p. Both were found to be significantly upregulated following delivery of BMS only. They are transcribed from

chromosome 17q22 and have not previously been reported as being involved in the vasculature. Previous reports have described miR-142 as being highly specific for haematopoietic cells and involved in immune regulation (Landgraf et al., 2007). They are also oncogenes with miR-142-3p being associated with leukaemia (Dahlhaus et al., 2013) and miR-142-5p with gastric mucosa-associated lymphoid tissue lymphoma (Saito et al., 2012). Interestingly, miR-155 has been shown to negatively regulate miR-142-3p expression, suggesting a further role in inflammation (Sun et al., 2013). My findings suggest that miR-142 may be involved in vascular cell-cycle regulation and ISR formation and further mechanistic insight is required to test this hypothesis and establish any potential therapeutic effect.

Other potential miRs of interest that arose from the qRT-PCR analysis were miR-23b, miR-30c and miR-99b. It has been reported that miR-23b acts as a tumour suppressor being found in high levels in tumours of the oesophagus, bladder, colon and prostate with possible involvement in human papilloma virus oncogenesis (Zheng and Wang, 2011). It acts as a cell-cycle regulator as a downstream target of the oncogene c-Myc (Dang, 2010). In the cardiovascular system it has been shown to block cell-cycle progression in EC *in-vitro* (Boon et al., 2012) and is felt to play an atheroprotective role in vessels subjected to shear stress (Neth et al., 2013).

As well as being dysregulated in lung, ovarian and breast carcinomas, miR-30c has an apparent effect on lipid metabolism in mice with hepatic overexpression reducing hyperlipidaemia and atherosclerosis and vice versa (Soh et al., 2013).

Lastly, miR-99b is another oncomir that is implicated as a tumour suppressor in non-small cell lung cancer (Kang et al., 2012) and as a biomarker of papillary thyroid carcinoma (Dettmer et al., 2013).

Further mechanistic and co-localisation experiments are clearly required to test the validity of these novel miRs as potential regulators of VSMC homeostasis and targets for therapeutic manipulation. These initial results are however, encouraging. All of these novel miRs play a role as either biomarkers or regulators of cell-cycle regulation in cancer and with the findings from the porcine stent model in conjunction with very similar parallel results from qRT-PCR analysis of porcine interposition grafts at 7 and 28 days it is highly likely that at least some are involved in the vascular response to injury, potentially as part

of a coexpressed microRNA regulatory network. Ongoing work within our institution will hope to clarify and expand on these initial findings in due course.

The use of a combination of qRT-PCR to assess overall vessel expression levels and *in-situ* hybridisation to localise microRNA presence within the vessel wall and emerging neointima has allowed a comprehensive longitudinal analysis of the dynamic changes in miR-21, miR-145 and miR-143 following stent delivery and vessel injury. To-date there are no published studies using large animal models to investigate the role of microRNAs in the development of ISR, thus adding novelty to the above findings. Assessment of the role of miRs in multiple pre-clinical models is required as differences may be present across different species (e.g. rodent vs. pig), different vascular beds (e.g. carotid artery vs. coronary artery) or even with different mechanisms of vascular injury (e.g. balloon dilatation injury vs. stent delivery). Knockdown of miR-143 and miR-145 has been shown to affect different vessels to different extents (Boettger et al., 2009), possibly due to variation in normal levels of expression which may reflect differences in the importance and/or function of the cluster.

Using a model of stent delivery is relevant to current clinical practice and would be hoped to provide more relevant findings that older models of balloon injury. It was also of interest to explore potential differences in miR levels in response to delivery of bare-metal versus drug-eluting stents. It is feasible that miRs may play an important role in mediating the effects of antiproliferative drugs on VSMC and EC proliferation or the sequelae of chronic inflammation and delayed arterial healing. In my experiments a second generation zotarolimus-eluting stent (Endeavor^{TM}, Medtronic, Minneapolis, MN, USA) was used due to easy availability of a range of sizes suitable for comparison with my chosen bare metal platform. Zotarolimus is a more lipophilic analogue of the immunosuppressant rapamycin (sirolimus). It acts as an anti-proliferative agent, blocking cell-cycle progression from G_1 to S phase through binding with the intracellular protein FKBP-12 and inhibiting VSMC and EC proliferation (Garcia-Touchard et al., 2006). When phosphorylcholine-coated Zotarolimus-eluting stents were tested in porcine coronary arteries *in-vivo* a 40% reduction of neointimal formation compared with a bare-metal platform at 28 days post-implantation was reported (Garcia-Touchard et al., 2006). In my experiments, a single 28 day time-point was used for the DES group to limit experimental costs and also due to limitations on available space for animal housing. The only vascular miR found to be significantly different between the two stent platforms used was miR-145. Of the novel miRs, both miR-30c (reduced in BMS at 28 days) and miR-99b (reduced in DES at 28 days) showed

potential differences. Also somewhat surprisingly, but in keeping with the qRT-PCR findings, mean neointimal thickness as assessed using OCT was similar in both the BMS and DES groups in my study. The reasons for these findings are not clear. The original Endeavor stent used has rapid drug-release kinetics with 95% of the zotarolimus eluted from the stent <15 days after implantation (Nakazawa et al., 2007). This has been suggested to potentially reduce local toxicity. In atherosclerotic plaques this highly lipophilic drug displays prolonged tissue retention (Nakazawa et al., 2007) however in my disease-free animals this is likely to be much less marked. Therefore my chosen 28 day time point, although normal for pathological studies, may have missed transient miR dysregulation in the presence of zotarolimus. It is also possible that the action of zotarolimus utilises a network of microRNAs distinct to those tested. This requires testing in *in-vitro* cell studies using miR microarray profiling. Lastly, the DES used in this chapter were all those that had passed their "use-by-date" and been removed from the shelf in a clinical catheter laboratory. Although unlikely, it is possible that the drug had degraded to become non-functional. This could explain the observed lack of difference in mean neointimal areas between BMS and DES at 28 days as observed by OCT. Clearly further and more rigorous experimental testing is required, utilising modern drug-eluting stent platforms to assess the role of microRNAs in both their antiproliferative action and delayed arterial healing.

Most pre-clinical models utilising stent insertion have been limited in the histological analysis that can be performed due to the methods of tissue processing commonly used. Normal tissue fixation, paraffin embedding and cutting with a microtome cannot be effectively performed with an *in-situ* metal scaffold as the metal/tissue interface results in excessive damage to the tissue architecture. Initially, stented arteries were carefully sectioned and the metal stent fragments removed by hand prior to tissue processing. This was, however, time consuming and maintenance of tissue architecture was challenging. Methods were therefore developed of tissue fixation and resin embedding which allowed tissue sectioning through use of precision saws and grinding/polishing to obtain sections of the required thickness (Malik et al., 1998). This allows for excellent morphometric analysis due to preservation of the stent/tissue interface but the incompatibility of organic solvents with the embedding resins limits the histochemical staining techniques that can be used (Malik et al., 1998). Further limitations include the requirement for specialist equipment, the overall cost of the procedure, time consuming processing steps, significant tissue depletion during processing, and a minimum obtainable section thickness of 8-10μm that can affect quality of morphometric studies (Rippstein et al., 2006). Lastly, it would not

have been possible to perform in-situ hybridisation on my samples if resin embedded, again due to lack of compatibility with the resins and solvents.

To circumvent these issues a novel method of stent dissolution using electrolysis was employed in the experiments in this chapter. By applying a differential voltage to an embedded stent and placing it in a mildly acidic salt solution, complete stent dissolution can be obtained (Samra et al., 2010, Bradshaw et al., 2009). This method is fast, cost-effective and results in significantly less tissue loss than resin embedding. It therefore allows for a more complete examination of the whole tissue segment and most importantly normal histological processing facilitating a complete range of histochemical staining methods, immunohistochemistry and in-situ hybridisation.

Complete dissolution of the cobalt chromium BMS platforms used in this chapter was achieved readily and consistently. Unfortunately, the DES platforms proved highly resistant to electrolysis and significant tissue destruction resulted, limiting the analysis that could be performed. It is noted that polymer-coated stents can impede process as the insulating coating prevents the continuity of the electrical circuit required for complete dissolution. This occurred despite using measures described in the original published methods (Bradshaw et al., 2009). As described in the above results section of this chapter, morphometric histology and in-situ hybridisation co-localisation of miRs was not obtained in the 28 day DES group.

It was however possible to obtain a measurement of mean neointimal area in 4% PFA-fixed stented arterial segments *ex-vivo* before dissolution and further processing using an optical coherence tomography catheter. This technique allows for accurate quantification of neointimal thickness and area and can also be used to assess strut coverage (Douglas et al., 2012). It is a useful adjunct to classical histological methods as neointimal measurements can be made along the whole vessel segment with a longitudinal reconstruction also being provided.

In summary, the experiments described in this chapter support the hypothesis that microRNAs play an important role in regulating the pathogenesis of acute vascular injury and the development of coronary ISR. A large animal model of ISR has not previously been used in this setting adding both novelty and clinical relevance to the described findings. As does the use of combined qRT-PCR measurement with *in-situ* hybridisation for histological co-localisation. Both miR-21 and the miR-143/miR-145 cluster appear to

play a key role in the regulation of VSMC phenotypic switch and are shown to be both dynamic and significantly upregulated in developing neointima following stent implantation. This localised upregulation in the miR-143/miR-145 cluster, despite a consistent overall "whole-vessel" downregulation, is particularly novel and differs from previously published findings. This has important implications towards future therapeutic manipulation. Furthermore, this chapter provides the first validation of suitable endogenous controls for qRT-PCR analysis in porcine vascular tissue and also shows the suitability of the electrolysis method to achieve atraumatic stent dissolution thus allowing a comprehensive range of histological techniques to be performed. Finally, and consistent with suggestions that microRNAs operate in regulatory networks, a panel of novel miRs have been identified that may play an important role in the development of ISR and merit future investigation.

Although the above findings do not fully explain the mechanisms behind this role they provide an important step towards our understanding. Although unsuccessful using the Endeavor zotarolimus-eluting platform the potential differences that may occur in microRNA expression following DES delivery remain intriguing. In our institution we therefore plan to repeat the porcine experiments using a widely used stainless-steel platform abluminally coated DES that we have recently shown to be amenable to dissolution and comparison with its BMS counterpart. This will allow both full microarray miR profiling and in-situ hybridisation in the DES arteries to fully investigate potential expression differences between the stent types. Lastly we plan to investigate the effect of systemically delivered antagomirs to miR-21 and miR-145, and miR-145 mimics on the development of ISR in the pig. If successful, it would be hoped to progress to local delivery via a suitable stent platform.

5 Dynamic changes in circulating microRNA levels in patients undergoing Coronary Artery Bypass Surgery

5.1 INTRODUCTION

Cardiovascular disease remains the principle contributing cause to mortality in Europe; responsible for approximately 4.3 million deaths per annum (48% of all deaths) (Allender et al., 2008). Coronary Artery Bypass Graft (CABG) surgery remains an important treatment modality in patients with severe coronary artery disease (CAD), and although numbers have stabilized due to the rise in use of percutaneous coronary intervention (PCI), more than 25,000 procedures are performed in the UK per annum (Scarborough et al., 2011) and greater than 400,000 in the U.S.A (Roger et al., 2012). Although effective, CABG remains limited by conduit graft failure with only 50-60% of vein grafts being patent at 10 years post-surgery (Motwani and Topol, 1998, Parang and Arora, 2009). As previously discussed, vein graft disease occurs as a result of multiple pathological processes including thrombosis, intimal hyperplasia and accelerated atherosclerosis (Motwani and Topol, 1998) and results in recurrent symptoms and MI leading to repeat revascularisation carrying excess morbidity and mortality (Mehilli et al., 2011, Lopes et al., 2012).

Risk factors for early graft occlusion are well characterized and include: female gender, obesity, unstable anginal symptoms, history of congestive heart failure, the artery to be bypassed (RCA>LAD), quality of the distal bed, diameter of the grafted vessel, lack of antiplatelet therapy and use of a nonsequential technique (Paz et al., 1993). However due to the heterogeneity of these patients it remains difficult to predict. The use of an extracorporeal circulation for cardiopulmonary bypass (CPB) is shown to be a major contributing factor to post-operative morbidity including neuropsychological impairment (Khan et al., 2004), systemic inflammatory response syndrome (Day and Taylor, 2005) and tissue injury due to ischaemia and reperfusion (Chandrasena et al., 2009, Nair et al., 2012). Early elevations in serum levels of cardiac enzymes (principally creatine kinase and troponin) post-CABG have been shown to correlate with increased intermediate- and long-term mortality (Domanski et al., 2011). Although markers of cardiac cell necrosis, these enzyme rises do not help to differentiate between the multiple potential causes of cell death such as graft failure, insufficient myocardial protection, air embolism, regional or global ischaemia or inflammation. There is therefore an unmet clinical need for reliable, sensitive and specific biomarkers that may predict particular complications or more accurately those at increased risk of a poor outcome post-surgery.

As previously discussed, microRNAs are short, non-coding ribonucleic acids (RNAs) that act to control gene expression at a posttranscriptional level and have been shown to play a key role in cellular function in both normal physiology and disease states. There has been a proliferation of studies in the literature describing miRs as being key regulators within the cardiovascular system. Through the display of distinct tissue expression profiles they appear to mediate cardiac development, vasculature homeostasis, response to vascular injury, neoangiogenesis and tissue repair (Latronico et al., 2007, Small et al., 2010).

More recently it has been shown that miRs can be detected in the circulation (Mitchell et al., 2008), either as a result of cellular damage or active secretion (Laterza et al., 2009), as regulators of an underlying pathological process (Gilad et al., 2008) or even as part of an inter-cellular signalling network (Zampetaki et al., 2012a). These circulating miRs are stable (Tsui et al., 2002b, Weber et al., 2010a), being packaged in microvesicles (exosomes, microparticles and apoptotic bodies) or bound to RNA-binding proteins or lipoprotein complexes, conferring resistance to degradation from circulating RNAse activity (Zampetaki et al., 2012a, Creemers et al., 2012). This, in combination with the poor risk prediction provided by traditional risk factors and existing soluble biomarkers, has lead to great interest in their potential as diagnostic and prognostic biomarkers.

There is an emerging body of literature associating specific circulating “miR signatures” with cancer, acute coronary syndromes/myocardial infarction, coronary artery disease, hypertension, heart failure, diabetes mellitus as well as many other non-cardiovascular conditions (Mitchell et al., 2008, Fichtlscherer et al., 2011, Creemers et al., 2012, Engelhardt, 2012). These studies suggest that the presence of miRs within the circulation may reflect the activation state of cells important to the disease process, such as smooth muscle cells, endothelial cells, platelets, monocytes and macrophages. They therefore provide an integrated read-out of both cell activation and tissue injury in response to cardiovascular risk factors and resulting tissue injury (Zampetaki et al., 2012a).

The aim of this chapter therefore, was to analyze, for the first time, the temporal expression profile of a selected group of miRs in the serum of patients undergoing CABG to investigate their future potential as biomarkers in this group of patients. Although not directly related to ISR, it was felt to be appropriate to include this Chapter within the thesis. To fully understand the complex regulatory role that miRs play within the developing neointima and damaged endothelium following vascular injury, it is important to recognise their presence and purpose within the circulation.

5.2 RESULTS

5.2.1 Demographics

Baseline characteristics from the cohort of 21 patients are shown in Table 5.1. Intra-operative characteristics are summarised in Table 5.2 and post-operative course described in Table 5.3. This cohort reflects a group of predominately male (76%), symptomatic (55% unstable symptoms) patients with extensive coronary disease (95% 3-vessel disease) and good LV systolic function (Mean Ejection Fraction: 57±11%), undergoing uncomplicated CABG at a single centre. Operations were performed by 4 surgeons with one senior operator being involved in 67% of procedures.

5.2.2 Panel of MicroRNAs Studied

A panel of miRs associated with both acute and stable chronic coronary artery disease were chosen (Fichtlscherer et al., 2011, Creemers et al., 2012). Muscle-enriched miRs-133a and -499 are elevated in pre-clinical models of, and patients with, MI/ACS (Wang et al., 2010a, D'Alessandra et al., 2010, Kuwabara et al., 2011, De Rosa et al., 2011) or stable CAD (Fichtlscherer et al., 2010). The cardiomyocyte-specific miR-208a and miR-208b cluster are undetectable in normal controls but elevated in patients with MI/ACS (Corsten et al., 2010, Widera et al., 2011, Wang et al., 2010a, De Rosa et al., 2011) and stable CAD (Fichtlscherer et al., 2010). Endothelial cell enriched miR-126 and miR-92a, leucocyte/inflammatory miR-155 and liver-specific miR-122 have also been identified as having potential as biomarkers in both acute and chronic coronary disease (Fichtlscherer et al., 2010, De Rosa et al., 2011). Furthermore, it was felt important to investigate miRs shown to be important in vascular injury (previously discussed in Chapter 4); namely miR-21, miR-143 and miR-145.

Table 5-1 Patient's Baseline Characteristics[2]

	CABG Group (n=21)
Sex (M/F)	16/5
Age (yrs)	66.3±9.5
Body weight (kg)	67.8±12.9
BSA (m^2)	1.71±0.18
Risk Factors	
Cigarette Smoking	10 (50%)
T2DM	9 (43%)
HBP	18 (86%)
Hyperlipidaemia	9 (43%)
Clinical Features	
Angina	
(≥CCS III)	15 (71%)
Unstable	12 (55%)
Previous MI	8 (38%)
Family H_x IHD	0 (0%)
CHF	1 (5%)
Ejection Fraction (%)	57±11
Angiographic Findings	
TVD	20 (95%)
LMS Involvement	14 (67%)
Calcification reported	2 (9%)
Medications	
Aspirin	21 (100%)
Clopidogrel	20 (95%)
Statin	19 (86%)
β-blocker	20 (95%)
ACEi/ARB	16 (76%)
OHA	9 (43%)
Insulin	1 (5%)
Heparin	3 (14%)
Warfarin	1 (5%)
ά-blocker	4 (19%)
Allopurinol	1 (5%)

[2] All numbers given as absolute values ± standard deviation as appropriate. Percentage of full cohort given in brackets. ACEi – Angiotensin Converting Enzyme inhibitors. ARB – Angiotensin Receptor Blockers. BSA – Body Surface Area. CABG – coronary artery bypass grafting. CCS – Canadian Cardiovascular Society. CHF – Congestive Heart Failure. HBP – hypertension. IHD – ischaemic heart disease. LMS – left main stem. MI – myocardial infarction. OHA – oral hypoglycaemic agents. T2DM – Type 2 diabetes mellitus. TVD – triple vessel disease.

Table 5-2 Intra-Operative Characteristics[3]

	CABG Group (n=21)
Procedural Urgency	
Emergency	1 (5%)
Urgent	2 (9%)
Elective	18 (86%)
Vein Harvest Technique	
Open	16 (76%)
EVH	5 (24%)
Number of Grafts	
3	17 (81%)
2	4 (19%)
LIMA used	17 (81%)
CPB Duration	
Bypass time (mins)	103±32
Ischemic time (mins)	58±21
Blood Product use	
RBC required	16 (76%)
1U	4 (25%)
2U	5 (31%)
3U	3 (19%)
4U	4 (25%)
Platelets required	13 (62%)
1U	1 (8%)
2U	1 (8%)
3U	2 (15%)
4U	8 (61%)
5U	0 (0%)
6U	1 (8%)
Fresh Frozen Plasma	6 (29%)
1U	1 (17%)
2U	2 (33%)
3U	2 (33%)
4U	1 (17%)
Cryoprecipitate (1U)	1 (5%)

[3] All numbers given as absolute values ± standard deviation as appropriate. Percentages given in brackets. CABG – coronary artery bypass grafting. CPB – cardiopulmonary bypass. EVH – endoscopic vein harvest. LIMA – left internal mammary artery. RBC – red blood cells. U – units.

Table 5-3 Post-Operative Course[4]

	CABG Group (n=21)
Time to Extubation (hrs)	8±4
Duration of ICU Stay (hrs)	20±2
Blood Products required (RBC)	2 (9%)
Post-op Medication Use	
Clopidogrel	18 (86%)
Aspirin	21 (100%)
Tramadol	17 (81%)
Complications	
Dysrhythmia	5 (24%)
Atrial Fibrillation	2
Atrial Flutter	1
Unspecified Tachycardia	2

[4] All numbers given as absolute values ± standard deviation as appropriate. Percentages given in brackets. AF – atrial fibrillation. CABG – coronary artery bypass grafting. ICU – intensive care unit. RBC – red blood cells. VR – ventricular rate.

5.2.3 Temporal Changes in Circulating MicroRNA Levels

All temporal comparisons were made to pre-op (PO) expression levels. Circulating levels of miR-133a showed a 6-fold elevation (RQ 5.89; $p<0.001$) on the first post-operative day (POD1) returning to baseline at day 5 post-op (POD5) (Figure 5.1). Levels of miR-122, previously shown to be down-regulated in patients with myocardial infarction (D'Alessandra et al., 2010), were significantly reduced on POD1 (77% reduction, RQ 0.23, $p<0.001$) but returned to baseline at POD5 with no significant difference when compared to PO levels (RQ 0.89, $p>0.05$) (Figure 5.2). These statistically significant associations persist when Ct values are normalized to the mean of all measured miRs (Figure 5.3-5.4). Levels of miR-92a (43% reduction, RQ 0.57, $p<0.05$, POD5) and miR-126 (33% reduction, RQ 0.67 $p<0.01$, POD1; 29% reduction, RQ 0.71, $p<0.05$, POD5) were reduced post-CABG (Figure 5.2) when normalized to “spiked-in” cel-miR-39. These significant associations at POD5 were lost when Ct values were normalized to the mean of all measured miRs, however this method is known to weaken observed associations (Zampetaki et al., 2012a) (Figure 5.5-5.6). No significant temporal changes in levels of miR-145, miR-143 or miR-21 were observed (Figure 5.1) with either normalization method. MiR-155 levels were also unchanged post-CABG (Figure 5.2). MiR-208a, miR-208b, and miR-499 were undetectable (Ct = Undetermined) in all patients at all time points, using the previously described experimental protocol.

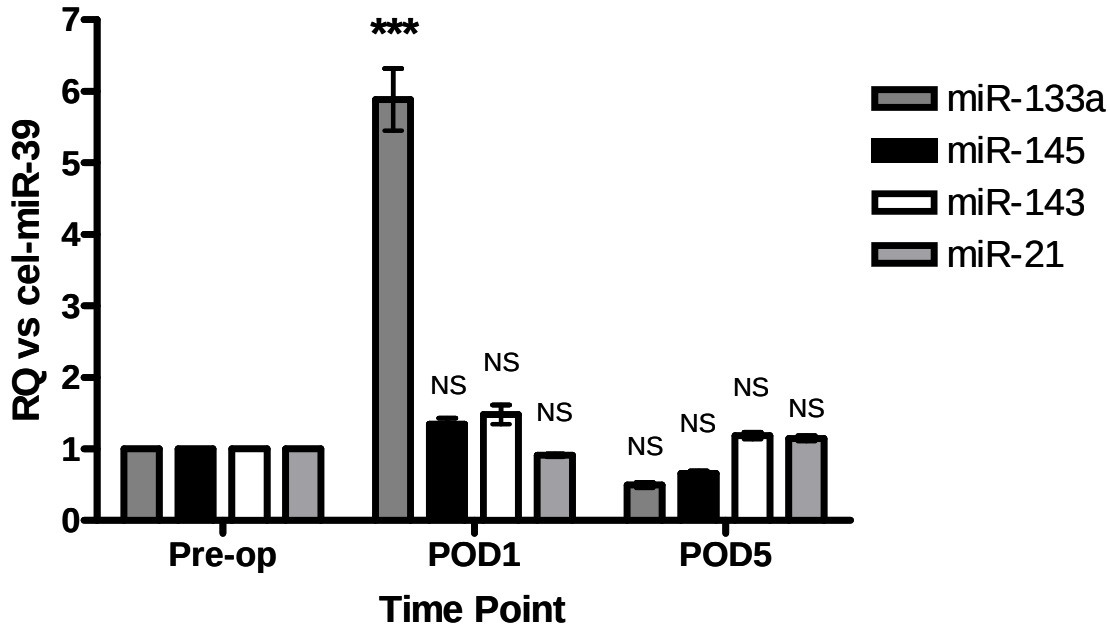

***** = p<0.05 ****** = p<0.01 ******* = p<0.001 NS = p>0.05

Figure 5-1 Circulating microRNA levels in serum from patients undergoing CABG – miRs showing increase or no change

RNA extraction from serum and levels determined by qRT-PCR. Ct values normalised to "spiked-in" cel-miR-39. RQ values calculated using $2^{-\Delta\Delta Ct}$ method and reported as RQ $\pm$ RQmax. p values are versus PO levels and calculated from ANOVA with Tukey adjustment for multiple comparisons. PO – Pre-op. POD1 – Post-op Day 1. POD5 – Post-op Day 5. RQ – Relative Quantity.

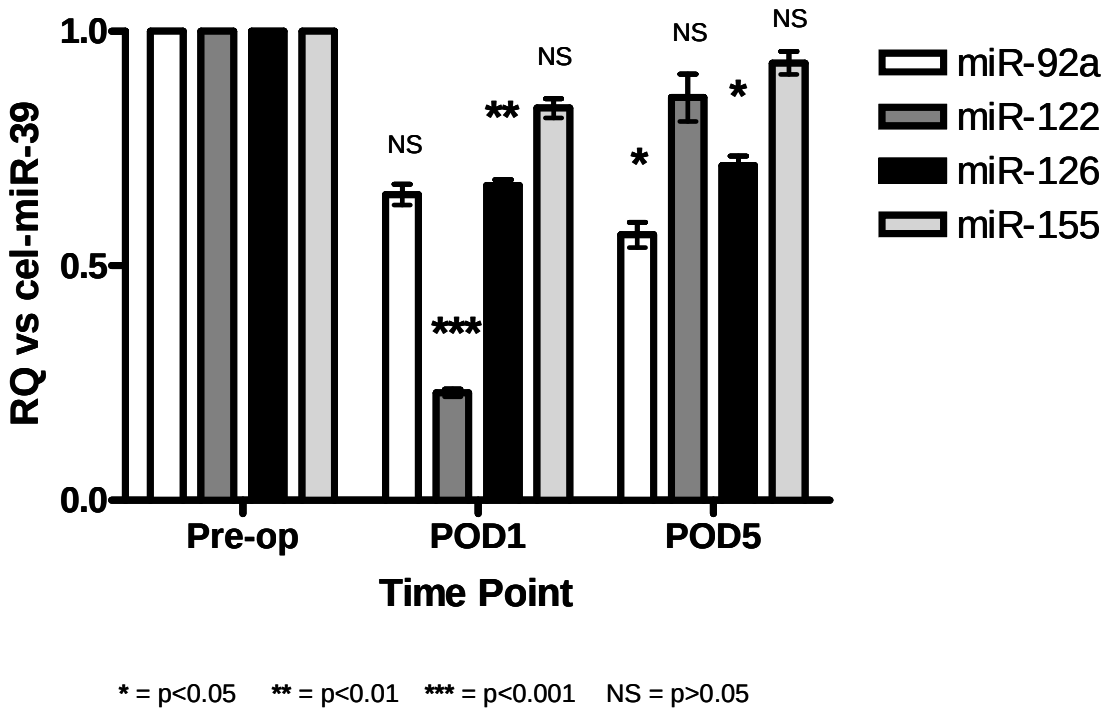

Figure 5-2 Circulating levels of microRNAs showing a post-op reduction

RNA extraction from serum and levels determined by qRT-PCR. Ct values normalised to "spiked-in" cel-miR-39. RQ values calculated using $2^{-\Delta\Delta Ct}$ method and reported as RQ $\pm$ RQmax. p values are versus PO levels and calculated from ANOVA with Tukey adjustment for multiple comparisons. PO – Pre-op. POD1 – Post-op Day 1. POD5 – Post-op Day 5. RQ – Relative Quantity.

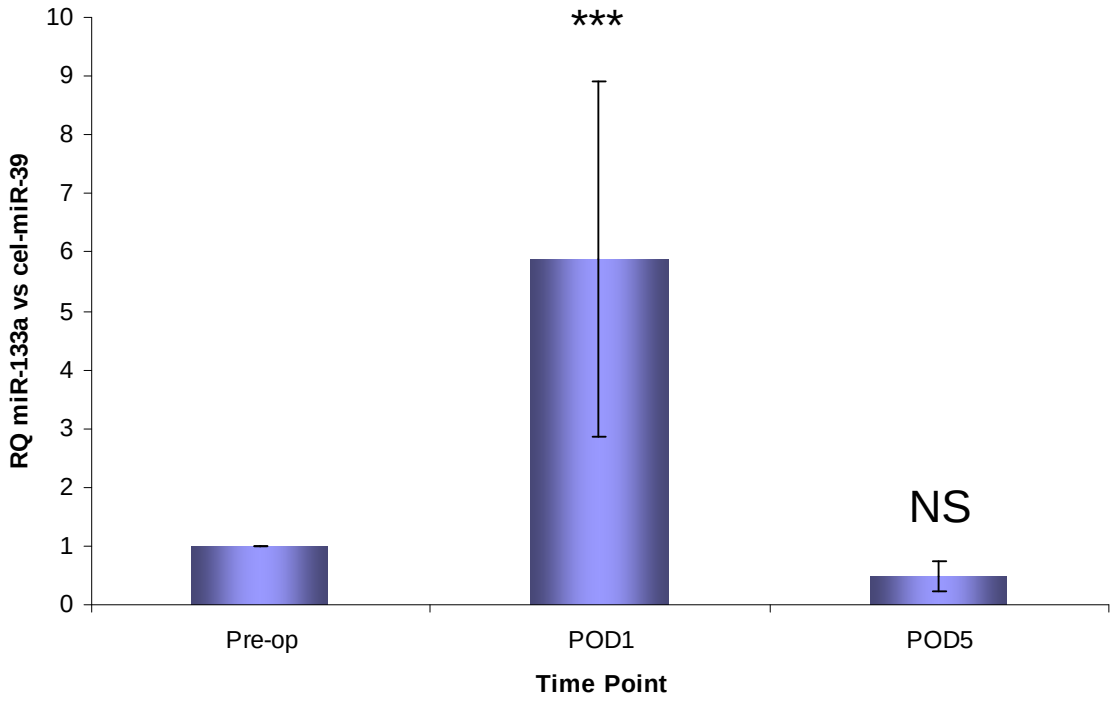

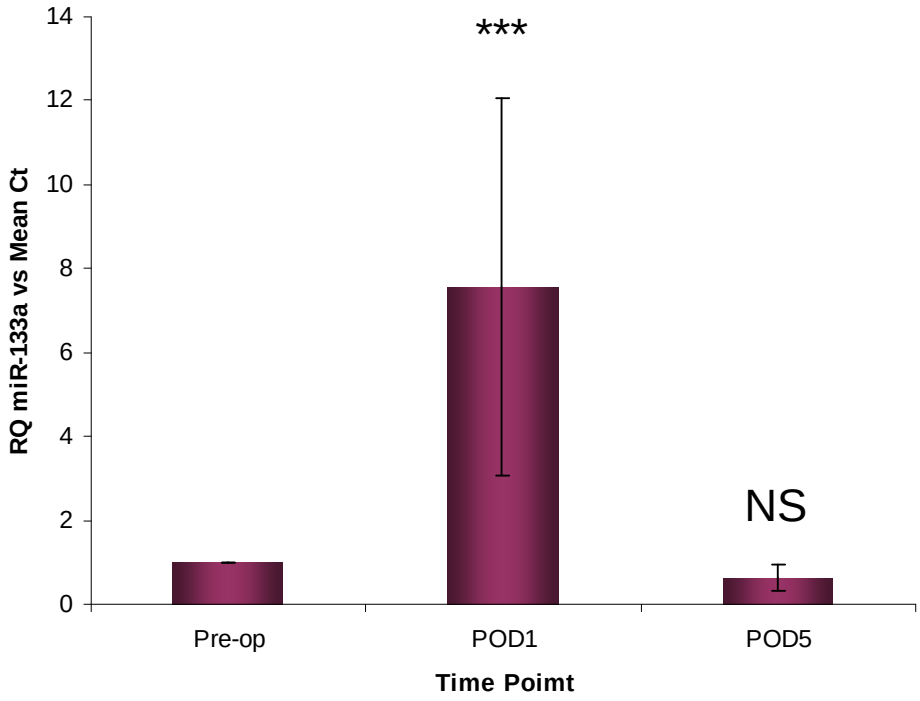

Figure 5-3 Comparison of normalisation methods for miR-133a

Quantitative real time PCR data for miR-133a normalised to both cel-mir-39 (above) and the mean of all measured microRNAs (below). RQ (Relative Quantity) ± RQmax. All comparisons made vs. control group (PO) using repeated measures ANOVA with Tukey's post test. *p<0.05, **p<0.01, ***p<0.001, NS p>0.05 (non-significant).

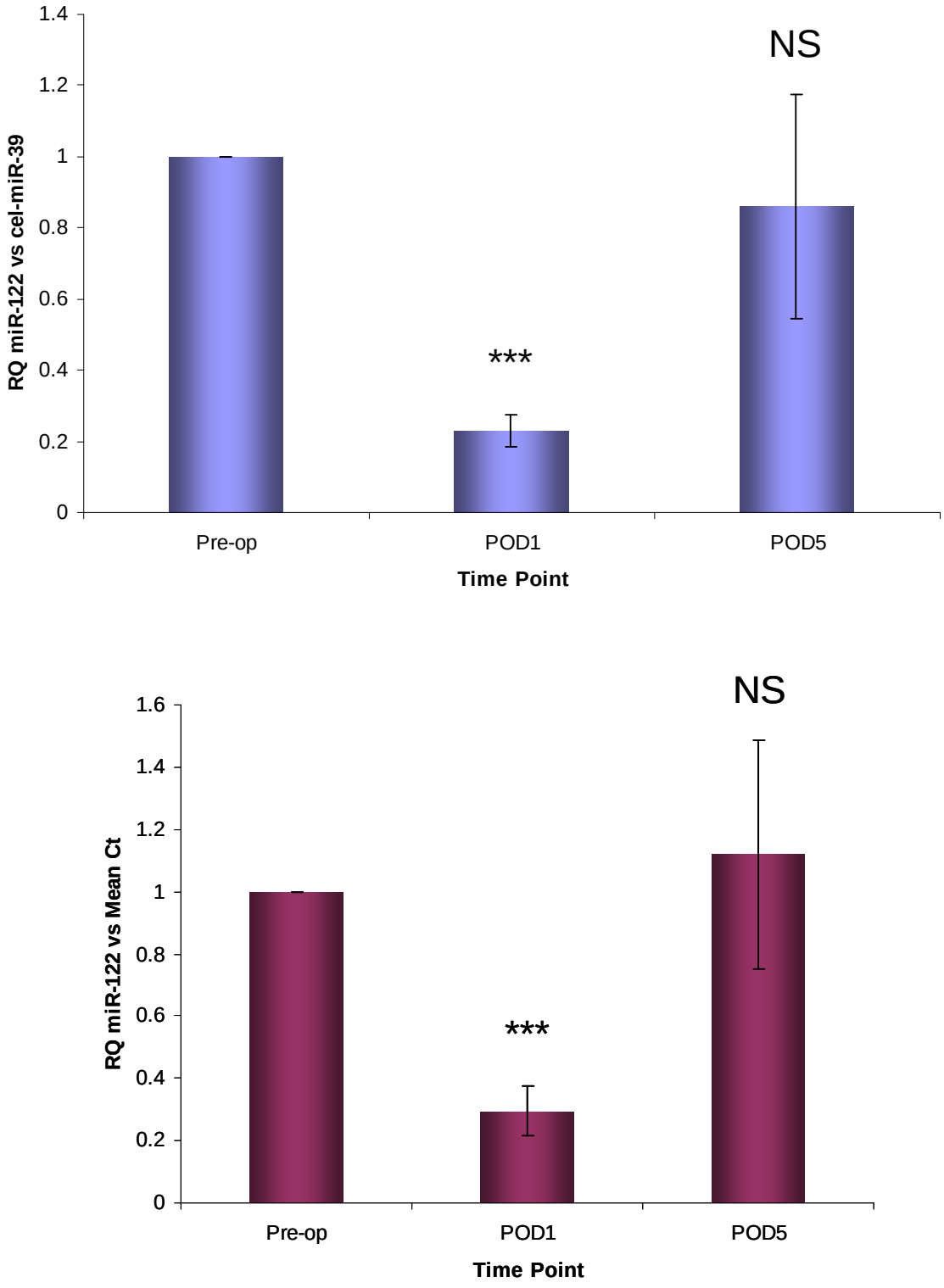

Figure 5-4 Comparison of normalisation methods for miR-122

Quantitative real time PCR data for miR-122 normalised to both cel-mir-39 (above) and the mean of all measured microRNAs (below). RQ (Relative Quantity) ± RQmax. All comparisons made vs. control group (PO) using repeated measures ANOVA with Tukey's post test. *p<0.05, **p<0.01, ***p<0.001, NS p>0.05 (non-significant).

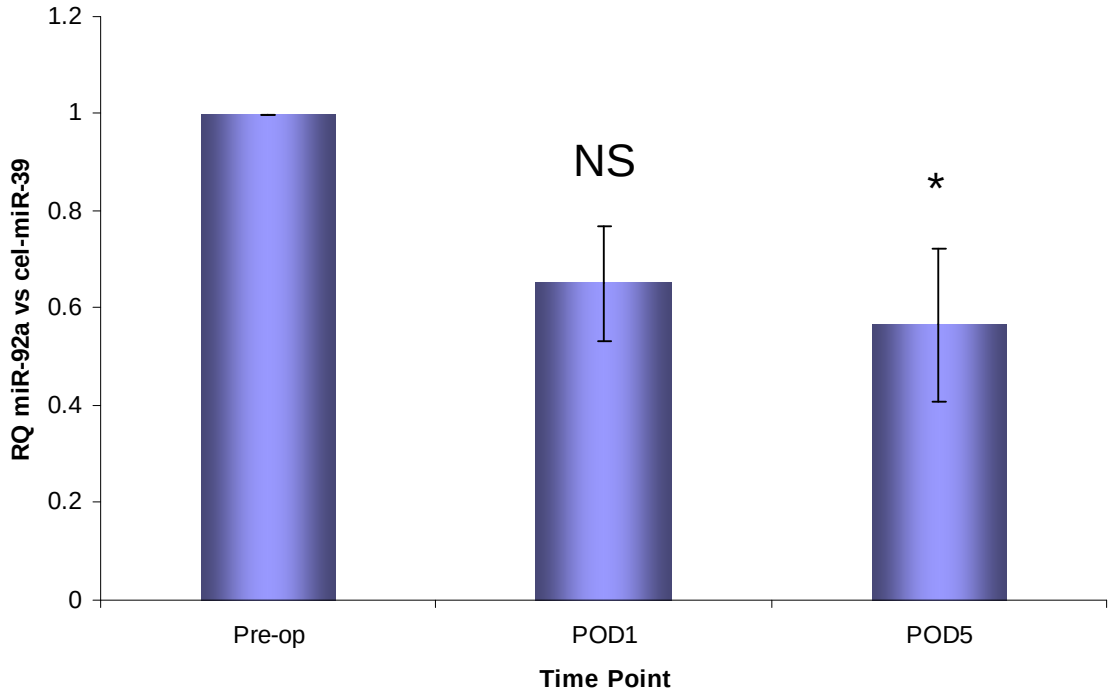

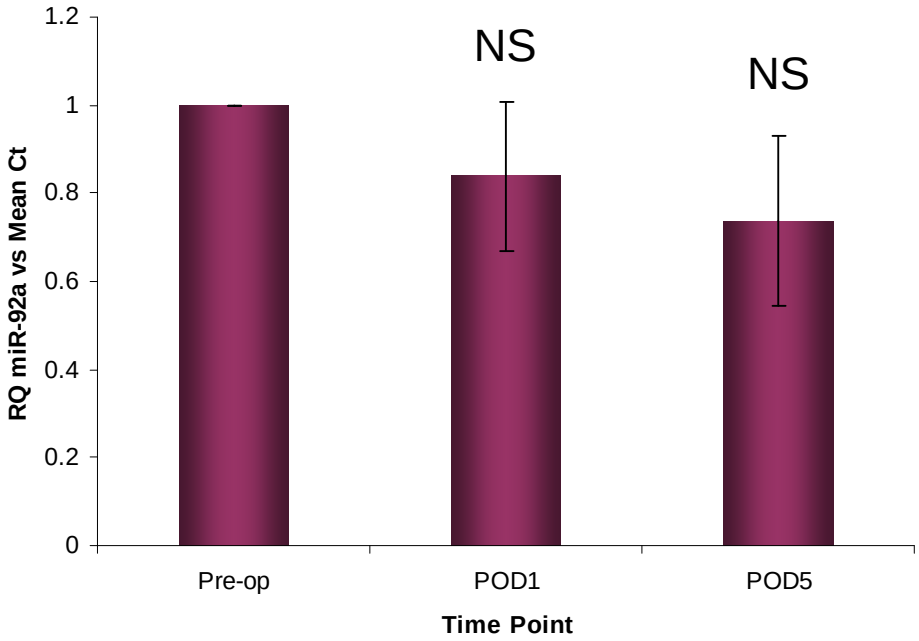

Figure 5-5 Comparison of normalisation methods for miR-92a

Quantitative real time PCR data for miR-92a normalised to both cel-mir-39 (above) and the mean of all measured microRNAs (below). RQ (Relative Quantity) $\pm$ RQmax. All comparisons made vs. control group (PO) using repeated measures ANOVA with Tukey's post test. *p<0.05, **p<0.01, ***p<0.001, NS p>0.05 (non-significant).

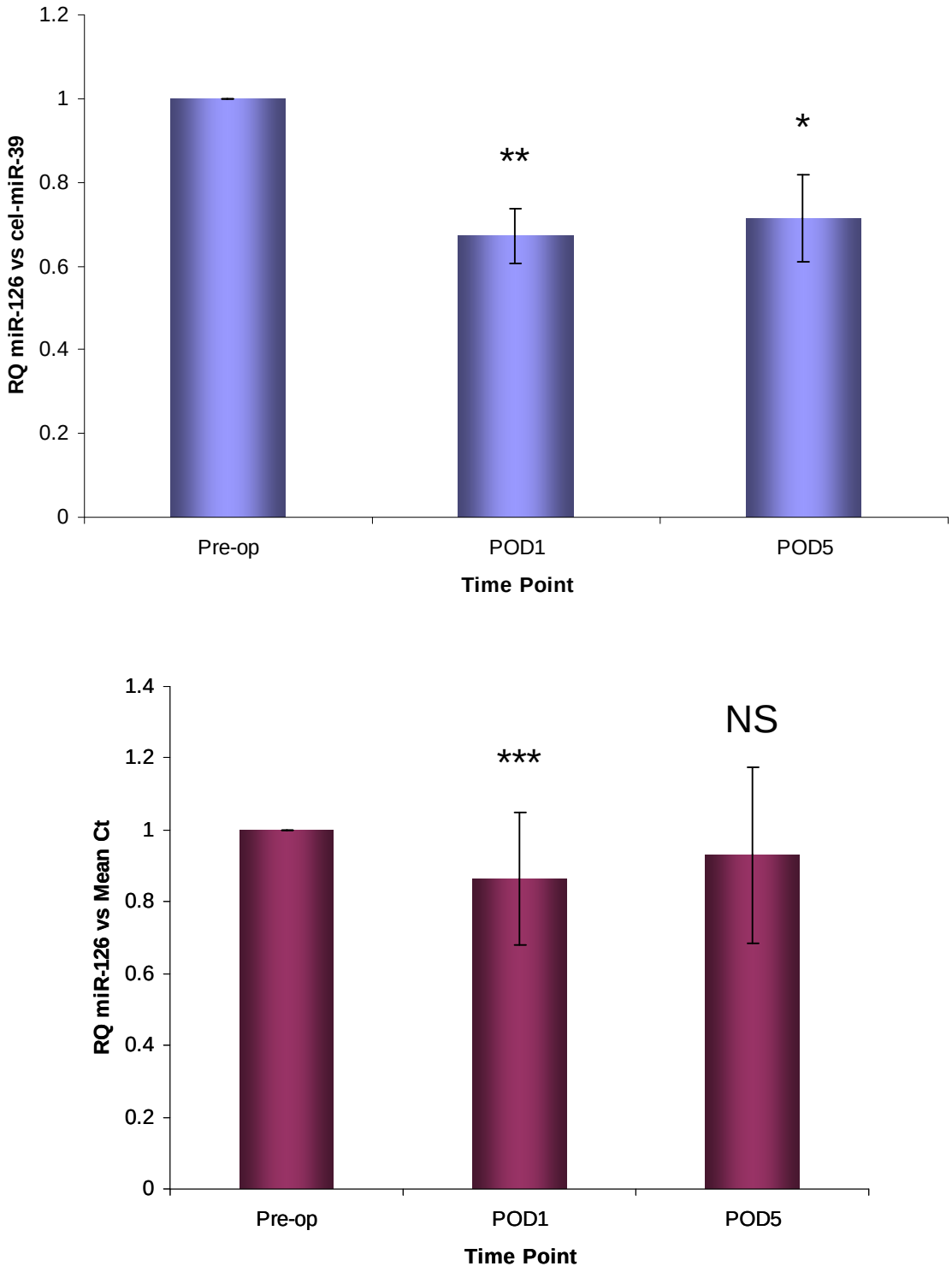

Figure 5-6 Comparison of normalisation methods for miR-126

Quantitative real time PCR data for miR-126 normalised to both cel-mir-39 (above) and the mean of all measured microRNAs (below). RQ (Relative Quantity) ± RQmax. All comparisons made vs. control group (PO) using repeated measures ANOVA with Tukey's post test. *p<0.05, **p<0.01, ***p<0.001, NS p>0.05 (non-significant).

5.2.4 Correlation with Existing Biomarkers

To investigate the potential of these dynamic circulating miRs for use as biomarkers we performed correlations with existing classical biomarkers. Serum cTnT levels (Table 5.4) increased from undetectable levels in all but one patient PO to median 0.16μg/L (Range 0.07-13.00μg/L) at POD1 ($p<0.001$) and 0.11μg/L (Range <0.03-9.60μg/L) at POD5 ($p<0.01$). The increase in miR-133a at POD1 correlated with the rise in cTnT ($p<0.0466$) (Figure 5.7). MiR-122, 92a and 126 levels showed no significant correlation with cTnT ($p>0.05$) at any time point (Figure 5.8). Serum CRP levels increased from 4.3±8.0mg/L PO to 159.7±11.7mg/L at POD1 and decreased to 106.4±54.4mg/L at POD5 (Table 5.4). There was no association between any of the studied miRs and serum CRP levels ($p>0.05$, all comparisons).

Table 5-4 Serum levels of C-reactive protein and cardiac isoform of Troponin T[5]

	CRP(mg/L)			cTnT (ug/L)		
Patient No	**Pre-op**	**POD1**	**POD5**	**Pre-op**	**POD1**	**POD5**
1	11.3	111.0	29.3	<0.03	0.18	0.13
2	<0.6	117.6	40.6	<0.03	0.13	0.11
3	<0.6	236.9	100.9	<0.03	0.10	0.07
4	1.7	130.0	112.1	<0.03	0.22	0.18
5	<0.6	124.0	25.9	<0.03	0.14	0.05
6	<0.6	100.9	67.0	<0.03	0.12	0.06
7	<0.6	157.0	164.9	<0.03	0.85	0.70
8	1.7	122.6	125.4	<0.03	0.10	<0.03
9	0.7	88.2	48.1	<0.03	0.07	<0.03
10	1.2	141.6	189.6	<0.03	0.15	1.10
11	35.9	158.6	115.4	<0.03	0.16	0.15
12	8.3	125.1	132.7	<0.03	0.32	0.33
13	7.4			<0.03		
14	2.9	147.0	60.3	<0.03	0.08	0.05
15	2.9	234.7	125.7	<0.03	0.42	0.37
16	8.3	157.3	240.5	0.15	0.58	0.33
17	8.3	257.3	136.4	<0.03	13.00	9.60
18	1	173.1	134.0	<0.03	0.13	0.04
19	<0.6	212.0	122.4	<0.03	0.37	0.09
20	<0.6	95.9	64.3	<0.03	0.11	<0.03
21	3.3	204.8	70.5	<0.03	0.48	0.09
22	<0.6	258.8	128.5	<0.03	0.79	0.58

[5] Patient 13 excluded from all analysis due to complicated post-operative course. POD1 = Post-operative day 1. POD 5 = Post-operative day 5

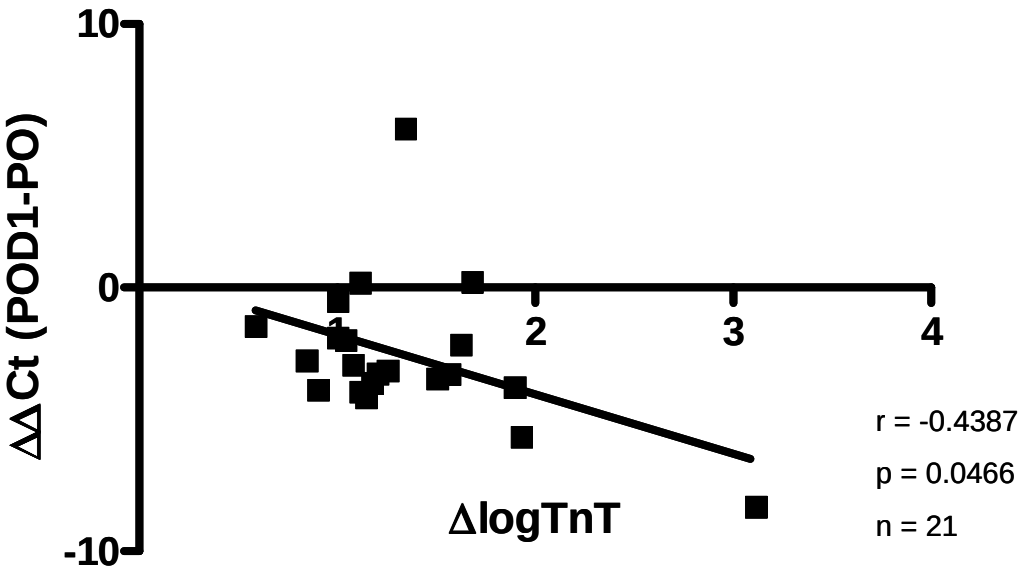

Figure 5-7 Correlation between change in circulating miR-133a levels and rise in serum Troponin T at day 1 post-op

ΔΔCt calculated by subtracting PO levels from POD1 levels. ΔlogTnT calculated by log transforming cTnT levels then subtracting PO from POD1. Increasing negative ΔΔCt values represent increasing serum levels of miR-133a at POD1 compared with corresponding PO. Ct – threshold cycle. PO – Pre-op POD1 – Post-op Day 1 POD5 – Post-op Day 5.

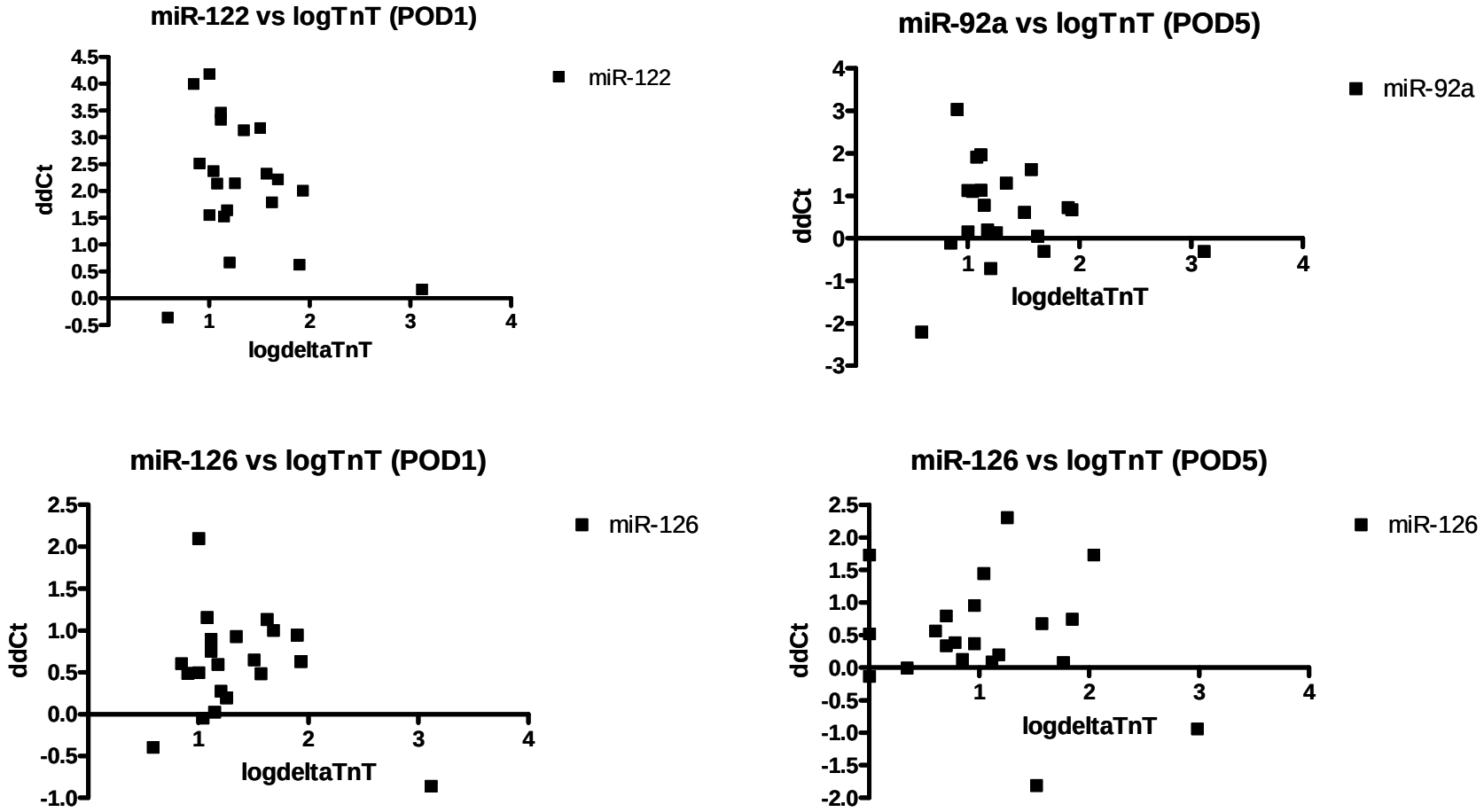

Figure 5-8 Absence of correlation between circulating microRNAs and rise in serum Troponin T

Scatter plots showing the lack of correlation (non-linear association) between rise in cardiac Troponin T (logΔTnT) from baseline and change in circulating microRNA (ddCt) levels at Day 1 (POD1) or Day 5 (POD5) post-op for miR-122, miR-92a or miR-126. Only graphs relating to significant changes in circulating microRNA levels are shown. $p>0.05$ for all comparisons (Pearson correlation).

5.2.5 Relationship to Intra-operative Factors

Despite protective measures (e.g. blood cardioplegia), cardiopulmonary bypass results in myocardial ischemia/reperfusion injury (Moens et al., 2005). It is therefore important to exclude any potential association between the change in circulating miR levels and important intra-operative variables, namely the duration of cardiopulmonary bypass (CPB) time and ischaemic time (length of time that the aorta is cross-clamped). No correlation was found between change in circulating levels of any of the studied miRs and ischemic or CPB time at either POD1 or POD5 (Figure 5.9-5.11).

5.2.6 Relationship to Renal and Liver Function

Animal studies have shown that although circulating miRs are protected from degradation by circulating ribonucleases, they are excreted by the renal (predominately), hepatic and gastrointestinal systems (Neal et al., 2011, Liu et al., 2007, Sepp-Lorenzino and Ruddy, 2008). It is therefore important to exclude relative changes in levels of circulating miRs due to alterations in renal and hepatic function secondary to operative factors that could result in impaired excretion. Small statistically significant increases in median urea and creatinine (Figure 5.12) and albumin, total bilirubin and ALP levels (Figure 5.13) were noted. No positive correlations were seen between these changes and levels of circulating miRs (Figure 5.14). These do not represent significant clinical alterations in renal or hepatic function and therefore would not explain the magnitude of change in miR levels that were identified.

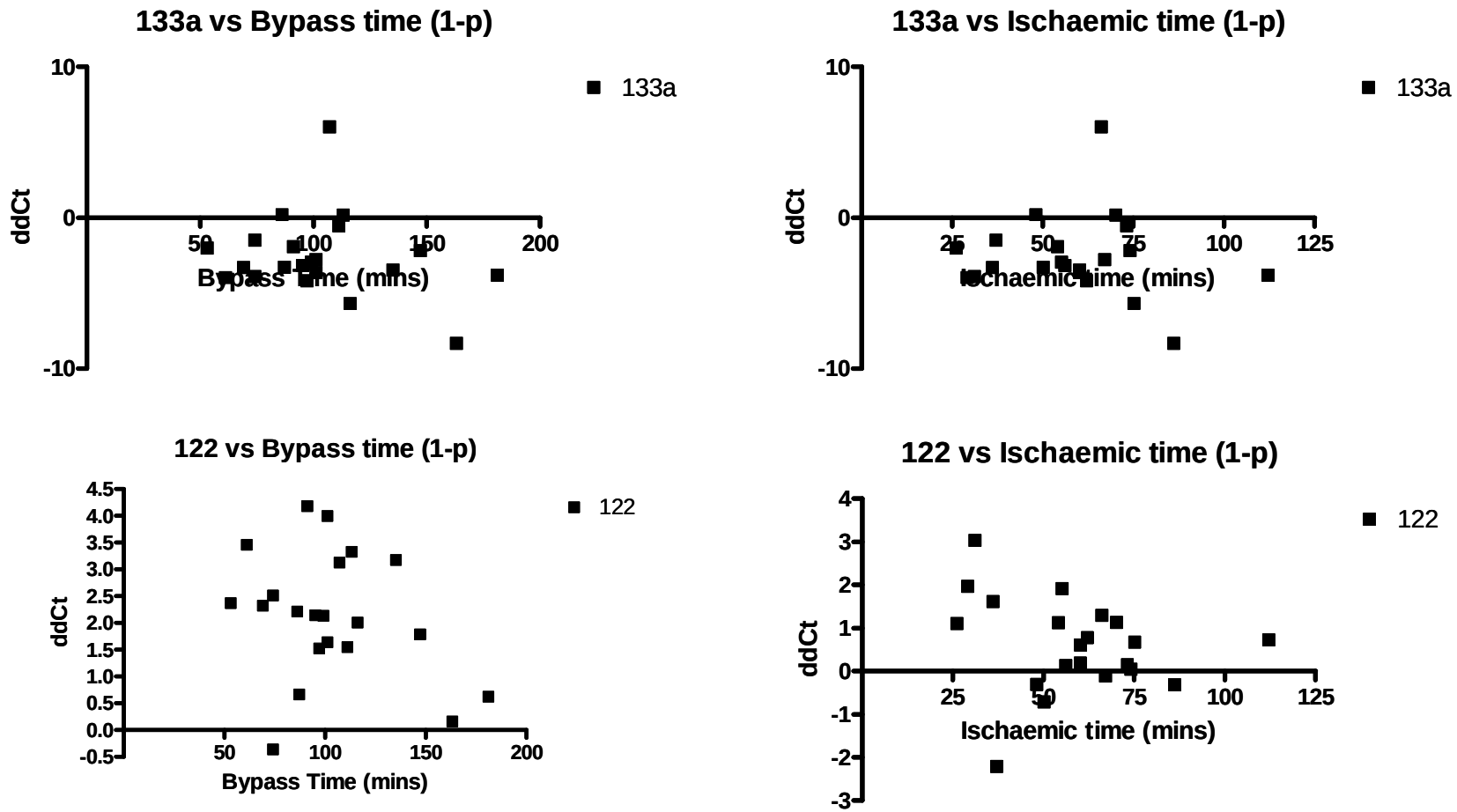

Figure 5-9 Absence of correlation between circulating miR-133a or miR-122 and intra-operative factors

Scatter plots showing the lack of correlation (non-linear association) between cardiopulmonary bypass time or ischaemic time and change in circulating microRNA (ddCt) levels at Day 1 (POD1) post-op for miR-133a and miR-122. Only graphs relating to significant changes in circulating microRNA levels are shown. $p>0.05$ for all comparisons (Pearson correlation).

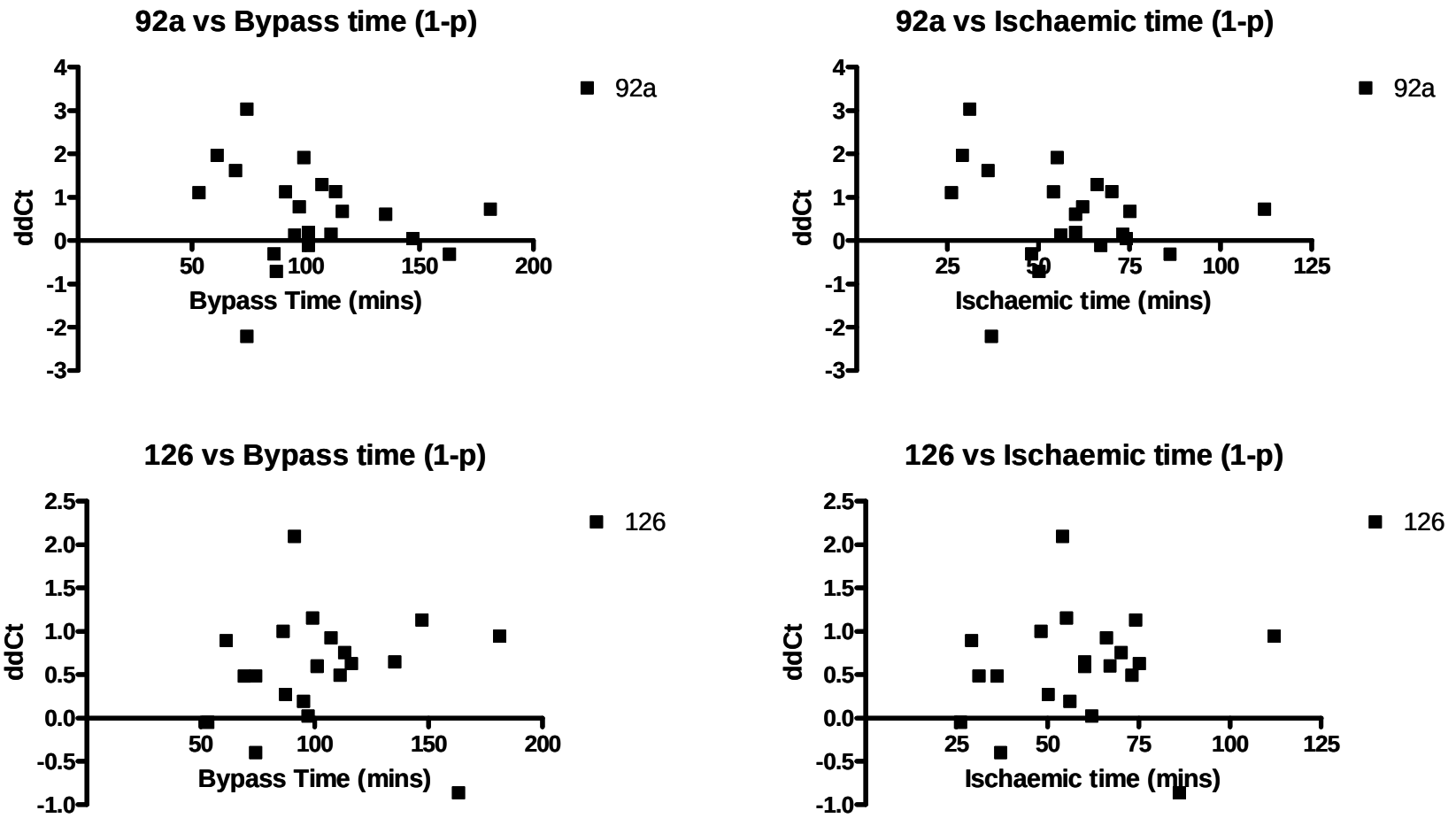

Figure 5-10 Absence of correlation between circulating miR-92a or miR-126 and intra-operative factors (POD1)

Scatter plots showing the lack of correlation (non-linear association) between cardiopulmonary bypass time or ischaemic time and change in circulating microRNA (ddCt) levels at Day 1 (POD1) post-op for miR-92a and miR-126. Only graphs relating to significant changes in circulating microRNA levels are shown. $p>0.05$ for all comparisons (Pearson correlation).

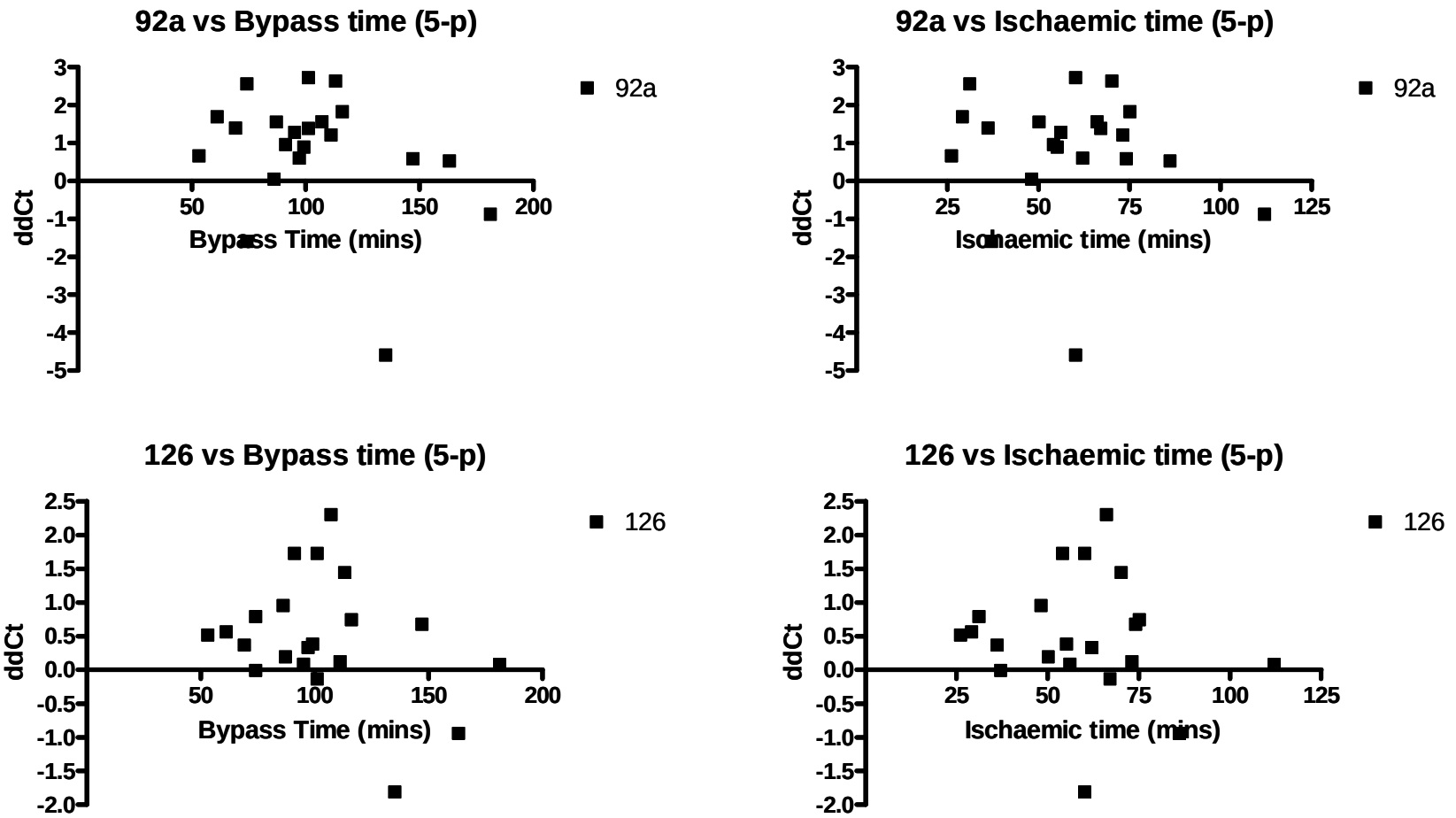

Figure 5-11 Absence of correlation between circulating miR-92a or miR-126 and intra-operative factors (POD5)

Scatter plots showing the lack of correlation (non-linear association) between cardiopulmonary bypass time or ischaemic time and change in circulating microRNA (ddCt) levels at Day 5 (POD5) post-op, compared with pre-op, for miR-92a and miR-126. Only graphs relating to significant changes in circulating microRNA levels are shown. $p>0.05$ for all comparisons (Pearson correlation).

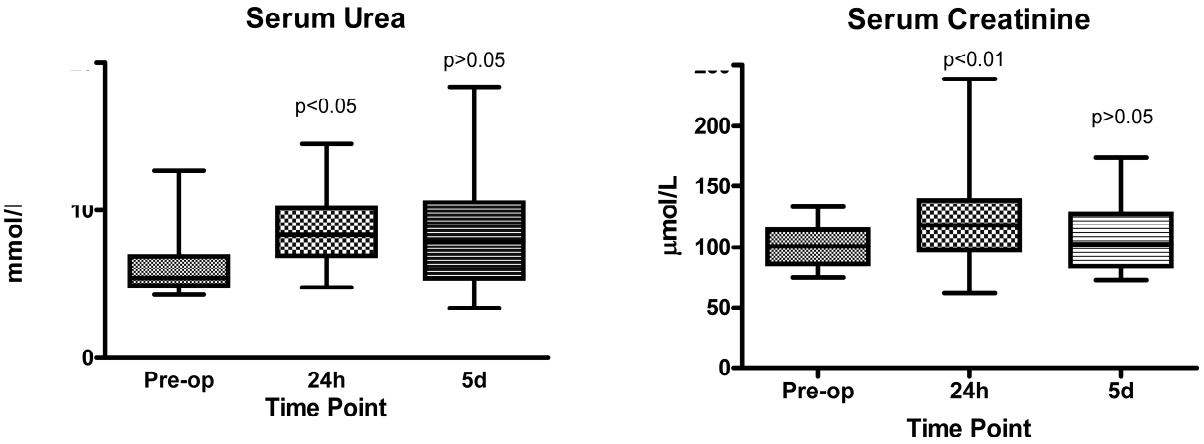

	Urea (mmol/L)			Creatinine (µmol/L)		
	Pre-op	24h	5d	Pre-op	24h	5d
Number of values	20	20	20	20	20	20
Minimum	4.3	4.8	3.4	75	62	73
25% Percentile	4.95	6.95	5.4	86.5	97.5	84
Median	5.45	8.35	7.9	101	117.5	102.5
75% Percentile	6.9	10.15	10.55	114	138.5	127
Maximum	12.7	14.5	18.4	133	239	174

Figure 5-12 Renal function in the peri-operative period

N = 20 as one-patient excluded due to pre-op end-stage renal failure and established renal replacement therapy. Statistical analysis made using a Friedman's test with Dunn's Multiple Comparisons. Comparisons made to pre-op levels. $p<0.05$ was considered statistically significant. Although statistically significant increases in serum Urea and Creatinine levels at POD1 were observed, these do not represent a significant clinical alteration in renal function.

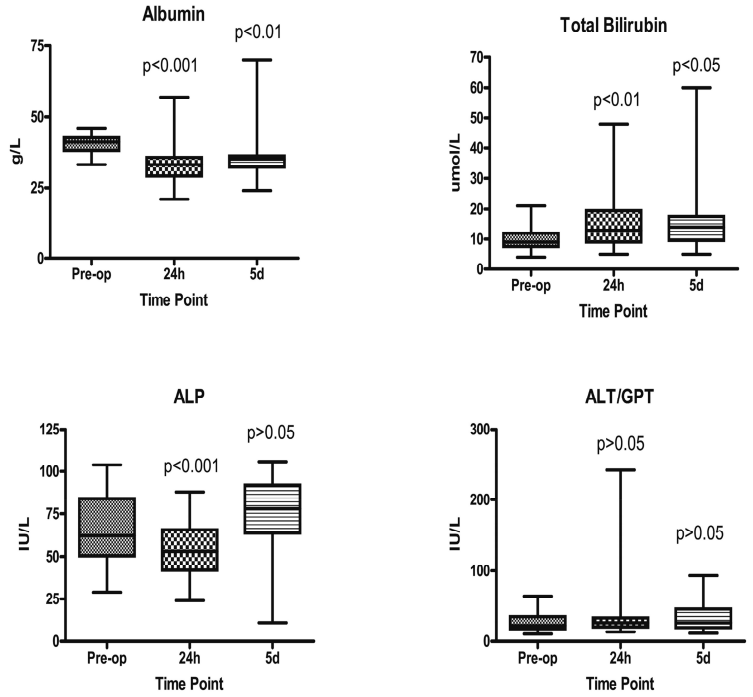

	Albumin (g/L)			Total Bilirubin (umol/L)		
	Pre-op	24h	5d	Pre-op	24h	5d
Number of values	21	21	21	21	21	21
Minimum	33	21	24	4	5	5
25% Percentile	38	29	32	7.5	9	9.5
Median	41	33	35	9	13	14
75% Percentile	42.5	35.5	36	12	19.5	17.5
Maximum	46	57	70	21	48	60
	ALP (IU/L)			ALT/GPT (IU/L)		
	Pre-op	24h	5d	Pre-op	24h	5d
Number of values	21	21	21	21	21	21
Minimum	29	24	11	10	13	11
25% Percentile	50.5	42	63.5	17.5	20	19
Median	62	53	78	22	26	26
75% Percentile	84	65.5	92	35	33	45.5
Maximum	104	88	106	64	242	93

Figure 5-13 Hepatic function in the peri-operative period

Statistical analysis made using a Friedman's test with Dunn's Multiple Comparisons. Comparisons made to pre-op levels. $p<0.05$ was considered statistically significant. All statistically significant differences between pre- and post-op levels do not equate to clinically significant changes in hepatic function. ALP – Alkaline Phosphatase. ALT/GPT - Alanine transaminase/Glutamic pyruvic transaminase.

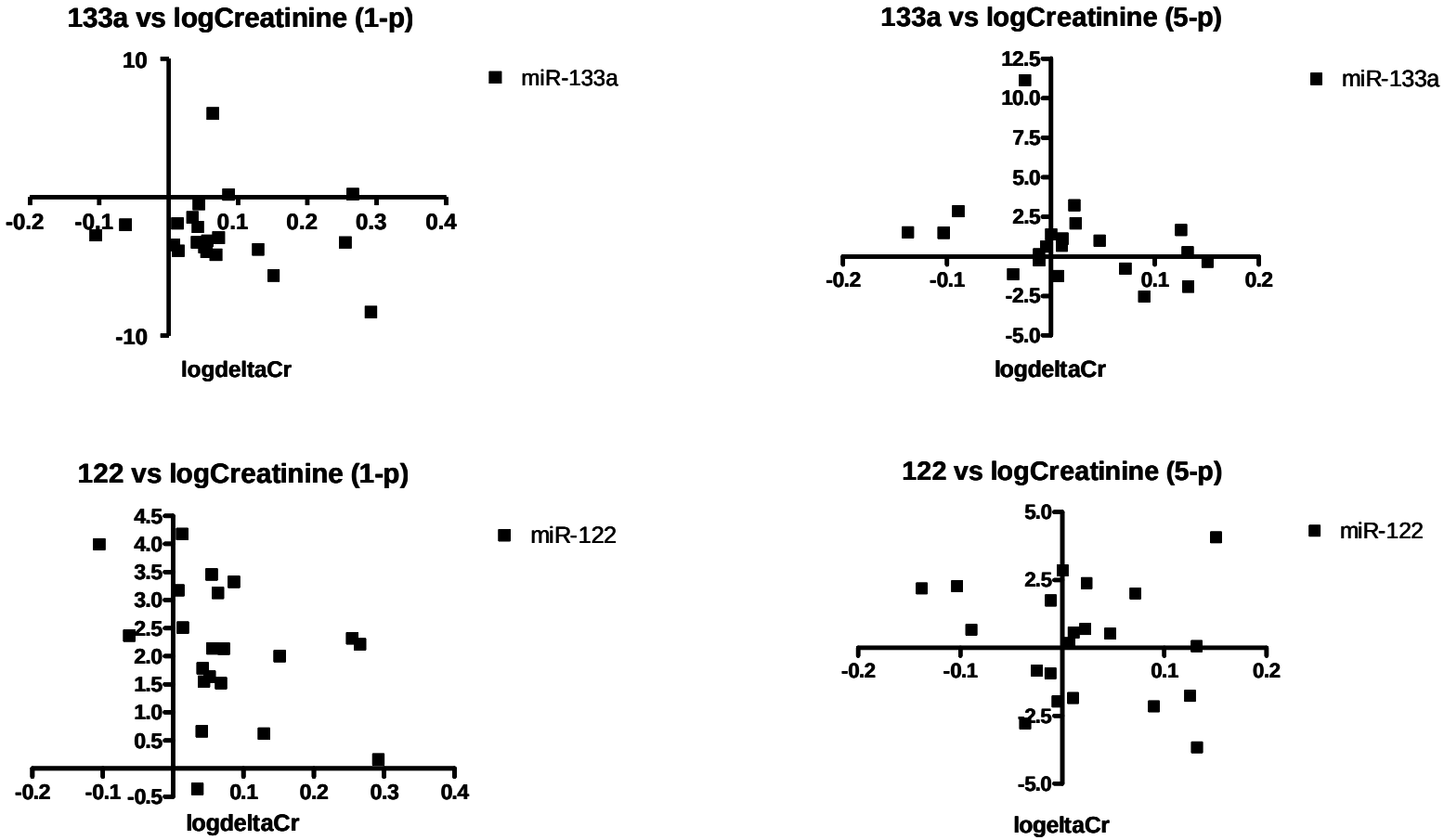

Figure 5-14 Absence of correlation between circulating microRNAs and change in serum creatinine

Representative scatter plots showing a lack of correlation (non-linear association) between change in circulating miR-133a or miR-122 levels (ddCt – y axis) and rise in serum creatinine from baseline (logΔCr) at Day 1 (1-p) or Day 5 (5-p) post-op. p>0.05 for all comparisons (Pearson correlation).

5.3 DISCUSSION

The experiments described in this chapter show altered levels of circulating miR-133a, miR-122, miR-92a and miR-126 in the serum of patients who have undergone CABG surgery.

Overexpression of miR-133a has been shown to inhibit cardiac hypertrophy and also may play a role in regulating cardiac electrical properties (Care et al., 2007). Expression of this miR-133a is reduced in areas of muscle infarction post-MI leading to the suggestion that it may play a protective role, being involved in the heart's repair mechanism following ischaemic damage (Care et al., 2007). Although shown to be increased in serum following ACS, it is not cardiac-specific, being expressed at high levels in both cardiac and skeletal muscle (De Rosa et al., 2011, Creemers et al., 2012, D'Alessandra et al., 2010). Although part of the marked increase in serum levels of miR-133a at POD1 in patients undergoing CABG may be explained by non-cardiac tissue damage, its correlation with the increase in cTnT suggests at least some degree of cardiac origin.

The observed reduction in circulating endothelial cell-enriched miR-92a and miR-126 expression levels parallel those seen in patients with stable CAD (Fichtlscherer et al., 2010) and ACS (De Rosa et al., 2011). MiR-126 is known to facilitate VEGF signalling and thus regulate endothelial homeostasis and vascular integrity (Wang et al., 2008). A recently published prospective study revealed that not only are serum miR-126 levels positively associated with future MI but also elevated in an ischaemia/reperfusion model, with platelets being a major contributor (Zampetaki et al., 2012b). The same group have previously shown a reduced circulating level in patients with Type 2 diabetes mellitus suggesting a predictive role for manifest disease (Zampetaki et al., 2010). There is an increasing body of evidence suggesting that circulating miR-126 levels may represent endothelial or platelet dysfunction and therefore be a useful predictor of future vascular events. In our patients, exposed to ischemia/reperfusion in the setting of CABG, the observed reduction in detectable serum miR-126 may reflect EC or platelet damage or be a component (or even trigger) of a reparative process. This merits further study and elucidation.

MiR-92a, although also highly endothelial cell enriched, is present in both cardiac fibroblasts and cardiomyocytes (Bonauer and Dimmeler, 2009). It is a negative regulator of angiogenesis and when inhibited was shown reduce infarct size, decrease apoptosis (thus

promoting cardiomyocyte survival) and promote neorevascularization in a murine coronary occlusion model (Bonauer et al., 2009). More recently, local catheter delivery of a locked nucleic acid-based inhibitor of miR-92a to a porcine model of ischemia/reperfusion has been shown to reduce miR-92a expression within the infarct zone, reduce infarction size and improve markers of cardiac function (Hinkel et al., 2013). The authors hypothesised that these effects were mediated through conferred endothelial protection, vascular (capillary) preservation or growth, suppression of post-ischaemic inflammation and direct cardiomyocyte protection (Hinkel et al., 2013). The observed reduction in circulating levels of miR-92a post-CABG supports the presence of a protective/reparative process for the endothelium and/or cardiac muscle occurring in response to tissue ischaemia, hyopoxia, hypothermia and inflammation.

MiR-122 levels were reduced on POD1 but had returned to baseline by POD5. This differs from patients with STEMI whose levels remained reduced out to 30 days (D'Alessandra et al., 2010). It has been generally accepted that miR-122 is liver specific, accounting for 70% of the livers total miR content and playing a key role in homeostasis and disease (Tsai et al., 2012, Ding et al., 2012). However, more recently miR-122 has been shown to be elevated in the plasma of patients post cardiac arrest, where it was found to correlate with neurological outcome (Stammet et al., 2012), and in a porcine model of cardiogenic shock where it was attenuated by therapeutic hypothermia (Andersson et al., 2012). In-vitro experiments have revealed that it can be released by neuronal cells (Stammet et al., 2012). The transient reduction observed in patients following CABG could possibly be explained by reduced liver perfusion, however clinically significant alterations in measures of hepatic function were not observed. Another more plausible explanation may be as part of a neuroprotective process activated in the setting of ischaemia/reperfusion.

MiR-208a, -208b and miR-499 have been shown to sensitively and specifically correlate with troponin in ACS studies and to be more cardiac specific than miR-133a (De Rosa et al., 2011, Corsten et al., 2010, Widera et al., 2011, Gidlof et al., 2012). However, in the post-CABG patient cohort these miRs were undetectable in serum pre- and post-op. The observed median cTnT rise in this study was relatively low, with only one patient suffering a marked rise consistent with periprocedural myocardial infarction (Table 5.4). It is therefore likely that miR-208a, miR-208b and miR-499 only become useful detectable biomarkers in the presence of significant myocardial necrosis. It is also possible that the experimental protocol, as designed, missed any potential rise in these miRs with the first sample not being taken until day 1 post-op. MiR-208a has been shown to be an early

marker of myocardial necrosis (within 4 hours) so transient changes in the circulation may have been missed (Wang et al., 2010a).

This chapter is the first to investigate a temporal serum profile of dynamic microRNAs in the setting of uncomplicated CABG and show early potential for use as biomarkers in this setting. It is currently unclear if these miRs represent only cell necrosis/damage or are acting as mediators of disease or protectors from the pathological process, or indeed in communication between cells, tissues and organs. It is becoming increasingly evident that microRNAs operate in co-expression networks and that any analysis of change in miR levels should ideally be examined within these set signatures (Zampetaki et al., 2012a). Comparison with reported findings from other models of CVD, suggests that these dynamic changes in miR expression may reflect part of a wider ischaemia/reperfusion network that merits further investigation.

The experiments in this chapter are limited by relatively small patient numbers. The findings can therefore only be considered as observational at this point. As temporal comparisons have been made within individual patients and not compared to healthy controls, this provides a reduction in bias (for example due to differing risk factor profiles or medications) and a more robust analysis. Unfortunately patient numbers are currently too small to allow for important sub-group analyses e.g. age, sex, diabetes mellitus, patient stability.

As previously mentioned, several miRs (e.g. miR-133a) are present in both cardiac and skeletal muscle. Although the correlation to troponin strongly suggests a cardiac origin, supportive data is required. Comparison to patients undergoing other surgical procedures would help in this regard. Samples from patients undergoing Aortic Valve Replacement on cardiopulmonary bypass but not requiring CABG (therefore not having significant CAD) are in the process of being collected from the same surgical centre. Repeat analysis of these miRs on these samples will be performed in the future and should provide clarification.

To fully assess the potential for these miRs as biomarkers in the setting of CABG will require several further studies. The results in this chapter are from a single surgical centre and therefore require replication in an independent, larger, study population. Corroboration with animal models is important to allow investigation of potential underlying mechanisms and assess cause versus effect. Lastly, and most importantly, a prospective analysis relating dynamic serum miR levels to patient outcome and occurrence of specific operative

complications is required. If it could be shown that changes in circulating miR profiles were predictive of poor operative outcome or of complications such as early vein-graft failure or impaired ventricular function then this would confer a clear advantage over existing protein biomarkers. Potential advantages in using miRs for this purpose are that current PCR technology allows both amplification and detection with high sensitivity and specificity. Many miRs can be detected simultaneously in a single experiment allowing assessment of coexpression networks to improve diagnostic and predictive accuracy. And lastly they are stable and protected from degradation within the circulation. However, qPCR-based analysis is also time consuming and expensive in comparison to laboratory-based protein assays which are cheaper and can provide results in minutes. Also accurate and reproducible normalisation remains a challenge. It has recently been shown that the presence of pre-analytical variation (e.g. haemolysis) can affect miR quantification, and that the spiking in of synthetic exogenous miRs does not correct for this or for variations in extraction efficiency (McDonald et al., 2011a, Duttagupta et al., 2011). There remain several hurdles to overcome for microRNAs to fulfil their potential in meeting the undoubted clinical need for accurate and reproducible disease biomarkers.

In summary, this data adds to the growing evidence for the presence of a circulating microRNA network for cardiovascular disease that may hold significant future potential as both biomarkers and potential therapeutic targets in specific pathological settings.

6 Final Discussion

This thesis has focused on the use of vascular gene therapy and potential role of microRNAs in the pathophysiological response to vascular injury, underpinning the development and treatment of coronary in-stent restenosis. Consideration has also been paid to vein graft failure following CABG surgery as this shares many pathological similarities. Lastly, following on from experience gained in the investigation of miRs, both *in-vitro* and *in-vivo*, attention was directed to their emerging use as cardiovascular disease biomarkers, in this case in the setting of CABG surgery.

Atherosclerotic coronary artery disease remains one of the major causes of morbidity and mortality worldwide (Libby et al., 2011). This progressive disease process leads to consequent flow-limiting vascular narrowing or acute vessel occlusion and resultant clinical sequelae, principally angina pectoris, cardiac dysrhythmia and myocardial infarction (Libby, 2013). Revascularization, either by percutaneous coronary intervention or coronary artery bypass surgery, are routinely performed to relieve symptoms and treat acute MI (Serruys et al., 2009). Also with respect to patient outcome (ie, decreasing the chance of premature death or myocardial infarction), revascularization of ischemia-associated lesions has proven effective (Tonino et al., 2009). Despite their widespread use and clinical effectiveness, both are limited by conduit failure - in-stent restenosis or thrombosis in PCI and vein graft failure in CABG.

Although ISR and VGD represent two distinct pathologies, many similarities exist, principally endothelial dysfunction and the development of intimal hyperplasia. The development of IH/NIH, occurring as a direct consequence of vascular injury, represents an important target for therapeutic interventions aimed at improving clinical outcomes following revascularisation. (Park et al., 2012). As previously discussed in detail, this dynamic process involves the complex interplay of multiple cell types and molecular mechanisms resulting in vascular remodelling and extracellular matrix deposition. Gene therapy remains an intuitive and attractive approach to both the prevention of ISR and VGD (Wan et al., 2012, Bradshaw and Baker, 2012).

In pre-clinical studies, the inhibition of cell proliferation and migration by arresting VSMCs in GO/G1 phase of the cell cycle has been a common approach. This has been achieved using either cell cycle regulatory proteins, or manipulation of mitogens, transcription factors, cytokines, growth factors, promoters of apoptosis or antioxidants. Treatment effects have been impressive, ranging from a 30% reduction in NIH at 28 days post-vein grafting in pigs with adenoviral gene transfer (Wan et al., 2004, Kibbe et al.,

2001) to a >90% reduction in intimal thickness in a rabbit model (Banno et al., 2006). Disappointingly, these impressive results have, as yet, failed to translate into measureable improved outcomes in clinical trials.

In pre-clinical studies of "gene-eluting" stent technology to-date, overall vessel transduction efficiency has been low and concerns have persisted regarding the role that a durable polymer coating may play in the development of arterial wall inflammation, delayed vascular healing and resultant late stent thrombosis. This has contributed to the lack of translation to the clinical setting. Furthermore, advancement in DES technology has been rapid. New second and third-generation DES with thinner stent struts, more biocompatible, less thrombogenic or biodegradable polymers, new antiproliferative agents and even completely biodegradable platforms have all appeared with excellent efficacy and safety data (particularly in regard to late and very-late stent thrombosis), at least in the short-to-medium term (Palmerini et al., 2013). In addition, improvements in individual stent performances have made the detection of statistically robust and clinically relevant differences between contemporary devices hugely difficult (Garg et al., 2013). As event rates continue to fall, the size of clinical trial required to show superiority continues to rise with the risk of becoming prohibitively expensive. Therefore, gene-eluting technology faces stiff competition. Despite this, a clinical need for novel and cost-effective approaches persists as stent thrombosis and delayed restenosis have been far from eliminated (Garg, 2013) and rates of vein graft failure remain high at 10 years post-surgery (Goldman et al., 2004). Targeted gene therapy remains perfectly placed to improve vascular healing, whilst still inhibiting the physiological repair processes leading to device/graft complications.

Ongoing research seeks to identify the optimal vector for vascular gene therapy. Viral vectors so far hold the most potential with retargeting and detargeting strategies in Ad and AAV vectors seeking to maximise transduction efficiency in the target tissue of choice and minimise toxicity, inflammation and interaction with circulating blood components. Helper-dependant adenoviruses hope to overcome problems with humoral immunity and lentiviruses show encouraging preclinical results in vascular tissues although some safety concerns need to be explored, namely the potential for insertional mutagenesis. It is unlikely that one single vector will emerge as an out-right choice for all situations but a selection of tailored options to suit the clinical scenario is entirely feasible. For example, adenoviruses may prove to be most effective in the setting of VGD where *ex-vivo* incubation removes problems with *in-vivo* interactions and allows a longer exposure time

(20-30mins), whereas an efficient lower dose lentivirus stably attached to a stent might be better placed to provide effective local inhibition of ISR.

With respect to failure of translation to the clinical setting, the variability of described effects across pre-clinical models, and also some conflicting results (e.g. use of VEGFs) have shown that there are many important considerations. Choice, design and dose of vector and therapeutic transgene are all clearly important. When pre-clinical animal models are used, species specific differences exist in arterial healing, atherogensis, response of the fibrinolytic system, inflammatory response, degree and rate of re-endothelialisation and host-virus interactions (Schachner et al., 2006, Havenga et al., 2001). This may reduce the effectiveness of a particular gene of interest, or viral vector, when translated to abnormal, inflamed, atherosclerotic human vessels. In stent studies, overall levels of cell transduction have been low, and this may contribute to a lack of clinically measurable effect so far. Also for ISR, the dose administered needs to correlate with the size of the target tissue to be transduced and the larger circulating blood volume in humans. It is likely that "combination gene therapy" targeting multiple regulators of the cell cycle, different points in the neointimal cascade or promoting re-endothelialisation while inhibiting NIH might result in improved efficacy in the clinical setting.

Lastly, finding the optimal method of delivery to target tissue is important. Vein grafts can be accessed *ex-vivo* allowing incubation with a chosen vector but with PCI this remains more difficult. Intuitively a "gene-eluting" stent platform seems most likely to be effective but achieving stable, controllable and reproducible vector binding and elution, as well as sufficient longevity of therapeutic gene expression is required to allow progression to clinical trials and compare favorably with current DES technology.

Taking into account these considerations, translation of gene therapy to clinical use will ultimately require the support of the large device companies. Pre-clinical studies to-date strongly suggest that targeted therapeutic viral vectors, tailored to augment positive vessel healing, could quite conceivably out-perform existing anti-proliferative agents with regards to the suppression of NIH. If a given vector can be proven to be effective in pre-clinical models and safe in phase I/II clinical trials then combining it with existing third-generation stent architecture, biocompatible/biodegradable polymers or even bioabsorbable platforms is commercially attractive and entirely feasible. This provides impetus and motivation to ongoing vascular gene therapy research.

With ongoing rapid improvement in gene delivery vectors, encouraging and robust pre-clinical mechanistic studies and evidence of safety and feasibility from clinical trials I do believe that gene therapy may still play an important future role in the prevention of the important clinical issues of in-stent restenosis and vein graft disease, despite the significant barriers that remain to be overcome Gene therapy has recovered from some of the early hurdles that reduced enthusiasm in the scientific and clinical communities and further developments are awaited with interest (Giacca and Baker, 2011, Verma, 2013).

Since their discovery 20 years ago (Lee et al., 1993), growth in the understanding of the key regulatory role played by small, non-coding, regulatory microRNA molecules in physiological development, homeostatsis and development of pathology has been exponential. Increasingly, pre-clinical research has shown their importance in the regulation of VSMC proliferation and migration in vascular pathologies (McDonald et al., 2011b). As discussed in chapter 4, dysregulation of specific miRs during the development of NIH and re-endothelialisation after vascular injury indicates that their dynamic regulation is a key determinant of VSMC phenotype. Consequently, this raises the possibility that the manipulation of these miRs could prevent neointimal formation, reduce thrombogenicity and promote re-endothelialisation after coronary stent or vein graft implantation. The rapidly evolving development of antisense oligonucleotide-mediated (antimiR/antagomir) knockdown and miR-mimic-mediated overexpression technologies provides opportunities for the therapeutic modulation of miRs in the clinical setting (Small et al., 2010).

As with vascular gene therapy, clinical translation is dependent on both choice of therapeutic strategy and method of delivery. Pre-clinical models have suggested that while systemic delivery (e.g. IV) of a miR-manipulating agent could achieve measurable changes in miR levels, it is unlikely to be clinically optimal, as in keeping with the complex role of miRs across many cell- and tissue-types, off-target effects could be apparent. In the setting of vascular disease the need for localized delivery of the therapeutic entitiy, requirement for short- or long-term manipulation to achieve a given effect, and whether reduction or augmentation of miR levels is required would all influence the choice of a given therapeutic strategy. The fields of vascular gene therapy and miR biology are clearly not exclusive and the development of viral or non-viral vector mediated mimic or antagonism approaches targeting miR(s) of interest hold promise as innovative therapies.

Further detailed mechanistic studies are required to define the importance and contribution of not only individual miRs, but miR clusters, their mRNA and pathway targets,

environmental factors (e.g. presence of atherosclerosis, ischaemia or inflammation) and co-expression networks in the settings of ISR and VGD. Concomitantly, evaluation and refinement of delivery techniques (*ex-vivo* incubation in vein grafts, local catheter or stent-based delivery *in-vivo*) including suppressing the risk of off-target effects is required. It is not inconceivable that in the setting of acute MI, a biocompatible polymer stent coupled with a synthetic miR-vehicle-complex, delivered to a culprit lesion could be tailored to provide a 3-fold benefit – plaque stabilization, prevention of ISR and promotion of positive vessel healing (re-endothelialisation) simultaneously addressing the 3 most significant current issues relating to PCI.

Several difficulties remain to be overcome before miRs can move forward as viable therapeutic targets. Across pre-clinical models, as shown with my findings in Chapter 4, levels of dysregulation in a given disease state and results obtained from the knockdown or overexpression of a given miR have been variable. An individual miR can have hundreds or even thousands of predicted mRNA targets but at a particular physiological expression level only affect a small percentage of them. Forced overexpression or inhibition may change this balance resulting in targeting of mRNAs not normally affected in the physiological state and therefore unwanted "off-target" effects. Given that miRs regulate the genome to a much greater degree than originally though, and that many have shown dysregulation in cancer studies, tumorigenesis is a specific concern that warrants attention (O'Sullivan et al., 2011). Recent data has suggested that miRs can act as endocrine molecules, mediating cell-cell and tissue-tissue signaling, a further important consideration when monitoring the effects of therapeutic modulation *in-vivo* (Polimeni et al., 2013). Additionally, recent work has shown that a single miR can exert its regulatory effect by targeting multiple points of a single pathway concurrently, and that any therapeutic effect could be diluted or ablated if all these conditions are not met, adding a further level of complexity (Ganesan et al., 2013). Lastly, it is now evident that miRs may not be the only important regulatory RNA involved in cardiovascular development and disease. Long non-coding RNAs (lncRNAs) are an emerging class of transcripts that regulate cellular processes by controlling gene expression and may hold potential for therapeutic modulation (Scheuermann and Boyer, 2013). Their biological and mechanistic functions are complex with initial evidence pointing towards an important role in regulatory networks (Schonrock et al., 2012). This area of cardiovascular research remains fast-paced and promises both an increased understanding of vascular biology and pathophysiology and potentially novel therapeutic opportunities. Encouragingly, significant recent progress was made in an early Phase II clinical trial where a course of systemic antimiR-122 was

not only well-tolerated but provided evidence of efficacy with suppression of viraemia in patients with Hepatitis C infection (van Rooij and Olson, 2012).

Additional interest in miRs has developed from the finding that they are present in stable and detectable levels within the circulation. Increasingly it has been suggested that these miRs are released into the circulation from injured tissue or are highly expressed in patients with specific cardiovascular diseases. The implication being, that these miRs could act as potential biomarkers for clinical diagnosis or prognosis in patients with cardiovascular diseases. However many question remain to be answered, including the basis for their altered expression (cause or effect), their relationship to disease progression and their power for predicting disease progression and clinical outcome (Fichtlscherer et al., 2011).

With respect to taking the results reported in this thesis forward, there were several avenues that could have been explored if time and financial constraints had allowed. The development of modified Ad vectors with improved vascular transduction efficiency is ongoing within our institution. Considerable success has been achieved thus far with the creation of a vector that combines hexon amino acid mutations to abrogate FX binding, fiber pseudotyping to improve vascular cell transduction lower immunogenicity (White et al., 2013). Unfortunately, this vector is not yet ready for *in-vivo* testing in the pig model as it utilises the CD46 receptor for cell-binding and a low level of homology exists between porcine and human CD46 (Havenga et al., 2001). Additionally, efficient and effective vascular gene transfer can be achieved using integrase-deficient lentiviral vectors (IDLV) *in-vitro* (Chick et al., 2012). It would have been interesting to administer novel modified Ad or IDLV to the porcine model using both the Clearway RX and GENIE systems to fully investigate the clinical potential of local delivery in this setting. Potentially even more useful would have been the direct spray coating of Yukon stents with IDLV expressing NogoB. The sand-blasted abluminal surface of the Yukon provides a series of crypts that could conceivably have stored enough lentivirus to allow efficacious local gene delivery. Unfortunately the cost required to perform this experiment is currently prohibitive.

Concurrently, work is ongoing between our institution and the Department of Chemistry to investigate chemical methods of binding Ad vectors to the surface of a metal stent allowing stable and controlled vector elution. Our plan is to test this in the *in-vivo* pig model in due course, although considerable attention will need to be paid to the biocompatibility of this technology and its effect on vessel inflammation. Should a given vector display proven effectiveness and compatibility in *in-vitro* models then we hope that collaboration with a

commercial stent company would allow us to move towards our aim of a gene-eluting stent platform suitable for clinical testing.

As previously mentioned, we are repeating the analysis of previously discussed levels of vascular-miRs in porcine neointima using a modern stainless steel DES platform with biodegradable polymer and limus agent (Biomatrix Flex^{TM}, Biosensors International, Singapore) and its sister BMS counterpart (Gazelle^{TM}, Biosensors International, Singapore) both of which are amenable to the electrolysis process. It would be expected to see differences in neointimal area between the two stents at 28 days and to establish potential differences in miR dysregulation using a microarray approach, qRT-PCR conformation and co-localisation using in-situ hybridisation. This would be hoped to provide further insights into the effect of DES on the vasculature. Ultimately, the porcine model will allow us to test both miR-mimic and antimiR approaches to the treatment of ISR prior to assessment in clinical trials.

List of References

ABDELLATIF, M. 2012. Differential expression of microRNAs in different disease states. *Circ Res,* 110**,** 638-50.

AHI, Y. S., BANGARI, D. S. & MITTAL, S. K. 2011. Adenoviral vector immunity: its implications and circumvention strategies. *Curr Gene Ther,* 11**,** 307-20.

AKOWUAH, E. F., GRAY, C., LAWRIE, A., SHERIDAN, P. J., SU, C. H., BETTINGER, T., BRISKEN, A. F., GUNN, J., CROSSMAN, D. C., FRANCIS, S. E., BAKER, A. H. & NEWMAN, C. M. 2005. Ultrasound-mediated delivery of TIMP-3 plasmid DNA into saphenous vein leads to increased lumen size in a porcine interposition graft model. *Gene Ther,* 12**,** 1154-7.

AL SUWAIDI, J., BERGER, P. B. & HOLMES, D. R., JR. 2000. Coronary artery stents. *Jama,* 284**,** 1828-36.

ALBA, R., BRADSHAW, A. C., COUGHLAN, L., DENBY, L., MCDONALD, R. A., WADDINGTON, S. N., BUCKLEY, S. M., GREIG, J. A., PARKER, A. L., MILLER, A. M., WANG, H., LIEBER, A., VAN ROOIJEN, N., MCVEY, J. H., NICKLIN, S. A. & BAKER, A. H. 2010. Biodistribution and retargeting of FX-binding ablated adenovirus serotype 5 vectors. *Blood,* 116**,** 2656-64.

ALBINSSON, S., SKOURA, A., YU, J., DILORENZO, A., FERNANDEZ-HERNANDO, C., OFFERMANNS, S., MIANO, J. M. & SESSA, W. C. 2011. Smooth muscle miRNAs are critical for post-natal regulation of blood pressure and vascular function. *PLoS One,* 6**,** e18869.

ALBINSSON, S., SUAREZ, Y., SKOURA, A., OFFERMANNS, S., MIANO, J. M. & SESSA, W. C. 2010. MicroRNAs are necessary for vascular smooth muscle growth, differentiation, and function. *Arterioscler Thromb Vasc Biol,* 30**,** 1118-26.

ALEMANY, R. & CURIEL, D. T. 2001. CAR-binding ablation does not change biodistribution and toxicity of adenoviral vectors. *Gene Ther,* 8**,** 1347-53.

ALI, Z. A., ALP, N. J., LUPTON, H., ARNOLD, N., BANNISTER, T., HU, Y., MUSSA, S., WHEATCROFT, M., GREAVES, D. R., GUNN, J. & CHANNON, K. M. 2007. Increased in-stent stenosis in ApoE knockout mice: insights from a novel mouse model of balloon angioplasty and stenting. *Arterioscler Thromb Vasc Biol,* 27**,** 833-40.

ALLENDER, S., SCARBOROUGH, P., PETO, V., RAYNER, M., LEAL, J., LUENGO-FERNANDEZ, R. & GRAY, A. 2008. European cardiovascular disease statistics 2008 edition

European Heart Network. Belgium.

ANDERSSON, P., GIDLOF, O., BRAUN, O. O., GOTBERG, M., VAN DER PALS, J., OLDE, B. & ERLINGE, D. 2012. Plasma levels of liver-specific miR-122 is massively increased in a porcine cardiogenic shock model and attenuated by hypothermia. *Shock,* 37**,** 234-8.

ASAHARA, T., CHEN, D., TSURUMI, Y., KEARNEY, M., ROSSOW, S., PASSERI, J., SYMES, J. F. & ISNER, J. M. 1996. Accelerated restitution of endothelial integrity and endothelium-dependent function after phVEGF165 gene transfer. *Circulation,* 94**,** 3291-302.

AUTIERI, M. V., YUE, T. L., FERSTEIN, G. Z. & OHLSTEIN, E. 1995. Antisense oligonucleotides to the p65 subunit of NF-kB inhibit human vascular smooth muscle cell adherence and proliferation and prevent neointima formation in rat carotid arteries. *Biochem Biophys Res Commun,* 213**,** 827-36.

AXEL, D. I., KUNERT, W., GOGGELMANN, C., OBERHOFF, M., HERDEG, C., KUTTNER, A., WILD, D. H., BREHM, B. R., RIESSEN, R., KOVEKER, G. & KARSCH, K. R. 1997. Paclitaxel inhibits arterial smooth muscle cell proliferation and migration in vitro and in vivo using local drug delivery. *Circulation,* 96**,** 636-45.

BAEK, D., VILLEN, J., SHIN, C., CAMARGO, F. D., GYGI, S. P. & BARTEL, D. P. 2008. The impact of microRNAs on protein output. *Nature,* 455**,** 64-71.

BAKER, A. H. 2002. Gene therapy for bypass graft failure and restenosis. *Pathophysiol Haemost Thromb,* 32**,** 389-91.

BAKER, A. H., ZALTSMAN, A. B., GEORGE, S. J. & NEWBY, A. C. 1998. Divergent effects of tissue inhibitor of metalloproteinase-1, -2, or -3 overexpression on rat vascular smooth muscle cell invasion, proliferation, and death in vitro. TIMP-3 promotes apoptosis. *J Clin Invest,* 101**,** 1478-87.

BANGALORE, S., KUMAR, S., FUSARO, M., AMOROSO, N., ATTUBATO, M. J., FEIT, F., BHATT, D. L. & SLATER, J. 2012. Short- and long-term outcomes with drug-eluting and bare-metal coronary stents: a mixed-treatment comparison analysis of 117 762 patient-years of follow-up from randomized trials. *Circulation,* 125**,** 2873-91.

BANNO, H., TAKEI, Y., MURAMATSU, T., KOMORI, K. & KADOMATSU, K. 2006. Controlled release of small interfering RNA targeting midkine attenuates intimal hyperplasia in vein grafts. *J Vasc Surg,* 44**,** 633-41.

BARATH, P., POPOV, A., DILLEHAY, G. L., MATOS, G. & MCKIERNAN, T. 1997. Infiltrator Angioplasty Balloon Catheter: a device for combined angioplasty and intramural site-specific treatment. *Cathet Cardiovasc Diagn,* 41**,** 333-41.

BARRAGAN, P., SAINSOUS, J., SILVESTRI, M., BOUVIER, J. L., COMET, B., SIMEONI, J. B., CHARMASSON, C. & BREMONDY, M. 1994. Ticlopidine and subcutaneous heparin as an alternative regimen following coronary stenting. *Cathet Cardiovasc Diagn,* 32**,** 133-8.

BARTEL, D. P. 2004. MicroRNAs: genomics, biogenesis, mechanism, and function. *Cell,* 116**,** 281-97.

BAYTURAN, O., TUZCU, E. M., UNO, K., LAVOIE, A. J., HU, T., SHREEVATSA, A., WOLSKI, K., SCHOENHAGEN, P., KAPADIA, S., NISSEN, S. E. & NICHOLLS, S. J. 2010. Comparison of rates of progression of coronary atherosclerosis in patients with diabetes mellitus versus those with the metabolic syndrome. *Am J Cardiol,* 105**,** 1735-9.

BERGELSON, J. M., CUNNINGHAM, J. A., DROGUETT, G., KURT-JONES, E. A., KRITHIVAS, A., HONG, J. S., HORWITZ, M. S., CROWELL, R. L. & FINBERG, R. W. 1997. Isolation of a common receptor for Coxsackie B viruses and adenoviruses 2 and 5. *Science,* 275**,** 1320-3.

BHARDWAJ, S., ROY, H., GRUCHALA, M., VIITA, H., KHOLOVA, I., KOKINA, I., ACHEN, M. G., STACKER, S. A., HEDMAN, M., ALITALO, K. & YLA-HERTTUALA, S. 2003. Angiogenic responses of vascular endothelial growth factors in periadventitial tissue. *Hum Gene Ther,* 14**,** 1451-62.

BHARDWAJ, S., ROY, H., HEIKURA, T. & YLA-HERTTUALA, S. 2005. VEGF-A, VEGF-D and VEGF-D(DeltaNDeltaC) induced intimal hyperplasia in carotid arteries. *Eur J Clin Invest,* 35**,** 669-76.

BHF. 2012. *Coronary Heart Disease Statistics 2012* [Online]. Available: http://www.bhf.org.uk/publications/view-publication.aspx?ps=1002097.

BODEN, W. E., O'ROURKE, R. A., TEO, K. K., HARTIGAN, P. M., MARON, D. J., KOSTUK, W. J., KNUDTSON, M., DADA, M., CASPERSON, P., HARRIS, C. L., CHAITMAN, B. R., SHAW, L., GOSSELIN, G., NAWAZ, S., TITLE, L. M., GAU, G., BLAUSTEIN, A. S., BOOTH, D. C., BATES, E. R., SPERTUS, J. A., BERMAN, D. S., MANCINI, G. B. & WEINTRAUB, W. S. 2007. Optimal medical therapy with or without PCI for stable coronary disease. *N Engl J Med,* 356**,** 1503-16.

BOETTGER, T., BEETZ, N., KOSTIN, S., SCHNEIDER, J., KRUGER, M., HEIN, L. & BRAUN, T. 2009. Acquisition of the contractile phenotype by murine arterial smooth muscle cells depends on the Mir143/145 gene cluster. *J Clin Invest,* 119**,** 2634-47.

BOHNSACK, M. T., CZAPLINSKI, K. & GORLICH, D. 2004. Exportin 5 is a RanGTP-dependent dsRNA-binding protein that mediates nuclear export of pre-miRNAs. *Rna,* 10**,** 185-91.

BONAUER, A., CARMONA, G., IWASAKI, M., MIONE, M., KOYANAGI, M., FISCHER, A., BURCHFIELD, J., FOX, H., DOEBELE, C., OHTANI, K., CHAVAKIS, E., POTENTE, M., TJWA, M., URBICH, C., ZEIHER, A. M. & DIMMELER, S. 2009. MicroRNA-92a controls angiogenesis and functional recovery of ischemic tissues in mice. *Science,* 324**,** 1710-3.

BONAUER, A. & DIMMELER, S. 2009. The microRNA-17-92 cluster: still a miRacle? *Cell Cycle,* 8**,** 3866-73.

BONCI, D. 2010. MicroRNA-21 as therapeutic target in cancer and cardiovascular disease. *Recent Pat Cardiovasc Drug Discov,* 5**,** 156-61.

BOON, R. A., HERGENREIDER, E. & DIMMELER, S. 2012. Atheroprotective mechanisms of shear stress-regulated microRNAs. *Thromb Haemost,* 108**,** 616-20.

BOUCHER, J. M., PETERSON, S. M., URS, S., ZHANG, C. & LIAW, L. 2011. The miR-143/145 cluster is a novel transcriptional target of Jagged-1/Notch signaling in vascular smooth muscle cells. *J Biol Chem,* 286**,** 28312-21.

BOUDRIOT, E., THIELE, H., WALTHER, T., LIEBETRAU, C., BOECKSTEGERS, P., POHL, T., REICHART, B., MUDRA, H., BEIER, F., GANSERA, B., NEUMANN, F. J., GICK, M., ZIETAK, T., DESCH, S., SCHULER, G. & MOHR, F. W. 2011. Randomized comparison of percutaneous coronary intervention with sirolimus-eluting stents versus coronary artery bypass grafting in unprotected left main stem stenosis. *J Am Coll Cardiol,* 57**,** 538-45.

BRADSHAW, A. C. & BAKER, A. H. 2012. Gene therapy for cardiovascular disease: perspectives and potential. *Vascul Pharmacol,* 58**,** 174-81.

BRADSHAW, S. H., KENNEDY, L., DEXTER, D. F. & VEINOT, J. P. 2009. A practical method to rapidly dissolve metallic stents. *Cardiovasc Pathol,* 18**,** 127-33.

BRIDGEWATER, B., KEOGH, B. & KINSMAN, R. 2009. *The Society for Cardiothoracic Surgery in Great Britain and Ireland. Sixth National Adult Cardiac Surgical Database Report 2008,* Oxfordshire: Dendrite Clinical Systems Limited.

BRIEGER, D. & TOPOL, E. 1997. Local drug delivery systems and prevention of restenosis. *Cardiovasc Res,* 35**,** 405-13.

BRYAN, A. J. & ANGELINI, G. D. 1994. The biology of saphenous vein graft occlusion: etiology and strategies for prevention. *Curr Opin Cardiol,* 9**,** 641-9.

BUSHATI, N. & COHEN, S. M. 2007. microRNA functions. *Annu Rev Cell Dev Biol,* 23**,** 175-205.

BUSZMAN, P. E., KIESZ, S. R., BOCHENEK, A., PESZEK-PRZYBYLA, E., SZKROBKA, I., DEBINSKI, M., BIALKOWSKA, B., DUDEK, D., GRUSZKA, A., ZURAKOWSKI, A., MILEWSKI, K., WILCZYNSKI, M., RZESZUTKO, L., BUSZMAN, P., SZYMSZAL, J., MARTIN, J. L. & TENDERA, M. 2008. Acute

and late outcomes of unprotected left main stenting in comparison with surgical revascularization. *J Am Coll Cardiol,* 51**,** 538-45.

BUTLER, S. L., HANSEN, M. S. & BUSHMAN, F. D. 2001. A quantitative assay for HIV DNA integration in vivo. *Nat Med,* 7**,** 631-4.

CALIN, G. A. & CROCE, C. M. 2006. MicroRNA signatures in human cancers. *Nat Rev Cancer,* 6**,** 857-66.

CAMENZIND, E., STEG, P. G. & WIJNS, W. 2007. Stent thrombosis late after implantation of first-generation drug-eluting stents: a cause for concern. *Circulation,* 115**,** 1440-55; discussion 1455.

CAO, Y., LINDEN, P., FARNEBO, J., CAO, R., ERIKSSON, A., KUMAR, V., QI, J. H., CLAESSON-WELSH, L. & ALITALO, K. 1998. Vascular endothelial growth factor C induces angiogenesis in vivo. *Proc Natl Acad Sci U S A,* 95**,** 14389-94.

CARE, A., CATALUCCI, D., FELICETTI, F., BONCI, D., ADDARIO, A., GALLO, P., BANG, M. L., SEGNALINI, P., GU, Y., DALTON, N. D., ELIA, L., LATRONICO, M. V., HOYDAL, M., AUTORE, C., RUSSO, M. A., DORN, G. W., 2ND, ELLINGSEN, O., RUIZ-LOZANO, P., PETERSON, K. L., CROCE, C. M., PESCHLE, C. & CONDORELLI, G. 2007. MicroRNA-133 controls cardiac hypertrophy. *Nat Med,* 13**,** 613-8.

CARLISLE, R. C., DI, Y., CERNY, A. M., SONNEN, A. F., SIM, R. B., GREEN, N. K., SUBR, V., ULBRICH, K., GILBERT, R. J., FISHER, K. D., FINBERG, R. W. & SEYMOUR, L. W. 2009. Human erythrocytes bind and inactivate type 5 adenovirus by presenting Coxsackie virus-adenovirus receptor and complement receptor 1. *Blood,* 113**,** 1909-18.

CEFAI, D., SIMEONI, E., LUDUNGE, K. M., DRISCOLL, R., VON SEGESSER, L. K., KAPPENBERGER, L. & VASSALLI, G. 2005. Multiply attenuated, self-inactivating lentiviral vectors efficiently transduce human coronary artery cells in vitro and rat arteries in vivo. *J Mol Cell Cardiol,* 38**,** 333-44.

CHAMBERLAIN, J., WHEATCROFT, M., ARNOLD, N., LUPTON, H., CROSSMAN, D. C., GUNN, J. & FRANCIS, S. 2010. A novel mouse model of in situ stenting. *Cardiovasc Res,* 85**,** 38-44.

CHANDRASENA, L. G., PEIRIS, H. & WAIKAR, H. D. 2009. Biochemical changes associated with reperfusion after off-pump and on-pump coronary artery bypass graft surgery. *Ann Clin Lab Sci,* 39**,** 372-7.

CHANG, M. W., BARR, E., LU, M. M., BARTON, K. & LEIDEN, J. M. 1995a. Adenovirus-mediated over-expression of the cyclin/cyclin-dependent kinase inhibitor, p21 inhibits vascular smooth muscle cell proliferation and neointima formation in the rat carotid artery model of balloon angioplasty. *J Clin Invest,* 96**,** 2260-8.

CHANG, M. W., BARR, E., SELTZER, J., JIANG, Y. Q., NABEL, G. J., NABEL, E. G., PARMACEK, M. S. & LEIDEN, J. M. 1995b. Cytostatic gene therapy for vascular proliferative disorders with a constitutively active form of the retinoblastoma gene product. *Science,* 267**,** 518-22.

CHANG, M. W., OHNO, T., GORDON, D., LU, M. M., NABEL, G. J., NABEL, E. G. & LEIDEN, J. M. 1995c. Adenovirus-mediated transfer of the herpes simplex virus thymidine kinase gene inhibits vascular smooth muscle cell proliferation and neointima formation following balloon angioplasty of the rat carotid artery. *Mol Med,* 1**,** 172-81.

CHEN, D., KRASINSKI, K., SYLVESTER, A., CHEN, J., NISEN, P. D. & ANDRES, V. 1997. Downregulation of cyclin-dependent kinase 2 activity and cyclin A promoter activity in vascular smooth muscle cells by p27(KIP1), an inhibitor of neointima formation in the rat carotid artery. *J Clin Invest,* 99**,** 2334-41.

CHEN, L., DAUM, G., FOROUGH, R., CLOWES, M., WALTER, U. & CLOWES, A. W. 1998. Overexpression of human endothelial nitric oxide synthase in rat vascular smooth muscle cells and in balloon-injured carotid artery. *Circ Res,* 82**,** 862-70.

CHEN, S., KAPTURCZAK, M., LOILER, S. A., ZOLOTUKHIN, S., GLUSHAKOVA, O. Y., MADSEN, K. M., SAMULSKI, R. J., HAUSWIRTH, W. W., CAMPBELL-THOMPSON, M., BERNS, K. I., FLOTTE, T. R., ATKINSON, M. A., TISHER, C. C. & AGARWAL, A. 2005. Efficient transduction of vascular endothelial cells with recombinant adeno-associated virus serotype 1 and 5 vectors. *Hum Gene Ther,* 16**,** 235-47.

CHEN, S. J., CHEN, Y. F., MILLER, D. M., LI, H. & OPARIL, S. 1994. Mithramycin inhibits myointimal proliferation after balloon injury of the rat carotid artery in vivo. *Circulation,* 90**,** 2468-73.

CHEN, T., HUANG, Z., WANG, L., WANG, Y., WU, F., MENG, S. & WANG, C. 2009. MicroRNA-125a-5p partly regulates the inflammatory response, lipid uptake, and ORP9 expression in oxLDL-stimulated monocyte/macrophages. *Cardiovasc Res,* 83**,** 131-9.

CHEN, T., LI, Z., JING, T., ZHU, W., GE, J., ZHENG, X., PAN, X., YAN, H. & ZHU, J. 2011. MicroRNA-146a regulates the maturation process and pro-inflammatory cytokine secretion by targeting CD40L in oxLDL-stimulated dendritic cells. *FEBS Lett,* 585**,** 567-73.

CHENG, L., MANTILE, G., PAULY, R., NATER, C., FELICI, A., MONTICONE, R., BILATO, C., GLUZBAND, Y. A., CROW, M. T., STETLER-STEVENSON, W. & CAPOGROSSI, M. C. 1998. Adenovirus-mediated gene transfer of the human tissue inhibitor of metalloproteinase-2 blocks vascular smooth muscle cell invasiveness in vitro and modulates neointimal development in vivo. *Circulation,* 98**,** 2195-201.

CHENG, Y., LIU, X., YANG, J., LIN, Y., XU, D. Z., LU, Q., DEITCH, E. A., HUO, Y., DELPHIN, E. S. & ZHANG, C. 2009. MicroRNA-145, a novel smooth muscle cell phenotypic marker and modulator, controls vascular neointimal lesion formation. *Circ Res,* 105**,** 158-66.

CHICK, H. E., NOWROUZI, A., FRONZA, R., MCDONALD, R. A., KANE, N. M., ALBA, R., DELLES, C., SESSA, W. C., SCHMIDT, M., THRASHER, A. J. & BAKER, A. H. 2012. Integrase-deficient lentiviral vectors mediate efficient gene transfer to human vascular smooth muscle cells with minimal genotoxic risk. *Hum Gene Ther,* 23**,** 1247-57.

CHIEFFO, A., MAGNI, V., LATIB, A., MAISANO, F., IELASI, A., MONTORFANO, M., CARLINO, M., GODINO, C., FERRARO, M., CALORI, G., ALFIERI, O. & COLOMBO, A. 2010. 5-year outcomes following percutaneous coronary intervention with drug-eluting stent implantation versus coronary artery bypass graft for unprotected left main coronary artery lesions the Milan experience. *JACC Cardiovasc Interv,* 3**,** 595-601.

CHO, C. W., CHO, Y. S., LEE, H. K., YEOM, Y. I., PARK, S. N. & YOON, D. Y. 2000. Improvement of receptor-mediated gene delivery to HepG2 cells using an amphiphilic gelling agent. *Biotechnol Appl Biochem,* 32 (Pt 1)**,** 21-6.

CHUNG, I. M., KIM, J., PAK, Y. K., JANG, Y., YANG, W. I., HAN, I., PARK, S. J., PARK, S. W., HUH, J., WIGHT, T. N. & UENO, H. 2010. Blockade of TGF-beta by catheter-based local intravascular gene delivery does not alter the in-stent neointimal response, but enhances inflammation in pig coronary arteries. *Int J Cardiol,* 145**,** 468-75.

CICHON, G., BOECKH-HERWIG, S., KUEMIN, D., HOFFMANN, C., SCHMIDT, H. H., WEHNES, E., HAENSCH, W., SCHNEIDER, U., ECKHARDT, U., BURGER, R. & PRING-AKERBLOM, P. 2003. Titer determination of Ad5 in blood: a cautionary note. *Gene Ther,* 10**,** 1012-7.

CIOFFI, C. L., GARAY, M., JOHNSTON, J. F., MCGRAW, K., BOGGS, R. T., HRENIUK, D. & MONIA, B. P. 1997. Selective inhibition of A-Raf and C-Raf mRNA expression by antisense oligodeoxynucleotides in rat vascular smooth muscle cells: role of A-Raf and C-Raf in serum-induced proliferation. *Mol Pharmacol,* 51**,** 383-9.

CLAUDIO, P. P., FRATTA, L., FARINA, F., HOWARD, C. M., STASSI, G., NUMATA, S., PACILIO, C., DAVIS, A., LAVITRANO, M., VOLPE, M., WILSON, J. M., TRIMARCO, B., GIORDANO, A. & CONDORELLI, G. 1999. Adenoviral RB2/p130 gene transfer inhibits smooth muscle cell proliferation and prevents restenosis after angioplasty. *Circ Res,* 85**,** 1032-9.

CLOWES, A. W., CLOWES, M. M. & REIDY, M. A. 1986. Kinetics of cellular proliferation after arterial injury. III. Endothelial and smooth muscle growth in chronically denuded vessels. *Lab Invest,* 54**,** 295-303.

COHEN, D. J., LAVELLE, T. A., VAN HOUT, B., LI, H., LEI, Y., ROBERTUS, K., PINTO, D., MAGNUSON, E. A., MCGARRY, T. F., LUCAS, S. K., HORWITZ, P. A., HENRY, C. A., SERRUYS, P. W., MOHR, F. W. & KAPPETEIN, A. P. 2012. Economic outcomes of percutaneous coronary intervention with drug-eluting stents versus bypass surgery for patients with left main or three-vessel coronary artery disease: one-year results from the SYNTAX trial. *Catheter Cardiovasc Interv,* 79**,** 198-209.

COLOMBO, A., HALL, P., NAKAMURA, S., ALMAGOR, Y., MAIELLO, L., MARTINI, G., GAGLIONE, A., GOLDBERG, S. L. & TOBIS, J. M. 1995. Intracoronary stenting without anticoagulation accomplished with intravascular ultrasound guidance. *Circulation,* 91**,** 1676-88.

CORDES, K. R., SHEEHY, N. T., WHITE, M. P., BERRY, E. C., MORTON, S. U., MUTH, A. N., LEE, T. H., MIANO, J. M., IVEY, K. N. & SRIVASTAVA, D. 2009. miR-145 and miR-143 regulate smooth muscle cell fate and plasticity. *Nature,* 460**,** 705-10.

CORSTEN, M. F., DENNERT, R., JOCHEMS, S., KUZNETSOVA, T., DEVAUX, Y., HOFSTRA, L., WAGNER, D. R., STAESSEN, J. A., HEYMANS, S. & SCHROEN, B. 2010. Circulating MicroRNA-208b and MicroRNA-499 reflect myocardial damage in cardiovascular disease. *Circ Cardiovasc Genet,* 3**,** 499-506.

COUGHLAN, L., ALBA, R., PARKER, A. L., BRADSHAW, A. C., MCNEISH, I. A., NICKLIN, S. A. & BAKER, A. H. 2010. Tropism-modification strategies for targeted gene delivery using adenoviral vectors. *Viruses,* 2**,** 2290-355.

CREEMERS, E. E., TIJSEN, A. J. & PINTO, Y. M. 2012. Circulating microRNAs: novel biomarkers and extracellular communicators in cardiovascular disease? *Circ Res,* 110**,** 483-95.

CRICK, S. J., SHEPPARD, M. N., HO, S. Y., GEBSTEIN, L. & ANDERSON, R. H. 1998. Anatomy of the pig heart: comparisons with normal human cardiac structure. *J Anat,* 193 (Pt 1)**,** 105-19.

CUTLIP, D. E., LEON, M. B., HO, K. K., GORDON, P. C., GIAMBARTOLOMEI, A., DIVER, D. J., LASORDA, D. M., WILLIAMS, D. O., FITZPATRICK, M. M., DESJARDIN, A., POPMA, J. J., KUNTZ, R. E. & BAIM, D. S. 1999. Acute and nine-month clinical outcomes after "suboptimal" coronary stenting: results from the STent Anti-thrombotic Regimen Study (STARS) registry. *J Am Coll Cardiol,* 34**,** 698-706.

D'ALESSANDRA, Y., DEVANNA, P., LIMANA, F., STRAINO, S., DI CARLO, A., BRAMBILLA, P. G., RUBINO, M., CARENA, M. C., SPAZZAFUMO, L., DE SIMONE, M., MICHELI, B., BIGLIOLI, P., ACHILLI, F., MARTELLI, F., MAGGIOLINI, S., MARENZI, G., POMPILIO, G. & CAPOGROSSI, M. C. 2010.

Circulating microRNAs are new and sensitive biomarkers of myocardial infarction. *Eur Heart J,* 31**,** 2765-73.

DAHLHAUS, M., ROOLF, C., RUCK, S., LANGE, S., FREUND, M. & JUNGHANSS, C. 2013. Expression and prognostic significance of hsa-miR-142-3p in acute leukemias. *Neoplasma,* 60**,** 432-8.

DANG, C. V. 2010. Rethinking the Warburg effect with Myc micromanaging glutamine metabolism. *Cancer Res,* 70**,** 859-62.

DANGAS, G. D., CLAESSEN, B. E., CAIXETA, A., SANIDAS, E. A., MINTZ, G. S. & MEHRAN, R. 2010. In-stent restenosis in the drug-eluting stent era. *J Am Coll Cardiol,* 56**,** 1897-907.

DAVIS-DUSENBERY, B. N., CHAN, M. C., RENO, K. E., WEISMAN, A. S., LAYNE, M. D., LAGNA, G. & HATA, A. 2011. down-regulation of Kruppel-like factor-4 (KLF4) by microRNA-143/145 is critical for modulation of vascular smooth muscle cell phenotype by transforming growth factor-beta and bone morphogenetic protein 4. *J Biol Chem,* 286**,** 28097-110.

DAVIS, B. N., HILYARD, A. C., LAGNA, G. & HATA, A. 2008. SMAD proteins control DROSHA-mediated microRNA maturation. *Nature,* 454**,** 56-61.

DAY, J. R. & TAYLOR, K. M. 2005. The systemic inflammatory response syndrome and cardiopulmonary bypass. *Int J Surg,* 3**,** 129-40.

DE FEYTER, P. J., DE JAEGERE, P. P. & SERRUYS, P. W. 1994. Incidence, predictors, and management of acute coronary occlusion after coronary angioplasty. *Am Heart J,* 127**,** 643-51.

DE KOK, J. B., ROELOFS, R. W., GIESENDORF, B. A., PENNINGS, J. L., WAAS, E. T., FEUTH, T., SWINKELS, D. W. & SPAN, P. N. 2005. Normalization of gene expression measurements in tumor tissues: comparison of 13 endogenous control genes. *Lab Invest,* 85**,** 154-9.

DE ROSA, S., FICHTLSCHERER, S., LEHMANN, R., ASSMUS, B., DIMMELER, S. & ZEIHER, A. M. 2011. Transcoronary concentration gradients of circulating microRNAs. *Circulation,* 124**,** 1936-44.

DEGUCHI, J., NAMBA, T., HAMADA, H., NAKAOKA, T., ABE, J., SATO, O., MIYATA, T., MAKUUCHI, M., KUROKAWA, K. & TAKUWA, Y. 1999. Targeting endogenous platelet-derived growth factor B-chain by adenovirus-mediated gene transfer potently inhibits in vivo smooth muscle proliferation after arterial injury. *Gene Ther,* 6**,** 956-65.

DEMAISON, C., PARSLEY, K., BROUNS, G., SCHERR, M., BATTMER, K., KINNON, C., GREZ, M. & THRASHER, A. J. 2002. High-level transduction and gene expression in hematopoietic repopulating cells using a human immunodeficiency [correction of imunodeficiency] virus type 1-based lentiviral vector containing an internal spleen focus forming virus promoter. *Hum Gene Ther,* 13**,** 803-13.

DENBY, L., NICKLIN, S. A. & BAKER, A. H. 2005. Adeno-associated virus (AAV)-7 and -8 poorly transduce vascular endothelial cells and are sensitive to proteasomal degradation. *Gene Ther,* 12**,** 1534-8.

DENLI, A. M., TOPS, B. B., PLASTERK, R. H., KETTING, R. F. & HANNON, G. J. 2004. Processing of primary microRNAs by the Microprocessor complex. *Nature,* 432**,** 231-5.

DETTMER, M. S., PERREN, A., MOCH, H., KOMMINOTH, P., NIKIFOROV, Y. E. & NIKIFOROVA, M. N. 2013. Comprehensive microRNA expression profiling identifies novel markers in follicular variant of papillary thyroid carcinoma. *Thyroid*.

DI PAOLO, N. C., MIAO, E. A., IWAKURA, Y., MURALI-KRISHNA, K., ADEREM, A., FLAVELL, R. A., PAPAYANNOPOULOU, T. & SHAYAKHMETOV, D. M. 2009. Virus binding to a plasma membrane receptor triggers interleukin-1 alpha-mediated proinflammatory macrophage response in vivo. *Immunity,* 31**,** 110-21.

DICHEK, D. A., NEVILLE, R. F., ZWIEBEL, J. A., FREEMAN, S. M., LEON, M. B. & ANDERSON, W. F. 1989. Seeding of intravascular stents with genetically engineered endothelial cells. *Circulation,* 80**,** 1347-53.

DING, X., DING, J., NING, J., YI, F., CHEN, J., ZHAO, D., ZHENG, J., LIANG, Z., HU, Z. & DU, Q. 2012. Circulating microRNA-122 as a potential biomarker for liver injury. *Mol Med Report*.

DISHART, K. L., DENBY, L., GEORGE, S. J., NICKLIN, S. A., YENDLURI, S., TUERK, M. J., KELLEY, M. P., DONAHUE, B. A., NEWBY, A. C., HARDING, T. & BAKER, A. H. 2003. Third-generation lentivirus vectors efficiently transduce and phenotypically modify vascular cells: implications for gene therapy. *J Mol Cell Cardiol,* 35**,** 739-48.

DOMANSKI, M. J., MAHAFFEY, K., HASSELBLAD, V., BRENER, S. J., SMITH, P. K., HILLIS, G., ENGOREN, M., ALEXANDER, J. H., LEVY, J. H., CHAITMAN, B. R., BRODERICK, S., MACK, M. J., PIEPER, K. S. & FARKOUH, M. E. 2011. Association of myocardial enzyme elevation and survival following coronary artery bypass graft surgery. *Jama,* 305**,** 585-91.

DOMMKE, C., HAASE, K. K., SUSELBECK, T., STREITNER, I., HAGHI, D., METZ, J., BORGGREFE, M. & HERDEG, C. 2007. Local paclitaxel delivery after coronary stenting in an experimental animal model. *Thromb Haemost,* 98**,** 674-80.

DOTTER, C. T. & JUDKINS, M. P. 1964. Transluminal Treatment of Arteriosclerotic Obstruction. Description of a New Technic and a Preliminary Report of Its Application. *Circulation,* 30**,** 654-70.

DOUGLAS, G., VAN KAMPEN, E., HALE, A. B., MCNEILL, E., PATEL, J., CRABTREE, M. J., ALI, Z., HOERR, R. A., ALP, N. J. & CHANNON, K. M. 2012. Endothelial cell repopulation after stenting determines in-stent neointima formation: effects of bare-metal vs. drug-eluting stents and genetic endothelial cell modification. *Eur Heart J*.

DUTTAGUPTA, R., JIANG, R., GOLLUB, J., GETTS, R. C. & JONES, K. W. 2011. Impact of cellular miRNAs on circulating miRNA biomarker signatures. *PLoS One,* 6**,** e20769.

EDELSTEIN, M. L., ABEDI, M. R. & WIXON, J. 2007. Gene therapy clinical trials worldwide to 2007--an update. *J Gene Med,* 9**,** 833-42.

EEFTING, D., DE VRIES, M. R., GRIMBERGEN, J. M., KARPER, J. C., VAN BOCKEL, J. H. & QUAX, P. H. 2010a. In vivo suppression of vein graft disease by nonviral, electroporation-mediated, gene transfer of tissue inhibitor of metalloproteinase-1 linked to the amino terminal fragment of urokinase (TIMP-1.ATF), a cell-surface directed matrix metalloproteinase inhibitor. *J Vasc Surg,* 51**,** 429-37.

EEFTING, D., SEGHERS, L., GRIMBERGEN, J. M., DE VRIES, M. R., DE BOER, H. C., LARDENOYE, J. W., JUKEMA, J. W., VAN BOCKEL, J. H. & QUAX, P. H. 2010b. A novel urokinase receptor-targeted inhibitor for plasmin and matrix metalloproteinases suppresses vein graft disease. *Cardiovasc Res,* 88**,** 367-75.

EGASHIRA, K., NAKANO, K., OHTANI, K., FUNAKOSHI, K., ZHAO, G., IHARA, Y., KOGA, J., KIMURA, S., TOMINAGA, R. & SUNAGAWA, K. 2007. Local delivery of anti-monocyte chemoattractant protein-1 by gene-eluting stents attenuates in-stent stenosis in rabbits and monkeys. *Arterioscler Thromb Vasc Biol,* 27**,** 2563-8.

ELEZI, S., KASTRATI, A., PACHE, J., WEHINGER, A., HADAMITZKY, M., DIRSCHINGER, J., NEUMANN, F. J. & SCHOMIG, A. 1998. Diabetes mellitus and the clinical and angiographic outcome after coronary stent placement. *J Am Coll Cardiol,* 32**,** 1866-73.

ELIA, L., QUINTAVALLE, M., ZHANG, J., CONTU, R., COSSU, L., LATRONICO, M. V., PETERSON, K. L., INDOLFI, C., CATALUCCI, D., CHEN, J., COURTNEIDGE, S. A. & CONDORELLI, G. 2009. The knockout of miR-143 and -145 alters smooth muscle cell maintenance and vascular homeostasis in mice: correlates with human disease. *Cell Death Differ,* 16**,** 1590-8.

ENGELHARDT, S. 2012. Small RNA biomarkers come of age. *J Am Coll Cardiol,* 60**,** 300-3.

FARB, A., HELLER, P. F., SHROFF, S., CHENG, L., KOLODGIE, F. D., CARTER, A. J., SCOTT, D. S., FROEHLICH, J. & VIRMANI, R. 2001. Pathological analysis of local delivery of paclitaxel via a polymer-coated stent. *Circulation,* 104**,** 473-9.

FARB, A., KOLODGIE, F. D., HWANG, J. Y., BURKE, A. P., TEFERA, K., WEBER, D. K., WIGHT, T. N. & VIRMANI, R. 2004. Extracellular matrix changes in stented human coronary arteries. *Circulation,* 110**,** 940-7.

FAVALORO, R. G. 1968. Saphenous vein autograft replacement of severe segmental coronary artery occlusion: operative technique. *Ann Thorac Surg,* 5**,** 334-9.

FAXON, D. P. 2002. Systemic drug therapy for restenosis: "deja vu all over again". *Circulation,* 106**,** 2296-8.

FELDMAN, L. J., PASTORE, C. J., AUBAILLY, N., KEARNEY, M., CHEN, D., PERRICAUDET, M., STEG, P. G. & ISNER, J. M. 1997. Improved efficiency of arterial gene transfer by use of poloxamer 407 as a vehicle for adenoviral vectors. *Gene Ther,* 4**,** 189-98.

FICHTLSCHERER, S., DE ROSA, S., FOX, H., SCHWIETZ, T., FISCHER, A., LIEBETRAU, C., WEBER, M., HAMM, C. W., ROXE, T., MULLER-ARDOGAN, M., BONAUER, A., ZEIHER, A. M. & DIMMELER, S. 2010. Circulating microRNAs in patients with coronary artery disease. *Circ Res,* 107**,** 677-84.

FICHTLSCHERER, S., ZEIHER, A. M. & DIMMELER, S. 2011. Circulating microRNAs: biomarkers or mediators of cardiovascular diseases? *Arterioscler Thromb Vasc Biol,* 31**,** 2383-90.

FISCHMAN, D. L., LEON, M. B., BAIM, D. S., SCHATZ, R. A., SAVAGE, M. P., PENN, I., DETRE, K., VELTRI, L., RICCI, D., NOBUYOSHI, M. & ET AL. 1994. A randomized comparison of coronary-stent placement and balloon angioplasty in the treatment of coronary artery disease. Stent Restenosis Study Investigators. *N Engl J Med,* 331**,** 496-501.

FISHBEIN, I., ALFERIEV, I., BAKAY, M., STACHELEK, S. J., SOBOLEWSKI, P., LAI, M., CHOI, H., CHEN, I. W. & LEVY, R. J. 2008. Local delivery of gene vectors from bare-metal stents by use of a biodegradable synthetic complex inhibits in-stent restenosis in rat carotid arteries. *Circulation,* 117**,** 2096-103.

FISHBEIN, I., ALFERIEV, I. S., NYANGUILE, O., GASTER, R., VOHS, J. M., WONG, G. S., FELDERMAN, H., CHEN, I. W., CHOI, H., WILENSKY, R. L. & LEVY, R. J. 2006. Bisphosphonate-mediated gene vector delivery from the metal surfaces of stents. *Proc Natl Acad Sci U S A,* 103**,** 159-64.

FLEISSNER, F., JAZBUTYTE, V., FIEDLER, J., GUPTA, S. K., YIN, X., XU, Q., GALUPPO, P., KNEITZ, S., MAYR, M., ERTL, G., BAUERSACHS, J. & THUM, T. 2010. Short communication: asymmetric dimethylarginine impairs angiogenic progenitor cell function in patients with coronary artery disease through a microRNA-21-dependent mechanism. *Circ Res,* 107**,** 138-43.

FLOTTE, T. R. & CARTER, B. J. 1995. Adeno-associated virus vectors for gene therapy. *Gene Ther,* 2**,** 357-62.

FLYNN, R., BUCKLER, J. M., TANG, C., KIM, F. & DICHEK, D. A. 2010. Helper-dependent adenoviral vectors are superior in vitro to first-generation vectors for endothelial cell-targeted gene therapy. *Mol Ther,* 18**,** 2121-9.

FLYNT, A. S. & LAI, E. C. 2008. Biological principles of microRNA-mediated regulation: shared themes amid diversity. *Nat Rev Genet,* 9**,** 831-42.

FREY, P., WATERS, D. D., DEMICCO, D. A., BREAZNA, A., SAMUELS, L., PIPE, A., WUN, C. C. & BENOWITZ, N. L. 2011. Impact of smoking on cardiovascular events in patients with coronary disease receiving contemporary medical therapy (from the Treating to New Targets [TNT] and the Incremental Decrease in End Points Through Aggressive Lipid Lowering [IDEAL] trials). *Am J Cardiol,* 107**,** 145-50.

FRIEDMAN, R. C., FARH, K. K., BURGE, C. B. & BARTEL, D. P. 2009. Most mammalian mRNAs are conserved targets of microRNAs. *Genome Res,* 19**,** 92-105.

FUJITA, S., ITO, T., MIZUTANI, T., MINOGUCHI, S., YAMAMICHI, N., SAKURAI, K. & IBA, H. 2008. miR-21 Gene expression triggered by AP-1 is sustained through a double-negative feedback mechanism. *J Mol Biol,* 378**,** 492-504.

GAFFNEY, M. M., HYNES, S. O., BARRY, F. & O'BRIEN, T. 2007. Cardiovascular gene therapy: current status and therapeutic potential. *Br J Pharmacol,* 152**,** 175-88.

GAGGAR, A., SHAYAKHMETOV, D. M. & LIEBER, A. 2003. CD46 is a cellular receptor for group B adenoviruses. *Nat Med,* 9**,** 1408-12.

GALLO, R., PADUREAN, A., TOSCHI, V., BICHLER, J., FALLON, J. T., CHESEBRO, J. H., FUSTER, V. & BADIMON, J. J. 1998. Prolonged thrombin inhibition reduces restenosis after balloon angioplasty in porcine coronary arteries. *Circulation,* 97**,** 581-8.

GANESAN, J., RAMANUJAM, D., SASSI, Y., AHLES, A., JENTZSCH, C., WERFEL, S., LEIERSEDER, S., LOYER, X., GIACCA, M., ZENTILIN, L., THUM, T., LAGGERBAUER, B. & ENGELHARDT, S. 2013. MiR-378 controls cardiac hypertrophy by combined repression of mitogen-activated protein kinase pathway factors. *Circulation,* 127**,** 2097-106.

GARCIA-TOUCHARD, A., BURKE, S. E., TONER, J. L., CROMACK, K. & SCHWARTZ, R. S. 2006. Zotarolimus-eluting stents reduce experimental coronary artery neointimal hyperplasia after 4 weeks. *Eur Heart J,* 27**,** 988-93.

GARG, S. 2013. The FIREHAWK stent: will it achieve its potential? *EuroIntervention,* 9**,** 15-9.

GARG, S., BOURANTAS, C. & SERRUYS, P. W. 2013. New concepts in the design of drug-eluting coronary stents. *Nat Rev Cardiol,* 10**,** 248-60.

GARG, S. & SERRUYS, P. 2010a. Benefits of and safety concerns associated with drug-eluting coronary stents. *Expert Rev Cardiovasc Ther,* 8**,** 449-70.

GARG, S. & SERRUYS, P. W. 2010b. Coronary stents: current status. *J Am Coll Cardiol,* 56**,** S1-42.

GARG, S. & SERRUYS, P. W. 2010c. Coronary stents: looking forward. *J Am Coll Cardiol,* 56**,** S43-78.

GARVEY, S. M., SINDEN, D. S., SCHOPPEE BORTZ, P. D. & WAMHOFF, B. R. 2010. Cyclosporine up-regulates Kruppel-like factor-4 (KLF4) in vascular smooth muscle cells and drives phenotypic modulation in vivo. *J Pharmacol Exp Ther,* 333**,** 34-42.

GEARY, R. L., WILLIAMS, J. K., GOLDEN, D., BROWN, D. G., BENJAMIN, M. E. & ADAMS, M. R. 1996. Time course of cellular proliferation, intimal hyperplasia, and remodeling following angioplasty in monkeys with established atherosclerosis. A nonhuman primate model of restenosis. *Arterioscler Thromb Vasc Biol,* 16**,** 34-43.

GEORGE, S. J., BAKER, A. H., ANGELINI, G. D. & NEWBY, A. C. 1998a. Gene transfer of tissue inhibitor of metalloproteinase-2 inhibits metalloproteinase activity and neointima formation in human saphenous veins. *Gene Ther,* 5**,** 1552-60.

GEORGE, S. J., JOHNSON, J. L., ANGELINI, G. D., NEWBY, A. C. & BAKER, A. H. 1998b. Adenovirus-mediated gene transfer of the human TIMP-1 gene inhibits smooth muscle cell migration and neointimal formation in human saphenous vein. *Hum Gene Ther,* 9**,** 867-77.

GEORGE, S. J., LLOYD, C. T., ANGELINI, G. D., NEWBY, A. C. & BAKER, A. H. 2000. Inhibition of late vein graft neointima formation in human and porcine

models by adenovirus-mediated overexpression of tissue inhibitor of metalloproteinase-3. *Circulation,* 101**,** 296-304.

GEORGE, S. J., WAN, S., HU, J., MACDONALD, R., JOHNSON, J. L. & BAKER, A. H. 2011. Sustained reduction of vein graft neointima formation by ex vivo TIMP-3 gene therapy. *Circulation,* 124**,** S135-42.

GIACCA, M. & BAKER, A. H. 2011. Heartening results: the CUPID gene therapy trial for heart failure. *Mol Ther,* 19**,** 1181-2.

GIDLOF, O., ANDERSSON, P., VAN DER PALS, J., GOTBERG, M. & ERLINGE, D. 2012. Cardiospecific microRNA plasma levels correlate with troponin and cardiac function in patients with ST elevation myocardial infarction, are selectively dependent on renal elimination, and can be detected in urine samples. *Cardiology,* 118**,** 217-26.

GILAD, S., MEIRI, E., YOGEV, Y., BENJAMIN, S., LEBANONY, D., YERUSHALMI, N., BENJAMIN, H., KUSHNIR, M., CHOLAKH, H., MELAMED, N., BENTWICH, Z., HOD, M., GOREN, Y. & CHAJUT, A. 2008. Serum microRNAs are promising novel biomarkers. *PLoS One,* 3**,** e3148.

GOLDMAN, S., ZADINA, K., MORITZ, T., OVITT, T., SETHI, G., COPELAND, J. G., THOTTAPURATHU, L., KRASNICKA, B., ELLIS, N., ANDERSON, R. J. & HENDERSON, W. 2004. Long-term patency of saphenous vein and left internal mammary artery grafts after coronary artery bypass surgery: results from a Department of Veterans Affairs Cooperative Study. *J Am Coll Cardiol,* 44**,** 2149-56.

GORDON, P. C., GIBSON, C. M., COHEN, D. J., CARROZZA, J. P., KUNTZ, R. E. & BAIM, D. S. 1993. Mechanisms of restenosis and redilation within coronary stents--quantitative angiographic assessment. *J Am Coll Cardiol,* 21**,** 1166-74.

GRANADA, J. F., ENSENAT, D., KESWANI, A. N., KALUZA, G. L., RAIZNER, A. E., LIU, X. M., PEYTON, K. J., AZAM, M. A., WANG, H. & DURANTE, W. 2005. Single perivascular delivery of mitomycin C stimulates p21 expression and inhibits neointima formation in rat arteries. *Arterioscler Thromb Vasc Biol,* 25**,** 2343-8.

GRANADA, J. F., KALUZA, G. L., WILENSKY, R. L., BIEDERMANN, B. C., SCHWARTZ, R. S. & FALK, E. 2009. Porcine models of coronary atherosclerosis

and vulnerable plaque for imaging and interventional research. *EuroIntervention,* 5**,** 140-8.

GREEN, N. K., HERBERT, C. W., HALE, S. J., HALE, A. B., MAUTNER, V., HARKINS, R., HERMISTON, T., ULBRICH, K., FISHER, K. D. & SEYMOUR, L. W. 2004. Extended plasma circulation time and decreased toxicity of polymer-coated adenovirus. *Gene Ther,* 11**,** 1256-63.

GREGOREVIC, P., BLANKINSHIP, M. J., ALLEN, J. M., CRAWFORD, R. W., MEUSE, L., MILLER, D. G., RUSSELL, D. W. & CHAMBERLAIN, J. S. 2004. Systemic delivery of genes to striated muscles using adeno-associated viral vectors. *Nat Med,* 10**,** 828-34.

GREGORY, R. I., YAN, K. P., AMUTHAN, G., CHENDRIMADA, T., DORATOTAJ, B., COOCH, N. & SHIEKHATTAR, R. 2004. The Microprocessor complex mediates the genesis of microRNAs. *Nature,* 432**,** 235-40.

GRIENDLING, K. K., SORESCU, D., LASSEGUE, B. & USHIO-FUKAI, M. 2000. Modulation of protein kinase activity and gene expression by reactive oxygen species and their role in vascular physiology and pathophysiology. *Arterioscler Thromb Vasc Biol,* 20**,** 2175-83.

GROSSHANS, H. & FILIPOWICZ, W. 2008. Molecular biology: the expanding world of small RNAs. *Nature,* 451**,** 414-6.

GROSSMAN, M., RAPER, S. E., KOZARSKY, K., STEIN, E. A., ENGELHARDT, J. F., MULLER, D., LUPIEN, P. J. & WILSON, J. M. 1994. Successful ex vivo gene therapy directed to liver in a patient with familial hypercholesterolaemia. *Nat Genet,* 6**,** 335-41.

GRUNTZIG, A. 1978. Transluminal dilatation of coronary-artery stenosis. *Lancet,* 1**,** 263.

GRUNTZIG, A. R., SENNING, A. & SIEGENTHALER, W. E. 1979. Nonoperative dilatation of coronary-artery stenosis: percutaneous transluminal coronary angioplasty. *N Engl J Med,* 301**,** 61-8.

GU, Y., LI, M., ZHANG, K., CHEN, L., JIANG, A. A., WANG, J., LV, X. & LI, X. 2011. Identification of suitable endogenous control microRNA genes in normal pig tissues. *Anim Sci J,* 82**,** 722-8.

GUNN, J., ARNOLD, N., CHAN, K. H., SHEPHERD, L., CUMBERLAND, D. C. & CROSSMAN, D. C. 2002. Coronary artery stretch versus deep injury in the development of in-stent neointima. *Heart,* 88**,** 401-5.

GUZMAN, R. J., HIRSCHOWITZ, E. A., BRODY, S. L., CRYSTAL, R. G., EPSTEIN, S. E. & FINKEL, T. 1994. In vivo suppression of injury-induced vascular smooth muscle cell accumulation using adenovirus-mediated transfer of the herpes simplex virus thymidine kinase gene. *Proc Natl Acad Sci U S A,* 91**,** 10732-6.

GUZMAN, R. J., LEMARCHAND, P., CRYSTAL, R. G., EPSTEIN, S. E. & FINKEL, T. 1993. Efficient gene transfer into myocardium by direct injection of adenovirus vectors. *Circ Res,* 73**,** 1202-7.

HACEIN-BEY-ABINA, S., VON KALLE, C., SCHMIDT, M., MCCORMACK, M. P., WULFFRAAT, N., LEBOULCH, P., LIM, A., OSBORNE, C. S., PAWLIUK, R., MORILLON, E., SORENSEN, R., FORSTER, A., FRASER, P., COHEN, J. I., DE SAINT BASILE, G., ALEXANDER, I., WINTERGERST, U., FREBOURG, T., AURIAS, A., STOPPA-LYONNET, D., ROMANA, S., RADFORD-WEISS, I., GROSS, F., VALENSI, F., DELABESSE, E., MACINTYRE, E., SIGAUX, F., SOULIER, J., LEIVA, L. E., WISSLER, M., PRINZ, C., RABBITTS, T. H., LE DEIST, F., FISCHER, A. & CAVAZZANA-CALVO, M. 2003. LMO2-associated clonal T cell proliferation in two patients after gene therapy for SCID-X1. *Science,* 302**,** 415-9.

HAMM, C. W., BASSAND, J. P., AGEWALL, S., BAX, J., BOERSMA, E., BUENO, H., CASO, P., DUDEK, D., GIELEN, S., HUBER, K., OHMAN, M., PETRIE, M. C., SONNTAG, F., UVA, M. S., STOREY, R. F., WIJNS, W. & ZAHGER, D. 2011. ESC Guidelines for the management of acute coronary syndromes in patients presenting without persistent ST-segment elevation: The Task Force for the management of acute coronary syndromes (ACS) in patients presenting without persistent ST-segment elevation of the European Society of Cardiology (ESC). *Eur Heart J,* 32**,** 2999-3054.

HANNA, A. K., FOX, J. C., NESCHIS, D. G., SAFFORD, S. D., SWAIN, J. L. & GOLDEN, M. A. 1997. Antisense basic fibroblast growth factor gene transfer reduces neointimal thickening after arterial injury. *J Vasc Surg,* 25**,** 320-5.

HARA, M., NISHINO, M., TANIIKE, M., MAKINO, N., KATO, H., EGAMI, Y., SHUTTA, R., YAMAGUCHI, H., TANOUCHI, J. & YAMADA, Y. 2010. Difference of neointimal formational pattern and incidence of thrombus formation among 3 kinds of stents: an angioscopic study. *JACC Cardiovasc Interv,* 3**,** 215-20.

HARRELL, R. L., RAJANAYAGAM, S., DOANES, A. M., GUZMAN, R. J., HIRSCHOWITZ, E. A., CRYSTAL, R. G., EPSTEIN, S. E. & FINKEL, T. 1997. Inhibition of vascular smooth muscle cell proliferation and neointimal accumulation by adenovirus-mediated gene transfer of cytosine deaminase. *Circulation,* 96**,** 621-7.

HARRIS, T. A., YAMAKUCHI, M., FERLITO, M., MENDELL, J. T. & LOWENSTEIN, C. J. 2008. MicroRNA-126 regulates endothelial expression of vascular cell adhesion molecule 1. *Proc Natl Acad Sci U S A,* 105**,** 1516-21.

HARTMAN, Z. C., APPLEDORN, D. M. & AMALFITANO, A. 2008. Adenovirus vector induced innate immune responses: impact upon efficacy and toxicity in gene therapy and vaccine applications. *Virus Res,* 132**,** 1-14.

HATA, M., SEZAI, A., NIINO, T., YODA, M., WAKUI, S., CHIKU, M., TAKAYAMA, T., HONYE, J., SAITOH, S. & MINAMI, K. 2007. What is the optimal management for preventing saphenous vein graft diseases?: early results of intravascular angioscopic assessment. *Circ J,* 71**,** 286-7.

HAVENGA, M. J., LEMCKERT, A. A., GRIMBERGEN, J. M., VOGELS, R., HUISMAN, L. G., VALERIO, D., BOUT, A. & QUAX, P. H. 2001. Improved adenovirus vectors for infection of cardiovascular tissues. *J Virol,* 75**,** 3335-42.

HEDMAN, M., HARTIKAINEN, J., SYVANNE, M., STJERNVALL, J., HEDMAN, A., KIVELA, A., VANNINEN, E., MUSSALO, H., KAUPPILA, E., SIMULA, S., NARVANEN, O., RANTALA, A., PEUHKURINEN, K., NIEMINEN, M. S., LAAKSO, M. & YLA-HERTTUALA, S. 2003. Safety and feasibility of catheter-based local intracoronary vascular endothelial growth factor gene transfer in the prevention of postangioplasty and in-stent restenosis and in the treatment of chronic myocardial ischemia: phase II results of the Kuopio Angiogenesis Trial (KAT). *Circulation,* 107**,** 2677-83.

HEISTAD, D. D. 2006. Gene therapy for vascular disease. *Vascul Pharmacol,* 45**,** 331-3.

HERDEG, C., GOHRING-FRISCHHOLZ, K., HAASE, K. K., GEISLER, T., ZURN, C., HARTMANN, U., WOHRLE, J., NUSSER, T., DIPPON, J., MAY, A. E. & GAWAZ, M. 2009. Catheter-based delivery of fluid paclitaxel for prevention of restenosis in native coronary artery lesions after stent implantation. *Circ Cardiovasc Interv,* 2**,** 294-301.

HERGENREIDER, E., HEYDT, S., TREGUER, K., BOETTGER, T., HORREVOETS, A. J., ZEIHER, A. M., SCHEFFER, M. P., FRANGAKIS, A. S., YIN, X., MAYR, M., BRAUN, T., URBICH, C., BOON, R. A. & DIMMELER, S. 2012. Atheroprotective communication between endothelial cells and smooth muscle cells through miRNAs. *Nat Cell Biol,* 14**,** 249-56.

HILTUNEN, M. O., LAITINEN, M., TURUNEN, M. P., JELTSCH, M., HARTIKAINEN, J., RISSANEN, T. T., LAUKKANEN, J., NIEMI, M., KOSSILA, M., HAKKINEN, T. P., KIVELA, A., ENHOLM, B., MANSUKOSKI, H., TURUNEN, A. M., ALITALO, K. & YLA-HERTTUALA, S. 2000a. Intravascular adenovirus-mediated VEGF-C gene transfer reduces neointima formation in balloon-denuded rabbit aorta. *Circulation,* 102**,** 2262-8.

HILTUNEN, M. O., TURUNEN, M. P., TURUNEN, A. M., RISSANEN, T. T., LAITINEN, M., KOSMA, V. M. & YLA-HERTTUALA, S. 2000b. Biodistribution of adenoviral vector to nontarget tissues after local in vivo gene transfer to arterial wall using intravascular and periadventitial gene delivery methods. *Faseb J,* 14**,** 2230-6.

HINKEL, R., PENZKOFER, D., ZUHLKE, S., FISCHER, A., HUSADA, W., XU, Q. F., BALOCH, E., VAN ROOIJ, E., ZEIHER, A. M., KUPATT, C. & DIMMELER, S. 2013. Inhibition of MicroRNA-92a Protects Against Ischemia/Reperfusion Injury in a Large-Animal Model. *Circulation,* 128**,** 1066-1075.

HLATKY, M. A., BOOTHROYD, D. B., BRAVATA, D. M., BOERSMA, E., BOOTH, J., BROOKS, M. M., CARRIE, D., CLAYTON, T. C., DANCHIN, N., FLATHER, M., HAMM, C. W., HUEB, W. A., KAHLER, J., KELSEY, S. F., KING, S. B., KOSINSKI, A. S., LOPES, N., MCDONALD, K. M., RODRIGUEZ, A., SERRUYS, P., SIGWART, U., STABLES, R. H., OWENS, D. K. & POCOCK, S. J. 2009. Coronary artery bypass surgery compared with percutaneous coronary interventions for multivessel disease: a collaborative analysis of individual patient data from ten randomised trials. *Lancet,* 373**,** 1190-7.

HOFFMANN, R., MINTZ, G. S., DUSSAILLANT, G. R., POPMA, J. J., PICHARD, A. D., SATLER, L. F., KENT, K. M., GRIFFIN, J. & LEON, M. B. 1996. Patterns and mechanisms of in-stent restenosis. A serial intravascular ultrasound study. *Circulation,* 94**,** 1247-54.

HOLMES, D. R., JR., KEREIAKES, D. J., GARG, S., SERRUYS, P. W., DEHMER, G. J., ELLIS, S. G., WILLIAMS, D. O., KIMURA, T. & MOLITERNO, D. J. 2010. Stent thrombosis. *J Am Coll Cardiol,* 56**,** 1357-65.

HOLMES, D. R., JR., SAVAGE, M., LABLANCHE, J. M., GRIP, L., SERRUYS, P. W., FITZGERALD, P., FISCHMAN, D., GOLDBERG, S., BRINKER, J. A., ZEIHER, A. M., SHAPIRO, L. M., WILLERSON, J., DAVIS, B. R., FERGUSON, J. J., POPMA, J., KING, S. B., 3RD, LINCOFF, A. M., TCHENG, J. E., CHAN, R., GRANETT, J. R. & POLAND, M. 2002. Results of Prevention of REStenosis with Tranilast and its Outcomes (PRESTO) trial. *Circulation,* 106**,** 1243-50.

HORITA, H. N., SIMPSON, P. A., OSTRIKER, A., FURGESON, S., VAN PUTTEN, V., WEISER-EVANS, M. C. & NEMENOFF, R. A. 2011. Serum response factor regulates expression of phosphatase and tensin homolog through a microRNA network in vascular smooth muscle cells. *Arterioscler Thromb Vasc Biol,* 31**,** 2909-19.

IACCARINO, G., SMITHWICK, L. A., LEFKOWITZ, R. J. & KOCH, W. J. 1999. Targeting Gbeta gamma signaling in arterial vascular smooth muscle proliferation: a novel strategy to limit restenosis. *Proc Natl Acad Sci U S A,* 96**,** 3945-50.

IACONETTI, C., POLIMENI, A., SORRENTINO, S., SABATINO, J., PIRONTI, G., ESPOSITO, G., CURCIO, A. & INDOLFI, C. 2012. Inhibition of miR-92a increases endothelial proliferation and migration in vitro as well as reduces neointimal proliferation in vivo after vascular injury. *Basic Res Cardiol,* 107**,** 296.

IALENTI, A., GRASSIA, G., GORDON, P., MADDALUNO, M., DI LAURO, M. V., BAKER, A. H., GUGLIELMOTTI, A., COLOMBO, A., BIONDI, G., KENNEDY, S. & MAFFIA, P. 2011. Inhibition of in-stent stenosis by oral administration of bindarit in porcine coronary arteries. *Arterioscler Thromb Vasc Biol,* 31**,** 2448-54.

INDOLFI, C., AVVEDIMENTO, E. V., RAPACCIUOLO, A., DI LORENZO, E., ESPOSITO, G., STABILE, E., FELICIELLO, A., MELE, E., GIULIANO, P.,

CONDORELLI, G. & ET AL. 1995. Inhibition of cellular ras prevents smooth muscle cell proliferation after vascular injury in vivo. *Nat Med,* 1**,** 541-5.

IP, J. H., FUSTER, V., BADIMON, L., BADIMON, J., TAUBMAN, M. B. & CHESEBRO, J. H. 1990. Syndromes of accelerated atherosclerosis: role of vascular injury and smooth muscle cell proliferation. *J Am Coll Cardiol,* 15**,** 1667-87.

ISHIDA, A., MURRAY, J., SAITO, Y., KANTHOU, C., BENZAKOUR, O., SHIBUYA, M. & WIJELATH, E. S. 2001. Expression of vascular endothelial growth factor receptors in smooth muscle cells. *J Cell Physiol,* 188**,** 359-68.

ISNER, J. M. 2002. Myocardial gene therapy. *Nature,* 415**,** 234-9.

ISNER, J. M., KEARNEY, M., BORTMAN, S. & PASSERI, J. 1995. Apoptosis in human atherosclerosis and restenosis. *Circulation,* 91**,** 2703-11.

JAMES, S. K., WALLENTIN, L. & LAGERQVIST, B. 2009. The SCAAR-scare in perspective. *EuroIntervention,* 5**,** 501-4.

JANSSENS, S., FLAHERTY, D., NONG, Z., VARENNE, O., VAN PELT, N., HAUSTERMANS, C., ZOLDHELYI, P., GERARD, R. & COLLEN, D. 1998. Human endothelial nitric oxide synthase gene transfer inhibits vascular smooth muscle cell proliferation and neointima formation after balloon injury in rats. *Circulation,* 97**,** 1274-81.

JEREMIAS, A. & KIRTANE, A. 2008. Balancing efficacy and safety of drug-eluting stents in patients undergoing percutaneous coronary intervention. *Ann Intern Med,* 148**,** 234-8.

JESSUP, M., GREENBERG, B., MANCINI, D., CAPPOLA, T., PAULY, D. F., JASKI, B., YAROSHINSKY, A., ZSEBO, K. M., DITTRICH, H. & HAJJAR, R. J. 2011. Calcium Upregulation by Percutaneous Administration of Gene Therapy in Cardiac Disease (CUPID): a phase 2 trial of intracoronary gene therapy of sarcoplasmic reticulum Ca2+-ATPase in patients with advanced heart failure. *Circulation,* 124**,** 304-13.

JI, R., CHENG, Y., YUE, J., YANG, J., LIU, X., CHEN, H., DEAN, D. B. & ZHANG, C. 2007. MicroRNA expression signature and antisense-mediated depletion reveal an

essential role of MicroRNA in vascular neointimal lesion formation. *Circ Res,* 100**,** 1579-88.

JIANG, B., QIAN, K., DU, L., LUTTRELL, I., CHITALEY, K. & DICHEK, D. A. 2011. Helper-dependent adenovirus is superior to first-generation adenovirus for expressing transgenes in atherosclerosis-prone arteries. *Arterioscler Thromb Vasc Biol,* 31**,** 1317-25.

JOHNSON, T. W., WU, Y. X., HERDEG, C., BAUMBACH, A., NEWBY, A. C., KARSCH, K. R. & OBERHOFF, M. 2005. Stent-based delivery of tissue inhibitor of metalloproteinase-3 adenovirus inhibits neointimal formation in porcine coronary arteries. *Arterioscler Thromb Vasc Biol,* 25**,** 754-9.

JOHNSTON, T. P. & MILLER, S. C. 1985. Toxicological evaluation of poloxamer vehicles for intramuscular use. *J Parenter Sci Technol,* 39**,** 83-9.

JONER, M., FINN, A. V., FARB, A., MONT, E. K., KOLODGIE, F. D., LADICH, E., KUTYS, R., SKORIJA, K., GOLD, H. K. & VIRMANI, R. 2006. Pathology of drug-eluting stents in humans: delayed healing and late thrombotic risk. *J Am Coll Cardiol,* 48**,** 193-202.

JONES, D. A., BENJAMIN, C. W. & LINSEMAN, D. A. 1995. Activation of thromboxane and prostacyclin receptors elicits opposing effects on vascular smooth muscle cell growth and mitogen-activated protein kinase signaling cascades. *Mol Pharmacol,* 48**,** 890-6.

JORGENSEN, S., BAKER, A., MOLLER, S. & NIELSEN, B. S. 2010. Robust one-day in situ hybridization protocol for detection of microRNAs in paraffin samples using LNA probes. *Methods,* 52**,** 375-81.

JOZKOWICZ, A. & DULAK, J. 2005. Helper-dependent adenoviral vectors in experimental gene therapy. *Acta Biochim Pol,* 52**,** 589-99.

JUKEMA, J. W., VERSCHUREN, J. J., AHMED, T. A. & QUAX, P. H. 2012. Restenosis after PCI. Part 1: pathophysiology and risk factors. *Nat Rev Cardiol,* 9**,** 53-62.

KABANOV, A., ZHU, J. & ALAKHOV, V. 2005. Pluronic block copolymers for gene delivery. *Adv Genet,* 53**,** 231-61.

KALYUZHNIY, O., DI PAOLO, N. C., SILVESTRY, M., HOFHERR, S. E., BARRY, M. A., STEWART, P. L. & SHAYAKHMETOV, D. M. 2008. Adenovirus serotype 5 hexon is critical for virus infection of hepatocytes in vivo. *Proc Natl Acad Sci U S A*, 105**,** 5483-8.

KANG, J., LEE, S. Y., LEE, S. Y., KIM, Y. J., PARK, J. Y., KWON, S. J., NA, M. J., LEE, E. J., JEON, H. S. & SON, J. W. 2012. microRNA-99b acts as a tumor suppressor in non-small cell lung cancer by directly targeting fibroblast growth factor receptor 3. *Exp Ther Med*, 3**,** 149-153.

KAPUR, A., HALL, R. J., MALIK, I. S., QURESHI, A. C., BUTTS, J., DE BELDER, M., BAUMBACH, A., ANGELINI, G., DE BELDER, A., OLDROYD, K. G., FLATHER, M., ROUGHTON, M., NIHOYANNOPOULOS, P., BAGGER, J. P., MORGAN, K. & BEATT, K. J. 2010. Randomized comparison of percutaneous coronary intervention with coronary artery bypass grafting in diabetic patients. 1-year results of the CARDia (Coronary Artery Revascularization in Diabetes) trial. *J Am Coll Cardiol*, 55**,** 432-40.

KARAS, S. P., GRAVANIS, M. B., SANTOIAN, E. C., ROBINSON, K. A., ANDERBERG, K. A. & KING, S. B., 3RD 1992. Coronary intimal proliferation after balloon injury and stenting in swine: an animal model of restenosis. *J Am Coll Cardiol*, 20**,** 467-74.

KARVINEN, H. & YLA-HERTTUALA, S. 2010. New aspects in vascular gene therapy. *Curr Opin Pharmacol*, 10**,** 208-11.

KASS-EISLER, A., FALCK-PEDERSEN, E., ALVIRA, M., RIVERA, J., BUTTRICK, P. M., WITTENBERG, B. A., CIPRIANI, L. & LEINWAND, L. A. 1993. Quantitative determination of adenovirus-mediated gene delivery to rat cardiac myocytes in vitro and in vivo. *Proc Natl Acad Sci U S A*, 90**,** 11498-502.

KASTRATI, A., MEHILLI, J., PACHE, J., KAISER, C., VALGIMIGLI, M., KELBAEK, H., MENICHELLI, M., SABATE, M., SUTTORP, M. J., BAUMGART, D., SEYFARTH, M., PFISTERER, M. E. & SCHOMIG, A. 2007. Analysis of 14 trials comparing sirolimus-eluting stents with bare-metal stents. *N Engl J Med*, 356**,** 1030-9.

KASTRATI, A., SCHUHLEN, H., HAUSLEITER, J., WALTER, H., ZITZMANN-ROTH, E., HADAMITZKY, M., ELEZI, S., ULM, K., DIRSCHINGER, J.,

NEUMANN, F. J. & SCHOMIG, A. 1997. Restenosis after coronary stent placement and randomization to a 4-week combined antiplatelet or anticoagulant therapy: six-month angiographic follow-up of the Intracoronary Stenting and Antithrombotic Regimen (ISAR) Trial. *Circulation,* 96**,** 462-7.

KAWAI-KOWASE, K. & OWENS, G. K. 2007. Multiple repressor pathways contribute to phenotypic switching of vascular smooth muscle cells. *Am J Physiol Cell Physiol,* 292**,** C59-69.

KHAN, N. E., DE SOUZA, A., MISTER, R., FLATHER, M., CLAGUE, J., DAVIES, S., COLLINS, P., WANG, D., SIGWART, U. & PEPPER, J. 2004. A randomized comparison of off-pump and on-pump multivessel coronary-artery bypass surgery. *N Engl J Med,* 350**,** 21-8.

KIANG, A., HARTMAN, Z. C., EVERETT, R. S., SERRA, D., JIANG, H., FRANK, M. M. & AMALFITANO, A. 2006. Multiple innate inflammatory responses induced after systemic adenovirus vector delivery depend on a functional complement system. *Mol Ther,* 14**,** 588-98.

KIBBE, M. R., TZENG, E., GLEIXNER, S. L., WATKINS, S. C., KOVESDI, I., LIZONOVA, A., MAKAROUN, M. S., BILLIAR, T. R. & RHEE, R. Y. 2001. Adenovirus-mediated gene transfer of human inducible nitric oxide synthase in porcine vein grafts inhibits intimal hyperplasia. *J Vasc Surg,* 34**,** 156-65.

KIPSHIDZE, N., IVERSEN, P., OVERLIE, P., DUNLAP, T., TITUS, B., LEE, D., MOSES, J., O'HANLEY, P., LAUER, M. & LEON, M. B. 2007. First human experience with local delivery of novel antisense AVI-4126 with Infiltrator catheter in de novo native and restenotic coronary arteries: 6-month clinical and angiographic follow-up from AVAIL study. *Cardiovasc Revasc Med,* 8**,** 230-5.

KIRBY, I., DAVISON, E., BEAVIL, A. J., SOH, C. P., WICKHAM, T. J., ROELVINK, P. W., KOVESDI, I., SUTTON, B. J. & SANTIS, G. 2000. Identification of contact residues and definition of the CAR-binding site of adenovirus type 5 fiber protein. *J Virol,* 74**,** 2804-13.

KLOOSTERMAN, W. P. & PLASTERK, R. H. 2006. The diverse functions of microRNAs in animal development and disease. *Dev Cell,* 11**,** 441-50.

KLUGHERZ, B. D., JONES, P. L., CUI, X., CHEN, W., MENEVEAU, N. F., DEFELICE, S., CONNOLLY, J., WILENSKY, R. L. & LEVY, R. J. 2000. Gene delivery from a DNA controlled-release stent in porcine coronary arteries. *Nat Biotechnol,* 18**,** 1181-4.

KLUGHERZ, B. D., SONG, C., DEFELICE, S., CUI, X., LU, Z., CONNOLLY, J., HINSON, J. T., WILENSKY, R. L. & LEVY, R. J. 2002. Gene delivery to pig coronary arteries from stents carrying antibody-tethered adenovirus. *Hum Gene Ther,* 13**,** 443-54.

KOMATSU, R., UEDA, M., NARUKO, T., KOJIMA, A. & BECKER, A. E. 1998. Neointimal tissue response at sites of coronary stenting in humans: macroscopic, histological, and immunohistochemical analyses. *Circulation,* 98**,** 224-33.

KOREN, B., WEISZ, A., FISCHER, L., GLUZMAN, Z., PREIS, M., AVRAMOVITCH, N., COHEN, T., COSSET, F. L., LEWIS, B. S. & FLUGELMAN, M. Y. 2006. Efficient transduction and seeding of human endothelial cells onto metallic stents using bicistronic pseudo-typed retroviral vectors encoding vascular endothelial growth factor. *Cardiovasc Revasc Med,* 7**,** 173-8.

KRATLIAN, R. G. & HAJJAR, R. J. 2012. Cardiac gene therapy: from concept to reality. *Curr Heart Fail Rep,* 9**,** 33-9.

KRONMAL, R. A., MCCLELLAND, R. L., DETRANO, R., SHEA, S., LIMA, J. A., CUSHMAN, M., BILD, D. E. & BURKE, G. L. 2007. Risk factors for the progression of coronary artery calcification in asymptomatic subjects: results from the Multi-Ethnic Study of Atherosclerosis (MESA). *Circulation,* 115**,** 2722-30.

KUEHBACHER, A., URBICH, C., ZEIHER, A. M. & DIMMELER, S. 2007. Role of Dicer and Drosha for endothelial microRNA expression and angiogenesis. *Circ Res,* 101**,** 59-68.

KUHNERT, F., MANCUSO, M. R., HAMPTON, J., STANKUNAS, K., ASANO, T., CHEN, C. Z. & KUO, C. J. 2008. Attribution of vascular phenotypes of the murine Egfl7 locus to the microRNA miR-126. *Development,* 135**,** 3989-93.

KULLO, I. J., MOZES, G., SCHWARTZ, R. S., GLOVICZKI, P., CROTTY, T. B., BARBER, D. A., KATUSIC, Z. S. & O'BRIEN, T. 1997. Adventitial gene transfer

of recombinant endothelial nitric oxide synthase to rabbit carotid arteries alters vascular reactivity. *Circulation,* 96**,** 2254-61.

KUTRYK, M. J., FOLEY, D. P., VAN DEN BRAND, M., HAMBURGER, J. N., VAN DER GIESSEN, W. J., DEFEYTER, P. J., BRUINING, N., SABATE, M. & SERRUYS, P. W. 2002. Local intracoronary administration of antisense oligonucleotide against c-myc for the prevention of in-stent restenosis: results of the randomized investigation by the Thoraxcenter of antisense DNA using local delivery and IVUS after coronary stenting (ITALICS) trial. *J Am Coll Cardiol,* 39**,** 281-7.

KUWABARA, Y., ONO, K., HORIE, T., NISHI, H., NAGAO, K., KINOSHITA, M., WATANABE, S., BABA, O., KOJIMA, Y., SHIZUTA, S., IMAI, M., TAMURA, T., KITA, T. & KIMURA, T. 2011. Increased microRNA-1 and microRNA-133a levels in serum of patients with cardiovascular disease indicate myocardial damage. *Circ Cardiovasc Genet,* 4**,** 446-54.

LAGERQVIST, B., JAMES, S. K., STENESTRAND, U., LINDBACK, J., NILSSON, T. & WALLENTIN, L. 2007. Long-term outcomes with drug-eluting stents versus bare-metal stents in Sweden. *N Engl J Med,* 356**,** 1009-19.

LAITINEN, M., HARTIKAINEN, J., HILTUNEN, M. O., ERANEN, J., KIVINIEMI, M., NARVANEN, O., MAKINEN, K., MANNINEN, H., SYVANNE, M., MARTIN, J. F., LAAKSO, M. & YLA-HERTTUALA, S. 2000. Catheter-mediated vascular endothelial growth factor gene transfer to human coronary arteries after angioplasty. *Hum Gene Ther,* 11**,** 263-70.

LAITINEN, M., ZACHARY, I., BREIER, G., PAKKANEN, T., HAKKINEN, T., LUOMA, J., ABEDI, H., RISAU, W., SOMA, M., LAAKSO, M., MARTIN, J. F. & YLA-HERTTUALA, S. 1997. VEGF gene transfer reduces intimal thickening via increased production of nitric oxide in carotid arteries. *Hum Gene Ther,* 8**,** 1737-44.

LANDGRAF, P., RUSU, M., SHERIDAN, R., SEWER, A., IOVINO, N., ARAVIN, A., PFEFFER, S., RICE, A., KAMPHORST, A. O., LANDTHALER, M., LIN, C., SOCCI, N. D., HERMIDA, L., FULCI, V., CHIARETTI, S., FOA, R., SCHLIWKA, J., FUCHS, U., NOVOSEL, A., MULLER, R. U., SCHERMER, B., BISSELS, U., INMAN, J., PHAN, Q., CHIEN, M., WEIR, D. B., CHOKSI, R., DE

VITA, G., FREZZETTI, D., TROMPETER, H. I., HORNUNG, V., TENG, G., HARTMANN, G., PALKOVITS, M., DI LAURO, R., WERNET, P., MACINO, G., ROGLER, C. E., NAGLE, J. W., JU, J., PAPAVASILIOU, F. N., BENZING, T., LICHTER, P., TAM, W., BROWNSTEIN, M. J., BOSIO, A., BORKHARDT, A., RUSSO, J. J., SANDER, C., ZAVOLAN, M. & TUSCHL, T. 2007. A mammalian microRNA expression atlas based on small RNA library sequencing. *Cell,* 129**,** 1401-14.

LAROCHELLE, N., DEOL, J. R., SRIVASTAVA, V., ALLEN, C., MIZUGUCHI, H., KARPATI, G., HOLLAND, P. C. & NALBANTOGLU, J. 2008. Downregulation of CD46 during muscle differentiation: implications for gene transfer to human skeletal muscle using group B adenoviruses. *Hum Gene Ther,* 19**,** 133-42.

LATERZA, O. F., LIM, L., GARRETT-ENGELE, P. W., VLASAKOVA, K., MUNIAPPA, N., TANAKA, W. K., JOHNSON, J. M., SINA, J. F., FARE, T. L., SISTARE, F. D. & GLAAB, W. E. 2009. Plasma MicroRNAs as sensitive and specific biomarkers of tissue injury. *Clin Chem,* 55**,** 1977-83.

LATRONICO, M. V., CATALUCCI, D. & CONDORELLI, G. 2007. Emerging role of microRNAs in cardiovascular biology. *Circ Res,* 101**,** 1225-36.

LEBHERZ, C., GAO, G., LOUBOUTIN, J. P., MILLAR, J., RADER, D. & WILSON, J. M. 2004. Gene therapy with novel adeno-associated virus vectors substantially diminishes atherosclerosis in a murine model of familial hypercholesterolemia. *J Gene Med,* 6**,** 663-72.

LEE, R. C., FEINBAUM, R. L. & AMBROS, V. 1993. The C. elegans heterochronic gene lin-4 encodes small RNAs with antisense complementarity to lin-14. *Cell,* 75**,** 843-54.

LEE, Y., AHN, C., HAN, J., CHOI, H., KIM, J., YIM, J., LEE, J., PROVOST, P., RADMARK, O., KIM, S. & KIM, V. N. 2003. The nuclear RNase III Drosha initiates microRNA processing. *Nature,* 425**,** 415-9.

LEE, Y., JEON, K., LEE, J. T., KIM, S. & KIM, V. N. 2002. MicroRNA maturation: stepwise processing and subcellular localization. *Embo J,* 21**,** 4663-70.

LEE, Y., KIM, M., HAN, J., YEOM, K. H., LEE, S., BAEK, S. H. & KIM, V. N. 2004. MicroRNA genes are transcribed by RNA polymerase II. *Embo J,* 23**,** 4051-60.

LEVINE, G. N., BATES, E. R., BLANKENSHIP, J. C., BAILEY, S. R., BITTL, J. A., CERCEK, B., CHAMBERS, C. E., ELLIS, S. G., GUYTON, R. A., HOLLENBERG, S. M., KHOT, U. N., LANGE, R. A., MAURI, L., MEHRAN, R., MOUSSA, I. D., MUKHERJEE, D., NALLAMOTHU, B. K. & TING, H. H. 2011. ACCF/AHA/SCAI Guideline for Percutaneous Coronary Intervention. A report of the American College of Cardiology Foundation/American Heart Association Task Force on Practice Guidelines and the Society for Cardiovascular Angiography and Interventions. *J Am Coll Cardiol,* 58**,** e44-122.

LEWIS, B. P., BURGE, C. B. & BARTEL, D. P. 2005. Conserved seed pairing, often flanked by adenosines, indicates that thousands of human genes are microRNA targets. *Cell,* 120**,** 15-20.

LIANG, C. C., PARK, A. Y. & GUAN, J. L. 2007. In vitro scratch assay: a convenient and inexpensive method for analysis of cell migration in vitro. *Nat Protoc,* 2**,** 329-33.

LIBBY, P. 2013. Mechanisms of acute coronary syndromes and their implications for therapy. *N Engl J Med,* 368**,** 2004-13.

LIBBY, P. & BRAUNWALD, E. 2008. *Braunwald's heart disease : a textbook of cardiovascular medicine,* Philadelphia, Saunders/Elsevier.

LIBBY, P., RIDKER, P. M. & HANSSON, G. K. 2011. Progress and challenges in translating the biology of atherosclerosis. *Nature,* 473**,** 317-25.

LIEBER, A., HE, C. Y., MEUSE, L., SCHOWALTER, D., KIRILLOVA, I., WINTHER, B. & KAY, M. A. 1997. The role of Kupffer cell activation and viral gene expression in early liver toxicity after infusion of recombinant adenovirus vectors. *J Virol,* 71**,** 8798-807.

LINCOFF, A. M., TOPOL, E. J. & ELLIS, S. G. 1994. Local drug delivery for the prevention of restenosis. Fact, fancy, and future. *Circulation,* 90**,** 2070-84.

LIU, N., DING, H., VANDERHEYDEN, J. L., ZHU, Z. & ZHANG, Y. 2007. Radiolabeling small RNA with technetium-99m for visualizing cellular delivery and mouse biodistribution. *Nucl Med Biol,* 34**,** 399-404.

LIU, N. & OLSON, E. N. 2010. MicroRNA regulatory networks in cardiovascular development. *Dev Cell,* 18**,** 510-25.

LIU, Q. & MURUVE, D. A. 2003. Molecular basis of the inflammatory response to adenovirus vectors. *Gene Ther,* 10**,** 935-40.

LONG, X. & MIANO, J. M. 2011. Transforming growth factor-beta1 (TGF-beta1) utilizes distinct pathways for the transcriptional activation of microRNA 143/145 in human coronary artery smooth muscle cells. *J Biol Chem,* 286**,** 30119-29.

LOPES, R. D., MEHTA, R. H., HAFLEY, G. E., WILLIAMS, J. B., MACK, M. J., PETERSON, E. D., ALLEN, K. B., HARRINGTON, R. A., GIBSON, C. M., CALIFF, R. M., KOUCHOUKOS, N. T., FERGUSON, T. B., JR. & ALEXANDER, J. H. 2012. Relationship Between Vein Graft Failure and Subsequent Clinical Outcomes After Coronary Artery Bypass Surgery. *Circulation,* 125**,** 749-756.

LOWE, H. C., CHESTERMAN, C. N. & KHACHIGIAN, L. M. 2002. Catalytic antisense DNA molecules targeting Egr-1 inhibit neointima formation following permanent ligation of rat common carotid arteries. *Thromb Haemost,* 87**,** 134-40.

LUO, Z., SATA, M., NGUYEN, T., KAPLAN, J. M., AKITA, G. Y. & WALSH, K. 1999. Adenovirus-mediated delivery of fas ligand inhibits intimal hyperplasia after balloon injury in immunologically primed animals. *Circulation,* 99**,** 1776-9.

LYONS, M., ONION, D., GREEN, N. K., ASLAN, K., RAJARATNAM, R., BAZAN-PEREGRINO, M., PHIPPS, S., HALE, S., MAUTNER, V., SEYMOUR, L. W. & FISHER, K. D. 2006. Adenovirus type 5 interactions with human blood cells may compromise systemic delivery. *Mol Ther,* 14**,** 118-28.

MAILLARD, L., VAN BELLE, E., SMITH, R. C., LE ROUX, A., DENEFLE, P., STEG, G., BARRY, J. J., BRANELLEC, D., ISNER, J. M. & WALSH, K. 1997. Percutaneous delivery of the gax gene inhibits vessel stenosis in a rabbit model of balloon angioplasty. *Cardiovasc Res,* 35**,** 536-46.

MAILLARD, L., VAN BELLE, E., TIO, F. O., RIVARD, A., KEARNEY, M., BRANELLEC, D., STEG, P. G., ISNER, J. M. & WALSH, K. 2000. Effect of percutaneous adenovirus-mediated Gax gene delivery to the arterial wall in double-injured atheromatous stented rabbit iliac arteries. *Gene Ther,* 7**,** 1353-61.

MALIK, N., GUNN, J., HOLT, C. M., SHEPHERD, L., FRANCIS, S. E., NEWMAN, C. M., CROSSMAN, D. C. & CUMBERLAND, D. C. 1998. Intravascular stents: a

new technique for tissue processing for histology, immunohistochemistry, and transmission electron microscopy. *Heart,* 80**,** 509-16.

MALLAWAARACHCHI, C. M., WEISSBERG, P. L. & SIOW, R. C. 2006. Antagonism of platelet-derived growth factor by perivascular gene transfer attenuates adventitial cell migration after vascular injury: new tricks for old dogs? *Faseb J,* 20**,** 1686-8.

MANO, T., LUO, Z., MALENDOWICZ, S. L., EVANS, T. & WALSH, K. 1999. Reversal of GATA-6 downregulation promotes smooth muscle differentiation and inhibits intimal hyperplasia in balloon-injured rat carotid artery. *Circ Res,* 84**,** 647-54.

MARCH, K. L., MADISON, J. E. & TRAPNELL, B. C. 1995. Pharmacokinetics of adenoviral vector-mediated gene delivery to vascular smooth muscle cells: modulation by poloxamer 407 and implications for cardiovascular gene therapy. *Hum Gene Ther,* 6**,** 41-53.

MATSUMOTO, T. & HWANG, P. M. 2007. Resizing the genomic regulation of restenosis. *Circ Res,* 100**,** 1537-9.

MAURI, L., HSIEH, W. H., MASSARO, J. M., HO, K. K., D'AGOSTINO, R. & CUTLIP, D. E. 2007. Stent thrombosis in randomized clinical trials of drug-eluting stents. *N Engl J Med,* 356**,** 1020-9.

MAXWELL, M. P., HEARSE, D. J. & YELLON, D. M. 1987. Species variation in the coronary collateral circulation during regional myocardial ischaemia: a critical determinant of the rate of evolution and extent of myocardial infarction. *Cardiovasc Res,* 21**,** 737-46.

MCDONALD, J. S., MILOSEVIC, D., REDDI, H. V., GREBE, S. K. & ALGECIRAS-SCHIMNICH, A. 2011a. Analysis of circulating microRNA: preanalytical and analytical challenges. *Clin Chem,* 57**,** 833-40.

MCDONALD, R. A., HATA, A., MACLEAN, M. R., MORRELL, N. W. & BAKER, A. H. 2011b. MicroRNA and vascular remodelling in acute vascular injury and pulmonary vascular remodelling. *Cardiovasc Res,* 93**,** 594-604.

MCDONALD, R. A., WHITE, K. M., WU, J., COOLEY, B. C., ROBERTSON, K. E., HALLIDAY, C. A., MCCLURE, J. D., FRANCIS, S., LU, R., KENNEDY, S., GEORGE, S. J., WAN, S., VAN ROOIJ, E. & BAKER, A. H. 2013. miRNA-21 is

dysregulated in response to vein grafting in multiple models and genetic ablation in mice attenuates neointima formation. *Eur Heart J*.

MEHILLI, J., KASTRATI, A., WESSELY, R., DIBRA, A., HAUSLEITER, J., JASCHKE, B., DIRSCHINGER, J. & SCHOMIG, A. 2006. Randomized trial of a nonpolymer-based rapamycin-eluting stent versus a polymer-based paclitaxel-eluting stent for the reduction of late lumen loss. *Circulation,* 113**,** 273-9.

MEHILLI, J., PACHE, J., ABDEL-WAHAB, M., SCHULZ, S., BYRNE, R. A., TIROCH, K., HAUSLEITER, J., SEYFARTH, M., OTT, I., IBRAHIM, T., FUSARO, M., LAUGWITZ, K. L., MASSBERG, S., NEUMANN, F. J., RICHARDT, G., SCHOMIG, A. & KASTRATI, A. 2011. Drug-eluting versus bare-metal stents in saphenous vein graft lesions (ISAR-CABG): a randomised controlled superiority trial. *Lancet,* 378**,** 1071-8.

MIANO, J. M., LONG, X. & FUJIWARA, K. 2007. Serum response factor: master regulator of the actin cytoskeleton and contractile apparatus. *Am J Physiol Cell Physiol,* 292**,** C70-81.

MILLETTE, E., RAUCH, B. H., DEFAWE, O., KENAGY, R. D., DAUM, G. & CLOWES, A. W. 2005. Platelet-derived growth factor-BB-induced human smooth muscle cell proliferation depends on basic FGF release and FGFR-1 activation. *Circ Res,* 96**,** 172-9.

MITCHELL, P. S., PARKIN, R. K., KROH, E. M., FRITZ, B. R., WYMAN, S. K., POGOSOVA-AGADJANYAN, E. L., PETERSON, A., NOTEBOOM, J., O'BRIANT, K. C., ALLEN, A., LIN, D. W., URBAN, N., DRESCHER, C. W., KNUDSEN, B. S., STIREWALT, D. L., GENTLEMAN, R., VESSELLA, R. L., NELSON, P. S., MARTIN, D. B. & TEWARI, M. 2008. Circulating microRNAs as stable blood-based markers for cancer detection. *Proc Natl Acad Sci U S A,* 105**,** 10513-8.

MITRA, A. K. & AGRAWAL, D. K. 2006. In stent restenosis: bane of the stent era. *J Clin Pathol,* 59**,** 232-9.

MOENS, A. L., CLAEYS, M. J., TIMMERMANS, J. P. & VRINTS, C. J. 2005. Myocardial ischemia/reperfusion-injury, a clinical view on a complex pathophysiological process. *Int J Cardiol,* 100**,** 179-90.

MOHR, F. W., MORICE, M. C., KAPPETEIN, A. P., FELDMAN, T. E., STAHLE, E., COLOMBO, A., MACK, M. J., HOLMES, D. R., JR., MOREL, M. A., VAN DYCK, N., HOULE, V. M., DAWKINS, K. D. & SERRUYS, P. W. 2013. Coronary artery bypass graft surgery versus percutaneous coronary intervention in patients with three-vessel disease and left main coronary disease: 5-year follow-up of the randomised, clinical SYNTAX trial. *Lancet,* 381**,** 629-38.

MOLITERNO, D. J. 2005. Healing Achilles--sirolimus versus paclitaxel. *N Engl J Med,* 353**,** 724-7.

MONAHAN, P. E. & SAMULSKI, R. J. 2000. Adeno-associated virus vectors for gene therapy: more pros than cons? *Mol Med Today,* 6**,** 433-40.

MORICE, M. C., SERRUYS, P. W., SOUSA, J. E., FAJADET, J., BAN HAYASHI, E., PERIN, M., COLOMBO, A., SCHULER, G., BARRAGAN, P., GUAGLIUMI, G., MOLNAR, F. & FALOTICO, R. 2002. A randomized comparison of a sirolimus-eluting stent with a standard stent for coronary revascularization. *N Engl J Med,* 346**,** 1773-80.

MORISHITA, R., GIBBONS, G. H., ELLISON, K. E., NAKAJIMA, M., VON DER LEYEN, H., ZHANG, L., KANEDA, Y., OGIHARA, T. & DZAU, V. J. 1994. Intimal hyperplasia after vascular injury is inhibited by antisense cdk 2 kinase oligonucleotides. *J Clin Invest,* 93**,** 1458-64.

MORISHITA, R., GIBBONS, G. H., ELLISON, K. E., NAKAJIMA, M., ZHANG, L., KANEDA, Y., OGIHARA, T. & DZAU, V. J. 1993. Single intraluminal delivery of antisense cdc2 kinase and proliferating-cell nuclear antigen oligonucleotides results in chronic inhibition of neointimal hyperplasia. *Proc Natl Acad Sci U S A,* 90**,** 8474-8.

MORISHITA, R., GIBBONS, G. H., HORIUCHI, M., ELLISON, K. E., NAKAMA, M., ZHANG, L., KANEDA, Y., OGIHARA, T. & DZAU, V. J. 1995. A gene therapy strategy using a transcription factor decoy of the E2F binding site inhibits smooth muscle proliferation in vivo. *Proc Natl Acad Sci U S A,* 92**,** 5855-9.

MOSES, J. W., LEON, M. B., POPMA, J. J., FITZGERALD, P. J., HOLMES, D. R., O'SHAUGHNESSY, C., CAPUTO, R. P., KEREIAKES, D. J., WILLIAMS, D. O., TEIRSTEIN, P. S., JAEGER, J. L. & KUNTZ, R. E. 2003. Sirolimus-eluting stents

versus standard stents in patients with stenosis in a native coronary artery. *N Engl J Med,* 349**,** 1315-23.

MOSHKOVITZ, Y., MOHR, R., MEDALION, B., HYAM, E., HERZ, I., DEITCH, I., URETZKY, G. & PEVNI, D. 2012. Drug-eluting stents compared with bilateral internal thoracic artery grafts for diabetic patients. *Ann Thorac Surg,* 94**,** 1455-62.

MOTWANI, J. G. & TOPOL, E. J. 1998. Aortocoronary saphenous vein graft disease: pathogenesis, predisposition, and prevention. *Circulation,* 97**,** 916-31.

NABEL, E. G., PLAUTZ, G., BOYCE, F. M., STANLEY, J. C. & NABEL, G. J. 1989. Recombinant gene expression in vivo within endothelial cells of the arterial wall. *Science,* 244**,** 1342-4.

NAIR, S., IQBAL, K., PHADKE, M., JADHAV, U. E., KHANDEKAR, J. & KHANDEPARKAR, J. M. 2012. Effect of cardiopulmonary bypass on tissue injury markers and endothelial activation during coronary artery bypass graft surgery. *J Postgrad Med,* 58**,** 8-13.

NAKAZAWA, G., FINN, A. V., JOHN, M. C., KOLODGIE, F. D. & VIRMANI, R. 2007. The significance of preclinical evaluation of sirolimus-, paclitaxel-, and zotarolimus-eluting stents. *Am J Cardiol,* 100**,** 36M-44M.

NAKAZAWA, G., OTSUKA, F., NAKANO, M., VORPAHL, M., YAZDANI, S. K., LADICH, E., KOLODGIE, F. D., FINN, A. V. & VIRMANI, R. 2011. The pathology of neoatherosclerosis in human coronary implants bare-metal and drug-eluting stents. *J Am Coll Cardiol,* 57**,** 1314-22.

NAYAK, S. & HERZOG, R. W. 2010. Progress and prospects: immune responses to viral vectors. *Gene Ther,* 17**,** 295-304.

NAZARI-JAHANTIGH, M., WEI, Y., NOELS, H., AKHTAR, S., ZHOU, Z., KOENEN, R. R., HEYLL, K., GREMSE, F., KIESSLING, F., GROMMES, J., WEBER, C. & SCHOBER, A. 2012. MicroRNA-155 promotes atherosclerosis by repressing Bcl6 in macrophages. *J Clin Invest,* 122**,** 4190-202.

NEAL, C. S., MICHAEL, M. Z., PIMLOTT, L. K., YONG, T. Y., LI, J. Y. & GLEADLE, J. M. 2011. Circulating microRNA expression is reduced in chronic kidney disease. *Nephrol Dial Transplant,* 26**,** 3794-802.

NETH, P., NAZARI-JAHANTIGH, M., SCHOBER, A. & WEBER, C. 2013. MicroRNAs in flow-dependent vascular remodelling. *Cardiovasc Res,* 99**,** 294-303.

NEWBY, A. C. 1997. Molecular and cell biology of native coronary and vein-graft atherosclerosis: regulation of plaque stability and vessel-wall remodelling by growth factors and cell-extracellular matrix interactions. *Coron Artery Dis,* 8**,** 213-24.

NEWBY, A. C. & GEORGE, S. J. 1993. Proposed roles for growth factors in mediating smooth muscle proliferation in vascular pathologies. *Cardiovasc Res,* 27**,** 1173-83.

NICHOLLS, S. J., HSU, A., WOLSKI, K., HU, B., BAYTURAN, O., LAVOIE, A., UNO, K., TUZCU, E. M. & NISSEN, S. E. 2010. Intravascular ultrasound-derived measures of coronary atherosclerotic plaque burden and clinical outcome. *J Am Coll Cardiol,* 55**,** 2399-407.

NICKLIN, S. A., BUENING, H., DISHART, K. L., DE ALWIS, M., GIROD, A., HACKER, U., THRASHER, A. J., ALI, R. R., HALLEK, M. & BAKER, A. H. 2001a. Efficient and selective AAV2-mediated gene transfer directed to human vascular endothelial cells. *Mol Ther,* 4**,** 174-81.

NICKLIN, S. A., VON SEGGERN, D. J., WORK, L. M., PEK, D. C., DOMINICZAK, A. F., NEMEROW, G. R. & BAKER, A. H. 2001b. Ablating adenovirus type 5 fiber-CAR binding and HI loop insertion of the SIGYPLP peptide generate an endothelial cell-selective adenovirus. *Mol Ther,* 4**,** 534-42.

NICKLIN, S. A., WHITE, S. J., WATKINS, S. J., HAWKINS, R. E. & BAKER, A. H. 2000. Selective targeting of gene transfer to vascular endothelial cells by use of peptides isolated by phage display. *Circulation,* 102**,** 231-7.

NICOL, C. G., DENBY, L., LOPEZ-FRANCO, O., MASSON, R., HALLIDAY, C. A., NICKLIN, S. A., KRITZ, A., WORK, L. M. & BAKER, A. H. 2009. Use of in vivo phage display to engineer novel adenoviruses for targeted delivery to the cardiac vasculature. *FEBS Lett,* 583**,** 2100-7.

NICOL, C. G., GRAHAM, D., MILLER, W. H., WHITE, S. J., SMITH, T. A., NICKLIN, S. A., STEVENSON, S. C. & BAKER, A. H. 2004. Effect of adenovirus serotype 5 fiber and penton modifications on in vivo tropism in rats. *Mol Ther,* 10**,** 344-54.

NICOLI, S., STANDLEY, C., WALKER, P., HURLSTONE, A., FOGARTY, K. E. & LAWSON, N. D. 2010. MicroRNA-mediated integration of haemodynamics and Vegf signalling during angiogenesis. *Nature,* 464**,** 1196-200.

NOKISALMI, P., PESONEN, S., ESCUTENAIRE, S., SARKIOJA, M., RAKI, M., CERULLO, V., LAASONEN, L., ALEMANY, R., ROJAS, J., CASCALLO, M., GUSE, K., RAJECKI, M., KANGASNIEMI, L., HAAVISTO, E., KARIOJA-KALLIO, A., HANNUKSELA, P., OKSANEN, M., KANERVA, A., JOENSUU, T., AHTIAINEN, L. & HEMMINKI, A. 2010. Oncolytic adenovirus ICOVIR-7 in patients with advanced and refractory solid tumors. *Clin Cancer Res,* 16**,** 3035-43.

NORDMANN, A. J., BRIEL, M. & BUCHER, H. C. 2006. Mortality in randomized controlled trials comparing drug-eluting vs. bare metal stents in coronary artery disease: a meta-analysis. *Eur Heart J,* 27**,** 2784-814.

O'CONNELL, R. M., TAGANOV, K. D., BOLDIN, M. P., CHENG, G. & BALTIMORE, D. 2007. MicroRNA-155 is induced during the macrophage inflammatory response. *Proc Natl Acad Sci U S A,* 104**,** 1604-9.

O'SULLIVAN, J. F., MARTIN, K. & CAPLICE, N. M. 2011. Microribonucleic acids for prevention of plaque rupture and in-stent restenosis: "a finger in the dam". *J Am Coll Cardiol,* 57**,** 383-9.

OHNO, T., GORDON, D., SAN, H., POMPILI, V. J., IMPERIALE, M. J., NABEL, G. J. & NABEL, E. G. 1994. Gene therapy for vascular smooth muscle cell proliferation after arterial injury. *Science,* 265**,** 781-4.

OKA, K., PASTORE, L., KIM, I. H., MERCHED, A., NOMURA, S., LEE, H. J., MERCHED-SAUVAGE, M., ARDEN-RILEY, C., LEE, B., FINEGOLD, M., BEAUDET, A. & CHAN, L. 2001. Long-term stable correction of low-density lipoprotein receptor-deficient mice with a helper-dependent adenoviral vector expressing the very low-density lipoprotein receptor. *Circulation,* 103**,** 1274-81.

ONG, A. T., SERRUYS, P. W., MOHR, F. W., MORICE, M. C., KAPPETEIN, A. P., HOLMES, D. R., JR., MACK, M. J., VAN DEN BRAND, M., MOREL, M. A., VAN ES, G. A., KLEIJNE, J., KOGLIN, J. & RUSSELL, M. E. 2006. The SYNergy between percutaneous coronary intervention with TAXus and cardiac surgery (SYNTAX) study: design, rationale, and run-in phase. *Am Heart J,* 151**,** 1194-204.

OTAKI, Y., GRANSAR, H., BERMAN, D. S., CHENG, V. Y., DEY, D., LIN, F. Y., ACHENBACH, S., AL-MALLAH, M., BUDOFF, M. J., CADEMARTIRI, F., CALLISTER, T. Q., CHANG, H. J., CHINNAIYAN, K., CHOW, B. J., DELAGO, A., HADAMITZKY, M., HAUSLEITER, J., KAUFMANN, P., MAFFEI, E., RAFF, G., SHAW, L. J., VILLINES, T. C., DUNNING, A. & MIN, J. K. 2013. Impact of family history of coronary artery disease in young individuals (from the CONFIRM registry). *Am J Cardiol,* 111**,** 1081-6.

PACAK, C. A., MAH, C. S., THATTALIYATH, B. D., CONLON, T. J., LEWIS, M. A., CLOUTIER, D. E., ZOLOTUKHIN, I., TARANTAL, A. F. & BYRNE, B. J. 2006. Recombinant adeno-associated virus serotype 9 leads to preferential cardiac transduction in vivo. *Circ Res,* 99**,** e3-9.

PALMERINI, T., BIONDI-ZOCCAI, G., DELLA RIVA, D., MARIANI, A., GENEREUX, P., BRANZI, A. & STONE, G. W. 2013. Stent Thrombosis with Drug-Eluting Stents: Is the Paradigm Shifting? *Journal of the American College of Cardiology***,** doi: 10.1016/j.jacc.2013.08.725.

PALOMEQUE, J., CHEMALY, E. R., COLOSI, P., WELLMAN, J. A., ZHOU, S., DEL MONTE, F. & HAJJAR, R. J. 2007. Efficiency of eight different AAV serotypes in transducing rat myocardium in vivo. *Gene Ther,* 14**,** 989-97.

PAN, Y., BALAZS, L., TIGYI, G. & YUE, J. 2011. Conditional deletion of Dicer in vascular smooth muscle cells leads to the developmental delay and embryonic mortality. *Biochem Biophys Res Commun,* 408**,** 369-74.

PANETTA, C. J., MIYAUCHI, K., BERRY, D., SIMARI, R. D., HOLMES, D. R., SCHWARTZ, R. S. & CAPLICE, N. M. 2002. A tissue-engineered stent for cell-based vascular gene transfer. *Hum Gene Ther,* 13**,** 433-41.

PARANG, P. & ARORA, R. 2009. Coronary vein graft disease: pathogenesis and prevention. *Can J Cardiol,* 25**,** e57-62.

PARIKH, V. N., JIN, R. C., RABELLO, S., GULBAHCE, N., WHITE, K., HALE, A., COTTRILL, K. A., SHAIK, R. S., WAXMAN, A. B., ZHANG, Y. Y., MARON, B. A., HARTNER, J. C., FUJIWARA, Y., ORKIN, S. H., HALEY, K. J., BARABASI, A. L., LOSCALZO, J. & CHAN, S. Y. 2012. MicroRNA-21 integrates pathogenic signaling to control pulmonary hypertension: results of a network bioinformatics approach. *Circulation,* 125**,** 1520-32.

PARK, D. W., SEUNG, K. B., KIM, Y. H., LEE, J. Y., KIM, W. J., KANG, S. J., LEE, S. W., LEE, C. W., PARK, S. W., YUN, S. C., GWON, H. C., JEONG, M. H., JANG, Y. S., KIM, H. S., KIM, P. J., SEONG, I. W., PARK, H. S., AHN, T., CHAE, I. H., TAHK, S. J., CHUNG, W. S. & PARK, S. J. 2010. Long-term safety and efficacy of stenting versus coronary artery bypass grafting for unprotected left main coronary artery disease: 5-year results from the MAIN-COMPARE (Revascularization for Unprotected Left Main Coronary Artery Stenosis: Comparison of Percutaneous Coronary Angioplasty Versus Surgical Revascularization) registry. *J Am Coll Cardiol,* 56**,** 117-24.

PARK, S. J., KANG, S. J., VIRMANI, R., NAKANO, M. & UEDA, Y. 2012. In-stent neoatherosclerosis: a final common pathway of late stent failure. *J Am Coll Cardiol,* 59**,** 2051-7.

PARK, S. J., KIM, Y. H., PARK, D. W., YUN, S. C., AHN, J. M., SONG, H. G., LEE, J. Y., KIM, W. J., KANG, S. J., LEE, S. W., LEE, C. W., PARK, S. W., CHUNG, C. H., LEE, J. W., LIM, D. S., RHA, S. W., LEE, S. G., GWON, H. C., KIM, H. S., CHAE, I. H., JANG, Y., JEONG, M. H., TAHK, S. J. & SEUNG, K. B. 2011. Randomized trial of stents versus bypass surgery for left main coronary artery disease. *N Engl J Med,* 364**,** 1718-27.

PARKER, A. L., WADDINGTON, S. N., NICOL, C. G., SHAYAKHMETOV, D. M., BUCKLEY, S. M., DENBY, L., KEMBALL-COOK, G., NI, S., LIEBER, A., MCVEY, J. H., NICKLIN, S. A. & BAKER, A. H. 2006. Multiple vitamin K-dependent coagulation zymogens promote adenovirus-mediated gene delivery to hepatocytes. *Blood,* 108**,** 2554-61.

PAZ, M. A., LUPON, J., BOSCH, X., POMAR, J. L. & SANZ, G. 1993. Predictors of early saphenous vein aortocoronary bypass graft occlusion. The GESIC Study Group. *Ann Thorac Surg,* 56**,** 1101-6.

PEKKANEN, J., LINN, S., HEISS, G., SUCHINDRAN, C. M., LEON, A., RIFKIND, B. M. & TYROLER, H. A. 1990. Ten-year mortality from cardiovascular disease in relation to cholesterol level among men with and without preexisting cardiovascular disease. *N Engl J Med,* 322**,** 1700-7.

PERK, J., DE BACKER, G., GOHLKE, H., GRAHAM, I., REINER, Z., VERSCHUREN, M., ALBUS, C., BENLIAN, P., BOYSEN, G., CIFKOVA, R., DEATON, C.,

EBRAHIM, S., FISHER, M., GERMANO, G., HOBBS, R., HOES, A., KARADENIZ, S., MEZZANI, A., PRESCOTT, E., RYDEN, L., SCHERER, M., SYVANNE, M., SCHOLTE OP REIMER, W. J., VRINTS, C., WOOD, D., ZAMORANO, J. L. & ZANNAD, F. 2012. European Guidelines on cardiovascular disease prevention in clinical practice (version 2012). The Fifth Joint Task Force of the European Society of Cardiology and Other Societies on Cardiovascular Disease Prevention in Clinical Practice (constituted by representatives of nine societies and by invited experts). *Eur Heart J,* 33**,** 1635-701.

PERRY, M. M., MOSCHOS, S. A., WILLIAMS, A. E., SHEPHERD, N. J., LARNER-SVENSSON, H. M. & LINDSAY, M. A. 2008. Rapid changes in microRNA-146a expression negatively regulate the IL-1beta-induced inflammatory response in human lung alveolar epithelial cells. *J Immunol,* 180**,** 5689-98.

PESONEN, S., NOKISALMI, P., ESCUTENAIRE, S., SARKIOJA, M., RAKI, M., CERULLO, V., KANGASNIEMI, L., LAASONEN, L., RIBACKA, C., GUSE, K., HAAVISTO, E., OKSANEN, M., RAJECKI, M., HELMINEN, A., RISTIMAKI, A., KARIOJA-KALLIO, A., KARLI, E., KANTOLA, T., BAUERSCHMITZ, G., KANERVA, A., JOENSUU, T. & HEMMINKI, A. 2010. Prolonged systemic circulation of chimeric oncolytic adenovirus Ad5/3-Cox2L-D24 in patients with metastatic and refractory solid tumors. *Gene Ther,* 17**,** 892-904.

PFISTERER, M., BRUNNER-LA ROCCA, H. P., BUSER, P. T., RICKENBACHER, P., HUNZIKER, P., MUELLER, C., JEGER, R., BADER, F., OSSWALD, S. & KAISER, C. 2006. Late clinical events after clopidogrel discontinuation may limit the benefit of drug-eluting stents: an observational study of drug-eluting versus bare-metal stents. *J Am Coll Cardiol,* 48**,** 2584-91.

PHILIPPE, S., SARKIS, C., BARKATS, M., MAMMERI, H., LADROUE, C., PETIT, C., MALLET, J. & SERGUERA, C. 2006. Lentiviral vectors with a defective integrase allow efficient and sustained transgene expression in vitro and in vivo. *Proc Natl Acad Sci U S A,* 103**,** 17684-9.

PINTO SLOTTOW, T. L., STEINBERG, D. H., ROY, P. K., BUCH, A. N., OKABE, T., XUE, Z., KANESHIGE, K., TORGUSON, R., LINDSAY, J., PICHARD, A. D., SATLER, L. F., SUDDATH, W. O., KENT, K. M. & WAKSMAN, R. 2008. Observations and outcomes of definite and probable drug-eluting stent thrombosis seen at a single hospital in a four-year period. *Am J Cardiol,* 102**,** 298-303.

POLIMENI, A., DE ROSA, S. & INDOLFI, C. 2013. Vascular miRNAs after balloon angioplasty. *Trends Cardiovasc Med,* 23**,** 9-14.

POLLMAN, M. J., HALL, J. L., MANN, M. J., ZHANG, L. & GIBBONS, G. H. 1998. Inhibition of neointimal cell bcl-x expression induces apoptosis and regression of vascular disease. *Nat Med,* 4**,** 222-7.

POON, M., MARX, S. O., GALLO, R., BADIMON, J. J., TAUBMAN, M. B. & MARKS, A. R. 1996. Rapamycin inhibits vascular smooth muscle cell migration. *J Clin Invest,* 98**,** 2277-83.

QI, J., RICE, S. J., SALZBERG, A. C., RUNKLE, E. A., LIAO, J., ZANDER, D. S. & MU, D. 2012. MiR-365 regulates lung cancer and developmental gene thyroid transcription factor 1. *Cell Cycle,* 11**,** 177-86.

QIAN, Z., HAESSLER, M., LEMOS, J. A., ARSENAULT, J. R., AGUIRRE, J. E., GILBERT, J. R., BOWLER, R. P. & PARK, F. 2006. Targeting vascular injury using Hantavirus-pseudotyped lentiviral vectors. *Mol Ther,* 13**,** 694-704.

QUINTAVALLE, M., ELIA, L., CONDORELLI, G. & COURTNEIDGE, S. A. 2010. MicroRNA control of podosome formation in vascular smooth muscle cells in vivo and in vitro. *J Cell Biol,* 189**,** 13-22.

RABER, L., WOHLWEND, L., WIGGER, M., TOGNI, M., WANDEL, S., WENAWESER, P., COOK, S., MOSCHOVITIS, A., VOGEL, R., KALESAN, B., SEILER, C., EBERLI, F., LUSCHER, T. F., MEIER, B., JUNI, P. & WINDECKER, S. 2011. Five-year clinical and angiographic outcomes of a randomized comparison of sirolimus-eluting and paclitaxel-eluting stents: results of the Sirolimus-Eluting Versus Paclitaxel-Eluting Stents for Coronary Revascularization LATE trial. *Circulation,* 123**,** 2819-28, 6 p following 2828.

RAINES, E. W. 2004. PDGF and cardiovascular disease. *Cytokine Growth Factor Rev,* 15**,** 237-54.

RAITOHARJU, E., LYYTIKAINEN, L. P., LEVULA, M., OKSALA, N., MENNANDER, A., TARKKA, M., KLOPP, N., ILLIG, T., KAHONEN, M., KARHUNEN, P. J., LAAKSONEN, R. & LEHTIMAKI, T. 2011. miR-21, miR-210, miR-34a, and miR-146a/b are up-regulated in human atherosclerotic plaques in the Tampere Vascular Study. *Atherosclerosis,* 219**,** 211-7.

RANGREZ, A. Y., MASSY, Z. A., METZINGER-LE MEUTH, V. & METZINGER, L. 2011. miR-143 and miR-145: molecular keys to switch the phenotype of vascular smooth muscle cells. *Circ Cardiovasc Genet,* 4**,** 197-205.

RAPER, S. E., CHIRMULE, N., LEE, F. S., WIVEL, N. A., BAGG, A., GAO, G. P., WILSON, J. M. & BATSHAW, M. L. 2003. Fatal systemic inflammatory response syndrome in a ornithine transcarbamylase deficient patient following adenoviral gene transfer. *Mol Genet Metab,* 80**,** 148-58.

REYNOLDS, P. N., ZINN, K. R., GAVRILYUK, V. D., BALYASNIKOVA, I. V., ROGERS, B. E., BUCHSBAUM, D. J., WANG, M. H., MILETICH, D. J., GRIZZLE, W. E., DOUGLAS, J. T., DANILOV, S. M. & CURIEL, D. T. 2000. A targetable, injectable adenoviral vector for selective gene delivery to pulmonary endothelium in vivo. *Mol Ther,* 2**,** 562-78.

RIPPSTEIN, P., BLACK, M. K., BOIVIN, M., VEINOT, J. P., MA, X., CHEN, Y. X., HUMAN, P., ZILLA, P. & O'BRIEN, E. R. 2006. Comparison of processing and sectioning methodologies for arteries containing metallic stents. *J Histochem Cytochem,* 54**,** 673-81.

RISSANEN, T. T., MARKKANEN, J. E., GRUCHALA, M., HEIKURA, T., PURANEN, A., KETTUNEN, M. I., KHOLOVA, I., KAUPPINEN, R. A., ACHEN, M. G., STACKER, S. A., ALITALO, K. & YLA-HERTTUALA, S. 2003. VEGF-D is the strongest angiogenic and lymphangiogenic effector among VEGFs delivered into skeletal muscle via adenoviruses. *Circ Res,* 92**,** 1098-106.

ROBINSON, H. C. & BAKER, A. H. 2012. How do microRNAs affect vascular smooth muscle cell biology? *Curr Opin Lipidol,* 23**,** 405-11.

RODRIGUEZ, A. E., GRINFELD, L., FERNANDEZ-PEREIRA, C., MIERES, J., RODRIGUEZ ALEMPARTE, M., BERROCAL, D., RODRIGUEZ-GRANILLO, A. M., VIGO, C. F., RUSSO FELSEN, M., O'NEILL, W. & PALACIOS, I. 2006. Revascularization strategies of coronary multiple vessel disease in the Drug Eluting Stent Era: one year follow-up results of the ERACI III Trial. *EuroIntervention,* 2**,** 53-60.

ROELVINK, P. W., LIZONOVA, A., LEE, J. G., LI, Y., BERGELSON, J. M., FINBERG, R. W., BROUGH, D. E., KOVESDI, I. & WICKHAM, T. J. 1998. The coxsackievirus-adenovirus receptor protein can function as a cellular attachment

protein for adenovirus serotypes from subgroups A, C, D, E, and F. *J Virol,* 72**,** 7909-15.

ROGER, V. L., GO, A. S., LLOYD-JONES, D. M., BENJAMIN, E. J., BERRY, J. D., BORDEN, W. B., BRAVATA, D. M., DAI, S., FORD, E. S., FOX, C. S., FULLERTON, H. J., GILLESPIE, C., HAILPERN, S. M., HEIT, J. A., HOWARD, V. J., KISSELA, B. M., KITTNER, S. J., LACKLAND, D. T., LICHTMAN, J. H., LISABETH, L. D., MAKUC, D. M., MARCUS, G. M., MARELLI, A., MATCHAR, D. B., MOY, C. S., MOZAFFARIAN, D., MUSSOLINO, M. E., NICHOL, G., PAYNTER, N. P., SOLIMAN, E. Z., SORLIE, P. D., SOTOODEHNIA, N., TURAN, T. N., VIRANI, S. S., WONG, N. D., WOO, D. & TURNER, M. B. 2012. Heart disease and stroke statistics--2012 update: a report from the American Heart Association. *Circulation,* 125**,** e2-e220.

ROSENZWEIG, A. 2003. Vectors for cardiovascular gene therapy. *J Mol Cell Cardiol,* 35**,** 731-3.

ROUBIN, G. S., CANNON, A. D., AGRAWAL, S. K., MACANDER, P. J., DEAN, L. S., BAXLEY, W. A. & BRELAND, J. 1992. Intracoronary stenting for acute and threatened closure complicating percutaneous transluminal coronary angioplasty. *Circulation,* 85**,** 916-27.

RUEF, J., HU, Z. Y., YIN, L. Y., WU, Y., HANSON, S. R., KELLY, A. B., HARKER, L. A., RAO, G. N., RUNGE, M. S. & PATTERSON, C. 1997. Induction of vascular endothelial growth factor in balloon-injured baboon arteries. A novel role for reactive oxygen species in atherosclerosis. *Circ Res,* 81**,** 24-33.

RUTANEN, J., TURUNEN, A. M., TEITTINEN, M., RISSANEN, T. T., HEIKURA, T., KOPONEN, J. K., GRUCHALA, M., INKALA, M., JAUHIAINEN, S., HILTUNEN, M. O., TURUNEN, M. P., STACKER, S. A., ACHEN, M. G. & YLA-HERTTUALA, S. 2005. Gene transfer using the mature form of VEGF-D reduces neointimal thickening through nitric oxide-dependent mechanism. *Gene Ther,* 12**,** 980-7.

SAITO, Y., SUZUKI, H., TSUGAWA, H., IMAEDA, H., MATSUZAKI, J., HIRATA, K., HOSOE, N., NAKAMURA, M., MUKAI, M., SAITO, H. & HIBI, T. 2012. Overexpression of miR-142-5p and miR-155 in gastric mucosa-associated

lymphoid tissue (MALT) lymphoma resistant to Helicobacter pylori eradication. *PLoS One,* 7**,** e47396.

SAMRA, A., BROWN, K., LEUNG, C., MEREDITH, A. & ALLARD, M. 2010. Method Evaluation of In Situ Dissolution of Metallic Coronary Artery Stent. *The Journal of Histotechnology,* 33**,** 182-86.

SANTIAGO, F. S., ISHII, H., SHAFI, S., KHURANA, R., KANELLAKIS, P., BHINDI, R., RAMIREZ, M. J., BOBIK, A., MARTIN, J. F., CHESTERMAN, C. N., ZACHARY, I. C. & KHACHIGIAN, L. M. 2007. Yin Yang-1 inhibits vascular smooth muscle cell growth and intimal thickening by repressing p21WAF1/Cip1 transcription and p21WAF1/Cip1-Cdk4-cyclin D1 assembly. *Circ Res,* 101**,** 146-55.

SARAF, S., ONG, P. J. & GOROG, D. A. 2008. ClearWay RX - Rapid exchange therapeutic perfusion catheter. *EuroIntervention,* 3**,** 639-42.

SATA, M., PERLMAN, H., MURUVE, D. A., SILVER, M., IKEBE, M., LIBERMANN, T. A., OETTGEN, P. & WALSH, K. 1998. Fas ligand gene transfer to the vessel wall inhibits neointima formation and overrides the adenovirus-mediated T cell response. *Proc Natl Acad Sci U S A,* 95**,** 1213-7.

SATO, J., MOHACSI, T., NOEL, A., JOST, C., GLOVICZKI, P., MOZES, G., KATUSIC, Z. S., O'BRIEN, T. & MAYHAN, W. G. 2000. In vivo gene transfer of endothelial nitric oxide synthase to carotid arteries from hypercholesterolemic rabbits enhances endothelium-dependent relaxations. *Stroke,* 31**,** 968-75.

SATO, T., LIU, X., NELSON, A., NAKANISHI, M., KANAJI, N., WANG, X., KIM, M., LI, Y., SUN, J., MICHALSKI, J., PATIL, A., BASMA, H., HOLZ, O., MAGNUSSEN, H. & RENNARD, S. I. 2010. Reduced miR-146a increases prostaglandin E(2)in chronic obstructive pulmonary disease fibroblasts. *Am J Respir Crit Care Med,* 182**,** 1020-9.

SCARBOROUGH, P., WICKRAMASINGHE, K., BHATNAGAR, P. & RAYNER, M. 2011. Trends in coronary heart disease 1961-2011. *British Heart Foundation. London.*

SCHACHNER, T., LAUFER, G. & BONATTI, J. 2006. In vivo (animal) models of vein graft disease. *European journal of cardio-thoracic surgery : official journal of the European Association for Cardio-thoracic Surgery,* 30**,** 451-63.

SCHEINMAN, M., ASCHER, E., LEVI, G. S., HINGORANI, A., SHIRAZIAN, D. & SETH, P. 1999. p53 gene transfer to the injured rat carotid artery decreases neointimal formation. *J Vasc Surg,* 29**,** 360-9.

SCHEUERMANN, J. C. & BOYER, L. A. 2013. Getting to the heart of the matter: long non-coding RNAs in cardiac development and disease. *Embo J,* 32**,** 1805-16.

SCHMIDT, A., LORKOWSKI, S., SEIDLER, D., BREITHARDT, G. & BUDDECKE, E. 2006. TGF-beta1 generates a specific multicomponent extracellular matrix in human coronary SMC. *Eur J Clin Invest,* 36**,** 473-82.

SCHMITTGEN, T. D. & LIVAK, K. J. 2008. Analyzing real-time PCR data by the comparative C(T) method. *Nat Protoc,* 3**,** 1101-8.

SCHOMIG, A., DIBRA, A., WINDECKER, S., MEHILLI, J., SUAREZ DE LEZO, J., KAISER, C., PARK, S. J., GOY, J. J., LEE, J. H., DI LORENZO, E., WU, J., JUNI, P., PFISTERER, M. E., MEIER, B. & KASTRATI, A. 2007. A meta-analysis of 16 randomized trials of sirolimus-eluting stents versus paclitaxel-eluting stents in patients with coronary artery disease. *J Am Coll Cardiol,* 50**,** 1373-80.

SCHOMIG, A., NEUMANN, F. J., KASTRATI, A., SCHUHLEN, H., BLASINI, R., HADAMITZKY, M., WALTER, H., ZITZMANN-ROTH, E. M., RICHARDT, G., ALT, E., SCHMITT, C. & ULM, K. 1996. A randomized comparison of antiplatelet and anticoagulant therapy after the placement of coronary-artery stents. *N Engl J Med,* 334**,** 1084-9.

SCHONROCK, N., HARVEY, R. P. & MATTICK, J. S. 2012. Long noncoding RNAs in cardiac development and pathophysiology. *Circ Res,* 111**,** 1349-62.

SCHWARTZ, R. S., CHRONOS, N. A. & VIRMANI, R. 2004. Preclinical restenosis models and drug-eluting stents: still important, still much to learn. *J Am Coll Cardiol,* 44**,** 1373-85.

SCHWARTZ, R. S., EDELMAN, E. R., CARTER, A., CHRONOS, N., ROGERS, C., ROBINSON, K. A., WAKSMAN, R., WEINBERGER, J., WILENSKY, R. L.,

JENSEN, D. N., ZUCKERMAN, B. D. & VIRMANI, R. 2002. Drug-eluting stents in preclinical studies: recommended evaluation from a consensus group. *Circulation,* 106**,** 1867-73.

SCHWARTZ, R. S., HUBER, K. C., MURPHY, J. G., EDWARDS, W. D., CAMRUD, A. R., VLIETSTRA, R. E. & HOLMES, D. R. 1992. Restenosis and the proportional neointimal response to coronary artery injury: results in a porcine model. *J Am Coll Cardiol,* 19**,** 267-74.

SCHWARTZ, R. S., MURPHY, J. G., EDWARDS, W. D., CAMRUD, A. R., VLIESTRA, R. E. & HOLMES, D. R. 1990. Restenosis after balloon angioplasty. A practical proliferative model in porcine coronary arteries. *Circulation,* 82**,** 2190-200.

SCHWARTZ, S. M., DEBLOIS, D. & O'BRIEN, E. R. 1995. The intima. Soil for atherosclerosis and restenosis. *Circ Res,* 77**,** 445-65.

SEIRADAKE, E., HENAFF, D., WODRICH, H., BILLET, O., PERREAU, M., HIPPERT, C., MENNECHET, F., SCHOEHN, G., LORTAT-JACOB, H., DREJA, H., IBANES, S., KALATZIS, V., WANG, J. P., FINBERG, R. W., CUSACK, S. & KREMER, E. J. 2009. The cell adhesion molecule "CAR" and sialic acid on human erythrocytes influence adenovirus in vivo biodistribution. *PLoS Pathog,* 5**,** e1000277.

SELBACH, M., SCHWANHAUSSER, B., THIERFELDER, N., FANG, Z., KHANIN, R. & RAJEWSKY, N. 2008. Widespread changes in protein synthesis induced by microRNAs. *Nature,* 455**,** 58-63.

SEPP-LORENZINO, L. & RUDDY, M. 2008. Challenges and opportunities for local and systemic delivery of siRNA and antisense oligonucleotides. *Clin Pharmacol Ther,* 84**,** 628-32.

SERRUYS, P. W., DE JAEGERE, P., KIEMENEIJ, F., MACAYA, C., RUTSCH, W., HEYNDRICKX, G., EMANUELSSON, H., MARCO, J., LEGRAND, V., MATERNE, P. & ET AL. 1994. A comparison of balloon-expandable-stent implantation with balloon angioplasty in patients with coronary artery disease. Benestent Study Group. *N Engl J Med,* 331**,** 489-95.

SERRUYS, P. W., KUTRYK, M. J. & ONG, A. T. 2006. Coronary-artery stents. *N Engl J Med,* 354**,** 483-95.

SERRUYS, P. W., MORICE, M. C., KAPPETEIN, A. P., COLOMBO, A., HOLMES, D. R., MACK, M. J., STAHLE, E., FELDMAN, T. E., VAN DEN BRAND, M., BASS, E. J., VAN DYCK, N., LEADLEY, K., DAWKINS, K. D. & MOHR, F. W. 2009. Percutaneous coronary intervention versus coronary-artery bypass grafting for severe coronary artery disease. *N Engl J Med,* 360**,** 961-72.

SERRUYS, P. W., ONUMA, Y., GARG, S., VRANCKX, P., DE BRUYNE, B., MORICE, M. C., COLOMBO, A., MACAYA, C., RICHARDT, G., FAJADET, J., HAMM, C., SCHUIJER, M., RADEMAKER, T., WITTEBOLS, K. & STOLL, H. P. 2010. 5-year clinical outcomes of the ARTS II (Arterial Revascularization Therapies Study II) of the sirolimus-eluting stent in the treatment of patients with multivessel de novo coronary artery lesions. *J Am Coll Cardiol,* 55**,** 1093-101.

SHAH, S. J., WATERS, D. D., BARTER, P., KASTELEIN, J. J., SHEPHERD, J., WENGER, N. K., DEMICCO, D. A., BREAZNA, A. & LAROSA, J. C. 2008. Intensive lipid-lowering with atorvastatin for secondary prevention in patients after coronary artery bypass surgery. *J Am Coll Cardiol,* 51**,** 1938-43.

SHARIF, F., DALY, K., CROWLEY, J. & O'BRIEN, T. 2004. Current status of catheter- and stent-based gene therapy. *Cardiovasc Res,* 64**,** 208-16.

SHARIF, F., HYNES, S. O., MCMAHON, J., COONEY, R., CONROY, S., DOCKERY, P., DUFFY, G., DALY, K., CROWLEY, J., BARTLETT, J. S. & O'BRIEN, T. 2006. Gene-eluting stents: comparison of adenoviral and adeno- associated viral gene delivery to the blood vessel wall in vivo. *Hum Gene Ther,* 17**,** 741-50.

SHARMA, S., CHRISTOPOULOS, C., KUKREJA, N. & GOROG, D. A. 2011. Local drug delivery for percutaneous coronary intervention. *Pharmacol Ther,* 129**,** 260-6.

SHASHKOVA, E. V., DORONIN, K., SENAC, J. S. & BARRY, M. A. 2008. Macrophage depletion combined with anticoagulant therapy increases therapeutic window of systemic treatment with oncolytic adenovirus. *Cancer Res,* 68**,** 5896-904.

SHAYAKHMETOV, D. M., EBERLY, A. M., LI, Z. Y. & LIEBER, A. 2005a. Deletion of penton RGD motifs affects the efficiency of both the internalization and the endosome escape of viral particles containing adenovirus serotype 5 or 35 fiber knobs. *J Virol,* 79**,** 1053-61.

SHAYAKHMETOV, D. M., GAGGAR, A., NI, S., LI, Z. Y. & LIEBER, A. 2005b. Adenovirus binding to blood factors results in liver cell infection and hepatotoxicity. *J Virol,* 79**,** 7478-91.

SHEARS, L. L., 2ND, KIBBE, M. R., MURDOCK, A. D., BILLIAR, T. R., LIZONOVA, A., KOVESDI, I., WATKINS, S. C. & TZENG, E. 1998. Efficient inhibition of intimal hyperplasia by adenovirus-mediated inducible nitric oxide synthase gene transfer to rats and pigs in vivo. *J Am Coll Surg,* 187**,** 295-306.

SHI, Y., FARD, A., GALEO, A., HUTCHINSON, H. G., VERMANI, P., DODGE, G. R., HALL, D. J., SHAHEEN, F. & ZALEWSKI, A. 1994. Transcatheter delivery of c-myc antisense oligomers reduces neointimal formation in a porcine model of coronary artery balloon injury. *Circulation,* 90**,** 944-51.

SHI, Y., PATEL, S., DAVENPECK, K. L., NICULESCU, R., RODRIGUEZ, E., MAGNO, M. G., ORMONT, M. L., MANNION, J. D. & ZALEWSKI, A. 2001. Oxidative stress and lipid retention in vascular grafts: comparison between venous and arterial conduits. *Circulation,* 103**,** 2408-13.

SHIBATA, M., SUZUKI, H., NAKATANI, M., KOBA, S., GESHI, E., KATAGIRI, T. & TAKEYAMA, Y. 2001. The involvement of vascular endothelial growth factor and flt-1 in the process of neointimal proliferation in pig coronary arteries following stent implantation. *Histochem Cell Biol,* 116**,** 471-81.

SIGWART, U., PUEL, J., MIRKOVITCH, V., JOFFRE, F. & KAPPENBERGER, L. 1987. Intravascular stents to prevent occlusion and restenosis after transluminal angioplasty. *N Engl J Med,* 316**,** 701-6.

SIGWART, U., URBAN, P., GOLF, S., KAUFMANN, U., IMBERT, C., FISCHER, A. & KAPPENBERGER, L. 1988. Emergency stenting for acute occlusion after coronary balloon angioplasty. *Circulation,* 78**,** 1121-7.

SIMARI, R. D., SAN, H., REKHTER, M., OHNO, T., GORDON, D., NABEL, G. J. & NABEL, E. G. 1996. Regulation of cellular proliferation and intimal formation following balloon injury in atherosclerotic rabbit arteries. *J Clin Invest,* 98**,** 225-35.

SIMONS, M., EDELMAN, E. R., DEKEYSER, J. L., LANGER, R. & ROSENBERG, R. D. 1992. Antisense c-myb oligonucleotides inhibit intimal arterial smooth muscle cell accumulation in vivo. *Nature,* 359**,** 67-70.

SIROIS, M. G., SIMONS, M. & EDELMAN, E. R. 1997. Antisense oligonucleotide inhibition of PDGFR-beta receptor subunit expression directs suppression of intimal thickening. *Circulation,* 95**,** 669-76.

SMALL, E. M., FROST, R. J. & OLSON, E. N. 2010. MicroRNAs add a new dimension to cardiovascular disease. *Circulation,* 121**,** 1022-32.

SMALL, E. M. & OLSON, E. N. 2011. Pervasive roles of microRNAs in cardiovascular biology. *Nature,* 469**,** 336-42.

SMITH, R. C., BRANELLEC, D., GORSKI, D. H., GUO, K., PERLMAN, H., DEDIEU, J. F., PASTORE, C., MAHFOUDI, A., DENEFLE, P., ISNER, J. M. & WALSH, K. 1997a. p21CIP1-mediated inhibition of cell proliferation by overexpression of the gax homeodomain gene. *Genes Dev,* 11**,** 1674-89.

SMITH, R. C., WILLS, K. N., ANTELMAN, D., PERLMAN, H., TRUONG, L. N., KRASINSKI, K. & WALSH, K. 1997b. Adenoviral constructs encoding phosphorylation-competent full-length and truncated forms of the human retinoblastoma protein inhibit myocyte proliferation and neointima formation. *Circulation,* 96**,** 1899-905.

SOH, J., IQBAL, J., QUEIROZ, J., FERNANDEZ-HERNANDO, C. & HUSSAIN, M. M. 2013. MicroRNA-30c reduces hyperlipidemia and atherosclerosis in mice by decreasing lipid synthesis and lipoprotein secretion. *Nat Med,* 19**,** 892-900.

SOUSA, J. E., COSTA, M. A., ABIZAID, A., ABIZAID, A. S., FERES, F., PINTO, I. M., SEIXAS, A. C., STAICO, R., MATTOS, L. A., SOUSA, A. G., FALOTICO, R., JAEGER, J., POPMA, J. J. & SERRUYS, P. W. 2001. Lack of neointimal proliferation after implantation of sirolimus-coated stents in human coronary arteries: a quantitative coronary angiography and three-dimensional intravascular ultrasound study. *Circulation,* 103**,** 192-5.

SOUZA, D. S., DASHWOOD, M. R., TSUI, J. C., FILBEY, D., BODIN, L., JOHANSSON, B. & BOROWIEC, J. 2002. Improved patency in vein grafts harvested with surrounding tissue: results of a randomized study using three harvesting techniques. *The Annals of thoracic surgery,* 73**,** 1189-95.

SPAULDING, C., DAEMEN, J., BOERSMA, E., CUTLIP, D. E. & SERRUYS, P. W. 2007. A pooled analysis of data comparing sirolimus-eluting stents with bare-metal stents. *N Engl J Med,* 356**,** 989-97.

STACHLER, M. D. & BARTLETT, J. S. 2006. Mosaic vectors comprised of modified AAV1 capsid proteins for efficient vector purification and targeting to vascular endothelial cells. *Gene Ther,* 13**,** 926-31.

STAHLBERG, A., HAKANSSON, J., XIAN, X., SEMB, H. & KUBISTA, M. 2004. Properties of the reverse transcription reaction in mRNA quantification. *Clin Chem,* 50**,** 509-15.

STAMMET, P., GORETTI, E., VAUSORT, M., ZHANG, L., WAGNER, D. R. & DEVAUX, Y. 2012. Circulating microRNAs after cardiac arrest. *Crit Care Med*.

STEG, P. G., JAMES, S. K., ATAR, D., BADANO, L. P., BLOMSTROM-LUNDQVIST, C., BORGER, M. A., DI MARIO, C., DICKSTEIN, K., DUCROCQ, G., FERNANDEZ-AVILES, F., GERSHLICK, A. H., GIANNUZZI, P., HALVORSEN, S., HUBER, K., JUNI, P., KASTRATI, A., KNUUTI, J., LENZEN, M. J., MAHAFFEY, K. W., VALGIMIGLI, M., VAN 'T HOF, A., WIDIMSKY, P. & ZAHGER, D. 2012. ESC Guidelines for the management of acute myocardial infarction in patients presenting with ST-segment elevation. *Eur Heart J,* 33**,** 2569-619.

STEG, P. G., TAHLIL, O., AUBAILLY, N., CAILLAUD, J. M., DEDIEU, J. F., BERTHELOT, K., LE ROUX, A., FELDMAN, L., PERRICAUDET, M., DENEFLE, P. & BRANELLEC, D. 1997. Reduction of restenosis after angioplasty in an atheromatous rabbit model by suicide gene therapy. *Circulation,* 96**,** 408-11.

STEPHAN, D., SAN, H., YANG, Z. Y., GORDON, D., GOELZ, S., NABEL, G. J. & NABEL, E. G. 1997. Inhibition of vascular smooth muscle cell proliferation and intimal hyperplasia by gene transfer of beta-interferon. *Mol Med,* 3**,** 593-9.

STETTLER, C., WANDEL, S., ALLEMANN, S., KASTRATI, A., MORICE, M. C., SCHOMIG, A., PFISTERER, M. E., STONE, G. W., LEON, M. B., DE LEZO, J. S., GOY, J. J., PARK, S. J., SABATE, M., SUTTORP, M. J., KELBAEK, H., SPAULDING, C., MENICHELLI, M., VERMEERSCH, P., DIRKSEN, M. T., CERVINKA, P., PETRONIO, A. S., NORDMANN, A. J., DIEM, P., MEIER, B., ZWAHLEN, M., REICHENBACH, S., TRELLE, S., WINDECKER, S. & JUNI, P.

2007. Outcomes associated with drug-eluting and bare-metal stents: a collaborative network meta-analysis. *Lancet,* 370**,** 937-48.

STONE, D., LIU, Y., SHAYAKHMETOV, D., LI, Z. Y., NI, S. & LIEBER, A. 2007a. Adenovirus-platelet interaction in blood causes virus sequestration to the reticuloendothelial system of the liver. *J Virol,* 81**,** 4866-71.

STONE, G. W., MOSES, J. W., ELLIS, S. G., SCHOFER, J., DAWKINS, K. D., MORICE, M. C., COLOMBO, A., SCHAMPAERT, E., GRUBE, E., KIRTANE, A. J., CUTLIP, D. E., FAHY, M., POCOCK, S. J., MEHRAN, R. & LEON, M. B. 2007b. Safety and efficacy of sirolimus- and paclitaxel-eluting coronary stents. *N Engl J Med,* 356**,** 998-1008.

SUN, S. G., ZHENG, B., HAN, M., FANG, X. M., LI, H. X., MIAO, S. B., SU, M., HAN, Y., SHI, H. J. & WEN, J. K. 2011. miR-146a and Kruppel-like factor 4 form a feedback loop to participate in vascular smooth muscle cell proliferation. *EMBO Rep,* 12**,** 56-62.

SUN, Y., SUN, J., TOMOMI, T., NIEVES, E., MATHEWSON, N., TAMAKI, H., EVERS, R. & REDDY, P. 2013. PU.1-dependent transcriptional regulation of miR-142 contributes to its hematopoietic cell-specific expression and modulation of IL-6. *J Immunol,* 190**,** 4005-13.

SWANSON, N., HOGREFE, K., JAVED, Q., MALIK, N. & GERSHLICK, A. H. 2003. Vascular endothelial growth factor (VEGF)-eluting stents: in vivo effects on thrombosis, endothelialization and intimal hyperplasia. *J Invasive Cardiol,* 15**,** 688-92.

TABATA, M., GRAB, J. D., KHALPEY, Z., EDWARDS, F. H., O'BRIEN, S. M., COHN, L. H. & BOLMAN, R. M., 3RD 2009. Prevalence and variability of internal mammary artery graft use in contemporary multivessel coronary artery bypass graft surgery: analysis of the Society of Thoracic Surgeons National Cardiac Database. *Circulation,* 120**,** 935-40.

TAHLIL, O., BRAMI, M., FELDMAN, L. J., BRANELLEC, D. & STEG, P. G. 1997. The Dispatch catheter as a delivery tool for arterial gene transfer. *Cardiovasc Res,* 33**,** 181-7.

TANSKI, W. J., ROZTOCIL, E., HEMADY, E. A., WILLIAMS, J. A. & DAVIES, M. G. 2004. Role of Galphaq in smooth muscle cell proliferation. *J Vasc Surg,* 39**,** 639-44.

TATOULIS, J. 2013. Total arterial coronary revascularization-patient selection, stenoses, conduits, targets. *Ann Cardiothorac Surg,* 2**,** 499-506.

TEIGLER, J. E., IAMPIETRO, M. J. & BAROUCH, D. H. 2012. Vaccination with adenovirus serotypes 35, 26, and 48 elicits higher levels of innate cytokine responses than adenovirus serotype 5 in rhesus monkeys. *J Virol,* 86**,** 9590-8.

TESCH, G. H., LAN, H. Y. & NIKOLIC-PATERSON, D. J. 2006. Treatment of tissue sections for in situ hybridization. *Methods Mol Biol,* 326**,** 1-7.

THACI, B., ULASOV, I. V., WAINWRIGHT, D. A. & LESNIAK, M. S. 2011. The challenge for gene therapy: innate immune response to adenoviruses. *Oncotarget,* 2**,** 113-21.

THIM, T., HAGENSEN, M. K., DROUET, L., BAL DIT SOLLIER, C., BONNEAU, M., GRANADA, J. F., NIELSEN, L. B., PAASKE, W. P., BOTKER, H. E. & FALK, E. 2010. Familial hypercholesterolaemic downsized pig with human-like coronary atherosclerosis: a model for preclinical studies. *EuroIntervention,* 6**,** 261-8.

THUM, T., GALUPPO, P., WOLF, C., FIEDLER, J., KNEITZ, S., VAN LAAKE, L. W., DOEVENDANS, P. A., MUMMERY, C. L., BORLAK, J., HAVERICH, A., GROSS, C., ENGELHARDT, S., ERTL, G. & BAUERSACHS, J. 2007. MicroRNAs in the human heart: a clue to fetal gene reprogramming in heart failure. *Circulation,* 116**,** 258-67.

THUM, T., GROSS, C., FIEDLER, J., FISCHER, T., KISSLER, S., BUSSEN, M., GALUPPO, P., JUST, S., ROTTBAUER, W., FRANTZ, S., CASTOLDI, M., SOUTSCHEK, J., KOTELIANSKY, V., ROSENWALD, A., BASSON, M. A., LICHT, J. D., PENA, J. T., ROUHANIFARD, S. H., MUCKENTHALER, M. U., TUSCHL, T., MARTIN, G. R., BAUERSACHS, J. & ENGELHARDT, S. 2008. MicroRNA-21 contributes to myocardial disease by stimulating MAP kinase signalling in fibroblasts. *Nature,* 456**,** 980-4.

TILEMANN, L., ISHIKAWA, K., WEBER, T. & HAJJAR, R. J. 2012. Gene therapy for heart failure. *Circ Res,* 110**,** 777-93.

TONINO, P. A., DE BRUYNE, B., PIJLS, N. H., SIEBERT, U., IKENO, F., VAN' T VEER, M., KLAUSS, V., MANOHARAN, G., ENGSTROM, T., OLDROYD, K. G., VER LEE, P. N., MACCARTHY, P. A. & FEARON, W. F. 2009. Fractional flow reserve versus angiography for guiding percutaneous coronary intervention. *N Engl J Med,* 360**,** 213-24.

TORELLA, D., IACONETTI, C., CATALUCCI, D., ELLISON, G. M., LEONE, A., WARING, C. D., BOCHICCHIO, A., VICINANZA, C., AQUILA, I., CURCIO, A., CONDORELLI, G. & INDOLFI, C. 2011. MicroRNA-133 controls vascular smooth muscle cell phenotypic switch in vitro and vascular remodeling in vivo. *Circ Res,* 109**,** 880-93.

TSAI, W. C., HSU, S. D., HSU, C. S., LAI, T. C., CHEN, S. J., SHEN, R., HUANG, Y., CHEN, H. C., LEE, C. H., TSAI, T. F., HSU, M. T., WU, J. C., HUANG, H. D., SHIAO, M. S., HSIAO, M. & TSOU, A. P. 2012. MicroRNA-122 plays a critical role in liver homeostasis and hepatocarcinogenesis. *J Clin Invest,* 122**,** 2884-97.

TSUI, J. C., SOUZA, D. S., FILBEY, D., KARLSSON, M. G. & DASHWOOD, M. R. 2002a. Localization of nitric oxide synthase in saphenous vein grafts harvested with a novel "no-touch" technique: potential role of nitric oxide contribution to improved early graft patency rates. *Journal of vascular surgery : official publication, the Society for Vascular Surgery [and] International Society for Cardiovascular Surgery, North American Chapter,* 35**,** 356-62.

TSUI, L. V., CAMRUD, A., MONDESIRE, J., CARLSON, P., ZAYEK, N., CAMRUD, L., DONAHUE, B., BAUER, S., LIN, A., FREY, D., RIVKIN, M., SUBRAMANIAN, A., FALOTICO, R., GYURIS, J., SCHWARTZ, R. & MCARTHUR, J. G. 2001. p27-p16 fusion gene inhibits angioplasty-induced neointimal hyperplasia and coronary artery occlusion. *Circ Res,* 89**,** 323-8.

TSUI, N. B., NG, E. K. & LO, Y. M. 2002b. Stability of endogenous and added RNA in blood specimens, serum, and plasma. *Clin Chem,* 48**,** 1647-53.

UENO, H., MASUDA, S., NISHIO, S., LI, J. J., YAMAMOTO, H. & TAKESHITA, A. 1997a. Adenovirus-mediated transfer of cyclin-dependent kinase inhibitor-p21 suppresses neointimal formation in the balloon-injured rat carotid arteries in vivo. *Ann N Y Acad Sci,* 811**,** 401-11.

UENO, H., YAMAMOTO, H., ITO, S., LI, J. J. & TAKESHITA, A. 1997b. Adenovirus-mediated transfer of a dominant-negative H-ras suppresses neointimal formation in balloon-injured arteries in vivo. *Arterioscler Thromb Vasc Biol,* 17**,** 898-904.

VALENCIA-SANCHEZ, M. A., LIU, J., HANNON, G. J. & PARKER, R. 2006. Control of translation and mRNA degradation by miRNAs and siRNAs. *Genes Dev,* 20**,** 515-24.

VAN BELLE, E., MAILLARD, L., RIVARD, A., FABRE, J. E., COUFFINHAL, T., KEARNEY, M., BRANELLEC, D., FELDMAN, L. J., WALSH, K. & ISNER, J. M. 1998. Effects of poloxamer 407 on transfection time and percutaneous adenovirus-mediated gene transfer in native and stented vessels. *Hum Gene Ther,* 9**,** 1013-24.

VAN BELLE, E., MAILLARD, L., TIO, F. O. & ISNER, J. M. 1997a. Accelerated endothelialization by local delivery of recombinant human vascular endothelial growth factor reduces in-stent intimal formation. *Biochem Biophys Res Commun,* 235**,** 311-6.

VAN BELLE, E., TIO, F. O., COUFFINHAL, T., MAILLARD, L., PASSERI, J. & ISNER, J. M. 1997b. Stent endothelialization. Time course, impact of local catheter delivery, feasibility of recombinant protein administration, and response to cytokine expedition. *Circulation,* 95**,** 438-48.

VAN DER GIESSEN, W. J., LINCOFF, A. M., SCHWARTZ, R. S., VAN BEUSEKOM, H. M., SERRUYS, P. W., HOLMES, D. R., JR., ELLIS, S. G. & TOPOL, E. J. 1996. Marked inflammatory sequelae to implantation of biodegradable and nonbiodegradable polymers in porcine coronary arteries. *Circulation,* 94**,** 1690-7.

VAN ROOIJ, E. 2011. The art of microRNA research. *Circ Res,* 108**,** 219-34.

VAN ROOIJ, E. 2012. Introduction to the series on microRNAs in the cardiovascular system. *Circ Res,* 110**,** 481-2.

VAN ROOIJ, E. & OLSON, E. N. 2012. MicroRNA therapeutics for cardiovascular disease: opportunities and obstacles. *Nat Rev Drug Discov,* 11**,** 860-72.

VAN WERKUM, J. W., HEESTERMANS, A. A., ZOMER, A. C., KELDER, J. C., SUTTORP, M. J., RENSING, B. J., KOOLEN, J. J., BRUEREN, B. R.,

DAMBRINK, J. H., HAUTVAST, R. W., VERHEUGT, F. W. & TEN BERG, J. M. 2009. Predictors of coronary stent thrombosis: the Dutch Stent Thrombosis Registry. *J Am Coll Cardiol,* 53**,** 1399-409.

VARENNE, O., PISLARU, S., GILLIJNS, H., VAN PELT, N., GERARD, R. D., ZOLDHELYI, P., VAN DE WERF, F., COLLEN, D. & JANSSENS, S. P. 1998. Local adenovirus-mediated transfer of human endothelial nitric oxide synthase reduces luminal narrowing after coronary angioplasty in pigs. *Circulation,* 98**,** 919-26.

VARGAS, J., JR., GUSELLA, G. L., NAJFELD, V., KLOTMAN, M. E. & CARA, A. 2004. Novel integrase-defective lentiviral episomal vectors for gene transfer. *Hum Gene Ther,* 15**,** 361-72.

VERMA, I. M. 2013. Medicine. Gene therapy that works. *Science,* 341**,** 853-5.

VETRINI, F. & NG, P. 2010. Gene therapy with helper-dependent adenoviral vectors: current advances and future perspectives. *Viruses,* 2**,** 1886-917.

VIGANT, F., DESCAMPS, D., JULLIENNE, B., ESSELIN, S., CONNAULT, E., OPOLON, P., TORDJMANN, T., VIGNE, E., PERRICAUDET, M. & BENIHOUD, K. 2008. Substitution of hexon hypervariable region 5 of adenovirus serotype 5 abrogates blood factor binding and limits gene transfer to liver. *Mol Ther,* 16**,** 1474-80.

VIRMANI, R., ATKINSON, J. B. & FORMAN, M. B. 1988. Aortocoronary saphenous vein bypass grafts. *Cardiovasc Clin,* 18**,** 41-62.

VIRMANI, R., FARB, A., GUAGLIUMI, G. & KOLODGIE, F. D. 2004. Drug-eluting stents: caution and concerns for long-term outcome. *Coron Artery Dis,* 15**,** 313-8.

VOELLENKLE, C., ROOIJ, J., GUFFANTI, A., BRINI, E., FASANARO, P., ISAIA, E., CROFT, L., DAVID, M., CAPOGROSSI, M. C., MOLES, A., FELSANI, A. & MARTELLI, F. 2012. Deep-sequencing of endothelial cells exposed to hypoxia reveals the complexity of known and novel microRNAs. *Rna,* 18**,** 472-84.

VON DER LEYEN, H. E., GIBBONS, G. H., MORISHITA, R., LEWIS, N. P., ZHANG, L., NAKAJIMA, M., KANEDA, Y., COOKE, J. P. & DZAU, V. J. 1995. Gene

therapy inhibiting neointimal vascular lesion: in vivo transfer of endothelial cell nitric oxide synthase gene. *Proc Natl Acad Sci U S A,* 92**,** 1137-41.

VON DER LEYEN, H. E., MUGGE, A., HANEFELD, C., HAMM, C. W., RAU, M., RUPPRECHT, H. J., ZEIHER, A. M. & FICHTLSCHERER, S. 2011. A Prospective, Single-Blind, Multicenter, Dose Escalation Study of Intracoronary iNOS Lipoplex (CAR-MP583) Gene Therapy for the Prevention of Restenosis in Patients with de novo or Restenotic Coronary Artery Lesion (REGENT I Extension). *Hum Gene Ther,* 22**,** 951-8.

WADDINGTON, S. N., MCVEY, J. H., BHELLA, D., PARKER, A. L., BARKER, K., ATODA, H., PINK, R., BUCKLEY, S. M., GREIG, J. A., DENBY, L., CUSTERS, J., MORITA, T., FRANCISCHETTI, I. M., MONTEIRO, R. Q., BAROUCH, D. H., VAN ROOIJEN, N., NAPOLI, C., HAVENGA, M. J., NICKLIN, S. A. & BAKER, A. H. 2008. Adenovirus serotype 5 hexon mediates liver gene transfer. *Cell,* 132**,** 397-409.

WALTER, D. H., CEJNA, M., DIAZ-SANDOVAL, L., WILLIS, S., KIRKWOOD, L., STRATFORD, P. W., TIETZ, A. B., KIRCHMAIR, R., SILVER, M., CURRY, C., WECKER, A., YOON, Y. S., HEIDENREICH, R., HANLEY, A., KEARNEY, M., TIO, F. O., KUENZLER, P., ISNER, J. M. & LOSORDO, D. W. 2004. Local gene transfer of phVEGF-2 plasmid by gene-eluting stents: an alternative strategy for inhibition of restenosis. *Circulation,* 110**,** 36-45.

WAN, S., GEORGE, S. J., BERRY, C. & BAKER, A. H. 2012. Vein graft failure: current clinical practice and potential for gene therapeutics. *Gene Ther,* 19**,** 630-6.

WAN, S., GEORGE, S. J., NICKLIN, S. A., YIM, A. P. & BAKER, A. H. 2004. Overexpression of p53 increases lumen size and blocks neointima formation in porcine interposition vein grafts. *Mol Ther,* 9**,** 689-98.

WANG, G. K., ZHU, J. Q., ZHANG, J. T., LI, Q., LI, Y., HE, J., QIN, Y. W. & JING, Q. 2010a. Circulating microRNA: a novel potential biomarker for early diagnosis of acute myocardial infarction in humans. *Eur Heart J,* 31**,** 659-66.

WANG, H., LI, Z. Y., LIU, Y., PERSSON, J., BEYER, I., MOLLER, T., KOYUNCU, D., DRESCHER, M. R., STRAUSS, R., ZHANG, X. B., WAHL, J. K., 3RD, URBAN, N., DRESCHER, C., HEMMINKI, A., FENDER, P. & LIEBER, A. 2010b.

Desmoglein 2 is a receptor for adenovirus serotypes 3, 7, 11 and 14. *Nat Med,* 17**,** 96-104.

WANG, S., AURORA, A. B., JOHNSON, B. A., QI, X., MCANALLY, J., HILL, J. A., RICHARDSON, J. A., BASSEL-DUBY, R. & OLSON, E. N. 2008. The endothelial-specific microRNA miR-126 governs vascular integrity and angiogenesis. *Dev Cell,* 15**,** 261-71.

WATT, J., KENNEDY, S., MCCORMICK, C., AGBANI, E. O., MCPHADEN, A., MULLEN, A., CZUDAJ, P., BEHNISCH, B., WADSWORTH, R. M. & OLDROYD, K. G. 2013. Succinobucol-eluting stents increase neointimal thickening and peri-strut inflammation in a porcine coronary model. *Catheter Cardiovasc Interv,* 81**,** 698-708.

WEAVER, M. E., PANTELY, G. A., BRISTOW, J. D. & LADLEY, H. D. 1986. A quantitative study of the anatomy and distribution of coronary arteries in swine in comparison with other animals and man. *Cardiovasc Res,* 20**,** 907-17.

WEBER, J. A., BAXTER, D. H., ZHANG, S., HUANG, D. Y., HUANG, K. H., LEE, M. J., GALAS, D. J. & WANG, K. 2010a. The microRNA spectrum in 12 body fluids. *Clin Chem,* 56**,** 1733-41.

WEBER, M., BAKER, M. B., MOORE, J. P. & SEARLES, C. D. 2010b. MiR-21 is induced in endothelial cells by shear stress and modulates apoptosis and eNOS activity. *Biochem Biophys Res Commun,* 393**,** 643-8.

WEI, Y., SCHOBER, A. & WEBER, C. 2013. Pathogenic arterial remodeling: the good and bad of microRNAs. *Am J Physiol Heart Circ Physiol,* 304**,** H1050-9.

WELT, F. G. & ROGERS, C. 2002. Inflammation and restenosis in the stent era. *Arterioscler Thromb Vasc Biol,* 22**,** 1769-76.

WEN, S., GRAF, S., MASSEY, P. G. & DICHEK, D. A. 2004. Improved vascular gene transfer with a helper-dependent adenoviral vector. *Circulation,* 110**,** 1484-91.

WENAWESER, P., DAEMEN, J., ZWAHLEN, M., VAN DOMBURG, R., JUNI, P., VAINA, S., HELLIGE, G., TSUCHIDA, K., MORGER, C., BOERSMA, E., KUKREJA, N., MEIER, B., SERRUYS, P. W. & WINDECKER, S. 2008. Incidence and correlates of drug-eluting stent thrombosis in routine clinical

practice. 4-year results from a large 2-institutional cohort study. *J Am Coll Cardiol,* 52**,** 1134-40.

WESSELY, R., HAUSLEITER, J., MICHAELIS, C., JASCHKE, B., VOGESER, M., MILZ, S., BEHNISCH, B., SCHRATZENSTALLER, T., RENKE-GLUSZKO, M., STOVER, M., WINTERMANTEL, E., KASTRATI, A. & SCHOMIG, A. 2005. Inhibition of neointima formation by a novel drug-eluting stent system that allows for dose-adjustable, multiple, and on-site stent coating. *Arterioscler Thromb Vasc Biol,* 25**,** 748-53.

WEST, N., GUZIK, T., BLACK, E. & CHANNON, K. 2001. Enhanced superoxide production in experimental venous bypass graft intimal hyperplasia: role of NAD(P)H oxidase. *Arterioscler Thromb Vasc Biol,* 21**,** 189-94.

WHITE, F. C., CARROLL, S. M., MAGNET, A. & BLOOR, C. M. 1992. Coronary collateral development in swine after coronary artery occlusion. *Circ Res,* 71**,** 1490-500.

WHITE, K. M., ALBA, R., PARKER, A. L., WRIGHT, A. F., BRADSHAW, A. C., DELLES, C., MCDONALD, R. A. & BAKER, A. H. 2013. Assessment of a novel, capsid-modified adenovirus with an improved vascular gene transfer profile. *J Cardiothorac Surg,* 8**,** 183.

WICKHAM, T. J., MATHIAS, P., CHERESH, D. A. & NEMEROW, G. R. 1993. Integrins alpha v beta 3 and alpha v beta 5 promote adenovirus internalization but not virus attachment. *Cell,* 73**,** 309-19.

WIDERA, C., GUPTA, S. K., LORENZEN, J. M., BANG, C., BAUERSACHS, J., BETHMANN, K., KEMPF, T., WOLLERT, K. C. & THUM, T. 2011. Diagnostic and prognostic impact of six circulating microRNAs in acute coronary syndrome. *J Mol Cell Cardiol,* 51**,** 872-5.

WIJNS, W., KOLH, P., DANCHIN, N., DI MARIO, C., FALK, V., FOLLIGUET, T., GARG, S., HUBER, K., JAMES, S., KNUUTI, J., LOPEZ-SENDON, J., MARCO, J., MENICANTI, L., OSTOJIC, M., PIEPOLI, M. F., PIRLET, C., POMAR, J. L., REIFART, N., RIBICHINI, F. L., SCHALIJ, M. J., SERGEANT, P., SERRUYS, P. W., SILBER, S., SOUSA UVA, M. & TAGGART, D. 2010. Guidelines on myocardial revascularization: The Task Force on Myocardial Revascularization of

the European Society of Cardiology (ESC) and the European Association for Cardio-Thoracic Surgery (EACTS). *Eur Heart J,* 31**,** 2501-55.

WILENSKY, R. L., TANGUAY, J. F., ITO, S., BARTORELLI, A. L., MOSES, J., WILLIAMS, D. O., BAILEY, S. R., MARTIN, J., BUCHER, T. A., GALLANT, P., GREENBERG, A., POPMA, J. J., WEISSMAN, N. J., MINTZ, G. S., KAPLAN, A. V. & LEON, M. B. 2000. Heparin infusion prior to stenting (HIPS) trial: final results of a prospective, randomized, controlled trial evaluating the effects of local vascular delivery on intimal hyperplasia. *Am Heart J,* 139**,** 1061-70.

WILLIAMS, P. D., MALIK, N. & KINGSTON, P. A. 2012. Coronary angiography and percutaneous coronary intervention in the porcine model: a practical guide to the procedure. *Animal,* 6**,** 311-20.

WORGALL, S., WOLFF, G., FALCK-PEDERSEN, E. & CRYSTAL, R. G. 1997. Innate immune mechanisms dominate elimination of adenoviral vectors following in vivo administration. *Hum Gene Ther,* 8**,** 37-44.

WORK, L. M., BUNING, H., HUNT, E., NICKLIN, S. A., DENBY, L., BRITTON, N., LEIKE, K., ODENTHAL, M., DREBBER, U., HALLEK, M. & BAKER, A. H. 2006. Vascular bed-targeted in vivo gene delivery using tropism-modified adeno-associated viruses. *Mol Ther,* 13**,** 683-93.

WORK, L. M., NICKLIN, S. A., BRAIN, N. J., DISHART, K. L., VON SEGGERN, D. J., HALLEK, M., BUNING, H. & BAKER, A. H. 2004a. Development of efficient viral vectors selective for vascular smooth muscle cells. *Mol Ther,* 9**,** 198-208.

WORK, L. M., RITCHIE, N., NICKLIN, S. A., REYNOLDS, P. N. & BAKER, A. H. 2004b. Dual targeting of gene delivery by genetic modification of adenovirus serotype 5 fibers and cell-selective transcriptional control. *Gene Ther,* 11**,** 1296-300.

WU, X., CHEN, Y., LIU, H., TEIRSTEIN, P. S., KIRTANE, A. J., GE, C., SONG, X., CHEN, X., GU, C., HUANG, F. & LV, S. 2010. Comparison of long-term (4-year) outcomes of patients with unprotected left main coronary artery narrowing treated with drug-eluting stents versus coronary-artery bypass grafting. *Am J Cardiol,* 105**,** 1728-34.

XIN, M., SMALL, E. M., SUTHERLAND, L. B., QI, X., MCANALLY, J., PLATO, C. F., RICHARDSON, J. A., BASSEL-DUBY, R. & OLSON, E. N. 2009. MicroRNAs miR-143 and miR-145 modulate cytoskeletal dynamics and responsiveness of smooth muscle cells to injury. *Genes Dev,* 23**,** 2166-78.

YAN, T. D., PADANG, R., POH, C., CAO, C., WILSON, M. K., BANNON, P. G. & VALLELY, M. P. 2011. Drug-eluting stents versus coronary artery bypass grafting for the treatment of coronary artery disease: a meta-analysis of randomized and nonrandomized studies. *J Thorac Cardiovasc Surg,* 141**,** 1134-44.

YANEZ-MUNOZ, R. J., BALAGGAN, K. S., MACNEIL, A., HOWE, S. J., SCHMIDT, M., SMITH, A. J., BUCH, P., MACLAREN, R. E., ANDERSON, P. N., BARKER, S. E., DURAN, Y., BARTHOLOMAE, C., VON KALLE, C., HECKENLIVELY, J. R., KINNON, C., ALI, R. R. & THRASHER, A. J. 2006. Effective gene therapy with nonintegrating lentiviral vectors. *Nat Med,* 12**,** 348-53.

YANG, G., PEI, Y., CAO, Q. & WANG, R. 2011. MicroRNA-21 represses human cystathionine gamma-lyase expression by targeting at specificity protein-1 in smooth muscle cells. *J Cell Physiol,* 227**,** 3192-200.

YANG, J., ZENG, Y., LI, Y., SONG, C., ZHU, W., GUAN, H. & LI, X. 2008. Intravascular site-specific delivery of a therapeutic antisense for the inhibition of restenosis. *Eur J Pharm Sci,* 35**,** 427-34.

YANG, S., BANERJEE, S., FREITAS, A., CUI, H., XIE, N., ABRAHAM, E. & LIU, G. 2012. miR-21 regulates chronic hypoxia-induced pulmonary vascular remodeling. *Am J Physiol Lung Cell Mol Physiol,* 302**,** L521-9.

YANG, Y., NUNES, F. A., BERENCSI, K., FURTH, E. E., GONCZOL, E. & WILSON, J. M. 1994. Cellular immunity to viral antigens limits E1-deleted adenoviruses for gene therapy. *Proc Natl Acad Sci U S A,* 91**,** 4407-11.

YANG, Z. Y., SIMARI, R. D., PERKINS, N. D., SAN, H., GORDON, D., NABEL, G. J. & NABEL, E. G. 1996. Role of the p21 cyclin-dependent kinase inhibitor in limiting intimal cell proliferation in response to arterial injury. *Proc Natl Acad Sci U S A,* 93**,** 7905-10.

YLA-HERTTUALA, S. & MARTIN, J. F. 2000. Cardiovascular gene therapy. *Lancet,* 355**,** 213-22.

YONEMITSU, Y., KANEDA, Y., TANAKA, S., NAKASHIMA, Y., KOMORI, K., SUGIMACHI, K. & SUEISHI, K. 1998. Transfer of wild-type p53 gene effectively inhibits vascular smooth muscle cell proliferation in vitro and in vivo. *Circ Res,* 82**,** 147-56.

YUSUF, S., ZHAO, F., MEHTA, S. R., CHROLAVICIUS, S., TOGNONI, G. & FOX, K. K. 2001. Effects of clopidogrel in addition to aspirin in patients with acute coronary syndromes without ST-segment elevation. *N Engl J Med,* 345**,** 494-502.

ZAMPETAKI, A., KIECHL, S., DROZDOV, I., WILLEIT, P., MAYR, U., PROKOPI, M., MAYR, A., WEGER, S., OBERHOLLENZER, F., BONORA, E., SHAH, A., WILLEIT, J. & MAYR, M. 2010. Plasma microRNA profiling reveals loss of endothelial miR-126 and other microRNAs in type 2 diabetes. *Circ Res,* 107**,** 810-7.

ZAMPETAKI, A., WILLEIT, P., DROZDOV, I., KIECHL, S. & MAYR, M. 2012a. Profiling of circulating microRNAs: from single biomarkers to re-wired networks. *Cardiovasc Res,* 93**,** 555-62.

ZAMPETAKI, A., WILLEIT, P., TILLING, L., DROZDOV, I., PROKOPI, M., RENARD, J. M., MAYR, A., WEGER, S., SCHETT, G., SHAH, A., BOULANGER, C. M., WILLEIT, J., CHOWIENCZYK, P. J., KIECHL, S. & MAYR, M. 2012b. Prospective Study on Circulating MicroRNAs and Risk of Myocardial Infarction. *J Am Coll Cardiol,* 60**,** 290-9.

ZENATI, M. A., SHROYER, A. L., COLLINS, J. F., HATTLER, B., OTA, T., ALMASSI, G. H., AMIDI, M., NOVITZKY, D., GROVER, F. L. & SONEL, A. F. 2011. Impact of endoscopic versus open saphenous vein harvest technique on late coronary artery bypass grafting patient outcomes in the ROOBY (Randomized On/Off Bypass) Trial. *J Thorac Cardiovasc Surg,* 141**,** 338-44.

ZERNECKE, A., BIDZHEKOV, K., NOELS, H., SHAGDARSUREN, E., GAN, L., DENECKE, B., HRISTOV, M., KOPPEL, T., JAHANTIGH, M. N., LUTGENS, E., WANG, S., OLSON, E. N., SCHOBER, A. & WEBER, C. 2009. Delivery of microRNA-126 by apoptotic bodies induces CXCL12-dependent vascular protection. *Sci Signal,* 2**,** ra81.

ZHAO, Y. & SRIVASTAVA, D. 2007. A developmental view of microRNA function. *Trends Biochem Sci,* 32**,** 189-97.

ZHENG, Z. M. & WANG, X. 2011. Regulation of cellular miRNA expression by human papillomaviruses. *Biochim Biophys Acta,* 1809**,** 668-77.

ZHOU, J., WANG, K. C., WU, W., SUBRAMANIAM, S., SHYY, J. Y., CHIU, J. J., LI, J. Y. & CHIEN, S. 2011. MicroRNA-21 targets peroxisome proliferators-activated receptor-alpha in an autoregulatory loop to modulate flow-induced endothelial inflammation. *Proc Natl Acad Sci U S A,* 108**,** 10355-60.

ZUCKERBRAUN, B. S. & TZENG, E. 2002. Vascular gene therapy: a reality of the 21st century. *Arch Surg,* 137**,** 854-61.